EVALUATION OF THE TRAC VARIABLE DIAMETER ROTOR: PRELIMINARY DESIGN OF A FULL-SCALE ROTOR AND PARAMETRIC MISSION ANALYSIS COMPARISONS

Evan A. Fradenburgh, et al

United Technologies Corporation

Prepared for:

Army Air Mobility Research and Development Laboratory

February 1976

USAAMRDL-TR- 75-54

EVALUATION OF THE TRAC VARIABLE DIAMETER ROTOR: PRELIMINARY DESIGN OF A FULL-SCALE ROTOR AND PARAMETRIC MISSION ANALYSIS COMPARISONS

Sikorsky Aircraft Division
United Technologies Corporation
Stratford, Conn. 06602

February 1976

Final Report

Prepared for

EUSTIS DIRECTORATE
U. S. ARMY AIR MOBILITY RESEARCH AND DEVELOPMENT LABORATORY
Fort Eustis, Va. 23604

EUSTIS DIRECTORATE POSITION STATEMENT

This report has been reviewed by the Eustis Directorate, U. S. Army Air Mobility Research and Development Laboratory and is considered technically sound.

This program was initiated to determine the potential of the Telescoping Rotor Aircraft Concept for projected Army operational missions. A preliminary design of a full-scale flightworthy rotor system and a comparative parametric analysis were conducted to evaluate TRAC-rotor compound helicopter and stowed-rotor concepts relative to conventional-rotor pure and compound helicopters.

The technical monitor for this contract was Mr. Patrick A. Cancro, Technology Applications Division.

DISCLAIMERS

The findings in this report are not to be construed as an official Department of the Army position unless so designated by other authorized documents.

When Government drawings, specifications, or other data are used for any purpose other than in connection with a definitely related Government procurement operation, the United States Government thereby incurs no responsibility nor any obligation whatsoever; and the fact that the Government may have formulated, furnished, or in any way supplied the said drawings, specifications, or other data is not to be regarded by implication or otherwise as in any manner licensing the holder or any other person or corporation, or conveying any rights or permission, to manufacture, use, or sell any patented invention that may in any way be related thereto.

Trade names cited in this report do not constitute an official endorsement or approval of the use of such commercial hardware or software.

DISPOSITION INSTRUCTIONS

Destroy this report when no longer needed. Do not return it to the originator.

Unclassified

SECURITY CLASSIFICATION OF THIS PAGE *(When Data Entered)*

REPORT DOCUMENTATION PAGE		READ INSTRUCTIONS BEFORE COMPLETING FORM
1. REPORT NUMBER USAAMRDL-TR-75-54	2. GOVT ACCESSION NO.	3. RECIPIENT'S CATALOG NUMBER
4. TITLE *(and Subtitle)* EVALUATION OF THE TRAC VARIABLE DIAMETER ROTOR: PRELIMINARY DESIGN OF A FULL-SCALE ROTOR AND PARAMETRIC MISSION ANALYSIS COMPARISONS		5. TYPE OF REPORT & PERIOD COVERED Final 6. PERFORMING ORG. REPORT NUMBER SER-50952
7. AUTHOR(s) Evan A. Fradenburgh Lee N. Hager Neville F. K. Keffort		8. CONTRACT OR GRANT NUMBER(s) DAAJ02-74-C-0048
9. PERFORMING ORGANIZATION NAME AND ADDRESS Sikorsky Aircraft Division United Technologies Corporation Stratford, Connecticut 06602		10. PROGRAM ELEMENT, PROJECT, TASK AREA & WORK UNIT NUMBERS 63211A 1F263211D157 11 001 EK
11. CONTROLLING OFFICE NAME AND ADDRESS Eustis Directorate, U. S. Army Air Mobility R&D Laboratory Fort Eustis, Virginia 23604		12. REPORT DATE February 1976 13. NUMBER OF PAGES 317
14. MONITORING AGENCY NAME & ADDRESS*(if different from Controlling Office)*		15. SECURITY CLASS. *(of this report)* Unclassified 15a. DECLASSIFICATION/DOWNGRADING SCHEDULE

16. DISTRIBUTION STATEMENT *(of this Report)*

Approved for public release; distribution unlimited.

17. DISTRIBUTION STATEMENT *(of the abstract entered in Block 20, if different from Report)*

18. SUPPLEMENTARY NOTES

19. KEY WORDS *(Continue on reverse side if necessary and identify by block number)*

Helicopter
TRAC Rotor
Variable Diameter
Telescoping Blade
Stowed Rotor
Compound Helicopter
Design Analysis
Performance
Mission Analysis

20. ABSTRACT *(Continue on reverse side if necessary and identify by block number)*

A two-phase analytical investigation was conducted to continue the development and evaluation of the variable-diameter telescoping rotor aircraft (TRAC) rotor system. The first phase was a preliminary design of a full-scale, flightworthy rotor system suitable for subsequent wind tunnel testing in the NASA-Ames 40-by 80-foot wind tunnel and for flight testing on an H-3 helicopter or the NASA/Army Rotor Systems Research Aircraft

DD FORM 1 JAN 73 1473 EDITION OF 1 NOV 65 IS OBSOLETE

Unclassified

SECURITY CLASSIFICATION OF THIS PAGE *(When Data Entered)*

Block 20. Abstract - Continued.

(RSRA). The second phase of the investigation was a comparative parametric analysis to evaluate TRAC rotor compound helicopter and stowed rotor aircraft concepts relative to conventional-rotor pure and compound helicopters.

The preliminary design of the flightworthy rotor indicated no serious unresolved problems. The design represents an improved modification of the basic concept successfully demonstrated in wind tunnel tests of a dynamically-scaled model, and successful full-scale development can be anticipated. The four-bladed, 56-foot-diameter rotor has a lifting capability in hover at 4000 ft 95° F conditions well in excess of 20,000 pounds, and an allowable flight speed in the compound helicopter mode of 300 knots at sea level and 360 knots at altitude. The blade incorporates fully redundant structure for the primary load path, and the diameter-change system incorporates safety devices to prevent inadvertent diameter changes or blade overtravel in case the normal diameter control system should malfunction. The rotor is also designed for stopping and blade folding in flight to demonstrate applicability to the stowed rotor configuration.

The parametric mission analysis phase of the investigation indicates that TRAC rotor aircraft, designed for high cruise speeds, provide distinct performance, operating envelope, and fleet life-cycle cost benefits compared to conventional rotor aircraft. The 400-knot stowed TRAC rotor aircraft shows the greatest potential for high productivity and low fleet costs, followed by the 300-knot full rpm TRAC compound helicopter. These benefits are in addition to special advantages that can derive from high cruise speed, such as increased mission versatility or reduced vulnerability. Aircraft designed for cruise speeds of 250 knots or less generally showed little or no performance cost advantages over the pure helicopter. Despite the high cruise speeds, the fuel consumption of the TRAC rotor aircraft are comparable in magnitude to the lower speed aircraft configurations. A TRAC compound helicopter designed for a cruise speed of 250 knots, or a stowed TRAC rotor aircraft designed for 300 knots, will have lower consumed fuel than will the 175-knot pure helicopter, because of substantially superior overall aircraft lift-drag ratios.

PREFACE

This investigation was conducted for the Eustis Directorate, U.S. Army Air Mobility Research and Development Laboratory, Ft. Eustis, Virginia, under contract DAAJ02-74-C-0048. Technical cognizance for the program was provided by Mr. Patrick A. Cancro.

Mr. Evan A. Fradenburgh was the Sikorsky Task Manager for the overall direction of this program. Messrs. Gordon G. Miller, Edward Hibyan, and Robert Faiz performed the preliminary design of the rotor blades and rotor head. Mr. Lee N. Hager was responsible for the preliminary design of the diameter-change mechanisms. Mr. Neville F. K. Kefford was responsible for the parametric mission analysis phase of the investigation. Mr. Anthony DiPierro was responsible for the development of weight-trending equations. Several other persons contributed substantially to the investigation.

TABLE OF CONTENTS

TABLE OF CONTENTS (CONTINUED)

LIST OF ILLUSTRATIONS

LIST OF TABLES

INTRODUCTION

The use of in-flight variable geometry to benefit aerodynamic performance characteristics in various flight modes has long been standard practice with fixed-wing aircraft. Perhaps the most notable example is the high-lift flap, but there are many other devices, such as variable pitch propellers, variable cowl flaps, speed brakes, jet engine thrust reversers, leading-edge slats, variable sweep wings, and retractable landing gear. Control surfaces are variable geometry devices of a different sort, their primary purpose being to control trim and angular accelerations rather than modify performance characteristics. Yet, except for retractable landing gears, helicopters generally have not used comparable variable geometry devices for control of performance. The helicopter main rotor incorporates collective and cyclic pitch control of the blades, but this variable geometry feature more nearly resembles the control surfaces of an airplane than a performance control device.

In-flight variable geometry features in fixed-wing aircraft provide increased capabilities and improved economy. Higher cruise speed, lower landing speed, longer range, greater maneuverability, reduced fuel consumption, and a smoother ride are all desirable attributes brought about by proper application of variable geometry concepts. While an increase in complexity usually accompanies these benefits, it is not necessarily true that acquisition and maintenance costs increase correspondingly after everything is considered. Unnecessary complexity is certainly undesirable. Historically, however, airplanes and many other products of technology have steadily increased in complexity over the years. The reason is that these complex devices really work, and the resulting increased capability or improved economy permits survival in a competitive environment.

The Sikorsky TRAC is an in-flight variable-diameter rotor system designed to extend the capabilities and to improve the performance of several categories of high-speed rotary-wing aircraft. Development of this rotor system began in 1966 at Sikorsky and has been supported by the Eustis Directorate of the U. S. Army Air Mobility Research and Development Laboratory since 1968.

Wind tunnel tests of a 9-foot-diameter aeroelastically scaled rotor model have demonstrated the feasibility and some of the benefits of the concept. This test program, reported in Reference (1), achieved all major objectives. The rotor was demonstrated successfully in every planned operating regime. Feasibility was established for both the high-speed compound helicopter and the stowed rotor aircraft configuration. The basic blade structural design and retraction system were

verified. Diameter changes were demonstrated at true forward speeds up to 150 knots at full rotational speed; rotor stops and starts at minimum diameter were demonstrated at true forward speeds up to 150 knots; and tests were conducted in the high-speed compound helicopter mode at true forward speeds up to 400 knots. The tests demonstrated many important benefits from the variable diameter capability, including improved performance and reduced vibration, stresses, and gust response. Other potential advantages of the TRAC rotor system have been reported in References (2) - (4).

The present investigation is intended to investigate the characteristics and long-term potential of the TRAC rotor system more thoroughly than past analytical studies have allowed. Two main tasks are included, the first of which is the preliminary design of a full-scale flightworthy rotor system. This rotor is specified to be four-bladed, with an extended diameter of 56 feet, and a lifting capability in hover at 4000 ft, 95°F, of approximately 20,000 pounds. The rotor is appropriate for wind tunnel testing in the NASA-Ames 40-by 80-foot wind tunnel and for flight testing on an H-3 (S-61 series) helicopter or NASA/Army Rotor Systems Research Aircraft (RSRA).

The second major task of the present investigation is to conduct parametric analyses to determine mission requirements for which TRAC rotor aircraft are competitive with other rotor VTOL aircraft configurations, including pure helicopter and compound helicopters with conventional rotor systems. A broad range of design cruise speeds, altitudes, payloads, and ranges are included.

PHASE I: FULL SCALE ROTOR PRELIMINARY DESIGN

GENERAL CONCEPT DESCRIPTION

A schematic arrangement of the TRAC rotor blade is shown in Figure 1. The basic retraction mechanism is a jackscrew which serves as a primary tension member of the blade. Rotation of this screw imparts a linear retraction or extension motion to the retention nut (actually a series of nuts) and, through tension-torsion straps, to the outboard half of the blade, which is the main lifting member. A torque tube, which is a streamlined ellipse in cross section, encloses the jackscrew, transmits blade pitch control motion to the outboard blade, and carries bending moments across the sliding joint. When the rotor diameter is reduced, the outboard blade slides over and encloses the torque tube. The outboard blade, with a full airfoil cross section, comprises the outer half of the radius when the blade is extended. The blade planform is unusual in that the effective root cutout is very large; however, even on a conventional blade the outboard half typically produces 90 percent of the total lift in hover, and the large root cutout produces only a few percent loss in hover efficiency (References 5 and 6). The schematic drawing of Figure 1 does not show a number of important features, including the multiple nut/strap assembly, redundant jackscrew structure, or nut reaction tube. These items are discussed in detail in the following section.

The means for actuating the blade jackscrew is shown schematically in Figure 2. The heart of the mechanism is a differential gear set contained within the rotor head. The differential consists of upper and lower bevel gears and one bevel pinion connected to each blade jackscrew through a universal joint. The universal joint is coincident with the rotor flap and lag hinges (not shown in the schematic). The upper and lower bevel gears are each connected by coaxial shafts to a clutch or brake at the bottom of the transmission. Stopping the lower bevel gear with respect to the fuselage, while the rotor is turning, forces the pinions of the differential to roll around the bevel gear and thus turn the jackscrews and retract the blades. Braking the upper bevel gear reverses the motion and extends the blades. With both clutches released, there is no relative motion and the rotor diameter remains fixed. The basic mechanism is as simple and reliable as an automobile differential. The gears are fully engaged at all times and the blades are completely synchronized. No separate power supply is required, as the system is driven in both directions by rotation of the main shaft. The rotor diameter is under direct control of the pilot and is not influenced by aerodynamic forces or torques. It is mandatory that the clutches be released when the blades reach the limit of extension or retraction. In normal operation the clutches are released electrically by means of limit switches;

however, mechanical safety systems are incorporated in the design to prevent over-retraction or extension in case of failure of the primary system. Figure 2 does not show a number of features, including these mechanical safety systems or a rotor head brake designed to ensure that the diameter change system is self-locking. These items are also discussed in detail in the following section.

DETAILED DESCRIPTION

ROTOR BLADES

A simplified drawing of the major blade components, showing retracted and extended positions and major dimensions, is shown in Figure 3. A blade assembly drawing is shown in Figure 4, and additional details of the root end assembly are shown in Figure 5. The design is basically similar to the previous design concept successfully demonstrated with the dynamically scaled model, reported in Reference 1. A photograph of the model blade components is shown in Figure 6. The physical arrangement and major components of the model and the present full-scale design are the same except that the latter incorporates an additional nut and pair of tension-torsion straps, plus a secondary, internal torque tube (nut reaction tube) designed to react nut torque during blade retractions or extensions, rather than having the outer torque tube carry this load. The model tests demonstrated that the nut torque caused a slight blade twist effect which, in turn, caused a blade flapping response during retraction. If the nut friction were different in the four blades, this difference would also cause the blades to go out of track, causing an increase in vibration level. The nut reaction tube avoids these potential problems by transmitting the nut torque directly to the main spindle in the sleeve/spindle assembly. The nut reaction tube will twist in response to the torsional moment, but an angular clearance ($\pm$ 20° from the mean position) is provided between this tube and the main torque tube so that no torsional contact results. This angular clearance also accommodates the pitch motion of the outer torque tube relative to the nut reaction tube, which is fixed in pitch.

The outer blade spar shown in Figure 4 is design number 2 discussed in the section on the evaluation of various blade spar concepts. This spar and number 6 were the two preferred spar concepts. Because number 2 requires a thicker spar wall dimension than number 6, any structural arrangement that will provide adequate clearances with design 2 will automatically accommodate spar design number 6.

The main load path for the blade, consisting of the jackscrew, nuts, and tension-torsion straps, is fully redundant. The multiple nut/strap arrangement (six nuts and twelve straps) distributes thread loads equally and provides a "fail-safe" arrangement. The hollow jackscrew is also structurally redundant. A central strap, anchored in a low stress area at the root of the screw by means of an integral flange, passes through the length of the screw and is retained by a nut at the tip. This strap is prestressed in tension, putting the screw in compression at zero centrifugal load and reducing the maximum stress in the screw at full centrifugal load. The reduced screw tension will improve the fatigue characteristics of the screw.

Should a fatigue crack occur, the redundant strap will carry the design ultimate load. To detect a crack in the screw, the screw is pressurized in the same manner as utilized in the Sikorsky BIM crack-detection system on the spars of conventional rotor blades. A crack through the jackscrew wall would allow the pressurized air to leak out, and the resulting drop in pressure will activate a pressure switch to warn the pilot and to deactivate the diameter-control system. The redundant strap and retaining nut serve to maintain pressure seals at the two ends of the screw.

The outboard end of the jackscrew is centered relative to the torque tube and the nut reaction tube by means of two bearings mounted on the tip of the redundant strap. One bearing housing is anchored to the torque tube and the other to the nut reaction tube. These bearings have been configured to retain any failed component that might otherwise be thrown out through the blade by centrifugal action and cause additional damage. Any of four major components - the jackscrew, redundant strap, nut reaction tube, and the torque tube - could conceivably fail due to fatigue, but would be retained by means of the tip bearing arrangement. It should be noted that if the redundant strap inside the jackscrew should fail, the portion outboard of the fracture will translate toward the tip a fraction of an inch so that the rubber seal at the tip of the jackscrew will fail and the jackscrew pressurization will be lost. Thus the pressurization serves to monitor the integrity of the redundant strap as well as that of the jackscrew.

The jackscrew has a double thread (sometimes referred to as a "two-start" thread) because the resulting increased thread pitch angle increases screw efficiency. It has a left-hand thread because this makes the outer shaft of the two coaxial diameter-change shafts (inside the main rotor shaft) serve the function of the retraction shaft. Because blade retraction corresponds to larger mechanical torques than does blade extension, it is desirable to make the outer shaft the retraction shaft. The jackscrew has a buttress-type thread profile, with the thread thickness less than the space between threads. This design minimizes the volume and therefore the weight penalty of the threads and also permits considerably greater thickness on the nut threads, which are fabricated from lower strength materials and which are subjected to greater wear rates.

There are six nuts, individually supported by a pair of tension-torsion straps, that transfer the centrifugal force from the 12 straps to the jackscrew. Nut number 1, closest to the rotor head, has one pair of holes, counterbored to retain its pair of straps. These straps pass freely through holes provided in the other five nuts. Nut number 2 has two pairs of holes, one pair of which is to retain its own pair of straps and one pair of which is to allow straps from nut 1 to pass through. The same

principle applies to all nuts, and nut number 6, closest to the blade tip, has six pairs of holes. The two retention straps for each nut are always diametrically opposite each other to avoid any moment transfer from the straps to the nuts.

The reason for the multiple nut/strap configuration, which is similar to that used on the dynamic model blade, is to provide structural redundancy in case of failure of any component and also to improve the thread loading distribution. If a single nut were to be provided with a large number of threads, only a few threads on each end would actually carry a significant loading because of elastic deformations which occur in both screw and nut. The threads in the middle would not carry much load. This would lead to overloading of the few end threads and excessive wear or progressive static failure. The problem is avoided by dividing the nut into a number of pieces with fewer threads each. The strap geometry ensures that each nut carries a full share of the load because the elastic stretch of the strap under load is large compared to intial errors in providing exactly correct strap lengths, particularly when the straps are "tuned" on the bench, i.e., the assembly loaded to part load and strap length adjusted as necessary to provide equal tension.

The blade incorporates the necessary features to provide these adjustments. The twelve tension-torsion straps are threaded at the tip and anchored into a drilled and tapped anchor block. The six nuts, twelve straps, and the anchor block constitute a subassembly which, by means of a bench installation on a jack-screw, can be adjusted for equal load sharing. Cylindrical lock nuts are then installed and the anchor block is bolted to the blade tip block when the blade assembly is completed. Lock plates, fitting over the squared ends of the tension-torsion straps, are then installed to be certain that the straps cannot turn in the anchor block.

The drawing of the six nuts shown in Figure 4 assumes that thread inserts will be used. In a materials evaluation test conducted under another Army contract, Reference (7), carbon-graphite proved to be a highly desirable nut material in several respects, including low friction and low wear rates at contact pressures and sliding velocities representative of the full scale TRAC blade application. However, the material strength is relatively low, and it would not be suitable as a material for a one-piece nut. Thus an insert of carbon graphite is shown, retained by a flange on the inboard end of the nut shell, which is fabricated from titanium. A safety thread of beryllium copper is also assumed. This thread does not normally touch the screw threads, but provides a backup in case of excessive wear or failure of the carbon graphite threads. The beryllium copper, which has excellent strength and was the second best of the various nut materials evaluated in the tests mentioned above, also provides the sliding contact with the inside of the

nut reaction tube, which fits closely around the nuts. Beryllium copper, used successfully in the model rotor tests, is also a candidate as the primary nut material. If this material is selected, no inserts or backup threads will be required; each nut will be a single piece.

The blade tip block is used to support the outboard blade spar, the tension-torsion strap anchor block, tip balance weights, and the tip cap. The tip balance weights are similar to standard Sikorsky blade balancing practice and permit adjustment of both span and chordwise moment balance. In addition to the tip balance weights there are additional balance weights provided at the root end of the outboard blade spar. This is to permit adjustment of outboard blade weight in addition to span balance. Conventional blades do not need to weigh exactly the same in a given rotor; as long as the span balance is the same, the centrifugal force will be the same. In the TRAC blade, however, the outboard blade moves during diameter change, and the weight of the moving portion must be the same on each blade of the rotor, or else the span moment will change by different amounts for different blades, and the rotor will go out of balance.

The bearing slide blocks for the blades are also similar to those used on the model. The material assumed is Nylatron GS, a molybdenum-disulfide filled nylon, which was entirely satisfactory on the model. Friction and wear properties are good, it is relatively lightweight, and its elasticity will accommodate minor dimensional variations that might occur along the length of the spar or torque tube.

The TRAC blade is retained at the root end by the sleeve/spindle assembly. The primary load path is through the jackscrew, retained by the jackscrew retention spindle and one set of angular-contact ball bearings. The nut reaction tube is bolted directly to the blade main spindle, and the torque tube is bolted to an aluminum cuff which is integral with the outer housing of the sleeve/spindle assembly and which is retained by a second set of angular-contact ball bearings. Additional details of the sleeve/spindle assembly are discussed in the following section.

ROTOR HEAD

Hub Plates

The rotor hub, shown in the rotor head assembly drawing (Figure 7), follows the classic Sikorsky two-plate design. The lower hub plate is splined to the main rotor shaft and is retained with a pair of split-cone members and a mast nut, which is locked and safetied to the main shaft. This retention system is identical in principle to most other Sikorsky main rotor hub designs. The lower hub plate transmits all of the vertical forces from the

rotor blades to the shaft. The four arms of this hub plate have "inverted omega" cross sections for high bending stiffness and light weight. The upper and lower hub plates share the centrifugal and tangential (torque) forces equally. The upper plate, which is essentially a flat ring with four radial arms, is fastened to the lower plate at the center of the hub through the differential gear housing.

Hinges

The four hinge members or hinge crosses are mounted between the upper and lower hub plates, and the flap and lag bearings are mounted on these hinge members. These bearings are identical to those used in the CH-53 series helicopters for the same purpose. These bearings were used because they have the desired load capacity and are readily available. The design of these hinge members differs from most designs in that the flapping bearings are mounted with a wider than normal separation. This permits a central hole in the hinge cross to accommodate the jackscrew drive shaft and the universal joint, which is coincident with the flap and lag axes. The hole in the hinge member is shaped to permit a blade lag or lead angle of up to 45 degrees, thus permitting the blade to be folded parallel to the fuselage when the rotor head arms are 45 degrees from the aircraft longitudinal axis. (See section on lag damper/fold actuator.)

Sleeve/Spindle Assembly

The flapping yoke is a three-piece member which connects the flapping bearings to the blade spindle through a bolted flange plate for ease of blade removal. The sleeve/spindle assembly contains two concentric sets of angular-contact ball bearings. The inner set, which uses the S-61 (H-3) series helicopter pitch-change bearings (except that only five bearings are used instead of seven), retains the jackscrew and carries the major portion of the centrifugal load. During a diameter change, these bearings rotate continuously, but at no time do they experience any cyclic feathering motion. The outer set of bearings accommodates collective and cyclic feathering motions. These bearings carry only a small fraction of the centrifugal load because they retain only the outer torque tube of the blade. Because the highly-loaded bearing experiences no cyclic motion and the cyclic-motion bearing carries only a small centrifugal load, each bearing can be considerably smaller and lighter than would be required if it had to carry both high load and cyclic motion. Analysis of these bearings indicate that a 1000-hour B-10 bearing life can be attained using grease as a lubricant. Oil lubrication is superior for bearing life, but grease lubrication is easier and less expensive for experimental, demonstration hardware.

The blade main spindle is the cylindrical member between the two concentric sets of ball bearings. This member is bolted directly to the flapping yoke, and all blade forces pass through it. The two sets of ball bearings are supported by this spindle, and the nut reaction tube (inner torque tube) is bolted directly to it.

A centrifugally operated flapping lock (labeled "anti-flap/droop stop" in Figure 7) is located inside the flapping yoke. This is a cylindrical member with an external taper that is spring loaded to contact a mating internal surface in the hinge cross. At rpm values above 50 percent of normal, the spring is compressed by centrifugal force to unlock the hinge. When rpm is decreased, the locking member automatically returns to the locked position. The taper provides a self-centering action so that it is not necessary to have the flapping angle at exactly zero degrees in order to function.

A conventional pitch horn is bolted to the outermost sleeve of the sleeve/spindle assembly. A "delta-three" angle of 30 degrees provides a pitch-to-flap coupling ratio of -0.577 (one degree of up flapping produces .577 degrees of down pitch angle). The delta-three hinge provides additional flapping stability and reduces control sensitivity at high rotor advance ratios. The hinge geometry is similar to that utilized in the TRAC model tests of Reference 1, except that the delta-three angle of the model rotor head was 26.5 degrees.

Lag Damper - Blade Fold Actuator

In the present design study the TRAC rotor is fully articulated and thus requires damping about the lag hinge to avoid potential ground resonance difficulties. In this respect it is no different than conventional articulated rotors. The TRAC rotor utilizes a linear, hydraulic damper in accordance with Sikorsky standard practice. In most Sikorsky main rotor designs the lag damper is located in the plane of the blades, between the upper and lower plates in the two-plate hub designs. Because of the differential gear package and jackscrew drive members located at the center of the TRAC rotor hub, it was not possible to locate the dampers in this conventional manner. Instead, the dampers are located below the lower hub plate as shown in Figure 7. A plan view in the plane of the dampers is shown in Figure 8. The housing of the damper is held by a trunion arrangement supported by a flange on the main rotor shaft. The piston rod is connected by conventional bearings to a horn or crank member which is splined to an extension of the vertical lag hinge member. Thus an angular motion of the blade about the lag hinge is transformed to an axial displacement of the damper piston.

If the rotor were designed for operation only in the extended blade mode and high-speed compound mode (blades retracted but still rotating), the damper would be entirely conventional, consisting of housing, piston with relief valves and orifices, and an external reservoir with differential check valve to accommodate the changing volume of fluid within the damper as the piston is displaced. This configuration is the one shown in Figure 8. In the present design study, the rotor is intended to demonstrate in-flight stopping and blade folding in addition to the other flight modes. Because the folding motion uses the lag hinge rather than a special folding hinge, it becomes possible to combine the lag damping and fold actuation functions in a single unit and to save weight relative to separate units for the two functions.

The folded positions of the blades are shown in Figure 9. This drawing assumes separate actuator cylinders on top of the rotor head rather than combined damper/actuator units, but the fold angles are the same. After rotor stopping but prior to blade folding, the rotor head is indexed so that the hub arms are 45 degrees to the aircraft longitudinal axis. There are two positions around the azimuth that will provide the desired fold positions; the rotor head is indexed by means of a small auxiliary drive unit clutched into the tail rotor drive shaft, with a detent to stop the head in the correct position. Rotor head indexing is a feature found on several Sikorsky helicopters having an automatic blade fold capability.

Two blades are folded forward and two folded aft, so that all four blades are parallel to the aircraft longitudinal axis. In an actual stowed rotor aircraft design there would be additional mechanisms for blade stowing (see description of possible systems in the mission studies portion of this report), but in the present preliminary design study only rotor stopping and blade folding are provided.

While the blades are being folded the rotating control rods remain connected to both the blade pitch horns and the swashplate. The pitch-lag coupling, which is designed to be essentially zero for in-flight lag motions, becomes significant for large lead or lag motions. This effect is utilized in providing blade pitch inclination in the folded positions and provides interblade clearance, allowing the blades to "nest" in a nose-down pitch attitude after initiating the blade fold cycle at zero pitch.

An integrated damper/actuator unit was investigated and is shown in Figure 10. It is actually a coaxial unit, with a damper system on the outside that is operationally independent of the fold actuator on the inside. The damper system is an entirely conventional hydraulic lag damper which provides a damping force whenever there is motion of the piston within the cylinder. The only unique feature of the damper is the fact the damper piston

rod is the housing of the coaxial hydraulic actuator. The piston of this actuator is contained within the damper piston rod. This piston is integral with its piston rod, which is connected to and is actually a part of the base of the damper housing. Thus the location of the actuator piston is fixed relative to the damper housing. Drilled holes through the actuator piston rod permit two oil lines to be connected to form fluid paths to either side of the piston.

A third small floating piston is at the very center of the unit to serve the purpose of providing a mechanical lock when the desired blade fold position is reached. It accomplishes this by means of chamfered surfaces which displace three lock dogs (equally spaced around the periphery) into the recessed groove provided on the inside surface of the damper piston rod. This floating piston and lock dog arrangement does not represent new or unusual technology; similar devices have been utilized in many applications, including use by Sikorsky Aircraft in landing gear retraction and tail rotor pylon folding systems.

Other components of the system include a follower arm and a spring-load roller and check valve system as shown in Figure 10. The spring on the roller exerts a force in the direction to hold the roller away from the follower arm. The system also includes a rotary fluid coupling (fluid slipring), at the bottom of the transmission, and a safety valve, shutoff valve, and a directional control valve, all located within the aircraft fuselage at a convenient point between the fluid slipring and the hydraulic pressure supply.

The operations of the system is described below:

1. Damping Mode

The rotor turns at full or reduced rpm and the blades are fully articulated. Damping is provided in a conventional manner by orifices and relief valves in the damper piston. Variable volume within the damper housing due to piston displacement is accommodated by the differential check valve and the external fluid reservoir. The hydraulic fluid in the actuator is free to move back and forth in a circuit which includes lines down the center of the rotor shaft, the fluid sliprings, the shutoff valves (in the unpowered, open condition), the directional control valves, where the two lines are vented together, and also to the hydraulic system reservoir through the "return" line. During damping motion, oil is pumped back and forth at low pressure through this circuit, with the reservoir serving to accommodate the changing fluid volume within the actuator cylinder.

2. Locking the Lag Motion for Rotor Stopping

During the rotor stopping mode, the hinges must be locked at speeds below approximately 50% rpm to prevent excessive blade motions. The flapping motion is locked automatically by a centrifugally-actuated spring device previously described. The lag motion is locked hydraulically, either manually by the pilot or by an rpm-sensitive switch. The hydraulic lock is effected simply by closing the shutoff valve in the circuit, preventing any fluid flow in either line. Because an axial motion of the damper/actuator assembly would require a change in fluid volume within the actuator cylinder, a hydraulic lock results whenever the shutoff valve is closed and the blade will stay in whatever position it was in just prior to the closing of the valve. Normally this position will be close to zero lag angle. Although leakage could allow very slow movement over a period of many minutes, the hydraulic lock is adequate for the short period required to stop the rotor.

3. Blade Folding

After the rotor is stopped and indexed to the proper overall azimuth position, the pilot activates the fold command, which affects all three valve units. The safety valve is energized, so that high pressure hydraulic fluid reaches the manifold which contains the other two valves. The directional control valve is energized to direct the high pressure fluid to the lower fluid line shown in Figure 10 and to connect the other line to the return (reservoir). The shutoff valve is de-energized to open both lines. This combination of events directs the high pressure supply to the line marked "Fold" in Figure 10 and vents the "Spread" line to the reservoir. Hydraulic oil flows through the "Fold" line, through the check valve assembly (the check valve is held open by the compression spring) and into the actuator cylinder, where the high pressure forces the damper piston to move to the left relative to the actuator piston, in turn forcing the blade to lag in the desired direction for the fold position. This motion continues until the blade is in the full 45° fold position, where the piston bottoms against the end of the cylinder. In this position the locking dogs are free to translate radially outward into the recess in the cylinder wall, and the floating piston, driven by its compression spring, drives the dogs into the recess. The motion of the floating piston actuates an electrical microswitch which tells the pilot that the blade is locked. When all four blades have been confirmed to be locked, the pilot disconnects the hydraulic pressure from the circuit and the blades remain positively locked by purely mechanical means, with no time limit.

4. Blade Unfolding

When the pilot wishes to unfold the blades, the "Spread" command affects three valves as before, except that the directional control valve connects the high pressure to the "Spread" line and the "Fold" line is connected to the return. High pressure oil flows to the check valve assembly. This pressure is vented to the chamber above the small piston in this assembly, and this pressure would overpower the compression spring and close the two check valves, except that the roller, in contact with the right end of the follower arm (not as shown in Figure 10) prevents such motion. Thus, the oil flows through the check valve assembly and into the actuator, where it is directed through the piston to the right side of the cylinder. The high pressure on the right side of the piston first forces the floating piston to the left, against its compression spring, thus unlocking the lock dogs. Then the pressure serves to force the damper piston rod to the right, and the lock dogs are displaced radially inward to their original position by the chamfered surface on the lock dogs and the recess. The actuator motion continues, with blades moving in the desired direction, until the curved recess in the follower arm allows the roller in the check valve assembly to drop down and shut off the oil flow. The high pressure oil then serves to keep the check valves closed and a hydraulic lock situation is again present, preventing the blade from moving. It is difficult to ensure that all four blades will fold or unfold at exactly the same rate, and so the follower arm/roller/check valve system is provided to stop each blade individually when it gets to the desired position (nominally 0° lag). Microswitches can be included to provide the pilot with a positive signal that the Spread cycle is completed as desired.

5. Unlocking the Lag Motion After Starting Rotation

The hydraulic lock is held automatically with the blades at 0° lag as long as the pressure is connected to the spread line. After the rotor is started and the desired rotational speed reached, the pilot unlocks the lag motion by disconnecting the pressure from the system via the directional control and safety valves. The compression spring in the check valve assembly returns the check valves to the open position, and the system is back in the damping mode described in paragraph 1 above.

It should be noted that the damper/actuator unit shown in Figure 10 folds the blade in the lag direction. Two of these units, for diametrically opposite blades, are required. The units for the other two blades are similar except that the actuator is configured to fold the blades in the lead direction instead.

This requirement is the same whether separate or integrated damper and fold actuator units are utilized.

DIAMETER CHANGE SYSTEM

The diameter change system, excluding the blades themselves, is shown in Figure 11. It is comprised of the differential gear assembly in the rotor head, coaxial shafts, clutches or brakes below the transmission, a friction brake on top of the rotor head, mechanical locking and safety devices, and a diameter measurement and control system.

Differential Assembly

The differential assembly, shown in Figures 7 and 11, is located within the main rotor center housing between the upper and lower hub plates. It is of a standard spiral bevel type having two input bevel gears and four output pinions. Gear ratio (pinion rpm/bevel rpm) is 3:2. The blade retraction input bevel gear utilizes the upper end of the main rotor shaft as its bearing support housing. A top cover plate mounted on the upper hub plate provides access to the internal portion of the rotor hub and differential assembly and also is the bearing support housing for the blade extension input bevel gear. The center housing provides the support and bearing housings for the four output pinions. The output pinions are lock-spline connected to their respective output shaft and universal assemblies. The output shafts are loose-spline connected to the blade jackscrew at the blade root.

Design investigation included the possibility of using standard straight bevel gears since the operation is bidirectional. However, analysis of operating loads showed that a spiral bevel gear arrangement with a pressure angle of 20° and spiral angle of 25° is preferred. The gear loads and load direction are significantly changed to permit use of much smaller bearing sizes.

The differential is designed so that complete disassembly of the differential may be made on the aircraft after blade removal has been accomplished.

Main Rotor Internal Shafting

Located within the S-61 main rotor shaft are three concentric shafts, as shown in Figures 11 and 12. The two outer shafts, each connected to one of the two input bevel gears of the differential, are a direct part of the diameter-change mechanism. They extend down from the differential assembly through the main rotor shaft to the base of the transmission where each terminates at a clutch disc. The shafts are supported at the upper

end by their respective bevel gear bearings. These bearings each consist of a pair of tapered roller bearings. The lower end of each shaft is supported radially by a needle bearing which reacts the clutch input torque loads. The outermost shaft of these two (just inside the main rotor drive shaft) is the retraction shaft; the inner shaft is the extension shaft).

The third (innermost) shaft is constrained to rotate with the rotor head and main shaft and provides three functions: (1) The shaft moves vertically and provides the normal mechanical means of operating the blade position lock. (2) The shaft moves vertically and operates the mechanical blade overtravel safety limit stop. (3) The shaft, which is a hollow tube, provides the passageway for blade-fold hydraulic lines and electrical instrumentation wires. The lower end of the shaft is equipped with both hydraulic and electrical sliprings. The shaft is supported by and actuated through a thrust bearing and connecting linkage to a lock-actuating cylinder.

Clutch Control System

Two clutch calipers are mounted in "piggy-back" fashion to a common mounting bracket attached to the lower transmission housing. The calipers are of standard disc brake type modified for the special mounting configuration and for use in a horizontal position, which includes relocation of input supply ports and bleed ports. The calipers are sized for operating static torque loads since the actual kinetic energy dissipation is negligible. System hydraulic supply pressures are obtained from the aircraft main hydraulic system. Each actuating clutch requires a different operating pressure, because of the specific torque load requirements, obtained through pressure regulators. A pressure of 2200 psi is required for the retraction clutch and a pressure of 650 psi is required for the extension clutch.

A schematic drawing of the clutch control system is shown in Figure 13. A three-position switch in the cockpit commands retract or extend operation, with a self-centering spring for the neutral or stop position (constant diameter operation). This switch controls the two solenoid valves shown on the right side of Figure 13, which direct the hydraulic oil through bypass valves to the retraction or extension clutch as appropriate.

Two solenoid-operated bypass valves provide automatic cutoff of the clutch hydraulic pressure when the blades are at their normal limit of travel. The diameter measurement system, described in a following section, actuates limit switches which control these valves. Thus, even if the pilot continues to command a diameter change after the normal blade travel limit is reached, the clutch will disengage at the proper point.

To provide for malfunction of either the bypass solenoid valves or the diameter measurement system, a mechanically controlled bypass valve is also incorporated. A traveling nut safety device, described in a following section, moves the instrumentation/lock shaft vertically downward in case the blades extend or retract beyond normal limits. Before physical limits in the blades are exceeded, the shaft motion, through a mechanical connection (shown schematically in Figure 13), will dump the clutch hydraulic pressures by means of this bypass valve.

Another function of the mechanically operated bypass valve is to ensure that the clutches will not operate inadvertently when the rotor diameter lock is engaged. The pilot must disengage this lock, by means of another switch which connects with the lock-control solenoid valve. The instrumentation/lock shaft must translate far enough to disengage the diameter lock mechanism on the rotor head before the bypass valves can be actuated to permit hydraulic pressure to reach the clutch calipers.

Rotor Diameter Indication

Located at the base of the transmission assembly between the two clutch discs is a miniature gear differential that is part of the mechanical system to measure and control rotor diameter (Figure 11). The differential senses relative motion of the retraction and extension shafts. During constant rotor diameter operation the two shafts rotate in unison at main rotor shaft speed but during a diameter change there is relative motion between the shafts. The miniature differential is geared to the two shafts by means of small ring gears located between the two clutch discs. One of these gears meshes directly with one of the spur gear inputs on the miniature differential, and the other is connected to the other gear input through an idler gear to reverse the direction. In this manner the centerbody of the differential does not rotate during constant rotor diameter operation, but does rotate during a rotor diameter change. The rotation of the differential centerbody, which is the output function which averages the two input rotations, is in one direction during a diameter decrease and in the opposite direction during a diameter increase. The number of turns of the centerbody is in direct relationship to the relative angular displacements of the two shafts.

The output (differential centerbody rotation) is mechanically geared to a multiple-turn potentiometer used for cockpit display of rotor diameter. The differential output also operates a miniature jackscrew with a traveling nut used to operate minimum and maximum rotor diameter limit switches, that are part of the clutch control system.

The diameter measurement and control system is identical in basic concept to the system utilized in the TRAC dynamic model tests, Reference 1. The model system was not equipped with the redundant safety features provided in the present design, but it functioned exactly as desired during the test program.

Rotor Head Friction Brake

An auxiliary friction device is incorporated on top of the rotor head to permit control of the overall mechanical efficiency of the retraction system. A disc brake is utilized, as shown in Figures 11, 12, and 14, with spring-loaded calipers. The brake disc is loose spline-connected to the extension shaft and thus, geared to the rotor head differential gear set. The disc also functions as part of the diameter lock system, described in the following section. The reason for adding friction is to avoid the possibility of an inadvertent, self-actuated diameter increase due to centrifugal force, when the lock system is disengaged. An overall system efficiency of slightly below 50 percent is desired, because any value less than 50 percent is desired, because any value less than 50 percent makes the system self-locking, a highly desirable attribute. The efficiency of the jackscrew in the blade will be higher than 50 percent in most cases, so the external brake is incorporated to add friction without contributing to heating or wear of the blade components. Another reason for desiring approximately 50 percent efficiency is that this value dissipates rotational kinetic energy at just the right rate to permit diameter reduction without a tendency to either increase or decrease rotational speed.

The brake disc is of conventional type. It is slotted for control of distortion due to heat generated during a diameter change. It should be noted that the brake functions only during a diameter change, which takes approximately 36 seconds for full travel at full rotor rpm. At all other times there is no relative motion between the brake disc and the rotor head.

A rotor head friction brake of similar basic concept was incorporated on the wind tunnel model of the TRAC rotor (Reference 1). This system performed as desired during the tests.

Diameter Lock System

The rotor diameter lock, shown in Figures 11, 12, and 14, is mounted on top of the rotor head and consists of two locking pawls and associated support brackets, over-center springs and connecting linkages. The friction brake disc is a common part to both the lock mechanism and the rotor head friction brake. Special slots located on the periphery of the disc mate with the locking pawls to prevent relative motion between the rotor head and the diameter change mechanism, mechanically locking the diameter at a constant value as long as the pawls remain engaged. Six equally-spaced slots (located midway between the

longer but narrower distortion-control slots) permit engagement of the lock at increments of 60 degrees of rotation. With the 3:2 gear ratio of the rotor head differential, this corresponds to 90-degree rotation increments of the pinions and the jackscrews. This in turn permits the universal joints in the jackscrew drive shafts to be oriented correctly, with one of the hinge axes vertical, facilitating the 45-degree fold angle about the lag hinge, required in the blade fold operation.

During normal operations the lock pawls are operated by vertical motion of the instrumentation/lock shaft, through the linkage on top of the rotor head. Raising the shaft fully releases the pawls from engagement with the slots in the disc and places the pawls in an 8-degree over-center position, where they stay during diameter change operations. When it is desired to reengage the lock, lowering the shaft brings the pawls back into contact with the disc. Usually the slots will not be in correct alignment initially, and the shaft will not move to the full down position. However, with a momentary diameter change command from the pilot, the desired alignment will take place and the pawls will snap into place by action of the over-center spring arrangement and circular arc slots provided in the locking pawls. The shaft will translate to the full down position and actuate a position switch to notify the pilot of a fully-locked condition. It should be noted that an override spring in series with the lock-actuating cylinder (Figure 13) permits the piston to travel the full distance required even when the shaft has not yet moved fully down. Another position switch, on the actuator, permits the pilot to verify that the lock command has been executed by the actuator even though the locking pawls might not have engaged.

Over-Travel Safety Stop System

A mechanical safety system has been incorporated in the design to provide automatic locking and shutoff of clutch hydraulic pressure if, for any reasons, the normal system fails to function properly. The heart of this safety system is a traveling nut located between the instrumentation/lock shaft and the extension shaft, as shown in Figures 11 and 12. The extension shaft is internally threaded (double thread, right hand) and the instrumentation/lock shaft is externally splined. The traveling nut is threaded externally and splined internally to mate loosely with the two shafts.

During constant rotor diameter operation there is no relative motion between the coaxial shafts, but during a diameter change a relative rotation occurs. The traveling nut is constrained by the spline to rotate with the instrumentation/lock shaft, and, because of the threaded interface with the extension shaft, it is constrained to translate axially, with the direction dependent on whether the rotor diameter is increasing or decreasing. A diameter increase causes the nut to travel upward,

and a diameter decrease results in the nut traveling downward. Before the rotor blades encounter physical limits to diameter change, the traveling nut reaches limits built into the diameter change mechanism. During a blade retraction overtravel the nut, translating downward, directly contacts a shoulder near the bottom of the lock/instrumentation shaft (Figure 12), forcing the shaft to move downward and engaging the lock system. Because of the override springs between the actuating arm and the lock actuating cylinder (Figure 13), the actuating arm will displace and cut off clutch hydraulic pressure in the normal fashion even if the lock actuating cylinder is in the full unlock position.

During a blade extension overtravel the traveling nut reaches the top of the rotor head and contacts a flanged sleeve which is loose-splined to the lock/instrumentation shaft (Figure 12). This flanged sleeve is mechanically connected through linkages to the shaft cross beam at the very top of the lock/instrumentation shaft in such a manner as to force the shaft to translate downward. Just as in the case of blade retraction overtravel, the locks then engage and the clutch hydraulic pressure is cut off.

It should be noted that during operation of this safety stop system, the brake disc may be rotating at full rpm relative to the rotor head. To allow the locking pawls to engage under these conditions, accelerating ramps are built into the disc (Figure 14) to allow the pawls to have an appreciable radial velocity when proper alignment occurs. The over-center springs are stiff enough and the pawls light enough to permit the pawls to engage even at full relative rpm. Fortunately, the angular momentum of the entire retraction system is quite small so that there is no shock load difficulty.

Once the overtravel safety stop system has engaged, subsequent disengagement in flight is not possible with the system as designed. It is entirely feasible to incorporate a special electric or hydraulic actuator on the rotor head to retract the pawls from the brake disc, thus freeing the system to revert to normal operation in flight. For an experimental demonstration rotor system, however, this was not felt to be required. If the rotor becomes locked at minimum diameter by the safety stop following a system malfunction, a fixed-wing type landing would be required, an operation for which the RSRA test vehicle has been designed. Unlocking the system and returning it to the normal operating condition would then be a ground maintenance item.

BIM Detection System

Located within the inboard end of the redundant strap is a BIM switch for monitoring the condition of the jackscrew at all

times. The pressurized portion of the jackscrew is ported through the head of the redundant strap to a pressure switch. The switch is normally held in a closed circuit condition by the pressure. The signal from this detector passes through two sets of electrical sliprings. One is located on the differential pinion output shaft and the second is the slipring below the main transmission. The control is such that a pressure drop in the jackscrew or an open circuit anywhere in the detection system renders the extension-retraction mechanism inoperative. If a blade jackscrew should fail, the redundant strap will carry the full centrifugal load, but it probably would not be possible to change diameter safely. The BIM system safety circuit will prevent a diameter change if the jackscrew develops a crack large enough to let the pressure bleed out.

Lubrication

Differential Gear Assembly

The center portion of the main rotor hub is designed to serve as an oil reservoir. All shaft and gear hub penetrations are sealed using standard type lip seals for oil retention and foreign matter exclusion. The output pinions and the retraction shaft tapered roller bearings are oil-lubricated. The extension shaft input bevel gear bearings are grease-lubricated.

Lower Shaft Bearing

The lower extension and retraction shaft needle bearings are grease lubricated and sealed.

Miniature Differential Assembly

The miniature differential bearings and support bracket idler bearings are prelubed and sealed.

Lock Shaft

The lock shaft actuation thrust bearing is prelubed and sealed.

Universal Joint

Jackshaft universal joints are grease-lubricated.

Lock Mechanism

All lock mechanism linkages and joints are dry film lubricated. The dry film lubricant has been selected because of the presence of friction-brake-lining dust in the area of the lock mechanisms, as well as normal airborne dust

and abrasive particles.

Mechanism Teardown and Inspection

The entire design of the blade retraction-extension system was developed for ease of assembly and disassembly. All shafts are removable from the top of the rotor head. The extension shaft and the lock/instrumentation shaft are easily removed for inspection of the traveling nut. All connections to shaft ends are through spline connections. The top of the rotor hub has a cover that serves also as the extension bevel gear bearing housing that can be removed for differential gear inspection.

Clutch calipers, clutch disc, miniature differential, lock actuating mechanism and control hydraulics are all external and located at the base of the transmission.

DESIGN ANALYSIS

PERFORMANCE AND SIZING

In accordance with the contract, the TRAC rotor should have a steady-state design lift capability in hover at 4000 ft, 95° F, of approximately 20,000 pounds. The criterion selected for the analysis was a rotor lift of 21,000 pounds, to provide a net lifting capability of 20,000 pounds with an airframe vertical drag allowance of 5 percent.

A diameter of 56 ft was tentatively selected as appropriate for the design requirements. An outer blade chord of 28 in. was also selected to provide a blade aspect ratio identical to that of the previous preliminary design study and the dynamic model reported in USAAVLABS Technical Report 73-32, Reference 1, because of the requirement to not deviate substantially from this successful baseline design. These dimensions provide a useful blade area ($b\bar{c}R$, where b is the number of blades, $\bar{c}$ is the thrust-weighted mean chord, and R is the extended radius) approximately the same as for the standard H-3 rotor system, which has a useful lifting capacity of 20,000 pounds or somewhat more, depending on the mission.

A comparison between the TRAC rotor and other Sikorsky rotor systems in the same general size category is shown in Table 1. It can be seen that in most respects the TRAC rotor has dimensional and blade loading parameters which are typical of other helicopter systems. The important parameter of dimensionless blade loading, C_T/σ, is essentially the same as for the H-3 and H-34 aircraft. The Sikorsky YUH-60A UTTAS is a higher performance pure helicopter than the other two and for this reason uses lower values of C_T/σ. Because the TRAC rotor will be used in aircraft configurations having wings and auxiliary propulsion systems, it is not necessary to utilize low C_T/σ values to achieve high speeds. In fact, in the mission studies comparisons described in the second major section of this report, all configurations with wings and auxiliary propulsion systems are assumed to operate at hover C_T/σ values of 0.12, substantially above the value selected for the flightworthy demonstration rotor. Thus, the present design is conservatively sized for a 20,000-pound lift capability. Rotor thrust at the normal design tip speed at 4000 ft, 95° F, for a C_T/σ values of 0.12, is over 24,000 pounds.

Table 1 indicates that the TRAC rotor utilizes a lower aspect ratio blade than do the conventional systems because of the fact that the outer blade half is in compression rather than tension, and the lower aspect ratio is needed to keep well clear of the compression buckling condition. Disc loading of the TRAC rotor is somewhat higher than for the comparison helicopters, but studies of compound helicopters or stowed rotor configurations have generally shown that optimum disc loadings are higher than for pure helicopters, and the value shown for TRAC is in line with this general trend. The mission analysis comparison studies described elsewhere in this report also confirm this trend.

Calculations of hover performance were made to verify the lifting capacity of the TRAC rotor. The calculation procedure used was the Sikorsky circulation - coupled wake program which utilizes a prescribed rotor vortex wake geometry which is based on the spanwise rotor load distribution and which generally agrees with experimental rotor performance to within $\pm$ 2 percent of thrust. Correlation of this method was conducted with the experimental results reported in References 5 and 6 to verify that the method would give reliable results for different twist values and high root cutout values. Generally good correlation results were obtained. The calculations confirmed that the assumed TRAC rotor geometry would provide the desired lift capacity in hover without encountering blade stall.

Forward flight performance calculations were also made, utilizing the Sikorsky Skewed Flow/Generalized Rotor Performance Method, for flight speeds in the range of 40 to 140 knots. For speeds below 40 knots, the results were faired into the hover power requirement. Results of these calculations are shown in Figures 15 and 16 for sea level standard and 4000 ft, 95° F operating conditions respectively. Rotor lift is held constant at 21,000 pounds and rotor propulsive force corresponds to an airframe parasite area of 20 ft^2. Curves are shown for blade twist values of 0° and -8° and for tip speeds of 100% normal (tip speed 660 ft/sec) and 105%. At sea level standard conditions, no significant blade stall is encountered at speeds up to 100 knots at any condition (blade stall parameter $\frac{b\ C_{Qd}}{\sigma}$ as defined in Reference 8). At the 4000 ft, 95°F condition (Figure 16), the 100% rpm, zero twist blade case is severely stalled at forward speeds above 60 knots. However, by the simple expedient of increasing rotor rpm by 5 percent (within the usual engine rpm control range) the stall is alleviated sufficiently to allow an increase in flight speed of approximately 40 knots for any degree of stall. Use of blade twist also alleviates stall and reduces power requirements throughout the speed range. One of the design criteria assumed for the TRAC rotor was that it should

be able to operate as a pure helicopter up to at least 100 knots forward speed. Although this capability is not absolutely required because of the presence of a wing and auxiliary propulsion system on all TRAC rotor configurations under consideration in this program, the operational flexibility afforded by such a capability is judged highly desirable. This criterion is barely met for the untwisted blade twist at 105% rpm at 4000 ft, 95° F, but the -8° twist provides a comfortable margin at the 105% rpm condition. Because of the performance benefits, the -8° twist was selected after the blade design and aeroelastic analysis studies established that desirably low vibratory stresses could be achieved with this twist.

It was concluded that the rotor dimensions selected are correct for achievement of program objectives.

INVESTIGATION OF OUTER BLADE SPAR DESIGN CONCEPTS

Eight distinct design concepts for the outer blade spar were considered during the preliminary design of the full-scale TRAC rotor system. Cross section drawings of these concepts are shown in Figure 17, and the calculated section properties are summarized in Table 2. The external airfoil dimensions (28-inch chord, 63_2A016 airfoil section) were kept constant during this investigation. Not all of the concepts were developed to the same degree; some were dropped from consideration before being refined because preliminary analysis indicated lack of promise. For this reason the Table 2 comparisons might be slightly misleading with regard to the relative merits of some of the configurations.

Configurations 2 and 6 were selected as the final candidates for the preliminary design of the full-scale flightworthy rotor, with number 6 considered to be the preferred choice. They are essentially equivalent in mass and stiffness properties which provide acceptable aeroelastic characteristics for the intended operating spectrum, and are believed to be satisfactory from the standpoint of manufacturing feasibility. The choice between the two has no significant impact on the design of other blade components, rotor head, or retraction system. Configuration 8 was investigated as a lighter weight solution that has a somewhat higher manufacturing risk at the present time, but is projected to be the preferred solution in the 1980 time frame.

The design constraints on the TRAC outer blade spar are different from those on a conventional blade. One difference is the requirement that the outer blade spar provide adequate space for the inboard blade components when the blade is telescoped. Another difference is that the TRAC outer blade spar is in compression, rather than tension. The compressive force dictates that the blade must be stiff enough overall to avoid column

buckling, and that the spar wall must be stiff enough to avoid local buckling. Thus, the TRAC outer blade utilizes somewhat thicker than normal blade airfoil sections; the spar is designed for higher than normal flapwise stiffness; and the spar wall thickness tends to be greater than for a conventional blade. Aeroelastic analysis has demonstrated that a key factor in keeping the outer blade vibratory stresses low is to provide a high ratio of blade flapwise bending stiffness to unit weight.

Blade configuration number 1 has a structural concept the same as that of the dynamic model blades described in Reference 1, except that the flapwise stiffness has been increased by the addition of boron fiber/epoxy elements as shown. The boron increases the stiffness to the point where a significant blade twist, desirable from a performance standpoint, can be introduced without incurring excessive vibratory stresses. As discussed in the following section, aeroelastic analysis indicates that the original blade spar structure, without the boron stiffening, is satisfactory for an untwisted blade, but not for the desired extended-twist value of -8°. Blade configuration 1 utilizes an extruded aluminum nose section, machined internally as required to provide the constant dimensions along the length to accommodate the bearing slide blocks which are mounted on the torque tube. The nose section is bonded to the aluminum honeycomb sandwich which forms the aft spar wall. The boron/epoxy elements are preformed and bonded in place with the outer spar skin. The trailing edge fairing is of generally conventional construction, but is one continuous structural unit rather than the multipocket nonstructural trailing edge used on most Sikorsky aluminum main rotor blades.

Blade configuration 2 is similar to configuration 1, but reduces weight by extending the honeycomb sandwich construction forward of the quarter chord line. Whereas spar 1 used the solid aluminum extrusion to provide chordwise balance about the quarter chord line, spar 2 utilizes brass (selected because of its relatively high density and its coefficient of thermal expansion which is similar to that for aluminum), located as far forward as possible. Fabrication is with formed sheet aluminum skins and aluminum flexcore honeycomb precut to the exact thickness desired. The spar components, including the brass counterweight and prefabricated boron/epoxy slabs, are bonded together in two steps in an autoclave, over a solid mandrel which provides the closely-controlled internal contour required. The trailing edge fairing is of the same relatively standard construction as that for blade configuration 1. The stiffness-to-weight ratio of blade 2 is not quite as high as for blade 1, but is high enough to provide the desired aeroelastic characteristics, and the weight is less. Blade configuration 2 was selected as one of the two preferred candidate designs for the present study.

Blade configuration 3 utilizes an open C-section aluminum extrusion, and a second open aluminum channel member to form the rear spar wall. Because both sections are open, they can be machined to provide the desired internal dimensions to accommodate the bearing slide block. However, it is anticipated that there might be some difficulty in matching the tapered joints between the two members to a sufficient accuracy along the full length of the spar to provide a reliable bond. Also, with the wall thickness required to avoid local buckling, the spar is considerably heavier than desired. Another disadvantage is that the stiffness-to-weight ratio is too low to permit the use of blade twist. This ratio could be increased by adding a high specific modulus material such as boron or graphite fibers, but only at a still higher weight penalty.

Blade configuration 4 also utilizes an open aluminum C-section extrusion. In this case, the section is closed with a steel channel for chordwise balance and a wet-layup graphite/epoxy nose splice to minimize the problems of providing a good bond in the joint. A layer of unidirectional boron/epoxy is applied to the rear spar wall to prevent the elastic axis of the spar from being too far forward. This configuration is also judged too heavy and has too low a stiffness-to-weight ratio.

Blade configuration 5 utilizes a single-piece closed aluminum D-section spar extrusion. Chordwise balance is achieved by a solid nose, and beads provide stiffness to avoid local buckling of the spar wall. Internal broaching can be used if required to achieve the required dimensional tolerances along the points of contact with the bearing slide blocks. Fabrication risks are relatively low, but it is not certain that the aft portion of the spar has sufficient resistance to vertical shear deformations in flight. This design is lighter than configurations 3 and 4, but still heavier than desired, and the stiffness-to-weight ratio is relatively low.

Blade configuration 6 utilizes a filament-wound graphite/epoxy spar. Because of the very high specific modulus (ratio of modulus of elasticity to density) of graphite, this material permits lighter weight, thinner spar walls, and higher bending stiffness-to-weight ratios than does an all-aluminum structure. The fiber orientation is mixed: 60 percent at $\pm$ 15° to the span axis and 40 percent at $\pm$ 45°. The low-angle fibers provide the desired beam bending stiffness and the 45° fibers provide torsional stiffness. The spar is wound over a mandrel with the internal stainless steel abrasion strips already in place. The external leading-edge abrasion strip and graphite and fiberglass cover sheets are laid over the wound spar, and this whole subassembly is cured in an autoclave in a single operation. The nonstructural leading-edge counterweight, such as lead shot in a rubber or epoxy matrix, is installed after the mandrel is removed. The trailing-edge fairing, made with fiberglass skins and Nomex honeycomb, is also bonded on in a separate operation.

Blade configuration 6 is relatively light weight and has the desired stiffness-to-weight ratio. Along with configuration 2, it was selected as one of two candidate designs for the present study. The cost of graphite fibers has been high in the past, but has dropped considerably in recent times and is expected to continue to drop for some time, to the point where cost relative to conventional materials is not a major consideration. Labor hours should be less than for most other configurations. For the long term it is expected that this material is to be preferred over the alternative materials shown in the various designs for the TRAC outer blade spar.

Blade configuration 7 is similar to blade 6, but assumes a hand layup of the upper and lower spar walls which are precured, followed by a wet layup of nose and trailing edge splices. The unidirectional fiber layers are oriented 55 percent at 0° (parallel to span axis) and 45 percent at $\pm$ 45°. Structural properties similar to blade design 6 are obtained, but the greater number of operations plus the four splices in the spar wall suggest that configuration 6 is to be preferred.

Blade configuration 8 combines the virtues of blades 2 and 6 and provides the lightest solution investigated. An extra-high modulus graphite (available commercially now) provides adequate stiffness with less material than for blade 6. A sandwich construction provides the necessary wall stiffness to avoid local buckling. This spar is also filament wound, but in two steps, with a layer of flex-core honeycomb mounted on the inner graphite skin and a counterweight installed prior to winding the outer graphite skin. The internal stainless steel liners, external abrasion strip, and outer cover are bonded integrally with the spar in the same manner as for blade 6. The fiber orientation mix is the same as for blade 6. Blade configuration 8 is believed feasible at present, but because it entails slightly higher manufacturing risks and higher material properties than blade 6, it was not considered a candidate for the preliminary design of the experimental full-scale rotor. Its superior weight properties make it an appropriate candidate for a 1980 time frame production prototype.

Fabrication of Spar Samples for Designs 1, 2, and 6

As part of the evaluation of the various spar concepts, full-size cross section samples of three of the designs were fabricated to investigate feasibility of manufacture. To evaluate manufacturing problems of blade spar configuration 1, a short sample ($\sim$ 10 inches) was fabricated and is shown in Figure 18. The aluminum nose was obtained from a scrap section of spar extrusion previously fabricated for the TRAC design selection test program, Reference 7. The unidirectional boron/epoxy elements were prefabricated in a separate mold, and the aluminum skins for the honeycomb sandwich were brake-formed. The components were bonded

together with AF-126 film adhesive over a wood (pine) mandrel, under vacuum bag pressure. Although several imperfections were noted in the finished product, partly due to shrinkage of the wood mandrel, the general feasibility of manufacture was established.

A 2-foot sample length of spar configuration 2 was also fabricated, as shown in Figure 19. As in the sample of spar 1, the aluminum skins were brake-formed to shape. In production, rolled or stretch-formed skins would be utilized. The unidirectional boron/epoxy slabs were prefabricated in a closed metal mold. The inner skins and the flex-core honeycomb were laid up over a mahogony mandrel, with AF-126 film adhesive, and cured under vacuum bag pressure in one operation. The tapered edges of the honeycomb were then machined by means of a circular saw blade in a milling cutter. The brass leading-edge counterweight (shaped in a separate operation), the boron/epoxy slabs, and the outer aluminum skins were then bonded to the inner components, in a second operation, using AF-126 adhesive between skins and other components and FM-37 foaming adhesive between the boron/epoxy slabs and brass leading-edge piece and the tapered edges of the honeycomb. The quality of this spar sample, although not perfect, was considered to be very good for the simple tooling utilized. It is believed that good quality, full-length spars of this design concept could be successfully produced.

To evaluate the filament-wound graphite/epoxy spar concept, design number 6, a 4-foot sample was fabricated and is shown in Figure 20. The "basket-weave" appearance results automatically from the winding technique in which a 1/2-inch-wide tape of graphite fibers is laid down in a helical pattern, back and forth between one end of the spar and the other. The exposed surface layers consist of $\pm$ 45° fibers; there are also internal layers at $\pm$ 15° to the span axis. This work was performed to Sikorsky specifications by a vendor, Fiber Science, Inc. The sample included the basic filament-wound structure and the internal stainless steel liners, but not the external leading-edge abrasion strip, the composite cover sheet, or the leading-edge counterweight. The spar was wound over a solid plaster mandrel which was shaped to the desired internal dimensions, and then cured under vacuum bag pressure. The sample was very successful, with excellent internal dimensional control, good external dimensions, and apparent good compaction and uniformity of the composite structure. The integral bonding of the internal stainless steel liners was also highly satisfactory. This sample provided convincing evidence that the material and particular fabrication technique can be used with confidence for production of full sized blade spars. It is anticipated that the completed spar can be produced at relatively low cost because of the minimum number of labor hours required. Based on the sample spar, this design is judged to be the most promising of the spar concepts investigated, and is the preferred choice for the rotor preliminary design.

AEROELASTIC ANALYSES

Preliminary Studies

Blade loads were calculated by means of the aeroelastic analyses described in Reference 9. These analyses were used initially to obtain gross effects of blade twist, tip speed, and spar stiffness on vibratory flapwise stress of the outer blade for the fully extended condition (helicopter mode). Blade properties were scaled up from the previously tested dynamic model blades, which were of all-aluminum construction. It was established that varying tip speed in the range of 650 to 700 feet per second had no appreciable effect on calculated loads. Twist had a significant effect; vibratory stress at a typical flight speed of 100 knots was increased by nearly 50 percent when twist was changed from zero to -8 degrees. Because previous studies had indicated that spar stiffness-to-weight ratio was important in determining vibratory stresses, the effects of adding a very high stiffness-to-weight material was investigated. The replacement of approximately 20 percent of the aluminum in the spar with unidirectional boron/epoxy reduced weight slightly and increased the bending stiffness of the outer blade by more than 60 percent. The aeroelastic analysis indicated a 50-percent drop in the vibratory stress. These effects are shown in Figure 21. Although the peak value shown is only about 4400 psi, correlation studies between theory and experiment indicated that the theory gave reasonable qualitative agreement but underpredicted the stress magnitude. This is at least partly attributable to fuselage-induced flow field effects present in the model tests, not considered by the theory. Although the ratio of experimental to predicted stress varies with the particular operating condition, a factor of 1.5 is believed to be reasonable for the critical conditions for a twisted blade. Thus, a calculated vibratory stress of 4400 psi corresponds to 6600 psi, near the allowable fatigue limit for aluminum. Other operating conditions investigated indicated stresses well beyond acceptable limits for the all-aluminum blade. Thus, the two-to-one drop in stress calculated for the boron-reinforced spar is an important factor in permitting the incorporation of blade twist into the design.

It should be noted that the boron-stiffened spar also reduced the calculated vibratory bending moment in the outer blade spar by approximately 20 percent. The drop in stress and deflection of approximately 50 percent results partly from this decreased moment and partly because of the higher effective structural moment of inertia of the spar. These calculations established the desirability of using an advanced composite material in the outer blade spar and the boron-stiffened aluminum spar design, otherwise similar to the dynamic model blade spar, became blade design no. 1 of this study. As noted in the section on the design of the outer blade spar, eight designs were considered. Spar designs 2 and 6, which were selected as most desirable for this preliminary design study, have essentially equal mass and stiffness properties.

Blade Natural Frequencies

The aeroelastic calculations were conducted using spar properties calculated for blade design 6, but may be considered to apply to blade 2 as well. Blade physical properties used in the calculations are tabulated in Table 3. It should be noted that although the proper mass distribution for tension-torsion straps are used in the analysis, the proper stiffness properties could not be used. For one thing, the actual blade design incorporates 12 straps, whereas the analysis is limited to two. Also, the analysis for natural frequencies and mode shapes would not converge when an appropriate representation of equivalent strap stiffness was incorporated; it was necessary to assume substantially higher strap stiffness values to make the program function. Thus, the calculated frequencies and loads for the straps are not correct, but it is believed that this fact has a negligible influence on the behavior of the other blade components.

Calculated natural frequencies for the full-scale TRAC rotor blade are presented in Figures 22 - 24 as a function of rotor speed for three blade length conditions: 100, 80, and 60 percent of full diameter, respectively. Because the analysis contains four major elastic structural element items, namely torque tube, outer blade, jackscrew and straps, each with their own degrees of freedom, the elastic modes are not as simply defined as for a conventional blade having a single major elastic structural element. Each natural frequency point has a mode shape similar to those shown in Reference 9, in which each of the four elastic elements participate to a greater or lesser degree. For the so-called "rigid body" modes, flap and lag, all elements move together except for small deviations about the mean. The torsion mode is well defined because only the torque tube and outer blade participate in this mode. The bending modes, however, might have either a single element showing prominent deflections or several. The letters adjacent to the calculation points on Figures 22 - 24 are a key for identification of the elements which participate in that mode. The label B (for blade) indicates that the outside elements, the torque tube and outer blade, show the predominant deflections. These two elements are always coupled, with the outer blade usually showing the greatest deflection magnitudes. These modes are the most significant ones in determining blade stresses. The label J indicates that the jackscrew is the primary participant, and the label S indicates that the strap is the primary participant. In some cases, two letters are shown - this indicates that the mode is more complex, with both identified elements participating substantially in the motion. (The first letter in such cases indicates the element with the greater deflection magnitude.) It should be noted that it is not always possible to identify a curve as representing deflections of only a particular element; as rotor speed changes, the nature of the vibratory mode can change. Thus, in Figure 22(a) the third circular-symbol curve above the horizontal axis (having a frequency of approximately 33 rad/sec at zero rotor speed)

represents a strap vibratory mode at low rotor speeds but becomes a blade mode at higher rotor speeds. Such a change in character usually results whenever there is a near-coalescence of frequencies of two components in either the flapwise or the edgewise planes.

Portions of some of the curves shown, such as in Figure 23(b), are extrapolated from calculated points. This was done because the computer program would not identify roots to the differential equations of motion in these regions, even though it is certain that roots exist. Despite considerable investigation of this phenomenon, the reason for the lack of success in establishing roots in these cases was not established. From the nature of the physical problem, the extrapolated frequencies cannot be too far wrong.

The variation of natural frequencies of the primary modes with changing rotor diameter, for the 100-percent rpm condition, is shown in Figure 25. The bending and torsion frequencies of the blades (external components) all increase as diameter is reduced, as would be expected by the reduction in length and addition of the stiffnesses of the telescoped components. Flapping and lag frequencies stay nearly constant. The jackscrew bending frequency, however, reduces as the diameter is decreased, because of the reduced centrifugal load supplied by the nut and the more inward location of the point of application of the centrifugal load.

Analysis of Selected Blade Design

An important part of the evaluation of the selected blade design was the calculation of vibratory stresses for a range of flight conditions. The conditions evaluated are summarized in Table 4, and include a range of forward speed from 100 to 360 knots, three values of diameter, variations of lift and propulsive force, and evaluations of the effects of gusts and operation at altitude.

The nominal design operating envelope and structural design envelopes are shown in Figure 26. The letters next to the indicated points reference the cases listed in Table 4. The solid line connect the points selected as the nominal design operating envelope. This represents the normal limit operating conditions assumed for the rotor. At 100 knots, case B, the rotor is designed to fly as a pure helicopter at a gross weight of 20,000 pounds (21,000 pounds lift specified to allow for an airframe download), with propulsive force adequate to overcome an airframe parasite area of 22 ft^2. At 150 knots, case D, the lift is reduced to 10,000 pounds and the propulsive force to zero. Cases F and G correspond to the diameter reduced to 80 percent, with lift requirements reduced as forward speed is increased. Cases J and M represent nominal zero lift conditions (zero collective pitch and rotor inflow - calculated lift was slightly negative) at minimum diameter.

The dashed line in Figure 26 represents the cases selected to represent the nominal structural design envelope, and was intended as a more severe operating envelope to be used for analysis of blade vibratory stresses, to provide a safety margin beyond the nominal design operating envelope. The first three cases, A, C, and E, are for operation in the pure helicopter mode at an assumed lift or 18,400 pounds. This value, rather than the higher lift previously discussed, was selected because it corresponds to the design gross weight of the NASA/Army Rotor Systems Research Aircraft (RSRA) in the pure helicopter mode. The other cases represent reduced diameter and reduced lift values following a trend similar to but more demanding than the nominal design operating envelope. The two highest speed points, L and Q, correspond to reduced rpm operation.

The maximum calculated blade vibratory flapwise moments for the cases indicated in Figure 26 are shown in Figure 27. As anticipated, the general trend was for vibratory moment to increase with forward speed, particularly at the design dive speed of 36 knots. Surprisingly, one of the points (L) thought to be a relatively severe operating condition at 300 knots, turned out to have relatively low stresses. Case J, with a lower lift at the same speed, had higher stresses. A similar phenomenon showed up again when the effect of a mild (8 ft/sec) vertical gust was investigated, as shown in Figure 28. In all cases the lift increased substantially due to the gust, but at full rpm the vibratory blade moments decreased, both at 300 and 360 knots. Only at 360 knots and reduced rpm did the calculated vibratory moment increase. Thus, in most cases it is preferable to carry a positive lift on the rotor to minimize stresses at high flight speeds. This phenomenon has not been explained but presumably results from the combination of blade twist and the high advance ratio operation.

The effect of altitude on rotor loads is shown in Figure 29. As anticipated, the magnitudes of both lift and vibratory moments decrease as altitude is increased. Whereas the blade vibratory moments are excessive for steady state operation at 360 knots at sea level, they are reduced to acceptable values at altitude.

The calculated spanwise distribution of vibratory flapwise moments and stresses are presented in Figure 30 for all of the conditions listed in Table 4. The calculations were made with the significant blade modes including flapwise, edgewise, and torsional degrees of freedom. Only flapwise results are shown because the edgewise and torsional moments and stresses were much lower in magnitude. In addition to the basic moment scale, which is common to all blade components, vibratory stress scales are also shown in Figure 30. These stress scales apply to the long-length, minimum stiffness, constant-cross-section portions of the various components as identified in Table 3.

In all cases shown in Figure 30, the maximum vibratory moment occurs on the outboard blade. However, because of the relatively high section modulus of the outboard blade relative to that of the torque tube, the maximum vibratory stress frequently is higher on the torque tube. Although allowable vibratory stresses cannot be precisely determined without considerable fatigue testing of full-scale components, the anticipated allowable vibratory stresses are on the order of 7,000-10,000 psi for the aluminum torque tube, 15,000-18,000 psi for the graphite/epoxy outer blade spar, and 15,000-20,000 psi for the steel jackscrew. On this basis, and allowing a 50 percent increase above calculated stresses, the outboard blade stresses are limiting only at 360 knots at sea level; the torque tube stresses are acceptable for all of the nominal design operating envelope points (Figures 26 and 27) at sea level, except at the maximum speed of 360 knots, but are excessive for some of the nominal structural design envelope at sea level; and the jackscrew stresses are acceptable except for 360 knots at sea level. At 360 knots, operation at altitude above 10,000 feet will provide acceptable stresses on all components.

Additional analyses were conducted of combined stresses in the outer blade spar and torque tube, and of bearing stresses in the sliding blocks of the blade components. These analyses were routine stress checks and did not indicate any unusual problems to be overcome. In addition to these checks, stress calculations were conducted for the blades in the minimum diameter, locked-hinge, zero rotation mode at 150 knots at sea level. At this flight condition a lift corresponding to the maximum lift coefficient along the full length of the blade could be sustained without exceeding the static strength limit of the components.

BLADE INTERNAL COMPONENT DESIGN

The design of the blade was an iterative process in which various assumptions of loads and blade properties were made and then modified as required to provide adequate strength and minimum weight. Description of the blade internal components is limited to the final configurations and ignores the iterative process.

The centrifugal load distribution in the various blade components at full blade extension is shown in Figure 31. The outboard blade starts at the 50% radial station (14 feet) and extends to the tip. This component is in compression. At the tip this load is picked up by the tension-torsion straps and is delivered through the set of six nuts to the jackscrew, and finally to the sleeve/spindle assembly, with each of these components adding its own centrifugal load. The torque tube and nut reaction tube are each independently supported by the sleeve/spindle assembly.

Jackscrew & Redundant Strap

The static design criteria for these members is that the ultimate load (1.5 times centrifugal force at 125% rpm at full blade extension) must be carried by either the jackscrew or the redundant strap, so that failure of either one will not result in system failure. The material assumed is maraging steel, such as Vascomax 300, with a minimum ultimate tensile strength of 280,000 psi.

Calculated centrifugal force at the nut at 100% rpm and 100% extension is 56,600 lb, and at the root end of the screw the CF is 67,000 lb (Figure 31). The ultimate static load at the root end is $67,000 \times 1.5 \times 1.25^2 = 157,000$ lb, and the required tensile area for both the jackscrew and redundant strap is $157,000/280,000 = 0.561$ in.^{2}. The maximum normal working stress with both members intact is $67,000/(2 \times 0.561) = 59,700$ psi. If the redundant strap is preloaded to 10 percent of the normal centrifugal load of 67,000 lb on assembly, the division of load between the strap and the jackscrew will be approximately 37,000 and 30,000 lb respectively, and the normal working stress at 100% rpm and 100% extension will be approximately 66,000 psi on the redundant strap and 53,500 psi on the jackscrew. The ground-air-ground (GAG) cycle stresses can be considered to be a steady stress plus a very low frequency vibratory stress, each of which is one-half of the above numbers, 33,000 and 26,750 psi for the strap and jackscrew respectively. These GAG cycle stress values are considered low for the selected material, even when a stress concentration factor of 3 is applied to account for the structural discontinuity of the jackscrew threads.

The threaded portion of the jackscrew has an outside diameter of 2.000 inches, a pitch diameter of 1.840 inches, and a minor diameter of 1.680 inches. The internal diameter (bore) of the jackscrew is 1.452 inches and the diameter of the internal redundant strap is 0.845 inches. The screw thread is double, left hand, with three threads to the inch and a lead of 2/3 inch. The threads are a buttress type, with a contact face angle of 14-1/2 degrees and the opposing face angle of 22-1/2 degrees. The thread is similar to that recently selected for full scale laboratory tests of jackscrew/nut combinations, Reference 7. At the full rotor rpm of 225 and the 3:2 gear ratio of the differential, the jackscrew rpm is 337.5. This provides a rate of change of blade length of 3.75 inches per second and a total time for diameter change between 100% and 60% of 36 seconds.

The reason for the double thread is the increased screw efficiency and consequent reduced heat dissipation requirements in the blade. This effect is illustrated in Figure 32. The key elements are coefficient of friction and thread pitch

(helix) angle; the double thread permits double the pitch angle for given thread proportions. An overall retraction system efficiency of slightly below 50% is desired in order to make the system self-locking, but it is better to introduce friction by means of the rotor head brake rather than in the jackscrew.

Tension-Torsion Straps

The structural design criterion established for the tension-torsion straps is that the strap package must carry the full ultimate load with two straps failed and the remaining 10 straps loaded unequally such that the highest strap stress is 110% of the mean stress of the remaining straps. For the rotor overspeed condition of 125% rpm and a factor of safety of 1.5, the relationship between normal working stress and material ultimate tensile stress which will satisfy the criterion is

$$\frac{\text{Ultimate tensile stress}}{\text{Normal working stress @ 100\% rpm}} = (1.25)^2 \times 1.5 \times \frac{12}{10} \times 1.10 = 3.094.$$

The material selected for the strap is maraging steel with a minimum ultimate tensile strength of 280,000 psi; the above factor permits a normal working stress of 90,500 psi.

At 100% rpm and full extension, the centrifugal force of the outboard blade, which is the value of the tension at the outboard end of the straps, is 45,100 pounds. The required total strap area at the tip is 0.498 $in.^2$, or an individual strap area of .0415 $in.^2$, requiring a strap diameter at the tip (excluding the enlarged diameter, threaded portion) of 0.230 inch. Inboard of the tip the diameter must be increased on a long taper to compensate for the increase in centrifugal force due to the strap mass. At the root end the strap diameter is 0.253 inch.

The straps are anchored in the nuts by means of a .450-inch-diameter, integral shoulder arrangement, as shown in Figure 33, to fit in counterbored holes in the nuts. The root end of the strap just outboard of the shoulder has a diameter of .350 inch, to fit snugly in the through-bore in the nut. This diameter is larger than the main body of the strap to permit passage of the .350 O.D. threaded tip of the strap during assembly. The increased diameter of the threaded end permits the full tensile strength of the strap to be developed. The square tip extension provides a means for wrenching for length adjustment and also a means for locking the rotation of the strap, as discussed in a previous section.

Blade Retention Nuts

Six nuts, each with five threads plus a safety thread (not normally in contact) are provided. The centrifugal force at the

nuts at 100% rpm and 100% extension is 56,600 pounds, or an average of 56,600/30 = 1887 pounds per thread. The nominal projected contract area per thread is .925 $in.^2$, so that the nominal contact pressure is 2040 psi. However, it cannot be assumed that the five threads of each nut carry equal load, even though the multiple nut/strap configuration provides that each nutcarries an equal load. Elastic deformations in both the jackscrew and the nuts will tend to load up the inboard end threads of each nut and unload the threads toward the tip. Lapping the nuts against the screw under load will permit a more even load distribution, and this operation is recommended to accomplish better thread load sharing. Wear in service will also tend to improve thread load sharing, provided that lubrication breakdown does not occur as a result of excessive initial contact pressure. In the present analysis it is assumed that lapping will provide at least an equivalent of 50 percent thread contact under load, so that the contact pressure of the effective threads is not more than double the nominal pressure. Thus, contact pressure = 4080 psi. The corresponding shear stress at the base of the nut thread is 2400 psi. This compares with an ultimate shear stress of approximately 8000 psi for the P-3310 carbon-graphite threads and very much higher values for the alternate nut material, beryllium copper.

Jackscrew Lubrication

The jackscrew is lubricated with Vitrolube dry film. This coating, consisting of molybdenum disulphide and other solid lubricant materials in a vitreous base, proved to be superior to other lubricants investigated in a materials study conducted under the Reference 7 contract. It worked very well with both carbon graphite nut material and beryllium copper. The carbon graphite by itself is also a good solid lubricant material. The recommended materials were tested extensively in combination in the Reference 7 tests at contact pressures (p) up to 6000 psi and sliding velocities (V) up to 190 feet per minute, for a "pV" value of 1.14 million. A limited number of overload tests were also conducted up to 10,000 psi contact pressure, up to pV values of 1.9 million. In the present design, the sliding velocity at the pitch diameter of the screw is 164 feet per minute at 100% rpm (225 rotor shaft rpm, corresponding to a jackscrew rotational speed of 337.5 rpm). With a calculated contact pressure of 4080 psi, the nominal pV for the present design is 669,000, substantially less than the maximum Reference 7 test values. Based on the referenced tests, it is anticipated that a coefficient of sliding friction on the order of .05 will be achieved. If all of the frictional heat were absorbed by the body of the jackscrew, the rise in temperature would be approximately 50°F. Thus dissipation of frictional heat is not anticipated to be a significant problem. Centrifugally pumped cooling airflow can be readily provided, however, by the simple technique of providing a small opening at the root of the blade

(with a filter to keep out dirt) and an exit at the blade tip. The total pressure drop available from the centrifugal pumping action is equal to the dynamic pressure corresponding to the rotor tip speed - over 500 lb/ft^2 for the fully extended blade at full tip speed at sea level.

DIAMETER-CHANGE SYSTEM LOADS

Loads in the diameter-change system are primarily a function of blade jackscrew torque, which in turn depends on thread pitch angle, coefficient of friction, applied centrifugal force (which is dependent on outer blade mass distribution and rotor rpm), and on whether the blade is being retracted or extended. The basic equations for jackscrew torque were defined, and the variation of torque per unit centrifugal force with coefficient of friction (between jackscrew and nuts) for the selected jackscrew design is shown in Figure 34. For blade extension, a negative torque is shown at friction coefficients less than approximately 0.12. This means that centrifugal force would cause the jackscrew to spin and the blades to extend without the extension clutch being applied; it is for this reason that the rotor head friction brake is incorporated to make the system self-locking.

Tests conducted under Reference 7 have indicated that coefficients of friction in the range of .05 to .10 should be anticipated as long as the dry film lubricant utilized remains intact. As the film gradually breaks down with extended usage, the friction increases, slowly at first and then rapidly, to approximately 0.2 at the end of the usable lubricant service life. The criteria selected for the design of the system, except for the rotor head friction brake, are C_f = .10 for normal operation (assumed 98% of time), C_f = .20 for incipient lubricant breakdown (2% of time) and C_f = .30 for maximum static load calculation. Because the rotor head friction brake is designed to add friction when the jackscrew friction is low, a jackscrew/nut coefficient of friction of only .05 was assumed in sizing the brake.

The loads are based on a centrifugal force applied to the jackscrew at the nuts of 57,000 pounds (full extension and full rpm). Torques are based on the criteria stated above and the relationship shown in Figure 34, increased by 5 percent to account for the friction between the nuts and the nut reaction tube, plus 900 in.-lb for jackscrew bearing friction. The resulting torque loads per blade are as follows:

For retraction case, torque is 12,800 in.-lb for normal operation (98% of the time), 18,500 in.-lb for incipient lubricant breakdown (2% of time), and 24,400 in.-lb for maximum static load.

The corresponding values for the extension cases are zero, 5300, and 10,500 in.-lb respectively.

The design of the differential gears and bearings is based on the above loads, with appropriate allowance for the decrease in loads as the blade retracts. The calculated prorated service life of the gears and bearings was more than double the design goal of 5000 complete diameter change cycles.

The coaxial shafts and clutch system were designed on the basis of maximum static loads, plus the rotor head friction brake torque. The friction brake design torque is 17,800 in.-lb, reacted by four spring-loaded calipers, each with two friction pads. In one retraction or extension, the energy dissipation by the brake is 1.26×10^6 foot pounds.

ROTOR WEIGHTS SUMMARY

Calculated weights for the TRAC blade and retention system are summarized in Table 5. The weight of each blade is 337 pounds; the division of this weight among the various blade components is illustrated in Figure 35. The outer blade is the heaviest of the four major assemblies, followed by the torque tube, the jackscrew, and the nut/strap assembly. The spanwise weight distribution for the blade and retention system is shown in Figure 36. Except for the mid-span region, where the blade segments overlap, the distribution is quite conventional.

Weights for the overall rotor system including blades, rotor head, and diameter change mechanism are summarized in Table 6. Total rotor system weight, including blade folding, is 2696 pounds. This value is 13.5 percent of the nominal design lift capability of 20,000 pounds. However, the rotor as designed is capable of higher lifts; for a blade loading parameter C_T/σ of 0.12 at 4000 ft 95°F, rotor lift is 24,000 pounds. The rotor of weight is 11.2 percent of this higher lift figure. Also shown in Table 6 are estimated weight savings that should be achievable if the rotor were designed for a 1980 initial operational capability (IOC). Most of these savings are based on use of a lighter outer blade spar (blade design 8 as discussed in the section on outer blade spar design concepts), which reduces blade centrifugal loads, rotor head loads, and retraction system loads. Some additional reduction in diameter change system weight is obtained by substituting titanium for steel. In total, the weight reduction is approximately 200 pounds. The 1980 IOC weights were used as the basis of the weight trending equations utilized for the parametric mission comparison studies, described in the other major section of this report.

A comparison between rotor system weights for the TRAC rotor and

corresponding values for the SH-3H helicopter (which has comparable total blade area and lifting capability - see Table 1) is shown in Figure 37. The SH-3H is a recent production model of the S-61 series and has a power blade fold system, as does the TRAC rotor. The blades of the TRAC rotor (present preliminary design) are 33% heavier than those of the SH-3H. Hub, hinge, and blade retention weight values are similar. Blade fold on the SH-3H is substantially heavier than for the TRAC rotor because of the need for separate folding hinges, not required on TRAC. Total rotor weight is 16% heavier than for the SH-3H; the 1980 IOC estimate is only 7% above the current SH-3H value (obviously, weight reductions should also be possible for the SH-3H rotor). In terms of total rotor weight per unit effective blade area ($bc\bar{R}$), the values are 11.26 lb/ft^2 for the present TRAC design, 10.40 for the 1980 TRAC, and 9.88 for the SH-3H. The value for the YUH-60A UTTAS, without power blade fold capability, is 8.12 lb/ft^2. Based on the present investigation, it is estimated that the weight penalty for the TRAC rotor system, compared to conventional rotor systems of comparable technology level, will be on the order of 15 to 25 percent, depending on the application.

PHASE II: AIRCRAFT PARAMETRIC MISSION STUDIES

Parametric analyses were conducted to determine mission requirements for which TRAC rotor aircraft are competitive with conventional rotor VTOL aircraft configurations. Prior analyses and model test results have shown that the variable-diameter TRAC rotor concept will provide positive aerodynamic benefits and other benefits in the cruise mode of high-performance rotary-wing aircraft. However, quantitative comparisons with conventional-rotor aircraft, including proper assessment of structural weight penalties of the TRAC system, had not previously been made. The present study is intended to provide a realistic assessment of the overall merits of the TRAC rotor system and to identify long-term potential applications.

The conventional rotor configurations considered include the pure helicopter and both full rpm and slowed rotor compound helicopters. The TRAC rotor configurations include both full rpm and slowed rotor compounds and the stowed-rotor aircraft wherein the rotor is stopped and folded away during cruise flight. Mission variables considered include a substantial range of design speeds, payloads, ranges, and cruise altitudes.

AIRCRAFT CONFIGURATIONS

There are seven rotary-wing aircraft configurations considered in this study. All are single main rotor designs, as follows:

1. Current technology pure helicopter. The pure helicopter derives all lift and propulsive force from the main rotor, and for this reason is relatively restricted in cruise speed and altitude capability by retreating blade stall limits. By "current technology" is meant the state of the art corresponding to helicopters presently in the development cycle, such as the Sikorsky/Army Utility Tactical Transport Aircraft System, YUH-60A (UTTAS).

1A. Helicopter with auxiliary propulsion. A limited evaluation of this configuration was added to the study. This aircraft derives all lift from the main rotor, but has an auxiliary propeller to provide all or part of the propulsive force in the cruise mode.

2. Full rpm conventional rotor compound helicopter. The compound helicopter is derived from a pure helicopter by the addition of a fixed wing to provide part or all of the lift in cruise flight and an auxiliary propulsion system (propellers, fans, or jets) to provide part or all of the propulsive force. In this manner the limitations of retreating blade stall are avoided and higher speeds and altitudes can be achieved than for the pure helicopter. "Full rpm" means an rpm variation of not

more than ±5 percent from the design hover rpm value, to avoid complexities in engine controls, transmission design, accessory systems, and vibration-control systems.

3. Slowed conventional rotor compound helicopter. This configuration operates at reduced main rotor rpm in cruise flight to avoid performance and noise penalties with excessive advancing blade Mach number. Cruise rpm will typically be in the range of 75 or 80 percent of the hover value and represents a compromise between performance considerations and rotor dynamics (blade stresses, flapping response, and aeroelastic stability). The slowed rotor compound provides higher speed potential than the full rpm compound, at the expense of possible complexities in engine controls, transmission design, accessory systems, and vibration-control systems.

4. Full rpm TRAC rotor compound helicopter. The TRAC rotor achieves a substantially lowered tip speed in cruise flight by means of reduction in diameter, so that the need for reduced rpm is eliminated except at very high forward speeds. As in the case of the conventional rotor compound, "full rpm" is taken to mean a variation of not more than ±5 percent from the design hover value.

5. Slowed TRAC rotor compound helicopter. The highest possible cruise speed potential for a compound helicopter is achieved by a combination of reduced diameter and reduced rpm, which serves to delay advancing blade Mach number limits to the maximum extent.

6. TRAC stowed rotor aircraft. The TRAC rotor makes feasible the stowed rotor concept, wherein the rotor is stopped in flight and folded away into the top of the fuselage, converting the aircraft from a helicopter at low speeds to a fixed-wing aircraft at high speeds. This concept would represent an extremely severe technological challenge with a conventional rotor system because of problems with stability, control, and blade aeroelastic behavior, but dynamic model tests have demonstrated that the stowed rotor configuration should be a straightforward development with the TRAC rotor. This aircraft category will have low drag and high specific range, with a virtually unlimited speed potential, at the expense of the additional structural weight and complexity associated with stowing the rotor in the fuselage.

ANALYTICAL METHOD AND ASSUMPTIONS

DESIGN MATH MODEL

The parametric mission studies were accomplished with the aid of the Sikorsky Aircraft Helicopter Design Model (HDM) computer program. This computerized math model permits a much more detailed analysis and better optimization of aircraft design than would otherwise be possible. A general description of HDM is presented in Appendix A.

GENERAL SPECIFICATIONS AND ASSUMPTIONS

In order to provide consistent ground rules for the parametric mission studies, a set of general specifications was established. These specifications, which influenced the studies through the mechanism of weight trending equations, fuel consumption rates, etc., were intended to be appropriate for typical Army mission requirements. The flight profile is generally representative of a transport mission. It is believed that the comparative results of this study can be applied to other types of missions as well; however, no mission evaluation in this sense were conducted.

The general specifications are listed in Appendix B. In brief, these specifications call for a single main rotor, with tail rotor or fan-in-fin, main rotor disc loading not greater than 15 psf, design limit load factor of 2.5g, retractable landing gear, and twin engines assuming rubberized characteristics. Performance requirements include specification of a vertical rate of climb of 500 feet per minute at design gross weight at 4000 ft 95°F at 95% of intermediate rated power (30 minute rating). Payloads from 2000 to 10,000 pounds and ranges from 200 to 500 nautical miles were considered.

Various general assumptions were required as inputs to the helicopter design model. For the most part, these assumptions follow standard state of the art practice. The important aerodynamic and dynamic assumptions and criteria that might have an impact on the comparisons between various aircraft configurations are presented in Appendix C. Items included are allowable blade twist and blade loadings, airframe parasite drag, weight allowance for vibration control, rotor gust response criteria, and wing aerodynamic design criteria.

The general weights trending methodology utilized in the present study is present in Appendix D. Included is a summary of weights equations developed for the TRAC rotor.

RANGE OF MISSION VARIABLES

The various combinations of aircraft configuration type and design mission parameters (payload, range, cruise altitude, and design cruise speed) which were investigated are summarized in Table 7. In addition to these combinations, there were a few additional cases investigated which fell outside the range of variables indicated. The total number of HDM cases was approximately 200. For each aircraft configuration, a baseline design point was specified, as indicated by the circled check marks in Table 7, at which optimization studies were conducted, including preliminary design layouts. Baseline mission payload, range, and cruise altitude were the same for all configurations (5000 pounds, 350 nautical miles, and 4000 ft 95°F respectively).

Each configuration had a range of design cruise speeds, selected to cover the anticipated range of interest and as limited by excessive advancing blade Mach number. As the configurations progress in sophistication from the pure helicopter, at the top of Table 7, to the TRAC stowed rotor, at the bottom, the range of possible design cruise speeds generally increases and so the number of combinations investigated generally increased. The baseline design speed also increases steadily from one configuration to the next, reflecting the anticipated result that the optimum cruise speed would increase from one configuration to the next in some sort of progressive fashion.

A range of disc loadings was investigated for each configuration at two or more design cruise speeds. Optimum disc loadings based on this study were used for the remainder of the design points. For each aircraft configuration, a parametric variation of each major mission variable was then made about the baseline mission. Two additional payloads were investigated for the baseline range and altitude, two different ranges were investigated for the baseline payload and altitude, and three different altitudes were investigated for the baseline payload and range. A range of design cruise speeds was also investigated for these various mission combinations. Direct comparisons of the various configurations for identical missions is possible where the range of design cruise speeds overlap. Many comparisons are also possible for missions which are identical except for cruise speed.

Based on results of the parametric investigation, a point design study was made for each of the aircraft configurations, for which more specific information was developed, including three-view drawings, performance curves, etc. The point design cases are indicated by the squared check marks in Table 7. The design cruise speeds selected were the same as for the baseline points, but different standard-day cruise altitudes were selected as more nearly optimum for the various configurations.

RESULTS AND ANALYSIS

DISC LOADING OPTIMIZATION

The initial task in evaluating the various aircraft configurations was to evaluate the effects of disc loading on overall performance and to select disc loadings for the remainder of the investigation. The criterion selected was that the optimum disc loading for a given configuration and design cruise speed was that which resulted in minimum gross weight. The disc loading optimization study, carried out for 4000 ft 95°F cruise conditions and for the baseline payload and range (5000 lb and 350 nautical miles, respectively), is summarized in Figure 38. For each of the seven aircraft configurations, the helicopter design model calculation was run for at least three disc loading values at various design cruise speeds. In each case, a minimum gross weight design solution could be defined, although the "bucket" of each curve is quite shallow. (If specific engines rather than "rubberized" engines were used in the analysis, the minimum points would be much more sharply defined.) These results indicate that the results of the investigation are not critically dependent on the disc loading assumption, as long as a value reasonably near the optimum is utilized. This also makes the use of the same disc loading over a range of mission payloads, ranges, and cruise altitudes a reasonable assumption, even though it is not entirely accurate. Comparisons between the various configurations, the main point of the investigation, should be valid.

Optimum disc loadings vary from 6 lb/ft^2 for the pure helicopter to 15 lb/ft^2 for the slowed rpm TRAC compound at 350 knots. The general trends are shown more clearly in Figure 39, which presents optimum loadings as a function of cruise speed. Bands rather than lines are shown because of the shallowness of the curves in Figure 38. It was found that results were divided into three separate bands: one for the configurations with high rotor tip speed in cruise, one for those with reduced tip speed in cruise, and one for the stowed rotor aircraft. The general upward trend of optimum disc loading with forward speed can be explained on the basis of the balance of power required in hover and in cruise. At high cruise speeds, the cruise power is high because of the combination of airframe drag and rotor equivalent drag. When cruise power is high, the same power can be utilized in hover, permitting higher disc loadings than could be used for a low-available-power aircraft. Because high disc loadings tend to minimize airframe weight, high cruise power favors high disc loading solutions. This tendency also explains the three separate bands. When tip speeds are reduced, rotor drag is reduced and, therefore, cruise power is lowered, favoring reduced disc loadings because of the hover power consideration. Similarly, the stowed rotor has the lowest drag in cruise and, therefore,

for a given cruise speed, lower optimum disc loadings than the various compound helicopter configurations.

BASELINE STUDIES AT 4000 FT 95°F CRUISE

A summary plot of gross weight, empty weight, and consumed fuel for the seven configurations for the range of design cruise speeds investigated is presented in Figure 40. These results are all for the baseline mission of 5000 lb payload and 350 nautical miles range. As can be seen, comparative trends shown by the curves of gross weight tend to be repeated in both the empty weight and consumed fuel data.

As was expected, the pure helicopter, configuration 1, shows the lightest weights of any of the aircraft, at least up to 175 knots cruise speed. At 190 knots, the combination of reduced allowable blade loading, which increases blade area required and thus, rotor weight, plus high advancing blade tip Mach number, which increases rotor equivalent drag and hence power required, greatly reduces the efficiency of the pure helicopter. In terms of productivity (payload times speed divided by weight), the best design cruise speed for the helicopter is 175 knots. This speed is higher than indicated by some previous studies, resulting from the relatively low levels of parasite drag utilized in this investigation (discussed in Appendix C).

Configuration 1A, the helicopter plus auxiliary propulsion (assumed to be a pusher propeller), shows an advantage over the pure helicopter at 190 knots. The basic benefit is the increased lifting capability of the rotor as it is relieved of the propulsive force requirement, so that rotor weight can be reduced.

The full rpm conventional rotor compound, configuration 2, provides, the lightest solution at 200 and 225 knots. At 200 knots or higher, a wing is a much more efficient lifting device than a rotor, so that the weight of the wing is more than offset by the reductions in rotor system weight and fuel weight that it permits. Because of the high tip speed, however (assumed 95% of hover tip speed for this configuration), the drag increases rapidly with increasing forward speed because of the increasing advancing tip Mach number encountered. Note that although this configuration has the lowest empty weight of any of the configurations analyzed at 225 knots, it has the highest fuel weight because of the high rotor drag. It should also be noted that the assumed operating temperature, 95°F, tends to favor the high tip speed configurations relative to the reduced tip speed configurations, because the high temperature results in a relatively high speed of sound and correspondingly low Mach numbers for any given speed. On a standard day, much more typical of average operating conditions, the drag rise due to Mach number occurs at lower forward speeds, and the empty weight advantage at 225 knots design cruise speed does not in fact occur. This comparison is shown in a subsequent section.

Configuration 3, the reduced rpm conventional rotor compound, provides the lightest solution by a slight margin at 250 knots for the 4000 ft 95°F condition, but as design cruise speed increases to 300 knots, it is no longer competitive with the TRAC rotor configurations. One reason for this result is the minimum tip speed imposed by the gust response criteria, discussed in Appendix C. The relatively high tip speed required to provide adequate blade flapping stability produces high rotor drag due to high rotor advancing tip Mach number.

The TRAC compound helicopters, configurations 4 and 5, become lighter than the conventional compound solution at forward speeds above 275 knots, because of the greatly reduced rotor drags resulting from the combination of reduced blade area and reduced tip speed. Consumed fuel is also less than for the conventional rotor. At the highest compound helicopter speeds, 325 and 350 knots, the reduced rpm TRAC compound (configuration 5) shows an advantage over the full rpm configuration (4), again because of the rotor drag factor.

The stowed TRAC rotor, configuration 6, shows a clear-cut advantage in consumed fuel starting at a design cruise speed of less than 250 knots and a gross weight advantage starting below 275 knots. At higher speeds these advantages become very large. The reason is the very large drag advantage obtained by eliminating rotor blades and hub from the airstream completely in cruise flight. The consequent savings in installed power required and consumed fuel more than make up the weight penalty in the mechanisms required to stow the rotor. The stowed rotor configuration has the highest productivity factor (payload times cruise speed divided by weight, indicated by the diagonal lines in Figure 40) of any of the aircraft types investigated.

To illustrate some of the factors involved in obtaining these results, a more detailed comparison between two of the cases is presented. The 300-knot conventional slowed rotor compound and the 300-knot full rpm TRAC compound configurations are compared in Figures 41 - 43. Disc loading is 13 lb/ft^2 for each case, so that this parameter does not enter into the comparison. As shown in Figure 41, the hover figure of merit is less for the TRAC rotor, despite a higher value of extended blade twist (-8° compared to -4° for the conventional rotor). This reduced hovering efficiency results from the large root cutout value (50% of blade radius), as discussed in Reference 5. The airframe vertical drag, however, is reduced by the relatively low downwash velocities in the central part of the disc, as discussed in Reference 6. Because of the reduced blade area and tip speed in cruise for the TRAC rotor, the rotor lift in cruise is smaller than for the conventional rotor, and for this reason the required wing area is higher, despite a lower gross weight for the TRAC rotor aircraft. The cruise tip speed is lower for the TRAC rotor, resulting automatically from the reduced diameter in cruise. The conventional rotor must maintain a higher tip speed

to provide adequate flapping stability, because of the higher blade Lock number, as discussed in Appendix C.

The weights of the same two aircraft are compared in Figure 42. The actual weights, on the left of this figure, show that gross weight, empty weight, and fuel weight are all less for the TRAC rotor. The weights expressed as percentage of gross weight are shown in the center of the figure. The empty weight fraction is slightly higher for the TRAC rotor case, but the fuel weight fraction is less. A summary of several major subsystem weight fractions is shown on the right of the figure. The rotor system is substantially heavier for the TRAC rotor, and the wing weight is higher. Most of this increased empty weight fraction is cancelled by modest weight reductions in drive system, engines, fuel system, and vibration suppression weights. The fuel weight reduction is of greater significance than the increase in empty weight fraction. It is this reduction that results in the decrease in actual overall weights.

The drag reduction benefit of the TRAC rotor, which is the key to the superiority of this configuration over the conventional rotor compound at 300 knots, is illustrated in Figure 43. The largest element of drag at the prescribed cruise speed and altitude is airframe parasite drag, which includes rotor head drag. This term is larger for the TRAC rotor aircraft, despite a lower gross weight, because of the slightly larger rotor head required to accommodate the differential gear system utilized to control diameter. Because of the lower rotor lift achievable in cruise, the wing is larger on the TRAC aircraft, and both the profile and induced drag terms are larger for that reason. The drag of the rotor itself, however, is greatly reduced by the small cruise diameter. The actual drag force is reduced and, just as significant from a performance standpoint, the rotor shaft power requirement is reduced. As a result, the total rotor equivalent drag (the sum of the actual drag force and the drag equivalent of the power) is only about one-third of the drag of the conventional rotor, which must operate at rpm approximately 25 percent below the hover value to achieve the level shown for it. Somewhat lower drags for the conventional rotor would result at still lower rpm values, but only at the expense of violating gust response criteria. The low drag afforded by the variable rotor diameter results in lower cruise power required and reduced fuel consumption.

EFFECT OF ALTITUDE ON PERFORMANCE COMPARISONS

The effects of design cruise altitude (standard day) on the configuration comparisons was investigated to determine if there were any significant changes from the results calculated for the 4000 ft 95°F cruise condition. It turned out that some of the qualitative comparisons did change. One reason was the fact that the high temperature condition produces a relatively high speed

of sound and correspondingly low Mach numbers, tending to favor the high tip speed configurations (pure helicopter, helicopter plus auxiliary propulsion, and full rpm conventional compound) relative to the other aircraft types. Because the standard day conditions are, by definition, more typical than hot day conditions, the comparisons conducted for the standard day cruise are considered more meaningful. It should be noted that the full required vertical performance capability at 4000 ft 95°F was retained for all cases. The other important factor was that the optimum cruise altitude tends to increase with cruise speed, so that comparing all configurations at the same altitude is somewhat misleading.

A summary of the effects of design cruise altitude on gross weight, empty weight, and consumed fuel is presented in Figure 44. This figure is comparable to the summary comparison shown in Figure 40, except that multiple design cruise altitudes are shown and the figure is divided into three parts to avoid an excessive number of overlapping lines.

For the pure helicopter, design for sea level cruise minimizes gross weight and empty weight, although minimum fuel consumption results for a design cruise altitude of 5000 ft. The competitiveness of the pure helicopter decreases rapidly at higher design altitudes. Comparison with Figure 40 indicates that the weights are higher at all cruise altitudes for the standard day than for the 4000 ft 95°F case. This is because of the temperature effect on Mach numbers as discussed above. The same effect is apparently true for the helicopter with auxiliary propulsion, although only the 5000-ft altitude case was calculated.

The full rpm conventional compound helicopter (configuration 2) shows the temperature/Mach number effect even more strongly. At 225 knots, the gross weight for a sea level standard design is more than 25 percent heavier than for the 4000 ft 95°F design condition. The 5000-ft-altitude design had a gross weight approaching 50,000 pounds, and there was no design solution at all at 10,000 feet. Whereas at the 4000-ft 95°F condition (Figure 40) the full rpm conventional rotor compound (configuration 2) was substantially lighter than the slowed rotor compound (3) at 225 knots, at the standard day design conditions the situation is reversed as shown in Figure 44(a). It is concluded that the full rpm conventional rotor compound is not really competitive at speeds much above 200 knots.

The slowed conventional rotor compound shows benefits of designing for cruise at altitude not evidenced by the slower aircraft. An altitude of 10,000 feet is beneficial up to the maximum design cruise speed of 300 knots, because of the reduction of drag with decreasing air density. At higher design altitude, the lower temperature and higher Mach numbers result in increasing rotor drag and, hence, weights at the higher cruise speeds. The restrictions on tip speed imposed by the criteria for blade

flapping response to gusts, discussed in Appendix C, prevent an optimum aerodynamic solution at higher altitudes.

The effect of design cruise altitude on the design weights for the two TRAC compound helicopters is shown in Figure 44(b). For these aircraft, the benefits of altitude continue past 10,000 feet to 20,000 feet. At the highest cruise speeds, the reduced rpm TRAC compound (configuration 5) shows small but distinct advantages in weights and fuel consumption over the full rpm cases (configuration 4). The TRAC compounds are superior to the conventional slowed rotor compound at 250 knots, and the competitive advantage increases at higher design speeds at all altitudes.

The effect of design cruise altitude on the stowed rotor configuration is shown in Figure 44(c). This aircraft type has by far the lowest fuel consumption of any of the aircraft for any given design speed in the range studied, the lowest gross weights at design speeds above about 260 knots, and the lowest empty weights at design speeds above about 290 knots. Consumed fuel is lower for the TRAC stowed rotor at a design speed of 300 knots at optimum altitude than for the 175-knot helicopter, despite a higher gross weight.

The aerodynamic advantages of the TRAC rotor are illustrated in Figure 45, which presents overall aircraft lift-drag ratio, equivalent to actual aircraft L/D times propulsive efficiency, as a function of design cruise speed and altitude. Despite the general trend for overall L/D to decrease with increasing forward speed, the TRAC configurations, particularly the stowed rotor, achieve higher overall L/D values and greatly increase the magnitudes of cruise speeds for which competitive L/D's are achieved.

VARIATION OF PAYLOAD AND RANGE REQUIREMENTS

Payload and range requirements on each side of the baseline values were investigated to establish whether the comparisons between aircraft types were significantly affected. Results of this investigation, all conducted for the 4000-ft 95°F cruise condition, are presented in Figures 46 and 47. In Figure 46, values of gross weight, empty weight, and consumed fuel are presented for the various configurations and various cruise speeds, all at a constant range of 350 nautical miles, for payloads from 2000 to 10,000 pounds. In general, the results indicate only minor changes in the relative merits of the various configurations, depending partly on the design cruise speed considered. All of the calculations indicate that larger aircraft become more efficient, i.e., the gross weight, empty weight, and consumed fuel increase by a substantially smaller percentage than the increase in payload. Conversely, the smaller design payload results in less efficient aircraft (lower payload to gross weight fractions).

Similar information for the effects of design range, from 200 to 500 nautical miles, are shown in Figure 47 for a constant payload of 5000 pounds. Again, the variations indicate small changes in the relative merits of the configurations. There is some evidence that at speeds in the range of 300 to 400 knots, the stowed rotor configuration improves its competitive advantage at longer ranges, as might be expected because its of the low drag.

It was concluded that configuration comparisons made at baseline missions are basically valid throughout the spectrum of design payloads and ranges investigated.

EVALUATION OF POINT DESIGN AIRCRAFT

As part of the mission studies investigation, a brief point design study was conducted for each of the basic aircraft configurations of the study. Initial design layouts were updated in accordance with results of the trending studies and performance and operating envelopes were defined. Design conditions were selected to optimize each of the aircraft types.

SELECTION OF DESIGN CONDITIONS

Each of the point designs selected was intended to represent an optimum choice for the particular aircraft type, with consistent ground rules to the extent possible. A standard day rather than a hot day was selected for all point design studies as being more typical of required operating conditions. Standard day conditions also provide more realistic comparisons between the high tip speed and reduced tip speed configurations because of the relationship between temperature and rotor Mach numbers on rotor drag, as discussed in the previous section. The altitude variation information developed in the parametric mission studies was utilized to optimize speed and altitude for each configuration. Full vertical performance capability (500 ft/min vertical rate of climb at design gross weight at 95% IRP) was retained at 4000 ft 95°F conditions for all configurations.

The point design conditions were selected largely on the basis of achieving maximum transport productivity consistent with a reasonable fuel consumption. For this purpose, productivity was defined as $\frac{PL \times V_{BL}}{WE}$ where PL is the payload, V_{BL} is block speed (mission range divided by the total mission time including ground time), and WE is weight empty. Productivity is frequently used as a measure of cost effectiveness of an aircraft, since the rate of doing useful work is proportional to payload and block speed, whereas the cost of the aircraft is generally proportional to empty weight. Charts of productivity and consumed fuel for the baseline missions (payload of 5000 pounds and range of 350 nautical miles) are presented in Figure 48 for a range of cruise speeds and altitudes for the six basic aircraft configurations. The selected points are indicated on each chart.

For the pure helicopter, Figure 48(a), only 175 knots cruise speed was investigated because the parametric studies at 4000 ft 95°F showed that this would be the optimum speed. The productivity is maximum for a sea level design cruise, and decreases at altitude. Despite this, 5000 ft was selected as the design cruise altitude because a sea level design is simply not realistic for typical Army missions where some altitude capability is

required for clearance over the local terrain. Consumed fuel is minimized by designing for 5000 ft, and a further benefit is that maneuver capability and operational envelopes will be enhanced compared to a sea level design.

For the full rpm conventional rotor compound, Configuration 2, the chart shows that a 200 knot cruise speed is clearly superior to a 225-knot design. Again, a minimum altitude of 5000 ft was legislated, but in this case very little penalty in productivity was involved.

No comparable chart was prepared for the helicopter with auxiliary propulsion (Configuration 1A) because fewer parametric variations were investigated for this aircraft. A point design speed of 190 knots (the best speed indicated by the 4000-ft 95°F studies), and a design cruise altitude of 5000 ft were selected. It is believed that this design point is close to optimum for this configuration, because it is an intermediate step between Configurations 1 and 2, both of which are better defined.

Charts for the reduced rpm conventional rotor compound and the full rpm TRAC rotor compound are shown in Figure 48(b). For this aircraft, a family of curves resulted which permit a reasonably clear-cut choice for the optimum design point. Although the maximum productivity point and minimum fuel point never coincide, the selected points, slightly below maximum productivity in the interest of conserving fuel, represent a good compromise. The selected points are 250 knots at 10,000 ft for the slowed rotor compound and 300 knots at 20,000 ft for the full rpm TRAC rotor compound.

For the slowed rpm TRAC compound, Figure 48(c), the selected design point of 350 knots at 20,000 ft is clearly not optimum from the fuel consumption standpoint; a lower design cruise speed would be better. However, the 350 knot speed was deliberately picked to explore the maximum possible cruise speed for a compound and to separate the design point from that selected for the full rpm TRAC compound.

The stowed rotor aircraft design trade-offs, also shown in Figure 48(c), permit a more reasonable compromise. A design speed of 400 knots at 20,000 ft was selected.

The design cruise speed and altitude for the seven design points are summarized in Figure 49. The optimum cruise altitude generally increases with design cruise speed because of the beneficial effects of reduced density on aircraft drag. The shape of the curve suggested that even higher cruise altitudes might be beneficial for Configurations 5 and 6. This possibility was investigated briefly, but there was little apparent benefit because of a relative deterioration in engine performance capabilities at higher altitudes.

DESCRIPTION OF POINT DESIGN AIRCRAFT

Three-view drawings of the point design aircraft are shown in Figures 50 - 56. Not included are drawings of the helicopter with auxiliary propulsion (which looks essentially identical to the full rpm conventional rotor compound, Configuration 2, except for the absence of a wing and for the number of blades), or of the reduced rpm TRAC compound (which looks identical to the full rpm TRAC compound, Configuration 4, except for the number of blades). Two versions of the stowed TRAC, Configuration 6, are shown. The helicopter design model computer printout summaries for the seven point design aircraft, including major dimensions, physical and aerodynamic attributes, summary weight statements, mission segment descriptions, and life-cycle cost information, are presented in Tables 8 - 14.

The 175-knot pure helicopter, Configuration 1, is shown in Figure 50. It is of conventional main rotor/tail rotor arrangement. Because of the relatively low optimum disc loading, 6 lb/ft^2, this aircraft has the largest diameter rotor of the seven point design aircraft, despite the lowest gross weight.

The 200-knot full rpm conventional rotor compound, Configuration 2, is shown in Figure 51. A pusher propeller, similar in concept to that of the AH-56 Cheyenne design, was assumed. This arrangement provides the simplest transmission and shafting layout and is entirely satisfactory at the design speed of 200 knots where the propulsive force and power required are relatively low. The wing on this aircraft supports about one-half of the weight in cruise flight. The 190-knot helicopter plus auxiliary propulsion, Configuration 1A, looks essentially the same as Configuration 2 except for the lack of a wing and the number of blades (five instead of four).

The 250-knot slowed conventional rotor compound, Configuration 3, is shown in Figure 52. Because of the increased propulsive power relative to that of Configuration 2, the pusher propeller configuration would be considerably heavier and would not balance satisfactorily. The best arrangement was to utilize two propulsive units on the wings, which are large enough to accommodate the two engines as well. Shaft-driven shrouded cruise fans, such as the Hamilton Standard Q-Fan, were assumed. At speeds of 250 knots or above, these fans are nearly as efficient as a propeller, require less rpm reduction, reduce noise, provide better clearance for main rotor flapping, and reduce hazard to ground personnel.

The 250-knot compound and all higher speed aircraft were assumed to have a fan-in-fin anti-torque and directional control system, similar to that demonstrated on the Sikorsky S-67 Blackhawk helicopter, Reference 10. The fan-in-fin concept is particularly appropriate for high-speed compound helicopters because it

provides reduced drag in cruise relative to a conventional tail rotor and is not subject to blade flapping instability problems at the high cruise advance ratios. Although the fan-in-fin increases hover power slightly, the higher speed aircraft tend to have a high installed power to satisfy cruise requirements, so that relatively little compromise is required.

The 300-knot full rpm TRAC rotor compound, Configuration 4, is shown in Figure 53. This aircraft looks very similar to the conventional compound, except that in cruise the rotor diameter is only 60 percent of the hover value. Because the TRAC rotor aircraft operates at 20,000 ft cruise altitude, it is assumed that the fuselage is pressurized, with appropriate weight allowances included in the helicopter design model.

The 350-knot slowed rpm TRAC rotor compound, Configuration 5, is similar in appearance and dimensions to Configuration 4, except that it has six blades instead of five. For this reason, a separate drawing was not prepared.

The 400-knot stowed TRAC rotor aircraft, Configuration 6, is shown in two versions in Figures 54 and 56. Both versions assume four blades and a fore-and-aft blade fold arrangement like the one described in the full-scale rotor preliminary design section of this report. The first version of the stowed rotor assumes that, after the blades are stopped and folded fore-and-aft, the rotor is stowed by means of an extensible rotor shaft arrangement, so that the rotor head and blades translate vertically downward without disturbing the main transmission. The extensible rotor shaft configuration, Figure 55, utilizes hydraulic pressure to lock, unlock, and to translate the moveable members, in a manner similar to that described in U.S. Patent No. 3,581,624, Reference 11. The locking arrangement, utilizing conical surfaces forced together by the hydraulic pressure, permits carrying the vibratory shaft bending moment required without the fretting action that would occur with a simple spline. The internal, coaxial diameter change shafts are active only during diameter changes and even then carry only torque, not bending moment, so that two-piece shafts with a simple loose-spline connection provides a satisfactory extensible arrangement.

In order to provide the vertical distance to accommodate the translation, a low-wing configuration is utilized, with the main transmission located below the floor of the cabin. The main rotor driveshaft extends through the fuselage inside a well which is sealed against the cabin pressurization. Although the obstruction in the cabin is undesirable from the point of view of flexibility of loading bulk cargo, the space around the well is wide enough to permit relatively easy fore and aft

movement of passengers, and there are many missions for which the obstruction would not be objectionable. In stowing the blades, doors on the top of the fuselage open when the rotor head and shaft translate downwards, then close again after the rotor is fully down, completely enclosing the blades. The top of the rotor head is a round fairing which forms part of the external fuselage contour.

The alternate stowed rotor aircraft configuration, Figure 56, avoids vertical translation of the rotor after fore-and-aft blade fold, thus simplifying the rotor system design. Instead, the upper fuselage fairing is designed to translate vertically to enclose the blades in cruise, and to retract to a lower position to expose the rotor for low speed operations. This configuration has a slightly humpback appearance in cruise, but the angles are low enough to permit avoidance of a significant drag penalty, and it has the advantage of an unobstructed cargo compartment.

The fan-in-fin unit for both stowed rotor configurations is assumed to have louvers which close off the duct to reduce parasite drag in cruise flight. The design layouts of this aircraft were defined in sufficient detail to allow weight trending information developed for the added rotor stowing features, as discussed in Appendix D.

COMPARISON OF AIRCRAFT WEIGHTS AND PERFORMANCE PARAMETERS

A summary comparison of gross weight, empty weight, and consumed fuel for the seven point design aircraft is shown in Figure 57. These data are consistent with the information previously presented in Figure 44, but represent the near-optimum design operating conditions selected for each type. Empty weight and gross weight generally increase with design cruise speed as expected, but for the three TRAC rotor aircraft, the speed increases more rapidly than the gross weight such that the productivity based on cruise speed, indicated by the diagonal lines in Figure 57, improves relative to the slower aircraft. The stowed rotor aircraft in particular shows a large gain in productivity.

Consumed fuel is surprisingly similar for the various aircraft. The 175-knot helicopter uses the least fuel of the seven aircraft shown, but the higher speed aircraft use relatively little more. For example, the 250, 300, and 400-knot aircraft each consume less than 25% more fuel than the 175-knot helicopter. This result stems from the reduced rotor drag and increased altitude in progressing from the slower to the faster aircraft. As pointed out in a previous section, if the full rpm TRAC compound were designed for 250 knots rather than 300, or the

stowed TRAC designed for 300 knots rather than 400, the consumed fuel in each case would be reduced to less than that of the 175 knot helicopter.

A comparison of transport productivity is presented in Figure 58. The upper half of the figure shows productivity based on cruise speed, consistent with Figure 57. Productivity is frequently based on block speed, which is less than cruise speed (Appendix C, Figure C-8), and this correction is shown on the lower half of Figure 58. The productivity values are all decreased, and the advantage of speed is diminished slightly, but the results are qualitatively similar. Although the slowed conventional rotor compound suffers slightly relative to the pure helicopter, the TRAC rotor aircraft, particularly the stowed rotor, show productivity advantages as well as the large speed advantage.

A comparison of overall weight fractions, expressed as percentages of gross weight, are presented in Figure 59. Note that each point on any given curve represents a different aircraft. The empty weight fraction generally increases as the configuration design cruise speed increases, with corresponding reductions in payload and useable fuel fractions.

A more detailed breakdown of subsystem weight fractions is shown in Figure 60. Considering the categories one at a time from the top of the figure, the engine weight fraction increases with design cruise speed as would be expected from the variation of power required with speed. The stowed rotor aircraft engine weight falls below this general trend because of the substantial reduction in parasite power that results from stowing the rotor. Empennage and tail rotor weight fraction increases with speed partly because of the increasing main rotor power and torque. The vibration suppression weight fraction increases with speed for the conventional rotor systems, but is reduced for the TRAC rotor aircraft because of the beneficial effects of diameter reduction on vibration, as discussed in Appendix C.

The drive system (transmissions and shafting) weight fraction increases substantially with increasing design cruise speed, because of the increase in installed power. The main rotor weight curve exhibits a more complex shape: the pure helicopter has the heaviest rotor weight fraction because of the requirement that it supply all of the lift and propulsive force in cruise. The helicopter with auxiliary propulsion benefits somewhat from the reduction in propulsive force requirement, and the conventional rotor compound helicopters benefit greatly by the unloading of rotor lift onto a wing, allowing substantially lower blade areas. The TRAC rotor compound helicopters pay a rotor weight penalty for the diameter change capability, and so the curve turns upward again at the higher speeds. The

rotor weight fraction for the stowed rotor configuration is still higher, partly because of the blade fold system requirement and partly because the denominator of the weight fraction, the gross weight, is less for Configuration 6 than for Configuration 5.

The body weight fraction is relatively constant, except for the stowed rotor, for which increased body length and the requirement for a stowage compartment adds a significant penalty. The wing weight fraction is nonexistent for the first two configurations (1 and 1A), reasonably constant for the four highest speed aircraft, and about one-half that value for Configuration 2 because of its smaller wing. The weight fraction for the propeller or fans is zero for the pure helicopter, moderate for the pusher prop aircraft (1A and 2), and highest for the compound helicopters with cruise fans. The fan weight for the stowed rotor is reduced by the relatively low propulsive force requirements corresponding to the low parasite drag. Finally, the fuel system weight is directly proportional to the useable fuel fraction.

Additional insight into the point design aircraft comparisons can be obtained by consideration of various rotor aerodynamic design parameters, presented in Figure 61. The disc loading variation follows the pattern previously established as optimum, as indicated in the discussion of Figure 39. The blade loading parameter, C_T/σ, follows the assumptions discussed in Appendix C. Rotor diameter is largest for the pure helicopter because of the low disc loading, and smallest for the three TRAC vehicles because of the higher disc loading. The curves for rotor solidity and blade area follow directly from the disc loading and blade loading results, and the number of blades is selected on the basis of the required blade area as well as upper and lower constraints placed on blade aspect ratio.

The rotor tip speed and advancing blade Mach number comparisons are shown in Figure 62. Although the assumed tip speed in hover is the same for all vehicles, the tip speed in cruise decreases steadily with the design cruise speed. The "full rpm" Configurations 1A and 2 actually operate at 95 percent rpm to minimize advancing blade Mach number which exceeds 0.9. The reduced tip speed compounds, Configurations 3, 4, and 5, operate at an advancing tip Mach number of slightly below 0.9, desirable from an efficiency standpoint.

Wing area and cruise wing lift are also shown in Figure 62. In the range of 200 to 300 knots, the wing lift curve follows the pattern of wing area with design cruise speed. Ordinarily, wing lift per unit area would increase with the square of the speed, but in this speed range, the cruise altitude is also increasing with speed. Above 300 knots, altitude is constant so that wing

lift per unit area increases. The wing area required for the TRAC stowed rotor follow different ground rules, as discussed in Appendix C, but wing loading remains similar to the next lower speed aircraft.

PERFORMANCE SUMMARIES FOR POINT DESIGN AIRCRAFT

Hover Performance Capability

The effect of altitude on out-of-ground effect (OGE) hover capability is shown in Figure 63 for both hot day and standard day conditions. The hot day temperatures are 50°F higher than for the standard atmosphere at all altitudes; at 4000 ft the temperature is 95°F. At design gross weight, indicated by the square symbols for each configuration, all aircraft can hover OGE at above 4000 ft on a hot day. The specification called for 500 feet per minute vertical rate of climb at 4000 ft 95°F; thus hover at zero rate of climb is possible at higher altitudes. The variation of hover capability (gross weight for OGE hover) with altitude varies in the expected manner. For the hot day conditions, engine power available limits the capability; for the standard day, engine power is limiting at high altitudes and transmission power capacity is limiting at low altitudes. For the standard day, the configurations with low blade loadings (the pure helicopter and the helicopter plus auxiliary propulsion, Configuration 1 and 1A), can hover at somewhat higher altitudes at design gross weight than the high-blade-loading aircraft. At lower altitudes, where the transmission limit is encountered, the improvement in lifting capability is much less for these two aircraft types than for the others. This behavior is explained by the fact that the high blade loading configurations are operating at a C_T/σ below the optimum value (usually on the order of .09 or .10) for maximum hover figure of merit. As altitude decreases, the blade loading gets still farther from optimum. Conversely, the high blade loading aircraft are designed for C_T/σ values above the optimum hover value, and so improve as altitude is decreased.

It is evident from Figure 63 that substantial increases in payload are available if the hover requirement are relaxed from the 4000 ft 95°F condition. Assuming that mission fuel requirements increase directly proportional to the increase in gross weight, the payloads available for sea level standard hover conditions were calculated and are presented in Figure 64. The corresponding increases in productivity are also shown. The increases are substantial: from 80 percent increase for the pure helicopter to as much as 120 percent increase for the TRAC rotor configurations. The increases for the higher speed aircraft are larger than for the slower speed aircraft primarily because the baseline payloads are smaller fractions of the

gross weight. A constant percentage increase in lift capability increase represents a larger actual increase of payload.

The productivity advantage of the TRAC rotor aircraft is increased substantially by relaxed hover requirements. The productivity (payload times block speed divided by empty weight) of the 400-knot stowed TRAC aircraft more than doubles, from 84 to 182 ton knots per ton, when the hover requirement is sea level standard rather than 4000 ft 95°F. Relative to the pure helicopter, the productivity advantage of the stowed TRAC aircraft increases from 20 to 45 percent. For most real missions, the hover requirements will be intermediate to the two conditions shown, with proportional effects on payload and productivity.

Power Required Curves

Power required curves for each of the seven point design aircraft are presented in Figure 65, for three altitudes (standard day) including sea level and the design cruise altitude. Also shown are power available curves corresponding to 95 percent of Intermediate Rated Power (IRP), specified as the limit in hover, and for Maximum Continuous Power (MCP), specified as the limit in cruise. The design cruise point is also indicated for each aircraft. For all configurations except the pure helicopter, the power required curves are broken into low-speed and high-speed regimes. The reason for this is that a transition regime exists at medium speeds in which auxiliary propulsion is applied, and, for some configurations, the rotor is slowed or stopped and stowed. Because there are many possible conversion techniques which influence the power required, no attempt was made to define the curves in the intermediate range. It was established, however, that the aircraft have adequate power and lift capability to fly through the transition corridor. Also indicated in Figure 65 are rotor stall limits and gust sensitivity limits where applicable.

Operating Envelopes

The allowable flight speed/altitude envelopes of the seven aircraft at design gross weight are shown in Figure 66 for both standard day and hot day conditions. The maximum speed boundaries are defined by available power limits except as indicated for rotor stall (the two wingless aircraft) and gust sensitivity as defined in Appendix C (the two slowed rotor compounds). At very low speeds the pure helicopter has somewhat greater altitude capability than the other aircraft, but at speeds higher than approximately 100 knots the winged aircraft configurations are all superior.

The three TRAC rotor aircraft have much larger flight envelopes than the lower speed aircraft. The pure helicopter and the helicopter plus auxiliary propulsion have the smallest overall envelopes, although the helicopter envelope is much larger than the envelopes of most current helicopters at design gross weight. In certain mountainous regions of the world, especially where hot weather prevails, the speed and altitude capability provided by the compound helicopter configurations, and particularly the TRAC compound and TRAC stowed rotor, could prove to be a distinct and perhaps decisive advantage.

The gust sensitivity limits as defined in Appendix C cut the allowable flight speed at low altitudes for the two slowed rotor compounds. These limits can probably be ignored in good weather, but must be considered for all-weather operation. The allowable speed for the 350-knot design slowed TRAC compound (Configuration 5) is cut to less than that for the 300-knot design full rpm TRAC compound (Configuration 4) at low altitudes. This limit could be alleviated by reverting to full rpm when operating at the lower altitudes; speeds at least as high as that for the nominally lower-speed TRAC compound could then be allowed.

Maneuver Envelopes

Speed/load factor diagrams for the six basic configurations are presented in Figure 67. The structural design load factor was 2.5 g's (3.75 g's ultimate) for all aircraft. Curves for maneuver load factor capability at sea level and the design cruise altitude are also shown. The pure helicopter has the best maneuver capability at low speeds, because of the low blade loading employed, but drops significantly with increasing speed and has very little margin above 1 g at cruise. The winged aircraft do very much better; they can all outmaneuver the helicopter at speeds above approximately 140 knots at sea level, and this advantage increases with altitude. If exceptionally maneuverable aircraft were desired, the aerodynamic capability provided by the wing could be fully utilized by accepting the necessary penalty in airframe structural weight.

Payload/Range Characteristics

A comparison of payload/range characteristics of the various point design aircraft, at their respective cruise speeds and altitudes, is shown in Figure 68. Both 4000 ft 95°F hover conditions and sea level standard hover (OGE) are shown. The curves for the 4000 ft 95°F condition all pass through the common point of 5000 pounds payload (design value) and 385 nautical miles (design range plus 10 percent for reserve fuel). For longer ranges auxiliary tanks are assumed, either two 150-gallon units for a range extension of 200-300 nautical miles, or two

350-gallon tanks for still greater capability.

At the 4000 ft 95°F condition, the 175-knot pure helicopter has the lowest consumed fuel for the design mission and therefore the least payload at zero range. Conversely, it has the longest range for a given auxiliary tank size. Next in line are the 400-knot stowed TRAC rotor, the 300-knot full rpm TRAC compound, and the 250-knot slowed conventional rotor compound.

When a sea level standard hover condition is available, the payloads increase substantially. There is no longer a common point because the payloads at the design range increase by different values for the various configurations, as indicated in Figure 64. The three TRAC rotor aircraft have the highest payloads for a given range for the sea level standard hover condition.

It should be noted that the range/payload curves are based on design cruise speed and not the speed for best range. All of the aircraft can achieve significantly longer ranges by operating at less than design cruise speed.

COST COMPARISONS

Aircraft unit acquisition cost and unit life-cycle cost, calculated in accordance with the methods described in Appendix A, are shown in Figures 69 and 70. These costs are based on the assumption of a fleet of aircraft capable of a specified rate of transporting cargo; the number of aircraft required is equivalent to 500 aircraft with a payload of 5000 pounds and a cruise speed of 300 knots. An 85 percent learning curve was assumed for the decrease in unit cost with increase in the number of aircraft produced. Costs are shown in 1974 dollars. Life-cycle costs are based on a utilization of 800 flight hours per year and a service life of 15 years.

As anticipated, the aircraft unit costs, both acquisition and life-cycle costs, are higher for the faster aircraft, partly because of the higher empty weight, greater installed power, etc., and partly because fewer aircraft are built so that there is less benefit from the learning curve. However, the important cost is not unit cost but fleet cost.

Fleet acquisition costs and life-cycle costs are shown in Figures 71 and 72, for three different criteria for the number of aircraft required. The middle value of each bar is consistent with the two previous figures; i.e., the payload is the design value of 5000 pounds and the number of aircraft is inversely proportional to cruise speed. On this basis all three TRAC rotor aircraft, because of the fewer number required, show a fleet life-cycle cost advantage relative to all of the conventional rotor

aircraft. The stowed TRAC configuration is least expensive by a substantial margin. Fleet acquisition cost is also slightly less for the stowed TRAC aircraft than for the pure helicopter.

Basing the number of aircraft on cruise speed, however, is not quite as realistic as using block speed in the equation. The tops of the bars in Figures 71 and 72 show costs and number of aircraft based on block speed rather than cruise speed, for the same 5000-pound payload. The benefits of a high cruise speed are somewhat diminished by this criterion, but the stowed TRAC configuration still has the lowest fleet life-cycle costs.

The most realistic comparison of costs is believed to result when the number of aircraft in the fleet is based on payload capability for typical operating conditions rather than on the design payload at 4000 ft 95°F conditions. The payload capacity for a sea level standard hover is substantially higher, as shown previously in Figure 64, but sea level standard is not a typical operating condition, either. For the present comparisons a payload capability halfway between these two operating conditions, i.e., hover out-of-ground-effect at 2000 ft 77°F, is assumed. The number of aircraft required and fleet life-cycle costs for this criterion are shown by the lowest level on the bars in Figures 71 and 72. On this basis the stowed TRAC rotor aircraft provides the lowest fleet acquisition costs, followed by the pure helicopter, with the other configurations more or less equal at a slightly higher level. With regard to fleet life-cycle costs, all three TRAC rotor aircraft are less expensive than any of the conventional rotor configurations. The 400-knot stowed TRAC life-cycle costs are the lowest, being 20 percent lower than for the lowest-cost conventional rotor aircraft, which is the 250-knot slowed rotor compound, and 21 percent lower than for the 175-knot pure helicopter.

Thus, even without crediting high cruise speed with special advantages that can derive from it, such as increased mission versatility or decreased vulnerability, the TRAC rotor permits increases in transport productivity which will reduce fleet life-cycle costs. There are certain missions, of course, for which high cruise speeds are extremely important. For example, high speed will contribute directly to the value of an aircraft in a search-and-rescue mission, for which the probability of rescue may be inversely proportional to the time required for the rescue aircraft to reach the scene.

Even for missions for which high speed or productivity are of secondary importance, there are potential advantages to be gained from the TRAC rotor. The Reference 1 model test results indicated that there are potential aircraft reliability and maintainability benefits to be gained from the reduced blade stresses and reduced vibration levels demonstrated. The tests also indicated

improved ride comfort because of low gust sensitivity and reduced rotor noise levels because of the low advancing blade Mach number levels. These factors all contribute to the desirability of the TRAC rotor relative to more conventional rotor systems.

CONCLUSIONS

A two-phase analytical investigation was conducted to continue the development and evaluation of the variable-diameter TRAC rotor system. The first phase of the investigation was a preliminary design of a full-scale, flightworthy rotor system suitable for subsequent wind tunnel testing in the NASA-Ames 40-x 80-foot wind tunnel and for flight testing on an H-3 helicopter or the NASA/Army Rotor Systems Research Aircraft (RSRA). The second phase of the investigation was a comparative parametric analysis to evaluate TRAC rotor compound helicopter and stowed rotor aircraft concepts relative to conventional-rotor pure and compound helicopters.

Conclusions from the preliminary design phase of the investigation include the following items:

1. The preliminary design of the flightworthy rotor indicated no serious unresolved problems. Because the basic concept remains unchanged from the design successfully demonstrated with a dynamically scaled model test (Reference 1), successful full-scale development can be anticipated.

2. The selected rotor design has four blades and a diameter of 56 feet in the extended condition; chord of the outer blade is 28 inches; blade twist (extended) is -8 degrees. This rotor has a lifting capability in hover at 4000 feet 95°F conditions well in excess of 20,000 pounds, and an allowable flight speed in excess of 300 knots with the rotor at minimum diameter. Thus, the design is particularly well suited for flight testing on the RSRA in the compound helicopter configuration. The rotor was also designed for in-flight stopping and fore-and-aft blade folding at 150 knots to demonstrate application to the stowed rotor configuration. This capability could be demonstrated both in the NASA Ames 40-x 80-foot wind tunnel and on the RSRA.

3. The blade design provides a fully redundant structure for the main centrifugal load path, so that the blade is potentially "fail-safe". In addition to a redundant strap capable of carrying full ultimate load, down the center of the jackscrew, a BIM type pressurization system is incorporated to monitor the jackscrew structural integrity at all times. The multiple nuts and tension-torsion straps are capable of carrying full ultimate load after failure of some of the members. Additional fail-safe features are also incorporated in the blade design.

4. The diameter change mechanism and diameter measurement system are similar to those previously demonstrated in model tests, except that a locking device and safety stop system were incorporated to prevent the possibility of inadvertent diameter changes or blade overtravel in case the normal diameter-control system malfunctions. In case a fatigue crack should develop in a blade jackscrew, a pressure-actuated switch in th BIM system will prevent actuation of the diameter change clutches.

5. The rotor head configuration is of conventional articulated design except for the incorporation of some of the diameter-change components. The hinge and blade retention system incorporates a number of standard bearings from production helicopter designs. The lag hinge is also utilized as a blade fold hinge; no special fold hinge is required. A design concept for an integrated lag damper/fold actuator was developed.

6. A number of outer blade spar structural concepts were evaluated and sample lengths were fabricated for some of the concepts. The preferred spar design employs a filament-wound graphite/epoxy structure, fabricated over a shaped mandrel for precise control over internal dimensions. This spar concept has the desired combination of high stiffness, low weight, and ease of fabrication.

7. At full rpm, the rotor will change diameter from 100 to 60 percent, or the reverse, in 36 seconds. No blade flapping response will result from initiation of a diameter reduction, a problem noted in the Reference 1 model tests and traced to the applied jackscrew torque reacting against the blade torque tube, resulting in a slight blade twist. The present design avoids this twisting effect by incorporation of a secondary, internal torque tube (nut reaction tube) which transmits the torque directly back to the rotor head.

8. Aeroelastic analysis of the selected blade design indicates that flight in the compound helicopter mode up to 300 knots at sea level and up to 360 knots at altitude can be achieved without exceeding allowable blade component vibratory stress limits. The analysis also shows that lower stresses result from moderate positive rotor lift conditions at high flight speeds than from zero rotor lift conditions.

9. Calculated main rotor group weight, including the diameter change and power blade fold mechanisms, in 2696 pounds. A lighter blade spar was investigated which would permit reduction of rotor weight to 2489 pounds

for a 1980 IOC design. These figures are 16 percent and 7 percent heavier than for an H-3 main rotor with power blade fold, with equivalent blade area and lifting capability. The weight penalty for the TRAC rotor, relative to conventional rotors at comparable technology levels, is estimated to be in the range of 15 to 25 percent, depending on the application.

The parametric mission analysis phase of the investigation included comparison of TRAC rotor aircraft (compound helicopters with either full or slowed rpm and stowed rotor aircraft) with conventional rotor aircraft (pure helicopter and compound helicopter with either full or slowed rpm). Conclusions from this phase include the following:

10. The TRAC rotor aircraft provide distinct performance, operating envelope, and fleet life-cycle cost benefits over conventional rotor aircraft. The 400-knot stowed TRAC rotor aircraft shows the greatest potential for high productivity and low fleet costs, followed by the 300-knot full rpm TRAC compound helicopter. These benefits are in addition to special advantages that can derive from high cruise speed, such as increased mission versatility or reduced vulnerability.

11. None of the concepts investigated show any large productivity or cost benefits over the 175-knot pure helicopter for design speeds less than 250 knots. The conventional rotor compound helicopters have at best only marginal productivity or costs benefits compared to the pure helicopter, because the increased block speeds that they provide do not generally compensate for the additional weight of wings and auxiliary propulsion systems. The TRAC rotor permits significantly higher cruise speeds with relatively little additional weight, resulting in improved productivity.

12. Although the TRAC rotor is heavier than a conventional rotor of equivalent lifting capability and requires a slightly larger wing, most of the empty weight penalty is compensated by reductions in engine and drive system weight, vibration suppression weight, and fuel system weight. Mission fuel weight is reduced significantly because of substantially lower rotor drag.

13. Optimum rotor disc loading increases with increasing design cruise speed. The rate of increase is highest for the high cruise tip speed aircraft, lower for reduced tip speed compound helicopters, and lowest for the stowed rotor configuration.

14. The optimum cruise speed for the pure helicopter was 175 knots. This is higher than for some previous studies because of the low parasite drag assumed. Above 175 knots, the pure helicopter rapidly becomes uncompetitive with the other configurations.

15. The helicopter plus auxiliary propulsion, investigated briefly, shows a small but distinct performance improvement over the pure helicopter at its optimum speed for 190 knots.

16. The full-rpm compound helicopter has a small region of application around 200 knots, but rapidly becomes unattractive at higher speeds because of excessive rotor drag caused by high advancing blade Mach numbers. It should be noted that evaluation of this configuration at hot day (95°F) conditions indicated favorable characteristics up to a design cruise speed of 225 knots, whereas for the more typical standard day conditions, the weights become unacceptable at 225 knots, because of the difference in Mach numbers corresponding to the temperature difference. It was concluded that standard day cruise mode conditions should be used for more realistic comparisons between configurations.

17. The slowed conventional rotor compound helicopter has an optimum cruise speed on the order of 250 knots. At this or higher speeds, it was not possible to design for the aerodynamically optimum operating conditions of altitude and tip speed because of rotor gust response limitations. Even when the gust criteria are satisfied at design cruise speed and altitude, it is necessary to restrict operating conditions at low altitudes to avoid violating the criteria.

18. The TRAC rotor allows increasing the cruise speeds of the compound helicopter configuration up to 350 knots. The low tip speed that results automatically from reducing the diameter reduces blade Mach numbers and rotor drag, and the low blade Lock number that results from telescoping the blades alleviates the gust response problem. The TRAC compound is superior to the conventional rotor compound at all speeds above 250 knots. Above 300 knots, additional tip speed reduction by slowing the rotor rpm shows modest additional benefits to performance and weights, but at the expense of a reduced operating envelope at low altitudes because of the gust criteria.

19. The stowed TRAC rotor configuration has the most attractive performance over the range of 300 to 400 knots,

and achieves higher productivities than any other configuration investigated. Design cruise speeds above 400 knots were not investigated but there is no apparent limitation that would prevent higher speeds.

20. Despite the higher cruise speeds, the fuel consumption of the TRAC rotor aircraft is comparable in magnitude to that of the lower speed aircraft configurations. A TRAC compound helicopter designed for a cruise speed of 250 knots, or a stowed TRAC rotor aircraft designed for 300 knots, will have lower consumed fuel for the baseline mission than the 175-knot pure helicopter, despite higher gross weights. This results from substantially superior overall aircraft lift-drag ratios for the TRAC rotor aircraft configurations.

21. Comparative performance results obtained for the baseline mission of 5000 pounds payload and 350 nautical miles range were generally confirmed for design payloads from 2000 to 10,000 pounds and for design ranges from 200 to 500 nautical miles.

22. All aircraft, designed to hover out of ground effect at 4000 feet 95°F, have substantially higher payloads and productivities if allowed to operate at less stringent ambient conditions. The increases allowed by a sea level standard hover out of ground effect ranges from 80 percent for the pure helicopter to as much as 120 percent for the TRAC rotor aircraft.

23. The pure helicopter investigated has a better speed/altitude operating envelope and better maneuver capability than most existing helicopters because of its relatively low blade loading. Despite this, the winged aircraft configurations exceed the capabilities of the helicopter by substantial margins except at low speeds. The winged aircraft can all outmaneuver the pure helicopter at speeds above approximately 140 knots at sea level, and this advantage increases with altitude. The winged aircraft can also operate at higher altitudes at speeds above approximately 100 knots. The TRAC rotor aircraft have better speed/altitude operating envelopes than any of the conventional rotor aircraft.

24. Despite higher gross weights, the TRAC rotor aircraft have smaller diameter rotors than the pure helicopter because of the difference in optimum design disc loading. All of the aircraft studied for the specified mission are of comparable overall size.

25. Two configurations were examined for the stowed TRAC rotor aircraft. One version utilizes an extensible main rotor shaft to retract the rotor head and blades after stopping and folding, and the other version encloses the rotor by means of a dual-position upper fuselage fairing. Neither version requires displacement of the transmission.

26. Relative aircraft unit costs tend to follow relative weights, with the pure helicopter being the least expensive because it is the lightest. Fleet costs, however, follow a different trend because fewer high-speed aircraft than low-speed aircraft are required for a given fleet transport capability. Fleet life-cycle costs show the benefit to a greater extent than acquisition costs. For typical operating conditions, the TRAC rotor aircraft investigated all have lower life-cycle costs than the conventional rotor aircraft. The 400-knot stowed TRAC rotor aircraft has the lowest fleet life-cycle costs, 20 percent below the best of the conventional rotor aircraft.

27. There are certain missions, e.g., search-and-rescue, for which the high cruise speeds made possible with the TRAC rotor will contribute directly to mission success. Even for missions where speed and productivity are of secondary importance, there are potential reliability and maintainability benefits resulting from reduced blade stresses and vibration levels, and reduced gust sensitivity and reduced noise levels from the reduced blade area and tip speed in cruise. These factors all contribute to the desirability of the TRAC rotor relative to more conventional rotor systems.

LITERATURE CITED

1. Fradenburgh, E. A., Murrill, R. J., and Kiely, E. F., DYNAMIC MODEL WIND TUNNEL TESTS OF A VARIABLE-DIAMETER, TELESCOPING-BLADE ROTOR SYSTEM (TRAC ROTOR), Sikorsky Aircraft Division, United Aircraft Corp., USAAMRDL Technical Report 73-32, Eustis Directorate, U.S. Army Air Mobility R&D Laboratory, Fort Eustis, Va., July 1973, AD771037.

2. Segel, R. M., and Fradenburgh, E. A., DEVELOPMENT OF THE TRAC VARIABLE DIAMETER ROTOR CONCEPT, Paper presented at the AIAA/AHS VTOL Research, Design, and Operations Meeting, Georgia Institute of Technology, Atlanta, Georgia, February 17-19, 1969. AIAA paper No. 69-221.

3. Fradenburgh, E. A., EXTENSION OF COMPOUND HELICOPTER PERFORMANCE BY MEANS OF THE TELESCOPING ROTOR, Paper presented at the Air Force V/STOL Technology and Planning Conference, Las Vegas, Nevada, September 23-25, 1969.

4. Fradenburgh, E. A., APPLICATION OF A VARIABLE DIAMETER ROTOR SYSTEM TO ADVANCED VTOL AIRCRAFT, Paper presented at the American Helicopter Society 31st National Forum, Washington, D. C., May 13-15, 1975.

5. Cassarino, S. J., EFFECT OF ROOT CUTOUT ON HOVER PERFORMANCE, U. S. Air Force Flight Dynamics Laboratory Technical Report AFFDL TR-70-70, June 1970.

6. Cassarino, S. J., EFFECT OF ROTOR BLADE ROOT CUTOUT ON VERTICAL DRAG, USAAVLABS Technical Report 70-59, U. S. Army Aviation Materiel Laboratories, Fort Eustis, Virginia, October 1970, AD877174.

7. USAAMRDL Contract Number DAAJ02-72-C-0049, DESIGN SELECTION TESTS OF TRAC RETRACTION MECHANISM, 1972.

8. Tanner, W. H., CHARTS FOR ESTIMATING ROTARY WING PERFORMANCE IN HOVER AND AT HIGH FORWARD SPEEDS, NASA CR-114, 1964.

9. Carlson, R. G., and Cassarino, S. J., AEROELASTIC ANALYSIS OF A TELESCOPING ROTOR BLADE, USAAMRDL Technical Report 73-48, U. S. Army Air Mobility R&D Laboratory, Fort Eustis, Virginia, August 1973, AD771963.

10. Meier, W. H., Groth, W. P., Clark, D. R., and Verzella, D., FLIGHT TESTING OF A FAN-IN-FIN ANTITORQUE AND DIRECTIONAL CONTROL SYSTEM AND A COLLECTIVE FORCE AUGMENTATION SYSTEM (CFAS), USAAMRDL Technical Report 75-19, Eustis Directorate, U. S. Army Air Mobility R&D Laboratory, Fort Eustis, VA., June 1975.

11. U. S. Patent 3,581,624 Issued June 1, 1971, TELESCOPING ROTOR SHAFT, by Robert A. Stone and Frederick C. Beurer.

12. Kefford, N. F. K., and Campbell, B., SIKORSKY HELICOPTER DESIGN MODEL USER'S GUIDE, Sikorsky Engineering Report SER-5851, November 1973.

13. Anon., GENERALIZED METHOD OF PROPELLER PERFORMANCE ESTIMATION, Hamilton Standard Corporation, Hamilton Standard Report PDB6101, Revision A, June 1963.

14. Anon., A PARAMETRIC LIFE CYCLE COST MODEL FOR ARMY HELICOPTERS, AVSCOM Report, March 1974.

15. Anon., ENGINEERING DESIGN HANDBOOK HELICOPTER ENGINEERING-PART ONE., PRELIMINARY DESIGN, Army Materiel Command Pamphlet 706-201.

16. Fradenburgh, E. A., AERODYNAMIC EFFICIENCY POTENTIALS OF ROTARY WING AIRCRAFT, Paper presented at the American Helicopter Society 16th Annual National Forum, May 1960.

17. Williams, R. M., and Montana, P. S., A COMPREHENSIVE PLAN FOR HELICOPTER DRAG REDUCTION, Paper presented at the American Helicopter Society National Symposium on Helicopter Aerodynamic Efficiency, Hartford, Conn., March 6-7, 1975.

18. Keys, Charles, and Wiesner, Robert, GUIDELINES FOR REDUCING HELICOPTER PARASITE DRAG, Paper presented at the American Helicopter Society National Symposium on Helicopter Aerodynamic Efficiency, Hartford, Conn., March 6-7, 1975. Also published in the Journal of the American Helicopter Society, January 1975.

19. Fenaughty, Ronald R., and Beno, Edward A., AIRLOAD, BLADE RESPONSE, AND HUB FORCE MEASUREMENTS ON THE NH-3A COMPOUND HELICOPTER, Journal of Aircraft, Vol. b, No. 5, September-October 1969 pp. 386-391.

20. Bain, Lawrence J., COMPARISON OF THEORETICAL AND EXPERIMENTAL MODEL ROTOR BLADE VIBRATORY SHEAR FORCES, USAAVLABS Technical Report 66-77, October 1967, AD671669.

TABLE 1. COMPARISON OF TRAC ROTOR AERODYNAMIC PARAMETERS WITH OTHER ROTOR SYSTEMS

	TRAC ROTOR PRELIM.DESIGN	H-3 (S-61)	H-34 (S-58)	YUH-60A (UTTAS)
Diameter (2R), ft	56 (fully extended)	62	56	53
Disk area (πR^2), ft^2	2463	3019	2463	2206
Number of blades (b)	4	5	4	4
Blade twist, θ_1, deg	-8 (fully extended)	-8	-8	-16
Mean blade chord ($\bar{c}$), ft	2.14	1.52	1.37	1.73
Blade aspect ratio ($\frac{R}{\bar{c}}$)	13.1	20.4	20.5	15.3
Solidity ($\frac{b\bar{c}}{\pi R}$)	.0972	.0780	.0621	.0831
Effective blade area ($b\bar{c}R$), ft^2	237.4	235.7	153.1	183.3
Typical Rotor Lift (L), lb	21,000	21,000	13,000	16,000
Disk Loading ($\frac{L}{\pi R^2}$) lb/ft^2	8.5	7.0	5.3	7.3
Blade Loading ($\frac{L}{b\bar{c}R}$), lb/ft^2	87.7	89.1	84.9	87.3
Normal Tip Speed (ΩR), ft/sec	660	660	649	730
$C_T/\sigma = L/\pi R^2 \rho (\Omega R)^2 \sigma$				
(a) Sea Level Standard	.0847	.0861	.0848	.0689
(b) 4000 ft 95°F	.1048	.1065	.1049	.0852

TABLE 2. PHYSICAL PROPERTIES OF TRAC OUTER BLADE CONCEPTS.

C = 28 inches 63_2A016 Airfoil

Design No.	Description of Spar	Unit Weight, w (lb/in.)	EI_{xx} x 10^{-6} ($lb\ in.^2$)	EI_{yy} x 10^{-6} ($lb\ in.^2$)	GJ x10^{-6} ($lb\ in.^2$)	$\frac{EI_{xx}}{w}$ x 10^{-6} ($in.^3$)
1	Alum, extrusion nose (integral L.E. ctrwgt.), alum. honeycomb sandwich, boron stiffeners	0.748	257	1795	108	344
2	Alum. honeycomb sandwich, brass L.E. ctrwgt., boron stiffners	0.627	200	1505	58	319
3	2-piece bonded alum. extrusion, brass L.E. ctrwgt.	0.886	195	2255	215	220
4	Alum. extrusion, steel L.E. ctrwgt., graphite/ epoxy L.E. splice	0.860	183	1655	145	213
5	Closed aluminum extrusion (integral L.E. ctrwgt.)	0.797	170	2235	209	213
6	Filament-wound graphite/epoxy, non-structural L.E. ctrwgt., stainless steel liner and abrasion strips	0.650	195	1630	99	300
7	4-piece graphite/epoxy (hand layup), non-structural L.E. ctrwgt.	0.656	198	1920	130	302
8	Filament-wound graphite/epoxy - alum. honeycomb sandwich, brass L.E. ctrwgt., stainless steel liner & abrasion strips	0.573	173	1775	91	302
	Reference Blade - CH-53A Aluminum Spar C=26", R=36' Section properties vary with radius. Values shown for sta. 200 & 400 in	~0.75 average Sta. 200-400	73(Sta. 200) 49(Sta. 400)	690(200) 450(400)	92(200) 52(400)	97(200) 65(400)

* Includes spar, L.E. counterweights, trailing edge fairings, abrasion strips, etc. Numbers apply to constant cross section region.

TABLE 3. MASS PROPERTIES USED IN AEROELASTIC ANALYSIS

Item	Radial Station Feet (Blade Extended)	W (lb/in.)	EI_{xx} $\times 10^{-6}$ ($lb\text{-}in.^2$)	$(I/C)_{xx}$ ($in.^3$)	EI_{yy} $\times 10^{-6}$ ($lb\text{-}in.^2$)	$(I/C)_{yy}$ (LE) ($in.^3$)	GJ $\times 10^{-6}$ ($lb\text{-}in.^2$)	I_B ($lb\ sec^2$)
Sleeve/ Spindle	1.08 - 2.25	9.00	500	12.0	500	12.0	400	.050
Torque* Tube	2.25 - 2.75	1.930	100	5.0	400	8.0	100	.020
	2.75 - 3.5	0.870	60	3.85	300	6.43	50	.010
	3.5 - 15.25	0.452	51.7	3.32	246	5.27	46.5	.0073
	15.25 - 16.33	0.950	60	3.85	400	6.40	50	.015
Outer Blade	14 - 15	1.150	235	9.40	2000	25.6	110	.140
	15 - 16	0.812	215	8.60	1800	23.0	100	.100
	16 - 27	0.650	195	7.80	1630	20.9	98.6	.081
	27 - 27.62	0.812	215	8.60	1800	23.0	100	.100
	27.62 - 28	2.00	250	10.00	2000	25.6	110	.200
Jackscrew	2.25 - 2.5	1.50	20.0	0.725	20.0	0.725	16.0	.0015
	2.5 - 15.5	0.419	5.34	0.235	5.34	0.235	4.35	.0004
Nut/Strap	14 - 15	0.92	10	0.4	15	0.5	8	.0012
	15 - 27.62	0.16	-	-	-	-	-	-

	100% Diam	80% Diam	60% Diam
Mass Moment of Inertia about Flapping Hinge, Slug ft^2	2373	1661	935
First Mass Moment about Flapping Hinge, Slug ft	138.5	123.3	90.8

Materials: Torque Tube - Aluminum, $E = 10 \times 10^6$ psi
Outer Blade - Graphite/Epoxy, $E = 11.2 \times 10^6$, $G = 2 \times 10^6$ psi
Jackscrew - Maraging Steel, $E = 27 \times 10^6$ psi

*For torque tube, W, EI_{xx}, and $(I/C)_{xx}$ include contribution from nut reaction tube. Other parameters neglect nut reaction tube.

TABLE 4. FLIGHT CONDITION FOR AEROELASTIC ANALYSIS

Case	Diameter (%)	V (kn)	RPM (%)	Altitude, ft (Standard Day)	Specified Rotor Operating Conditions			
					Rotor Lift (lb)	Propulsive Force (lb)	Collective Pitch $\theta_{.75}$ (deg)	Rotor Inflow λ
A	100	100	100	Sea Level	18,400	746	-	-
B	100	100	100	Sea Level	21,000	746	-	-
C	100	120	100	Sea Level	18,400	1074	-	-
D	100	150	100	Sea Level	10,000	0	-	-
E	100	150	100	Sea Level	18,400	0	-	-
F	80	175	100	Sea Level	7,000	-	0	-
G	80	200	100	Sea Level	4,000	-	0	-
H	80	220	100	Sea Level	10,000	-	0	-
I	80	260	100	Sea Level	5,000	-	0	-
J	60	300	100	Sea Level	-	-	0	0
K	60	300	100	Sea Level	-	-	0	.020
L	60	300	80	Sea Level	2,000	-	0	-
M	60	360	100	Sea Level	-	-	0	0
N	60	360	100	Sea Level	-	-	0	.020
O	60	360	80	Sea Level	-	-	0	0
P	60	360	80	Sea Level	-	-	0	.025
Q	60	360	80	Sea Level	1,000	-	0	-
R	60	300	100	10,000	-	-	0	0
S	60	300	100	10,000	-	-	[illegible]	.020
T	60	360	80	10,000	-	-	[illegible]	0
U	60	360	80	10,000	-	-	0	.025
V	60	360	80	20,000	-	-	0	0
W	60	360	80	20,000	-	-	0	.025

Blade twist = -8 degrees (Fully Extended). Delta-three angle 30 degrees

TABLE 5. UNIT WEIGHTS SUMMARY - BLADE, RETENTION, AND HINGE

Blade		
Outer Blade Assembly		122.5 lb
Spar and L.E. Counterweights	86.5	
Trailing Edge Pocket	22.3	
Bearing Blocks	3.4	
Tip Block and Misc.	10.3	
Torque Tube Assembly		92.6
Outer Torque Tube and Cuff	60.9	
Nut Reaction Tube	25.3	
Bearing Blocks	6.4	
Jackscrew Assembly		84.9
Jackscrew	58.1	
Redundant Strap	26.8	
Nut/Strap Assembly		37.1
Nut Package (6)	10.4	
Tension-Torsion Straps (12)	26.7	
Total Blade		337.1
Hinge and Blade Retention		
Main Spindle	14.7	
Jackscrew Retention Spindle	3.5	
Yoke	34.7	
Pitch Horn	8.6	
Blade Attachment Hardware	1.3	
Flapping Lock	8.0	
Blade Pitch Bearing System	22.4	
Jackscrew Retention Bearing System	10.5	
Flapping Bearing System	21.5	
Total Hinge and Retention		125.2 lb
Total Flapping Mass		462.3 lb

TABLE 6. OVERALL ROTOR SYSTEM WEIGHTS SUMMARY

	TRAC Rotor Present Preliminary Design		TRAC Rotor 1980 IOC	
	Material	Weight	% Saving	Weight
Blades -				
Outer blade assy. -				
Spar (4)	Graphite/Epoxy	346.0	11.0	304.8
Pocket (4)		89.2	11.9	78.6
Bearing blocks (8)		13.6	-	13.6
Misc.		41.2	-	41.2
Torque tube assy. -				
Outer torque tube (4)	Aluminum	243.6	-	243.6
Nut reaction tube (4)	Steel	101.2	10.6	90.5
Bearing blocks (8)		25.6	-	25.6
Jackscrew assy. -				
Jackscrew (4)	Steel	232.4	10.6	207.8
Redundant strap (4)	Steel	107.2	10.6	95.8
Tension - torsion straps (48)	Steel	106.8	10.6	95.5
Nut package (24)		41.6	10.6	37.2
Total - Blades		1348.4	8.5	1234.2
Diameter Change Mechanism				
Shafts	Steel	93.2	14.4	79.8
Gears	Steel	51.2	10.6	45.8
Housings	Aluminum	44.9	30.0	31.4
Bearings		15.7	10.6	14.0
Brakes	Steel	108.3	18.8	87.9
Misc.		17.0	-	17.0
Total - Diam. Change Mech.		330.2	16.5	275.9
Rotor Head -				
Hub	Ti	170.9	4.2	163.7
Hinge & blade retention -				
Flap	Ti Comp	381.0	4.2	365.0
Lead-Lag	Ti Comp	167.7	4.2	160.7
Pitch	Ti Comp	182.8	4.2	175.1
Blade attach.		5.2	-	5.2
Blade fold		109.3	-	109.3
Total Rotor Head		1016.9	3.7	979.0
Total Rotor Group Weight		2695.6	7.7	2489.1

TABLE 7. SELECTED OPERATING CONDITIONS FOR PARAMETRIC MISSION INVESTIGATIONS

Configuration	Disc Loading	Payload (lb)			Range (Naut. Mile)			Cruise Altitude (ft)					Design Cruise Speed (Kn)											
								95°	Std. Day															
		2000	5000	10,000	200	350	500	4000'	SL	5000	10,000	20,000	150	175	180	190	200	225	250	275	300	325	350	375	400
1. Pure Helicopter	3 values		⊘			⊘		⊘					✓	⊘		✓									
	optimum	✓		✓		✓		✓					✓	✓											
	"		✓		✓		✓	✓					✓	✓											
	"		☑			☑			✓	☑	✓			☑											
1A Helicopter + Aux. Propulsion	3 values		⊘			⊘		⊘							⊘	✓									
	optimum		✓			✓		✓							✓										
	"		☑			☑				☑					☑										
2. Conventional Rotor Compound - Full rpm	3 values		⊘			⊘		⊘								⊘	✓								
	optimum		✓			✓		✓							✓										
	"	✓		✓		✓		✓								✓	✓								
	"		✓		✓		✓									✓	✓								
	"		☑			☑			✓	☑	✓					☑	✓								
3. Conventional Rotor Compound - Slowed	3 values		⊘			⊘		⊘									✓	⊘	✓	✓					
	optimum		✓			✓		✓								✓									
	"	✓		✓		✓		✓									✓	✓							
	"		✓		✓		✓										✓	✓							
	"		☑			☑			✓		☑	✓					✓	☑	✓	✓					
4. TRAC Compound - Full rpm	3 values		⊘			⊘		⊘									✓		✓	✓	✓				
	optimum		✓			✓		✓								✓		✓							
	"	✓		✓		✓		✓									✓	✓		✓					
	"		✓		✓		✓	✓									✓	✓		✓					
	"		☑			☑			✓		✓	✓						✓		☑	✓				
5. TRAC Compound - Slowed	3 values		⊘			⊘		⊘												✓	✓	⊘			
	optimum	✓		✓		✓		✓												✓		✓			
	"		✓		✓		✓	✓												✓		✓			
	"		☑			☑			✓		✓	☑								✓		☑			
6. Stowed TRAC	3 values		⊘			⊘		⊘												✓		✓		⊘	
	optimum		✓			✓		✓									✓	✓							
	"	✓		✓		✓		✓										✓		✓		✓		✓	
	"		✓		✓		✓	✓										✓		✓		✓		✓	
	"		☑			☑			✓		✓	☑						✓		✓		✓		☑	

⊘ Operating Conditions for Baseline Designs

☑ Operating Conditions for Selected Point-Design Investigations

TABLE 8. COMPUTER PRINTOUT SUMMARY FOR POINT DESIGN AIRCRAFT - CONFIGURATION 1 - PURE HELICOPTER - DESIGN CRUISE SPEED 175 KNOTS

DESIGN ATTRIBUTES

GENERAL		MAIN ROTOR		TAIL ROTOR/FAN	
DESIGN G.W.(LB)	19223.	RADIUS (FT)	31.93	RADIUS (FT)	4.89
PAYLOAD (LB)	5000.	CHORD (FT)	2.234	CHORD (FT)	.989
WEIGHT EMPTY (LB)	11260.	NO.OF BLADES	4.0	NO.OF BLADES	4.0
FUEL (LB)	2439.	ROTOR SOLIDITY	.0891	ROTOR SLDTY/AF	.2577
HOVER POWER (SHP)	2382.	TIP SPEED (FPS)	730.0	TIP SPEED (FPS)	700.0
POWER + CLIMB HP	2558.	ASPECT RATIO	14.293	ASPECT RATIO	4.941
MAIN ROTOR DESIGN HP	2151.	CT/SIGMA	.0680	CT/SIGMA	.1223
TAIL ROTOR CANT(DEG)	.00	MAIN ROTOR LIFT	19223.1	TAIL ROTOR LIFT	.0
M.R.DISC LOADING(PSF)	6.00	FIGURE OF MERIT	.7251	FIGURE OF MERIT	.6685
MAIN G.B. DESIGN HP	2942.	BLADE AREA(SQ.FT)	285.4	BLADE AREA(SQ.FT)	19.3

SUMMARY WEIGHT STATEMENT

GROUP	WEIGHT		% GW
MAIN ROTOR GROUP		2896.	15.07
WING GROUP		0.	.00
TAIL GROUP		341.	1.77
TAIL ROTOR/FAN	131.		.68
TAIL SURFACES	210.		1.09
BODY GROUP		1566.	8.15
ALIGHTING GEAR		565.	2.94
FLIGHT CONTROLS		593.	3.08
ENGINE SECTION		136.	.71
PROPULSION GROUP		3154.	16.41
ENGINES	697.		3.63
AIR INDUCTION	19.		.10
EXHAUST SYSTEM	12.		.06
LUBRICATING SYSTEM	0.		.00
FUEL SYSTEM	470.		2.45
ENGINE CONTROLS	19.		.10
STARTING SYSTEM	49.		.26
AUXILIARY PROPULSION PROPELLERS	0.		.00
DRIVE SYSTEM	1888.		9.82
AUXILIARY POWER UNIT		193.	1.00
INSTRUMENTS		183.	.95
HYDRAULICS		82.	.43
ELECTRICAL GROUP		306.	1.59
AVIONICS		325.	1.69
ARMAMENT GROUP		0.	.00
FURNISHINGS		392.	2.04
AIR CONDITIONING AND ANTI-ICE		86.	.45
AUXILIARY GEAR		59.	.31
VIBRATION SUPPRESSION		269.	1.40
TECHNOLOGY SAVINGS		0.	.00
CONTINGENCY		113.	.59
WEIGHT EMPTY		11260.	58.57
FIXED USEFUL LOAD		525.	2.73
PILOT	235.		
CO-PILOT	235.		
OIL-ENGINE	30.		
-TRAPPED	10.		
FUEL TRAPPED	15.		
MISSION EQUIPMENT	0.		
OTHER FUL.	0.		
PAYLOAD		5000.	26.01
FUEL-USABLE		2439.	12.69
GROSS WEIGHT		19223.	

TABLE 8 - Continued

SELECTED DESIGN PARAMETERS

HINGE OFFSET (FT)	1.5329	HINGE LENGTH (FT)	1.5201
MAIN ROTOR BLADE TWIST(DEG)	-14.0000	MAIN ROTOR DESIGN HP	2151.146
MAIN ROTOR RPM	216.290	MAIN ROTOR DESIGN ADV.RATIO	.52668
MAIN ROTOR SHAFT LENGTH(IN)	63.071	TAIL ROTOR SHAFT LENGTH(IN)	14.665
TAIL DRIVE SHAFT LENGTH(IN)	452.921	MAX.TR SUSTAINED THRUST(LB)	2225.15
TAIL ROTOR RPM	1367.45	MRB LOCK NUMBER	8.3163
HORIZONTAL TAIL AREA(SQ.FT)	50.05895	VERTICAL TAIL AREA (SQ.FT)	38.79101
DESIGN HOV. ANTI-TORQUE HP	255.862	HOV.ANTI-TORQUE MOMT(FT-LB)	54345.
REQ.YAW ACCEL.(RAD/SEC/SEC)	.71543	MAX.SUST.YAW MOMENT(FT-LB)	83047.
VERTICAL DRAG	.033143	FUSELAGE WETTED AREA(SQ.FT)	809.9811
ENGINE SCALE FACTOR	.92749	WING AREA (SQ.FT)	.00000
CRUISE PROPULSOR SHAFT HP	.000	TOTAL INSTALLED POWER (HP)	3617.210
PROPULSOR RPM	.000	PROPULSOR DIAMETER (FT)	.00000
MAIN GEARBOX INPUT RPM	20767.08	ENGINE OUTPUT RPM	20767.08
DESIGN HOVER SHAFT HP	2558.171	ALTERNATE HOVER SHAFT HP	2558.171
EQUIV.SLS DESIGN HOVER HP	3617.210	EQUIV.SLS ALTERNATE HOV.HP	3617.210
DESIGN HOVER LAPSE RATE	.70722	ALTERNATE HOVER LAPSE RATE	.70722
HOV.OVERALL MECH.EFFICIENCY	.840892	HOVER FIXED LOSSES (HP)	100.0000
DES.DYNAMIC PRESS(LB/SQ.FT)	100.0000	ACTUAL CRUISE SPEED (KTS)	174.9756
DESIGN CRUISE HP	2239.818	DESIGN CRUISE ROTOR HP	2081.023
EQUIV.SLS STATIC HP-CRUISE	2959.916	CRUISE LAPSE RATE	.75672
CRUISE FIXED LOSSES (HP)	100.0000	DES.CRUISE PROP.THRUST(LB)	.00
CRUISE TIP SPEED (FPS)	730.000	DESIGN CRUISE ADV.RATIO	.40508
DES.CRUISE WING LIFT(LB)	.00	PARASITE DRAG (SQ.FT)	16.371
ULTIMATE LOAD FACTOR	3.7500	HEAD MOMT.CONST.(FT-LB/DEG)	4956.3
PLANFORM HOR.TAIL (SQ.FT)	25.0295	PLANFORM VER.TAIL (SQ.FT)	38.7910
TAIL CANT ANGLE (DEG)	.00	MAIN ROTOR ASPECT RATIO	14.2927
NUMBER OF ROTORS	1.	MAINROTOR SOLIDITY	.08908
MAIN ROTOR RADIUS	31.9346	MAIN ROTOR CHORD	2.23432
MAIN ROTOR TIPSPEED	730.00	NUMBER OF MAIN ROTOR BLADES	4.
ROTOR BLADE CUTOUT/R	.20000	MR BLADE TAPER RATIO	1.000
MAIN ROTOR LIFT (LB)	19223.06	NUMBER OF TAIL ROTOR BLADES	4.
TAIL ROTOR RADIUS (FT)	4.6883	TAIL ROTOR CHORD (FT)	.9893
TAIL ROTOR ASPECT RATIO	4.94119	TAIL ROTOR SOLIDITY/AC.FAC.	.25768
PERCENT POWER,ANTI-TORQUE	10.7425	TAIL ROTOR FM,ANTI-TORQUE	.6685
% HP,ANTI-TORQUE,GIVEN TR	.0000	TR CT/SIG RATIO,ANTI-TORQUE	.1223
TR CT/SIG,MAX.CONT.THRUST	.08000	TR DL,MAX.CON.THR(LB/SQ.FT)	29.6409
TR FM,MAX.CONT.THRUST	.66850	AVAILABLE TR ANTI-TORQUE HP	256.09
TR AN-TORQ.MOMENT(FT-LB)	54345.03	TAIL ROTOR TIPSPEED (FPS)	700.00
MAIN GEARBOX DESIGN HP	2941.90	TR HP,MAX.CONT.THRUST	686.23

TABLE 8 - Concluded

MISSION ANALYSIS

TOGW= 19223.1 LBS., ROTOR RADIUS= 31.93 FT., PARASITE DRAG= 16.4 SQ.FT.

MODE	GR.WT (LBS)	TEMP (DEG.F)	ALT (FT)	OPTN (FPM)	SPEED (KTS)	VSTALL (KTS)	DIST (N.MI)	TIME (MIN)	FL.AR. (SQ.FT)	SHP	FUEL (LBS)	SFC	WARNG
ARMUP	19186.	59.	0.	--	--	--	--	8.0	--	615.9	73.7	.8547	
HOVER	19131.	59.	0.	1000.000	--	--	--	2.0	--	2249.6	36.7	.4667	
CLIMB	19070.	50.	2500.	1000.00	120.0	182.3	10.0	5.0	16.37	2070.3	84.2	.4644	
CRUISE	18535.	41.	5000.	.00	175.0	177.2	165.0	56.6	16.37	2212.3	980.3	.4476	
CRUISE	17562.	41.	5000.	.00	175.0	180.2	165.0	56.6	16.37	2173.6	966.4	.4491	
DESCNT	17059.	50.	2500.	-1000.00	120.0	187.1	10.0	5.0	16.37	679.1	45.1	.7598	
HOVER	17020.	59.	0.	1000.000	--	--	--	2.0	--	1975.7	33.5	.4852	

RESERVE FUEL(10.%)= 222.0 LBS.

TOTAL MISSION FUEL IS 2442.0 LBS.
TOTAL MISSION TIME IS 135.1 MINS

LIFE CYCLE COST SUMMARY		DOLLARS
DEVELOPMENT COST PER AIRCRAFT		70101.
PROTOTYPE COST PER PRODUCTION AIRCRAFT		20768.
RECURRING PRODUCTION COST	798587.	
GFE AVIONICS	100000.	
ENGINE COST	153341.	
(FLYAWAY COST)	(1051928.)	
INITIAL SPARES	331682.	
GROUND SUPPORT EQUIPMENT	63115.	
INIT.TRAINING AND TRAVEL	55948.	
ACQUISITION COST		1502674.
FLIGHT CREW	457200.	
FUEL + OIL	461269.	
REPLENISHMENT SPARES	1369587.	
ORG+D/S+G/S-MAINT	513592.	
DEPOT MAINTENANCE	505140.	
RECURRING TRAINING	293992.	
MAINTENANCE OF GSE	30562.	
OPERATING COST		3631342.
LIFE CYCLE COST		5224885.
PRODUCTIVITY		.03885
FLEET LIFE CYCLE COST		4479098496.

TABLE 9. COMPUTER PRINTOUT SUMMARY FOR POINT DESIGN AIRCRAFT - CONFIGURATION 1A - HELICOPTER PLUS AUXILIARY PROPULSION, DESIGN CRUISE SPEED 190 KNOTS

DESIGN ATTRIBUTES

GENERAL		MAIN ROTOR		TAIL ROTOR/FAN	
DESIGN G.W.(LB)	21429.	RADIUS (FT)	29.20	RADIUS (FT)	4.73
PAYLOAD (LB)	5000.	CHORD (FT)	1.983	CHORD (FT)	.763
WEIGHT EMPTY (LB)	12412.	NO.OF BLADES	5.0	NO.OF BLADES	6.0
FUEL (LB)	3493.	ROTOR SOLIDITY	.1084	ROTOR SLDTY/AF	.3080
HOVER POWER (SHP)	3083.	TIP SPEED (FPS)	730.0	TIP SPEED (FPS)	700.0
HOVER + CLIMB HP	3286.	ASPECT RATIO	14.686	ASPECT RATIO	6.202
MAIN ROTOR DESIGN HP	2729.	CT/SIGMA	.0750	CT/SIGMA	.1294
TAIL ROTOR CANT(DEG)	.00	MAIN ROTOR LIFT	21429.4	TAIL ROTOR LIFT	.0
M.R.DISC LOADING(PSF)	8.60	FIGURE OF MERIT	.7362	FIGURE OF MERIT	.6393
MAIN G.B. DESIGN HP	3779.	BLADE AREA(SQ.FT)	290.3	BLADE AREA(SQ.FT)	21.7

SUMMARY WEIGHT STATEMENT

GROUP	WEIGHT		% GW
MAIN ROTOR GROUP		2907.	13.56
WING GROUP		0.	.00
TAIL GROUP		365.	1.70
TAIL ROTOR/FAN	148.		.69
TAIL SURFACES	217.		1.01
BODY GROUP		1564.	7.30
ALIGHTING GEAR		617.	2.88
FLIGHT CONTROLS		647.	3.02
ENGINE SECTION		168.	.78
PROPULSION GROUP		4104.	19.15
ENGINES	831.		3.88
AIR INDUCTION	23.		.11
EXHAUST SYSTEM	14.		.07
LUBRICATING SYSTEM	0.		.00
FUEL SYSTEM	672.		3.14
ENGINE CONTROLS	23.		.11
STARTING SYSTEM	61.		.28
AUXILIARY PROPULSION PROPELLERS	409.		1.91
DRIVE SYSTEM	2071.		9.66
AUXILIARY POWER UNIT		193.	.90
INSTRUMENTS		183.	.85
HYDRAULICS		88.	.41
ELECTRICAL GROUP		310.	1.45
AVIONICS		325.	1.52
ARMAMENT GROUP		0.	.00
FURNISHINGS		424.	1.98
AIR CONDITIONING AND ANTI-ICE		126.	.59
AUXILIARY GEAR		59.	.28
VIBRATION SUPPRESSION		208.	.97
TECHNOLOGY SAVINGS		0.	.00
CONTINGENCY		124.	.58
WEIGHT EMPTY		12412.	57.92
FIXED USEFUL LOAD		525.	2.45
PILOT	235.		
CO-PILOT	235.		
OIL-ENGINE	30.		
-TRAPPED	10.		
FUEL TRAPPED	15.		
MISSION EQUIPMENT	0.		
OTHER FUL.	0.		
PAYLOAD		5000.	23.33
FUEL-USABLE		3493.	16.30
GROSS WEIGHT		21429.	

TABLE 9 - Continued

SELECTED DESIGN PARAMETERS

HINGE OFFSET (FT) =	1.4916	HINGE LENGTH (FT) =	1.3899
MAIN ROTOR BLADE TWIST(DEG) =	-12.0000	MAIN ROTOR DESIGN HP =	2729.313
MAIN ROTOR RPM =	238.731	MAIN ROTOR DESIGN ADV.RATIO =	.57182
MAIN ROTOR SHAFT LENGTH(IN) =	57.670	TAIL ROTOR SHAFT LENGTH(IN) =	14.193
TAIL DRIVE SHAFT LENGTH(IN) =	417.353	MAX.TR SUSTAINED THRUST(LB) =	2636.40
TAIL ROTOR RPM =	1812.93	MRB LOCK NUMBER =	7.8059
HORIZONTAL TAIL AREA(SQ.FT) =	34.15912	VERTICAL TAIL AREA (SQ.FT) =	37.89832
DESIGN HOV. ANTI-TORQUE HP =	390.685	HOV.ANTI-TORQUE MOMT(FT-LB) =	63047.
REQ.YAW ACCEL.(RAD/SEC/SEC) =	.69149	MAX.SUST.YAW MOMENT(FT-LB) =	90645.
VERTICAL DRAG =	.039641	FUSELAGE WETTED AREA(SQ.FT) =	601.4811
ENGINE SCALE FACTOR =	1.19127	WING AREA (SQ.FT) =	.00000
CRUISE PROPULSOR SHAFT HP =	2120.881	TOTAL INSTALLED POWER (HP) =	4645.940
PROPULSOR RPM =	1809.342	PROPULSOR DIAMETER (FT) =	9.50000
MAIN GEARBOX INPUT RPM =	18324.22	ENGINE OUTPUT RPM =	18324.22
DESIGN HOVER SHAFT HP =	3285.712	ALTERNATE HOVER SHAFT HP =	3285.712
EQUIV.SLS DESIGN HOVER HP =	4645.940	EQUIV.SLS ALTERNATE HOV.HP =	4645.939
DESIGN HOVER LAPSE RATE =	.70722	ALTERNATE HOVER LAPSE RATE =	.70722
HOV.OVERALL MECH.EFFICIENCY =	.830661	HOVER FIXED LOSSES (HP) =	100.0000
DES.DYNAMIC PRESS(LB/SQ.FT) =	104.4398	ACTUAL CRUISE SPEED (KTS) =	190.0000
DESIGN CRUISE HP =	3660.152	DESIGN CRUISE ROTOR HP =	1395.074
EQUIV.SLS STATIC HP-CRUISE =	4635.917	CRUISE LAPSE RATE =	.78952
CRUISE FIXED LOSSES (HP) =	100.0000	DES.CRUISE PROP.THRUST(LB) =	2992.06
CRUISE TIP SPEED (FPS) =	694.000	DESIGN CRUISE ADV.RATIO =	.46268
DES.CRUISE WING LIFT(LB) =	.00	PARASITE DRAG (SQ.FT) =	15.425
ULTIMATE LOAD FACTOR =	3.7500	HEAD MOMT.CONST.(FT-LB/DEG) =	4910.8
PLANFORM HOR.TAIL (SQ.FT) =	17.0796	PLANFORM VER.TAIL (SQ.FT) =	37.8983
TAIL CANT ANGLE (DEG) =	.00	MAIN ROTOR ASPECT RATIO =	14.6864
NUMBER OF ROTORS =	1.	MAINROTOR SOLIDITY =	.10837
MAIN ROTOR RADIUS =	29.2002	MAIN ROTOR CHORD =	1.98824
MAIN ROTOR TIPSPEED =	730.00	NUMBER OF MAIN ROTOR BLADES =	5.
ROTOR BLADE CUTOUT/R =	.20000	MR BLADE TAPER RATIO =	1.000
MAIN ROTOR LIFT (LB) =	21429.41	NUMBER OF TAIL ROTOR BLADES =	6.
TAIL ROTOR RADIUS (FT) =	4.7310	TAIL ROTOR CHORD (FT) =	.7628
TAIL ROTOR ASPECT RATIO =	6.20178	TAIL ROTOR SOLIDITY/AC.FAC. =	.30795
PERCENT POWER,ANTI-TORQUE =	12.6742	TAIL ROTOR FM,ANTI-TORQUE =	.6393
% HP,ANTI-TORQUE,GIVEN TR =	.0000	TR CT/SIG RATIO,ANTI-TORQUE =	.1294
TR CT/SIG,MAX.CONT.THRUST =	.09000	TR DL,MAX.CON.THR(LB/SQ.FT) =	37.4941
TR FM,MAX.CONT.THRUST =	.63929	AVAILABLE TR ANTI-TORQUE HP =	389.90
TR AN-TORQ.MOMENT(FT-LB) =	63047.50	TAIL ROTOR TIPSPEED (FPS) =	700.00
MAIN GEARBOX DESIGN HP =	3776.57	TR HP,MAX.CONT.THRUST =	1352.42

TABLE 9 - Concluded

MISSION ANALYSIS

TOGW= 21429.4 LBS., ROTOR RADIUS= 29.20 FT., PARASITE DRAG= 15.4 SQ.FT.

MODE	GR.WT (LBS)	TEMP (DEG.F)	ALT (FT)	OPTN (ZR/FPM)	SPEED (KTS)	VSTALL (KTS)	DIST (N.MI)	TIME (MIN)	FL.AR. (SQ.FT)	SHP	FUEL (LBS)	SFC	WARNG
WARMUP	21362.	59.	0.	--	--	--	--	8.0	--	791.0	94.7	.8547	
HOVER	21311.	59.	0.	1000.000	--	--	--	2.0	--	2850.1	46.7	.8645	
CLIMB	21236.	58.	2500.	1000.00	120.0	*****	10.0	5.0	15.43	2499.3	103.4	.4728	
CRUISE	20467.	41.	5000.	.00	190.0	*****	165.0	52.1	15.43	3618.5	1424.7	.4318	
CRUISE	19053.	41.	5000.	.00	190.0	*****	165.0	52.1	15.43	3558.6	1403.2	.4324	
DESCNT	18327.	50.	2500.	-1000.00	120.0	*****	10.0	5.0	15.43	928.8	59.5	.7327	
HOVER	18277.	59.	0.	1000.000	--	--	--	2.0	--	2365.3	41.1	.4970	

RESERVE FUEL(10.1)= 317.3 LBS.

TOTAL MISSION FUEL IS 3490.8 LBS.
TOTAL MISSION TIME IS 126.2 MINS

LIFE CYCLE COST SUMMARY		DOLLARS
DEVELOPMENT COST PER AIRCRAFT		80751.
PROTOTYPE COST PER PRODUCTION AIRCRAFT		26936.
RECURRING PRODUCTION COST	969137.	
GFE AVIONICS	100000.	
ENGINE COST	187335.	
(FLYAWAY COST)	(1256471.)	
INITIAL SPARES	401503.	
GROUND SUPPORT EQUIPMENT	75388.	
INIT.TRAINING AND TRAVEL	56881.	
ACQUISITION COST		1790243.
FLIGHT CREW	457200.	
FUEL + OIL	706043.	
REPLENISHMENT SPARES	1498384.	
ORG+D/S+G/S MAINT	553727.	
DEPOT MAINTENANCE	554233.	
RECURRING TRAINING	299420.	
MAINTENANCE OF GSE	33239.	
OPERATING COST		4102246.
LIFE CYCLE COST		6000175.
PRODUCTIVITY		.03827
FLEET LIFE CYCLE COST		4736980608.

TABLE 10. COMPUTER PRINTOUT SUMMARY FOR POINT DESIGN AIRCRAFT - CONFIGURATION 2 - CONVENTIONAL COMPOUND HELICOPTER - FULL RPM, DESIGN CRUISE SPEED 200 KNOTS

DESIGN ATTRIBUTES

GENERAL		MAIN ROTOR		TAIL ROTOR/FAN	
DESIG. G.W.(LB)	21666.	RADIUS (FT)	26.26	RADIUS (FT)	5.19
PAYLOAD (LB)	5000.	CHORD (FT)	1.794	CHORD (FT)	.868
WEIGHT EMPTY (LB)	12578.	NO.OF BLADES	4.0	NO.OF BLADES	6.0
FUEL (LB)	3563.	ROTOR SOLIDITY	.0870	ROTOR SLDTY/AF	.3197
HOVER POWER (SHP)	3983.	TIP SPEED (FPS)	730.0	TIP SPEED (FPS)	700.0
HOVER + CLIMB HP	4193.	ASPECT RATIO	14.642	ASPECT RATIO	5.973
MAIN ROTOR DESIGN HP	3506.	CT/SIGMA	.1200	CT/SIGMA	.1206
TAIL ROTOR CANT(DEG)	.00	MAIN ROTOR LIFT	21666.1	TAIL ROTOR LIFT	.0
M.R.DISC LOADING(PSF)	10.30	FIGURE OF MERIT	.6656	FIGURE OF MERIT	.6326
MAIN G.B. DESIGN HP	4822.	BLADE AREA(SQ.FT)	188.4	BLADE AREA(SQ.FT)	27.0

SUMMARY WEIGHT STATEMENT

GROUP	WEIGHT		% GW
MAIN ROTOR GROUP		1751.	8.08
WING GROUP		465.	2.15
TAIL GROUP		476.	2.20
TAIL ROTOR/FAN	188.		.87
TAIL SURFACES	288.		1.33
BODY GROUP		1571.	7.25
ALIGHTING GEAR		622.	2.87
FLIGHT CONTROLS		724.	3.34
ENGINE SECTION		206.	.95
PROPULSION GROUP		4581.	21.14
ENGINES	985.		4.55
AIR INDUCTION	28.		.13
EXHAUST SYSTEM	18.		.08
LUBRICATING SYSTEM	0.		.00
FUEL SYSTEM	687.		3.17
ENGINE CONTROLS	28.		.13
STARTING SYSTEM	75.		.34
AUXILIARY PROPULSION PROPELLERS	579.		2.67
DRIVE SYSTEM	2180.		10.06
AUXILIARY POWER UNIT		193.	.89
INSTRUMENTS		183.	.84
HYDRAULICS		89.	.41
ELECTRICAL GROUP		310.	1.43
AVIONICS		325.	1.50
ARMAMENT GROUP		0.	.00
FURNISHINGS		424.	1.96
AIR CONDITIONING AND ANTI-ICE		126.	.58
AUXILIARY GEAR		59.	.27
VIBRATION SUPPRESSION		347.	1.60
TECHNOLOGY SAVINGS		0.	.00
CONTINGENCY		126.	.58
WEIGHT EMPTY		12578.	58.05
FIXED USEFUL LOAD		525.	2.42
PILOT	235.		
CO-PILOT	235.		
OIL-ENGINE	30.		
-TRAPPED	10.		
FUEL TRAPPED	15.		
MISSION EQUIPMENT	0.		
OTHER FUL.	0.		
PAYLOAD		5000.	23.08
FUEL-USABLE		3563.	16.45
GROSS WEIGHT		21666.	

TABLE 10 - Continued

SELECTED DESIGN PARAMETERS

HINGE OFFSET (FT) =	1.2685	HINGE LENGTH (FT) =	1.2500
MAIN ROTOR BLADE TWIST(DEG) =	-12.0000	MAIN ROTOR DESIGN HP =	3507.660
MAIN ROTOR RPM =	265.448	MAIN ROTOR DESIGN ADV.RATIO =	.41671
MAIN ROTOR SHAFT LENGTH(IN) =	51.866	TAIL ROTOR SHAFT LENGTH(IN) =	15.556
TAIL DRIVE SHAFT LENGTH(IN) =	386.793	MAX.TR SUSTAINED THRUST(LB) =	3064.79
TAIL ROTOR RPM =	1289.12	MRB LOCK NUMBER =	8.0507
HORIZONTAL TAIL AREA(SQ.FT) =	47.02951	VERTICAL TAIL AREA (SQ.FT) =	48.70618
DESIGN HOV. ANTI-TORQUE HP =	501.789	HOV.ANTI-TORQUE MOMT(FT-LB) =	72372.
REQ.YAW ACCEL.(RAD/SEC/SEC) =	.69605	MAX.SUST.YAW MOMENT(FT-LB) =	97650.
VERTICAL DRAG =	.167843	FUSELAGE WETTED AREA(SQ.FT) =	792.6719
ENGINE SCALE FACTOR =	1.52033	WING AREA (SQ.FT) =	166.70766
CRUISE PROPULSOR SHAFT HP =	2546.804	TOTAL INSTALLED POWER (HP) =	5929.268
PROPULSOR RPM =	1562.613	PROPULSOR DIAMETER (FT) =	11.00000
MAIN GEARBOX INPUT RPM =	16220.41	ENGINE OUTPUT RPM =	16220.41
DESIGN HOVER SHAFT HP =	4193.310	ALTERNATE HOVER SHAFT HP =	4193.310
EQUIV.SLS DESIGN HOVER HP =	5929.268	EQUIV.SLS ALTERNATE HOV.HP =	5929.268
DESIGN HOVER LAPSE RATE =	.70722	ALTERNATE HOVER LAPSE RATE =	.70722
HOV.OVERALL MECH.EFFICIENCY =	.836489	HOVER FIXED LOSSES (HP) =	100.0000
DES.DYNAMIC PRESS(LB/SQ.FT) =	115.7227	ACTUAL CRUISE SPEED (KTS) =	200.0000
DESIGN CRUISE HP =	3801.066	DESIGN CRUISE ROTOR HP =	1114.907
EQUIV.SLS STATIC HP-CRUISE =	4789.936	CRUISE LAPSE RATE =	.79355
CRUISE FIXED LOSSES (HP) =	100.0000	DES.CRUISE PROP.THRUST(LB) =	3389.75
CRUISE TIP SPEED (FPS) =	694.000	DESIGN CRUISE ADV.RATIO =	.48703
DES.CRUISE WING LIFT(LB) =	10144.86	PARASITE DRAG (SQ.FT) =	15.377
ULTIMATE LOAD FACTOR =	3.7500	HEAD MOMT.CONST.(FT-LB/DEG) =	2779.4
PLANFORM HOR.TAIL (SQ.FT) =	23.5148	PLANFORM VER.TAIL (SQ.FT) =	48.7062
TAIL CANT ANGLE (DEG) =	.00	MAIN ROTOR ASPECT RATIO =	14.6416
NUMBER OF ROTORS =	1.	MAINROTOR SOLIDITY =	.08696
MAIN ROTOR RADIUS =	26.2612	MAIN ROTOR CHORD =	1.79360
MAIN ROTOR TIPSPEED =	730.00	NUMBER OF MAIN ROTOR BLADES =	4.
ROTOR BLADE CUTOUT/R =	.20000	MR BLADE TAPER RATIO =	1.000
MAIN ROTOR LIFT (LB) =	21666.05	NUMBER OF TAIL ROTOR BLADES =	6.
TAIL ROTOR RADIUS (FT) =	5.1853	TAIL ROTOR CHORD (FT) =	.8681
TAIL ROTOR ASPECT RATIO =	5.97331	TAIL ROTOR SOLIDITY/AC.FAC. =	.31973
PERCENT POWER,ANTI-TORQUE =	12.5992	TAIL ROTOR FM,ANTI-TORQUE =	.6326
% HP,ANTI-TORQUE,GIVEN TR =	.0000	TR CT/SIG RATIO,ANTI-TORQUE =	.1206
TR CT/SIG,MAX.CONT.THRUST =	.09000	TR DL,MAX.CON.THR(LB/SQ.FT) =	36.2827
TR FM,MAX.CONT.THRUST =	.63258	AVAILABLE TR ANTI-TORQUE HP =	501.09
TR ANTI-TORQ.MOMENT(FT-LB) =	72872.17	TAIL ROTOR TIPSPEED (FPS) =	700.00
MAIN GEARBOX DESIGN HP =	4822.31	TR HP,MAX.CONT.THRUST =	1164.25

TABLE 10 - Concluded

MISSION ANALYSIS

TOGW= 21666.1 LBS., ROTOR RADIUS= 26.26 FT., PARASITE DRAG= 15.4 SQ.FT.

MODE	GR.WT (LBS)	TEMP (DEG.F)	ALT (FT)	OPTN (FR/FPM)	SPEED (KTS)	VSTALL (KTS)	DIST (N.MI)	TIME (MIN)	FL.AR. (SQ.FT)	SHP	FUEL (LBS)	SFC	WARNG
WARMUP	21666.	59.	0.	--	--	--	--	8.0	--	1009.5	120.8	.8547	
HOVER	21517.	59.	0.	1000.000	--	--	--	2.0	--	3326.1	56.0	.4899	
CLIMB	21456.	50.	2500.	2000.00	150.0	*****	6.2	2.5	15.38	3264.3	67.1	.4697	
CRUISE	20678.	41.	5000.	.00	200.0	*****	168.7	50.6	15.38	3732.5	1472.0	.4452	
CRUISE	19222.	41.	5000.	.00	200.0	*****	168.7	50.6	15.38	3643.9	1443.6	.4472	
DESCNT	18490.	50.	2500.	-2000.00	150.0	*****	6.2	2.5	15.38	887.6	33.8	.8706	
HOVER	18449.	59.	0.	1000.000	--	--	--	2.0	--	2615.9	48.0	.5245	

RESERVE FUEL(10.%)= 324.1 LBS.

TOTAL MISSION FUEL IS 3565.5 LBS.
TOTAL MISSION TIME IS 118.3 MINS

LIFE CYCLE COST SUMMARY		DOLLARS
DEVELOPMENT COST PER AIRCRAFT		85694.
PROTOTYPE COST PER PRODUCTION AIRCRAFT		28611.
RECURRING PRODUCTION COST	940163.	
GFE AVIONICS	100000.	
ENGINE COST	227699.	
(FLYAWAY COST)	(1267862.)	
INITIAL SPARES	431166.	
GROUND SUPPORT EQUIPMENT	76072.	
INIT.TRAINING AND TRAVEL	57015.	
ACQUISITION COST		1832115.
FLIGHT CREW	457200.	
FUEL + OIL	769697.	
REPLENISHMENT SPARES	1516916.	
ORG+D/S+G/S MAINT	559502.	
DEPOT MAINTENANCE	561297.	
RECURRING TRAINING	300201.	
MAINTENANCE OF GSE	33624.	
OPERATING COST		4198437.
LIFE CYCLE COST		6144057.
PRODUCTIVITY		.03975
FLEET LIFE CYCLE COST		4608642688.

TABLE 11. COMPUTER PRINTOUT SUMMARY FOR POINT DESIGN AIRCRAFT - CONFIGURATION 3 - CONVENTIONAL COMPOUND HELICOPTER - SLOWED, DESIGN CRUISE SPEED 250 KNOTS

DESIGN ATTRIBUTES

GENERAL		MAIN ROTOR		TAIL ROTOR/FAN	
DESIGN G.W.(LB)	24654.	RADIUS (FT)	29.53	RADIUS (FT)	2.45
PAYLOAD (LB)	5000.	CHORD (FT)	1.811	CHORD (FT)	********
WEIGHT EMPTY (LB)	16138.	NO.OF BLADES	4.0	NO.OF BLADES	13.0
FUEL (LB)	2991.	ROTOR SOLIDITY	.0781	ROTOR SLDTY/AF	1220.0547
HOVER POWER (SHP)	4575.	TIP SPEED (FPS)	730.0	TIP SPEED (FPS)	700.0
HOVER + CLIMB HP	4824.	ASPECT RATIO	16.335	ASPECT RATIO	********
MAIN ROTOR DESIGN HP	3849.	CT/SIGMA	.1200	CT/SIGMA	.0000
TAIL ROTOR CANT(DEG)	.00	MAIN ROTOR LIFT	24654.3	TAIL ROTOR LIFT	.0
M.R.DISC LOADING(PSF)	9.00	FIGURE OF MERIT	.6538	FIGURE OF MERIT	1.0726
MAIN G.B. DESIGN HP	5546.	BLADE AREA(SQ.FT)	213.9	BLADE AREA(SQ.FT)	*******

SUMMARY WEIGHT STATEMENT

GROUP	WEIGHT		% GW
MAIN ROTOR GROUP		1978.	8.02
WING GROUP		906.	3.67
TAIL GROUP		616.	2.50
TAIL ROTOR/FAN	266.		1.08
TAIL SURFACES	350.		1.42
BODY GROUP		1978.	8.02
ALIGHTING GEAR		690.	2.80
FLIGHT CONTROLS		809.	3.28
ENGINE SECTION		651.	2.64
PROPULSION GROUP		5893.	23.90
ENGINES	1087.		4.41
AIR INDUCTION	0.		.00
EXHAUST SYSTEM	20.		.08
LUBRICATING SYSTEM	0.		.00
FUEL SYSTEM	576.		2.34
ENGINE CONTROLS	33.		.13
STARTING SYSTEM	85.		.35
AUXILIARY PROPULSION PROPELLERS	1308.		5.31
DRIVE SYSTEM	2784.		11.29
AUXILIARY POWER UNIT		193.	.78
INSTRUMENTS		183.	.74
HYDRAULICS		96.	.39
ELECTRICAL GROUP		434.	1.76
AVIONICS		325.	1.32
ARMAMENT GROUP		0.	.00
FURNISHINGS		424.	1.72
AIR CONDITIONING AND ANTI-ICE		126.	.51
AUXILIARY GEAR		59.	.24
VIBRATION SUPPRESSION		616.	2.50
TECHNOLOGY SAVINGS		0.	.00
CONTINGENCY		161.	.65
WEIGHT EMPTY		16138.	65.46
FIXED USEFUL LOAD		525.	2.13
PILOT	235.		
CO-PILOT	235.		
OIL-ENGINE	30.		
-TRAPPED	10.		
FUEL TRAPPED	15.		
MISSION EQUIPMENT	0.		
OTHER FUL.	0.		
PAYLOAD		5000.	20.28
FUEL-USABLE		2991.	12.13
GROSS WEIGHT		24654.	

TABLE 11 - Continued

SELECTED DESIGN PARAMETERS

HIN F OFFSET (FT) =	1.4765	HINGE LENGTH (FT) =	1.4026
MAIN ROTOR BLADE TWIST(DEG) =	-6.0000	MAIN ROTOR DESIGN HP =	3949.382
MAIN ROTOR RPM =	238.072	MAIN ROTOR DESIGN ADV.RATIO =	.41671
MAIN ROTOR SHAFT LENGTH(IN) =	59.320	TAIL ROTOR SHAFT LENGTH(IN) =	7.350
TAIL DRIVE SHAFT LENGTH(IN) =	383.879	MAX.TR SUSTAINED THRUST(LB) =	2460.26
TAIL ROTOR RPM =	2728.52	MRP LOCK NUMBER =	7.6793
HORIZONTAL TAIL AREA(SQ.FT) =	67.19399	VERTICAL TAIL AREA (SQ.FT) =	53.45122
DESIGN HOV. ANTI-TORQUE HP =	778.067	HOV.ANTI-TORQUE MOMT(FT-LB) =	85641.
REQ.YAW ACCEL.(RAD/SEC/SEC) =	.68667	MAX.SUST.YAW MOMENT(FT-LB) =	114759.
VERTICAL DRAG =	.065486	FUSELAGE WETTED AREA(SQ.FT) =	922.5864
ENGINE SCALE FACTOR =	1.74896	WING AREA (SQ.FT) =	252.59372
CRUISE PROPULSOR SHAFT HP =	1775.964	TOTAL INSTALLED POWER (HP) =	6820.951
PROPULSOR RPM =	.000	PROPULSOR DIAMETER (FT) =	4.24209
MAIN GEARBOX INPUT RPM =	6041.02	ENGINE OUTPUT RPM =	15123.07
DESIGN HOVER SHAFT HP =	4823.928	ALTERNATE HOVER SHAFT HP =	4823.928
EQUIV.SLS DESIGN HOVER HP =	6820.951	EQUIV.SLS ALTERNATE HOV.HP =	6820.951
DESIGN HOVER LAPSE RATE =	.70722	ALTERNATE HOVER LAPSE RATE =	.70722
HOV.OVERALL MECH.EFFICIENCY =	.797977	HOVER FIXED LOSSES (HP) =	100.0000
DES.DYNAMIC PRESS(LB/SQ.FT) =	193.8167	ACTUAL CRUISE SPEED (KTS) =	250.0000
DESIGN CRUISE HP =	3965.562	DESIGN CRUISE ROTOR HP =	282.019
EQUIV.SLS STATIC HP-CRUISE =	5563.703	CRUISE LAPSE RATE =	.71276
CRUISE FIXED LOSSES (HP) =	100.0000	DES.CRUISE PROP.THRUST(LB) =	1842.29
CRUISE TIP SPEED (FPS) =	525.000	DESIGN CRUISE ADV.RATIO =	.80476
DES.CRUISE WING LIFT(LB) =	20594.74	PARASITE DRAG (SQ.FT) =	12.299
ULTIMATE LOAD FACTOR =	3.7500	HEAD MOMT.CONST.(FT-LB/DEG) =	3321.1
PLANFORM HOR.TAIL (SQ.FT) =	33.5970	PLANFORM VER.TAIL (SQ.FT) =	53.4512
TAIL CANT ANGLE (DEG) =	.00	MAIN ROTOR ASPECT RATIO =	16.3049
NUMBER OF ROTORS =	1.	MAINROTOR SOLIDITY =	.07809
MAIN ROTOR RADIUS =	29.5291	MAIN ROTOR CHORD =	1.81106
MAIN ROTOR TIPSPEED =	730.00	NUMBER OF MAIN ROTOR BLADES =	4.
ROTOR BLADE CUTOUT/R =	.20000	MR BLADE TAPER RATIO =	1.000
MAIN ROTOR LIFT (LB) =	24654.33	NUMBER OF TAIL ROTOR BLADES =	13.
TAIL ROTOR RADIUS (FT) =	2.4499	TAIL ROTOR CHORD (FT) =	**********
TAIL ROTOR ASPECT RATIO =	**********	TAIL ROTOR SOLIDITY/AC.FAC. =	1220.05466
PERCENT POWER,ANTI-TORQUE =	17.0086	TAIL ROTOR FM,ANTI-TORQUE =	1.0726
% HP,ANTI-TORQUE,GIVEN TR =	.0000	TR CT/SIG RATIO,ANTI-TORQUE =	.0000
TR CT/SIG,MAX.CONT.THRUST =	.00000	TR DL,MAX.CON.THR(LB/SQ.FT) =	131.5416
TR FM,MAX.CONT.THRUST =	1.07264	AVAILABLE TR ANTI-TORQUE HP =	778.07
TR AN-TORQ.MOMENT(FT-LB) =	85640.95	TAIL ROTOR TIPSPEED (FPS) =	700.00
MAIN GEARBOX DESIGN HP =	5547.52	TR HP,MAX.CONT.THRUST =	1242.71

TABLE 11 - Concluded

WGT= 24654.3 LBS., ROTOR RADIUS= 29.53 FT., PARASITE DRAG= 12.3 SQ.FT.

MODE	GR.WT (LBS)	TEMP (DEG.F)	ALT (FT)	OPTN (ZR/FPM)	SPEED (KTS)	VSTALL (KTS)	DIST (N.MI)	TIME (MIN)	FL.AR. (SQ.FT)	SPD	FUEL (LBS)	SFC	WARNG
WARMUP	24565.	59.	0.	--	--	--	--	8.0	--	1161.3	139.0	.857	
HOVER	24483.	59.	0.	1000.000	--	--	--	2.0	--	3651.8	64.7	.4748	
CLIMB	24391.	41.	5000.	2000.00	160.0	*****	15.0	5.0	12.30	2687.7	119.2	.5069	
CRUISE	23761.	23.	10000.	.00	250.0	*****	158.1	38.0	12.30	3894.7	1130.5	.4371	
CRUISE	22641.	23.	10000.	.00	250.0	*****	156.1	36.0	12.30	3610.4	1109.4	.4364	
DESCNT	22642.	41.	5000.	-2000.00	225.0	*****	18.7	5.0	12.30	1949.4	99.1	.5087	
HOVER	21963.	59.	0.	1000.000	--	--	--	2.0	--	3244.5	57.8	.5043	

RESERVE FUEL(10.%)= 272.0 LBS.

TOTAL MISSION FUEL IS 2991.7 LBS.
TOTAL MISSION TIME IS 97.9 MINS

LIFE CYCLE COST SUMMARY		DOLLARS
DEVELOPMENT COST PER AIRCRAFT		125240.
PROTOTYPE COST PER PRODUCTION AIRCRAFT		49313.
RECURRING PRODUCTION COST	1393525.	
GFE AVIONICS	100000.	
ENGINE COST	254704.	
(FLYAWAY COST)	(1748229.)	
INITIAL SPARES	559744.	
GROUND SUPPORT EQUIPMENT	104894.	
INIT.TRAINING AND TRAVEL	59896.	
ACQUISITION COST		2472763.
FLIGHT CREW	457200.	
FUEL + OIL	780083.	
REPLENISHMENT SPARES	1914894.	
O&G+D/S+G/S MAINT	683519.	
DEPOT MAINTENANCE	712993.	
RECURRING TRAINING	316974.	
MAINTENANCE OF GSE	41895.	
OPERATING COST		4907558.
LIFE CYCLE COST		7554875.
PRODUCTIVITY		.03873
FLEET LIFE CYCLE COST		4532924864.

TABLE 12. COMPUTER PRINTOUT SUMMARY FOR POINT DESIGN AIRCRAFT - CONFIGURATION 4 - TRAC COMPOUND HELICOPTER - FULL RPM, DESIGN CRUISE SPEED 300 KNOTS

DESIGN ATTRIBUTES

GENERAL		MAIN ROTOR		TAIL ROTOR/FAN	
DESIGN G.W.(LB)	25469.	RADIUS (FT)	24.97	RADIUS (FT)	2.72
PAYLOAD (LB)	5000.	CHORD (FT)	1.798	CHORD (FT)	********
WEIGHT EMPTY (LB)	16965.	NO.OF BLADES	5.0	NO.OF BLADES	13.0
FUEL (LB)	2979.	ROTOR SOLIDITY	.1146	ROTOR SLDTY/AF	1111.0612
HOVER POWER (SHP)	6192.	TIP SPEED (FPS)	730.0	TIP SPEED (FPS)	700.0
HOVER + CLIMB HP	6442.	ASPECT RATIO	13.689	ASPECT RATIO	********
MAIN ROTOR DESIGN HP	5168.	CT/SIGMA	.1200	CT/SIGMA	.0000
TAIL ROTOR CANT(DEG)	.0	MAIN ROTOR LIFT	25468.9	TAIL ROTOR LIFT	.0
M.R.DISC LOADING(PSF)	13.00	FIGURE OF MERIT	.6117	FIGURE OF MERIT	1.0705
MAIN G.B. DESIGN HP	7409.	BLADE AREA(SQ.FT)	224.5	BLADE AREA(SQ.FT)	*******

SUMMARY WEIGHT STATEMENT

GROUP	WEIGHT		% GW
MAIN ROTOR GROUP		2418.	9.49
WING GROUP		1109.	4.32
TAIL GROUP		775.	3.04
TAIL ROTOR/FAN	327.		1.28
TAIL SURFACES	448.		1.76
BODY GROUP		1922.	7.55
ALIGHTING GEAR		708.	2.78
FLIGHT CONTROLS		844.	3.31
ENGINE SECTION		719.	2.82
PROPULSION GROUP		6366.	25.07
ENGINES	1331.		5.22
AIR INDUCTION	0.		.00
EXHAUST SYSTEM	26.		.10
LUBRICATING SYSTEM	0.		.00
FUEL SYSTEM	574.		2.25
ENGINE CONTROLS	41.		.16
STARTING SYSTEM	109.		.43
AUXILIARY PROPULSION PROPELLERS	1367.		5.37
DRIVE SYSTEM	2939.		11.54
AUXILIARY POWER UNIT		193.	.76
INSTRUMENTS		193.	.76
HYDRAULICS		98.	.38
ELECTRICAL GROUP		310.	1.22
AVIONICS		325.	1.28
ARMAMENT GROUP		0.	.00
FURNISHINGS		424.	1.66
AIR CONDITIONING AND ANTI-ICE		126.	.49
AUXILIARY GEAR		59.	.23
VIBRATION SUPPRESSION		196.	.77
TECHNOLOGY SAVINGS		0.	.00
CONTINGENCY		170.	.67
WEIGHT EMPTY		16965.	66.61
FIXED USEFUL LOAD		525.	2.06
PILOT	235.		
CO-PILOT	235.		
OIL-ENGINE	10.		
-TRAPPED	10.		
FUEL TRAPPED	15.		
MISSION EQUIPMENT	0.		
OTHER FUL.	0.		
PAYLOAD		5000.	19.63
FUEL-USABLE		2979.	11.70
GROSS WEIGHT		25469.	

TABLE 12 - Continued

SELECTED DESIGN PARAMETERS

HINGE OFFSET (FT)	1.2496	HINGE LENGTH (FT)	1.1862
MAIN ROTOR BLADE TWIST(DEG)	-8.0000	MAIN ROTOR DESIGN HP	5168.312
MAIN ROTOR RPM	279.149	MAIN ROTOR DESIGN ADV.RATIO	.41671
MAIN ROTOR SHAFT LENGTH(IN)	49.320	TAIL ROTOR SHAFT LENGTH(IN)	8.167
TAIL DRIVE SHAFT LENGTH(IN)	324.640	MAX.TR SUSTAINED THRUST(LB)	7235.51
TAIL ROTOR RPM	2456.42	MRE LOCK NUMBER	1.4126
HO I.ONTAL TAIL AREA(SQ.FT)	70.22145	VERTICAL TAIL AREA (SQ.FT)	71.76543
DESIGN HOV. ANTI-TORQUE HP	1045.314	HOV.ANTI-TORQUE MOMT(FT-LB)	97241.
R.D.YAW ACCEL.(RAD/SEC/SEC)	.69071	MAX.SUST.YAW MOMENT(FT-LB)	121420.
VERTICAL DRAG	.082397	FUSELAGE WETTED AREA(SQ.FT)	900.0000
ENGINE SCALE FACTOR	2.33578	WING AREA (SQ.FT)	292.24369
CRUISE PROPULSOR SHAFT HP	2164.965	TOTAL INSTALLED POWER (HP)	9109.549
PROPULSOR RPM	.000	PROPULSOR DIAMETER (FT)	4.22446
MAIN GEARBOX INPUT RPM	4500.00	ENGINE OUTPUT RPM	13096.21
DESIGN HOVER SHAFT HP	6442.475	ALTERNATE HOVER SHAFT HP	6442.474
EQUIV.SLS DESIGN HOVER HP	9109.549	EQUIV.SLS ALTERNATE HOV.HP	9109.548
DESIGN HOVER LAPSE RATE	.70722	ALTERNATE HOVER LAPSE RATE	.70722
HOV.OVERALL MECH.EFFICIENCY	.802275	HOVER FIXED LOSSES (HP)	100.0000
DES.DYNAMIC PRESS(LB/SQ.FT)	260.3761	ACTUAL CRUISE SPEED (KTS)	300.0000
DESIGN CRUISE HP	4536.556	DESIGN CRUISE ROTOR HP	71.134
EQUIV.SLS STATIC HP-CRUISE	6687.811	CRUISE LAPSE RATE	.52217
CRUISE FIXED LOSSES (HP)	100.0000	DES.CRUISE PROP.THRUST(LB)	1871.52
CRUISE TIP SPEED (FPS)	415.000	DESIGN CRUISE ADV.RATIO	1.22169
DES.CRUISE WING LIFT(LB)	24456.18	PARASITE DRAG (SQ.FT)	12.886
ULTIMATE LOAD FACTOR	3.7500	HEAD MOMT.CONST.(FT-LB/DEG)	1317.8
PLANFORM HOR.TAIL (SQ.FT)	39.1107	PLANFORM VER.TAIL (SQ.FT)	71.7654
TAIL CANT ANGLE (DEG)	.00	MAIN ROTOR ASPECT RATIO	13.6893
NUMBER OF ROTORS	1.	MAINROTOR SOLIDITY	.11459
MAIN ROTOR RADIUS	24.9723	MAIN ROTOR CHORD	1.79796
MAIN ROTOR TIPSPEED	730.00	NUMBER OF MAIN ROTOR BLADES	5.
ROTOR BLADE CUTOUT/R	.50000	MR BLADE TAPER RATIO	1.000
MAIN ROTOR LIFT (LB)	25468.94	NUMBER OF TAIL ROTOR BLADES	13.
TAIL ROTOR RADIUS (FT)	2.7223	TAIL ROTOR CHORD (FT)	**********
TAIL ROTOR ASPECT RATIO	**********	TAIL ROTOR SOLIDITY/AC.FAC.	1111.06122
PERCENT POWER,ANTI-TORQUE	16.9687	TAIL ROTOR FM,ANTI-TORQUE	1.0705
TR HP,ANTI-TORQUE,GIVEN TR	.0000	TR CT/SIG RATIO,ANTI-TORQUE	.0000
TR CT/SIG,MAX.CONT.THRUST	.00000	TR DL,MAX.CON.THR(LB/SQ.FT)	138.9651
TR FM,MAX.CONT.THRUST	1.07051	AVAILABLE TR ANTI-TORQUE HP	1045.31
TR ANTI-TORQ.MOMENT(FT-LB)	97240.58	TAIL ROTOR TIPSPEED (FPS)	700.00
MAIN GEARBOX DESIGN HP	7408.85	TR HP,MAX.CONT.THRUST	1448.96

TABLE 12 - Concluded

MISSION ANALYSIS

TOGW= 25468.9 LBS.. ROTOR RADIUS= 24.97 FT.. PARASITE DRAG= 12.9 SQ.FT.

MODL	GR.WT (LBS)	TEMP (DEG.F)	ALT (FT)	OPTN (ZR/FPM)	SPEED (KTS)	VSTALL (KTS)	DIST (...MI)	TIME (MIN)	FL.AR. (SQ.FT)	SHP	FUEL (LBS)	SFC	WARNG
WARMUP	25376.	59.	0.	--	--	--	--	8.0	--	1551.0	185.6	.8547	
HOVER	25241.	59.	0.	1000.000	--	--	--	2.0	--	4984.8	84.6	.4849	
CLIMB	25048.	23.	10000.	2000.00	200.0	*****	33.3	10.0	12.89	3646.9	300.4	.4707	
CRUISE	24447.	-12.	20000.	.00	300.0	*****	135.0	27.0	12.89	4448.0	894.2	.4255	
CRUISE	23561.	-12.	20000.	.00	300.0	*****	135.0	27.0	12.89	4367.1	879.2	.4241	
DESCNT	22681.	23.	10000.	-2000.00	260.0	*****	46.7	10.0	12.89	3434.0	287.9	.4790	
HOVER	22799.	59.	0.	1000.000	-	--	--	2.0	--	4207.1	75.8	.5149	

RESERVE FUEL(10.1)= 270.6 LBS.

TOTAL MISSION FUEL IS 2978.5 LBS.
TOTAL MISSION TIME IS 86.0 MINS

LIFE CYCLE COST SUMMARY		DOLLARS
DEVELOPMENT COST PER AIRCRAFT		155196.
PROTOTYPE COST PER PRODUCTION AIRCRAFT		66629.
RECURRING PRODUCTION COST	1547376.	
GFE AVIONICS	100000.	
ENGINE COST	321038.	
(FLYAWAY COST)	(1968414.)	
INITIAL SPARES	654831.	
GROUND SUPPORT EQUIPMENT	118105.	
INIT.TRAINING AND TRAVEL	60565.	
ACQUISITION COST		2801916.
FLIGHT CREW	457200.	
FUEL + OIL	884096.	
REPLENISHMENT SPARES	2007359.	
ORG+D/S+G/S MAINT	712333.	
DEPOT MAINTENANCE	748238.	
RECURRING TRAINING	320870.	
MAINTENANCE OF GSE	43017.	
OPERATING COST		5173912.
LIFE CYCLE COST		8197653.
PRODUCTIVITY		.04421
FLEET LIFE CYCLE COST		4098826656.

TABLE 13. COMPUTER PRINTOUT SUMMARY FOR POINT DESIGN AIRCRAFT - CONFIGURATION 5 - TRAC COMPOUND HELICOPTER - SLOWED, DESIGN CRUISE SPEED 350 KNOTS

DESIGN ATTRIBUTES

GENERAL		MAIN ROTOR		TAIL ROTOR/FAN	
DESIGN G.W.(LB)	28716.	RADIUS (FT)	24.69	RADIUS (FT)	3.32
PAYLOAD (LB)	5000.	CHORD (FT)	1.701	CHORD (FT)	********
WEIGHT EMPTY (LB)	19287.	NO.OF BLADES	6.0	NO.OF BLADES	13.9
FUEL (LB)	3907.	ROTOR SOLIDITY	.1316	ROTOR SLDTY/AF	871.0894
HOVER POWER (SHP)	7769.	TIP SPEED (FPS)	730.0	TIP SPEED (FPS)	700.0
HOVER + CLIMB HP	8061.	ASPECT RATIO	14.511	ASPECT RATIO	********
MAIN ROTOR DESIGN HP	648..	CT/SIGMA	.1200	CT/SIGMA	.0000
TAIL ROTOR CANT(DEG)	.00	MAIN ROTOR LIFT	28718.5	TAIL ROTOR LIFT	.0
M.R.DISC LOADING(PSF)	15.00	FIGURE OF MERIT	.5842	FIGURE OF MERIT	.9596
MAIN G.B. DESIGN HP	9270.	BLADE AREA(SQ.FT)	252.0	BLADE AREA(SQ.FT)	******

SUMMARY WEIGHT STATEMENT

GROUP	WEIGHT		% GW
MAIN ROTOR GROUP		2629.	9.16
WING GROUP		1029.	3.58
TAIL GROUP		1075.	3.74
TAIL ROTOR/FAN	472.		1.64
TAIL SURFACES	604.		2.10
BODY GROUP		2022.	7.04
ALIGHTING GEAR		779.	2.71
FLIGHT CONTROLS		933.	3.25
ENGINE SECTION		818.	2.85
PROPULSION GROUP		7725.	26.90
ENGINES	1688.		5.88
AIR INDUCTION	0.		.00
EXHAUST SYSTEM	34.		.12
LUBRICATING SYSTEM	0.		.00
FUEL SYSTEM	754.		2.62
ENGINE CONTROLS	55.		.19
STARTING SYSTEM	145.		.50
AUXILIARY PROPULSION PROPELLERS	1485.		5.17
DRIVE SYSTEM	3565.		12.41
AUXILIARY POWER UNIT		193.	.67
INSTRUMENTS		193.	.67
HYDRAULICS		106.	.37
ELECTRICAL GROUP		434.	1.51
AVIONICS		325.	1.13
ARMAMENT GROUP		0.	.00
FURNISHINGS		424.	1.48
AIR CONDITIONING AND ANTI-ICE		126.	.44
AUXILIARY GEAR		59.	.21
VIBRATION SUPPRESSION		223.	.78
TECHNOLOGY SAVINGS		0.	.00
CONTINGENCY		193.	.67
WEIGHT EMPTY		19287.	67.16
FIXED USEFUL LOAD		525.	1.83
PILOT	235.		
CO-PILOT	235.		
OIL-ENGINE	30.		
-TRAPPED	10.		
FUEL TRAPPED	15.		
MISSION EQUIPMENT	0.		
OTHER FUL.	0.		
PAYLOAD		5000.	17.41
FUEL-USABLE		3907.	13.60
GROSS WEIGHT		28718.	

TABLE 13 - Continued

SELECTED DESIGN PARAMETERS

HINGE OFFSET (FT)	1.2343	HINGE LENGTH (FT)	1.1726
MAIN ROTOR BLADE TWIST(DEG)	-4.0000	MAIN ROTOR DESIGN HP	6482.456
MAIN ROTOR RPM	282.380	MAIN ROTOR DESIGN ADV.RATIO	.41671
MAIN ROTOR SHAFT LENGTH(IN)	48.756	TAIL ROTOR SHAFT LENGTH(IN)	9.9967
TAIL DRIVE SHAFT LENGTH(IN)	320.925	MAX.TR SUSTAINED THRUST(LB)	4007.93
TAIL ROTOR RPM	2012.03	MRP LOCK NUMBER	1.4185
HORIZONTAL TAIL AREA(SQ.FT)	90.96999	VERTICAL TAIL AREA (SQ.FT)	90.01318
DESIGN HOV. ANTI-TORQUE HP	1317.453	HOV.ANTI-TORQUE MOMT(FT-LB)	120570.
RLD.YAW ACCEL.(RAD/SEC/SEC)	.65607	MAX.SUST.YAW MOMENT(FT-LB)	147286.
VERTICAL DRAG	.077491	FUSELAGE WETTED AREA(SQ.FT)	900.0000
ENGINE SCALE FACTOR	3.28001	WING AREA (SQ.FT)	244.81263
CRUISE PROPULSOR SHAFT HP	3399.128	TOTAL INSTALLED POWER (HP)	12792.037
PROPULSOR RPM	.000	PROPULSOR DIAMETER (FT)	4.27252
MAIN GEARBOX INPUT RPM	4500.00	ENGINE OUTPUT RPM	11043.14
DESIGN HOVER SHAFT HP	6061.131	ALTERNATE HOVER SHAFT HP	6061.130
EQUIV.SLS DESIGN HOVER HP	11398.301	EQUIV.SLS ALTERNATE HOV.HP	11398.299
DESIGN HOVER LAPSE RATE	.70722	ALTERNATE HOVER LAPSE RATE	.70722
HOV.OVERALL MECH.EFFICIENCY	.804162	HOVER FIXED LOSSES (HP)	100.0000
DES.DYNAMIC PRESS(LB/SQ.FT)	354.4008	ACTUAL CRUISE SPEED (KTS)	350.0000
DESIGN CRUISE HP	6995.072	DESIGN CRUISE ROTOR HP	53.306
EQUIV.SLS STATIC HP-CRUISE	12792.037	CRUISE LAPSE RATE	.54683
CRUISE FIXED LOSSES (HP)	100.0000	DES.CRUISE PROP.THRUST(LB)	2518.63
CRUISE TIP SPEED (FPS)	332.000	DESIGN CRUISE ADV.RATIO	1.78163
DES.CRUISE WING LIFT(LB)	27569.75	PARASITE DRAG (SQ.FT)	13.713
ULTIMATE LOAD FACTOR	3.7500	HEAD MOMT.CONST.(FT-LB/DEG)	1458.2
PLANFORM HOR.TAIL (SQ.FT)	45.4850	PLANFORM VER.TAIL (SQ.FT)	90.0132
TAIL CANT ANGLE (DEG)	.00	MAIN ROTOR ASPECT RATIO	14.5106
NUMBER OF ROTORS	1.	MAINROTOR SOLIDITY	.13162
MAIN ROTOR RADIUS	24.6666	MAIN ROTOR CHORD	1.70128
MAIN ROTOR TIPSPEED	730.00	NUMBER OF MAIN ROTOR BLADES	6.
ROTOR BLADE CUTOUT/R	.50000	MR BLADE TAPER RATIO	1.000
MAIN ROTOR LIFT (LB)	28718.49	NUMBER OF TAIL ROTOR BLADES	13.
TAIL ROTOR RADIUS (FT)	3.3223	TAIL ROTOR CHORD (FT)	**********
TAIL ROTOR ASPECT RATIO	**********	TAIL ROTOR SOLIDITY/AC.FAC.	871.08939
PERCENT POWER,ANTI-TORQUE	16.9580	TAIL ROTOR FM,ANTI-TORQUE	.9596
% HP,ANTI-TORQUE,GIVEN TR	.0000	TR CT/SIG RATIO,ANTI-TORQUE	.0000
TR CT/SIG,MAX.CONT.THRUST	.00000	TR DL,MAX.CON.THR(LB/SQ.FT)	115.5843
TR FM,MAX.CONT.THRUST	.95957	AVAILABLE TP ANTI-TORQUE HP	1317.45
TR AN-TORQ.MOMENT(FT-LB)	120570.16	TAIL ROTOR TIPSPEED (FPS)	700.00
MAIN GEARBOX DESIGN HP	9270.30	TR HP,MAX.CONT.THRUST	1900.89

TABLE 13 - Concluded

MISSION ANALYSIS

TOGW= 28718.5 LBS., ROTOR RADIUS= 24.69 FT., PARASITE DRAG= 13.7 SQ.FT.

MODE	GR.WT (LBS)	TEMP (DEG.F)	ALT (FT)	OPTN (ZR/FPM)	SPEED (KTS)	VSTALL (KTS)	DIST (N.MI)	TIME (MIN)	FL.AR. (SQ.FT)	SHP	FUEL (LBS)	SFC	WARNG
WARMUP	28588.	59.	0.	--	--	--	--	8.0	--	2177.9	260.6	.8547	
HOVER	28403.	59.	0.	1000.000	--	--	--	2.0	--	6170.8	108.9	.6062	
CLIMB	28151.	23.	10000.	2000.00	230.0	*****	38.3	10.0	13.71	4660.1	395.0	.4844	
CRUISE	27389.	-12.	20000.	.00	350.0	*****	128.7	22.1	13.71	6870.6	1121.6	.4226	
CRUISE	26276.	-12.	20000.	.00	350.0	*****	128.7	22.1	13.71	6752.4	1103.6	.4231	
DESCNT	25493.	23.	10000.	-2000.00	325.0	*****	54.2	10.0	13.71	5945.2	471.7	.4534	
HOVER	25209.	59.	0.	1000.000	--	--	--	2.0	--	5004.9	96.7	.5521	

RESERVE FUEL(10.%)= 355.8 LBS.

TOTAL MISSION FUEL IS 3913.9 LBS.
TOTAL MISSION TIME IS 76.1 MINS

LIFE CYCLE COST SUMMARY		DOLLARS
DEVELOPMENT COST PER AIRCRAFT		196845.
PROTOTYPE COST PER PRODUCTION AIRCRAFT		92849.
RECURRING PRODUCTION COST	1829958.	
GFE AVIONICS	100000.	
ENGINE COST	421222.	
(FLYAWAY COST)	(2351180.)	
INITIAL SPARES	809990.	
GROUND SUPPORT EQUIPMENT	141071.	
INIT.TRAINING AND TRAVEL	62444.	
ACQUISITION COST		3364685.
FLIGHT CREW	457200.	
FUEL + OIL	1312138.	
REPLENISHMENT SPARES	2266873.	
ORG+D/S+G/S MAINT	793202.	
DEPOT MAINTENANCE	847156.	
RECURRING TRAINING	331807.	
MAINTENANCE OF GSE	49211.	
OPERATING COST		6057587.
LIFE CYCLE COST		9711967.
PRODUCTIVITY		.04537
FLEET LIFE CYCLE COST		4162271808.

TABLE 14. COMPUTER PRINTOUT SUMMARY FOR POINT DESIGN AIRCRAFT - CONFIGURATION 6 - STOWED TRAC ROTOR AIRCRAFT, DESIGN CRUISE SPEED 400 KNOTS

DESIGN ATTRIBUTES

GENERAL		MAIN ROTOR		TAIL ROTOR/FAN	
DESIGN G.W.(LB)	26662.	RADIUS (FT)	25.55	RADIUS (FT)	2.77
PAYLOAD (LB)	5000.	CHORD (FT)	2.274	CHORD (FT)	********
WEIGHT EMPTY (LB)	18201.	NO.OF BLADES	4.0	NO.OF BLADES	13.0
FUEL (LB)	2937.	ROTOR SOLIDITY	.1133	ROTOR SLDTY/AF	1091.9659
HOVER POWER (SHP)	6355.	TIP SPEED (FPS)	730.0	TIP SPEED (FPS)	700.0
HOVER + CLIMB HP	6625.	ASPECT RATIO	11.234	ASPECT RATIO	********
MAIN ROTOR DESIGN HP	5315.	CT/SIGMA	.1200	CT/SIGMA	.0000
TAIL ROTOR CANT(DEG)	.00	MAIN ROTOR LIFT	26662.4	TAIL ROTOR LIFT	.0
M.R.DISC LOADING(PSF)	13.00	FIGURE OF MERIT	.6128	FIGURE OF MERIT	1.0641
MAIN G.B. DESIGN HP	7618.	BLADE AREA(SQ.FT)	232.5	BLADE AREA(SQ.FT)	******

SUMMARY WEIGHT STATEMENT

GROUP	WEIGHT		% GW
MAIN ROTOR GROUP		2902.	10.88
WING GROUP		1032.	3.87
TAIL GROUP		946.	3.55
TAIL ROTOR/FAN	410.		1.54
TAIL SURFACES	536.		2.01
BODY GROUP		2487.	9.33
ALIGHTING GEAR		734.	2.75
FLIGHT CONTROLS		910.	3.41
ENGINE SECTION		438.	1.64
PROPULSION GROUP		6706.	25.15
ENGINES	1435.		5.38
AIR INDUCTION	0.		.00
EXHAUST SYSTEM	28.		.11
LUBRICATING SYSTEM	0.		.00
FUEL SYSTEM	565.		2.12
ENGINE CONTROLS	45.		.17
STARTING SYSTEM	119.		.45
AUXILIARY PROPULSION PROPELLERS	918.		3.44
DRIVE SYSTEM	3595.		13.48
AUXILIARY POWER UNIT		193.	.72
INSTRUMENTS		193.	.72
HYDRAULICS		101.	.38
ELECTRICAL GROUP		310.	1.16
AVIONICS		325.	1.22
ARMAMENT GROUP		0.	.00
FURNISHINGS		424.	1.59
AIR CONDITIONING AND ANTI-ICE		126.	.47
AUXILIARY GEAR		59.	.22
VIBRATION SUPPRESSION		133.	.50
TECHNOLOGY SAVINGS		0.	.00
CONTINGENCY		182.	.68
WEIGHT EMPTY		18201.	68.26
FIXED USEFUL LOAD		525.	1.97
PILOT	235.		
CO-PILOT	235.		
OIL-ENGINE	30.		
-TRAPPED	10.		
FUEL TRAPPED	15.		
MISSION EQUIPMENT	0.		
OTHER FUL.	0.		
PAYLOAD		5000.	18.75
FUEL-USABLE		2937.	11.01
GROSS WEIGHT		26662.	

TABLE 14 - Continued

SELECTED DESIGN PARAMETERS

HINGE OFFSET (FT)	1.2775	HINGE LENGTH (FT)	1.2137
MAIN ROTOR BLADE TWIST(DEG)	-8.0000	MAIN ROTOR DESIGN HP	5314.506
MAIN ROTOR RPM	272.830	MAIN ROTOR DESIGN ADV.RATIO	.41671
MAIN ROTOR SHAFT LENGTH(IN)	50.463	TAIL ROTOR SHAFT LENGTH(IN)	8.310
TAIL DRIVE SHAFT LENGTH(IN)	332.159	MAX.TR SUSTAINED THRUST(LB)	3327.03
TAIL ROTOR RPM	2413.11	MRP LOCK NUMBER	1.3694
HORIZONTAL TAIL AREA(SQ.FT)	96.66072	VERTICAL TAIL AREA (SQ.FT)	73.79543
DESIGN HOV. ANTI-TORQUE HP	1077.684	HOV.ANTI-TORQUE MOMT(FT-LB)	102307.
REQ.YAW ACCEL.(RAD/SEC/SEC)	.67548	MAX.SUST.YAW MOMENT(FT-LB)	128142.
VERTICAL DRAG	.070620	FUSELAGE WETTED AREA(SQ.FT)	964.0000
ENGINE SCALE FACTOR	2.60139	WING AREA (SQ.FT)	251.53215
CRUISE PROPULSOR SHAFT HP	2873.351	TOTAL INSTALLED POWER (HP)	10145.408
PROPULSOR RPM	.000	PROPULSOR DIAMETER (FT)	3.46220
MAIN GEARBOX INPUT RPM	4500.00	ENGINE OUTPUT RPM	12400.17
DESIGN HOVER SHAFT HP	6624.684	ALTERNATE HOVER SHAFT HP	6624.683
EQUIV.SLS DESIGN HOVER HP	9367.189	EQUIV.SLS ALTERNATE HOV.HP	9367.188
DESIGN HOVER LAPSE RATE	.70722	ALTERNATE HOVER LAPSE RATE	.70722
HOV.OVERALL MECH.EFFICIENCY	.802228	HOVER FIXED LOSSES (HP)	100.0000
DES.DYNAMIC PRESS(LB/SQ.FT)	462.8909	ACTUAL CRUISE SPEED (KTS)	400.0000
DESIGN CRUISE HP	5846.701	DESIGN CRUISE ROTOR HP	.000
EQUIV.SLS STATIC HP-CRUISE	10145.408	CRUISE LAPSE RATE	.57629
CRUISE FIXED LOSSES (HP)	100.0000	DES.CRUISE PROP.THRUST(LB)	1862.92
CRUISE TIP SPEED (FPS)	730.000	DESIGN CRUISE ADV.RATIO	.92603
DES.CRUISE WING LIFT(LB)	26662.41	PARASITE DRAG (SQ.FT)	8.655
ULTIMATE LOAD FACTOR	3.7500	HEAD MOMT.CONST.(FT-LB/DEG)	1429.5
PLANFORM HOR.TAIL (SQ.FT)	46.3404	PLANFORM VER.TAIL (SQ.FT)	73.7954
TAIL CANT ANGLE (DEG)	.00	MAIN ROTOR ASPECT RATIO	11.2336
NUMBER OF ROTORS	1.	MAINROTOR SOLIDITY	.11334
MAIN ROTOR RADIUS	25.5567	MAIN ROTOR CHORD	2.27448
MAIN ROTOR TIPSPEED	730.00	NUMBER OF MAIN ROTOR BLADES	4.
ROTOR BLADE CUTOUT/R	.50000	MR BLADE TAPER RATIO	1.000
MAIN ROTOR LIFT (LB)	26662.41	NUMBER OF TAIL ROTOR BLADES	13.
TAIL ROTOR RADIUS (FT)	2.7701	TAIL ROTOR CHORD (FT)	**********
TAIL ROTOR ASPECT RATIO	**********	TAIL ROTOR SOLIDITY/AC.FAC.	1091.96594
PERCENT POWER,ANTI-TORQUE	16.9576	TAIL ROTOR FM,ANTI-TORQUE	1.0641
% HP,ANTI-TORQUE,GIVEN TR	.0000	TR CT/SIG RATIO,ANTI-TORQUE	.0000
TR CT/SIG,MAX.CONT.THRUST	.00000	TR DL,MAX.CON.THR(LB/SQ.FT)	138.0132
TR FM,MAX.CONT.THRUST	1.06406	AVAILABLE TR ANTI-TORQUE HP	1077.68
TR AN-TORQ.MOMENT(FT-LB)	102307.15	TAIL ROTOR TIPSPEED (FPS)	700.00
MAIN GEARBOX DESIGN HP	7616.39	TR HP,MAX.CONT.THRUST	1499.75

TABLE 14 - Concluded

MISSION ANALYSIS

TOGW= 26662.4 LBS., ROTOR RADIUS= 25.55 FT., PARASITE DRAG= 8.7 SQ.FT.

MODE	GR.WT (LBS)	TEMP (DEG.F)	ALT (FT)	OPT (ZRA PM)	SPEED (KTS)	VSTALL (KTS)	DIST (N.MI)	TIME (MIN)	FL.AR. (SQ.FT)	SHP	FUEL (LBS)	SFC	WARNG
WARMUP	26559.	59.	0.	--	--	--	--	8.0	--	1727.3	206.7	.8547	
HOVER	26411.	59.	0.	1000.000	--	--	--	2.0	--	5126.7	89.4	.4953	
CLIMB	26166.	23.	10000.	2000.00	260.0	*****	43.3	10.0	8.66	5105.3	398.8	.4464	
CRUISE	25577.	-12.	20000.	.00	400.0	*****	122.1	18.3	8.66	5758.6	771.1	.4211	
CRUISE	24809.	-12.	20000.	.00	400.0	*****	122.1	18.3	8.66	5697.9	769.4	.4214	
DESCNT	24249.	23.	10000.	-2000.00	325.0	*****	62.5	10.0	8.66	4262.8	346.5	.4649	
HOVER	24034.	59.	0.	1000.000	--	--	--	2.0	--	4378.6	81.1	.5293	

RESERVE FUEL(10.%)= 266.9 LBS.

TOTAL MISSION FUEL IS 2935.9 LBS.
TOTAL MISSION TIME IS 68.6 MINS

LIFE CYCLE COST SUMMARY		DOLLARS
DEVELOPMENT COST PER AIRCRAFT		216586.
PROTOTYPE COST PER PRODUCTION AIRCRAFT		99151.
RECURRING PRODUCTION COST	1746979.	
GFE AVIONICS	100000.	
ENGINE COST	349925.	
(FLYAWAY COST)	(2196904.)	
INITIAL SPARES	726738.	
GROUND SUPPORT EQUIPMENT	131814.	
INIT.TRAINING AND TRAVEL	61565.	
ACQUISITION COST		3117022.
FLIGHT CREW	457200.	
FUEL + OIL	1092125.	
REPLENISHMENT SPARES	2145479.	
ORG+D/S+G/S MAINT	755373.	
DEPOT MAINTENANCE	800885.	
RECURRING TRAINING	326691.	
MAINTENANCE OF GSE	46688.	
OPERATING COST		5624441.
LIFE CYCLE COST		9057200.
PRODUCTIVITY		.05494
FLEET LIFE CYCLE COST		3396449952.

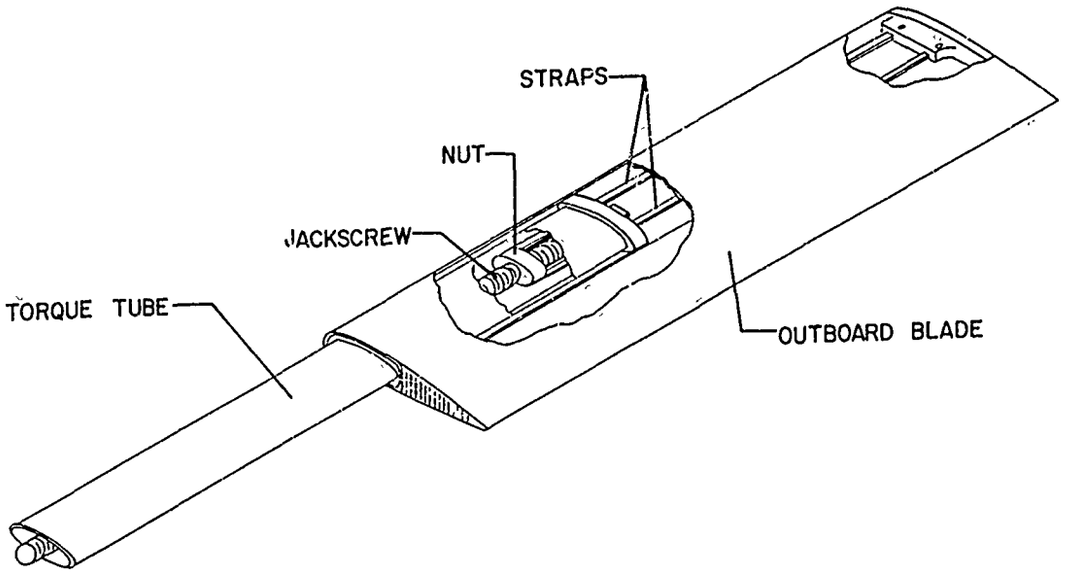

Figure 1. TRAC Rotor Blade Schematic Arrangement.

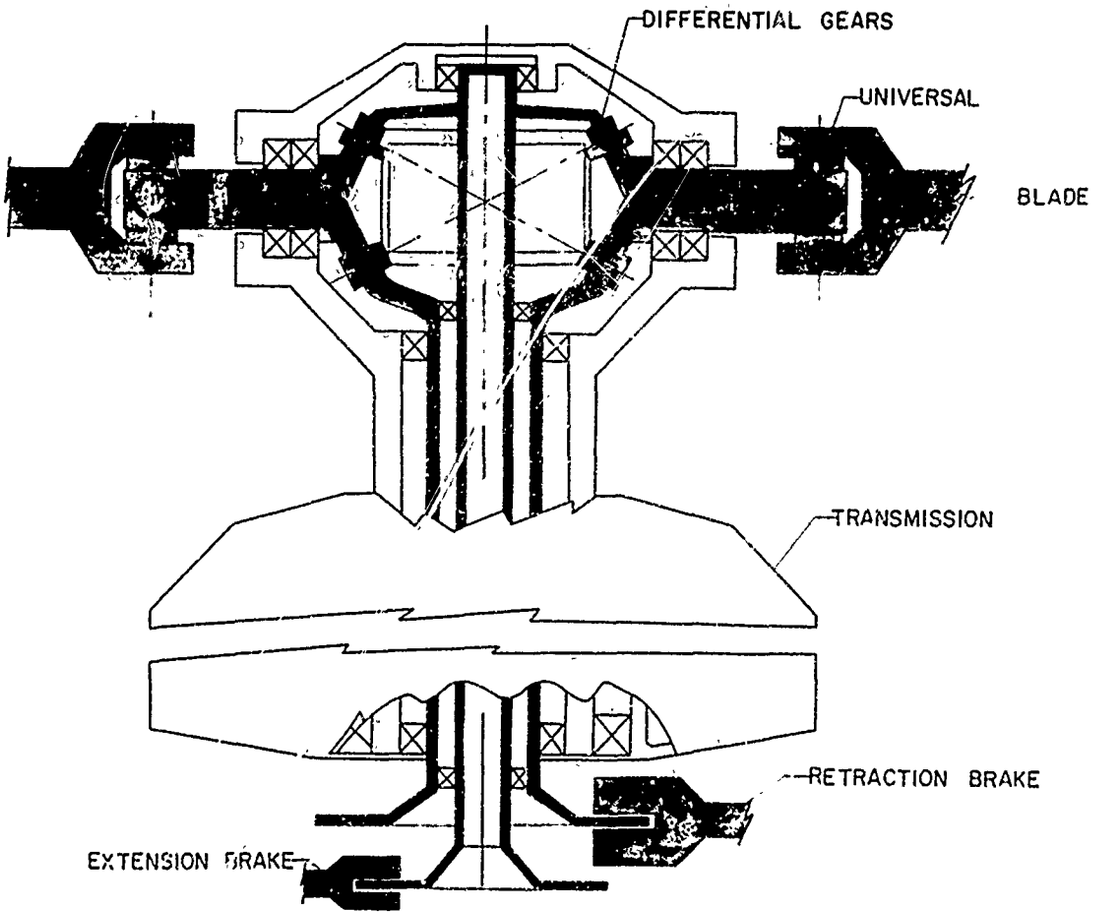

Figure 2. TRAC Rotor Head Schematic Arrangement.

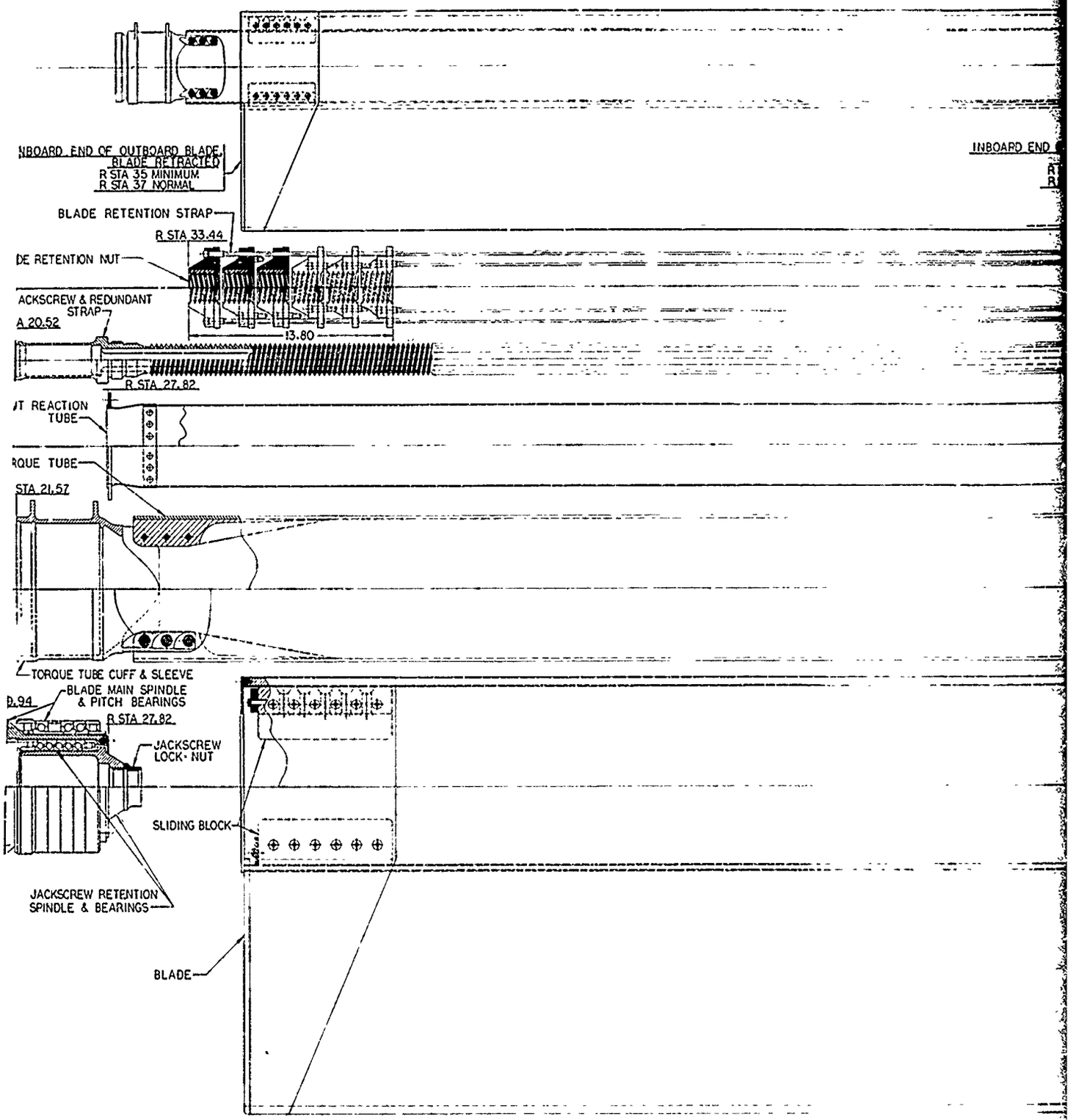

Figure 3. TRAC Rotor Blade Major Components.

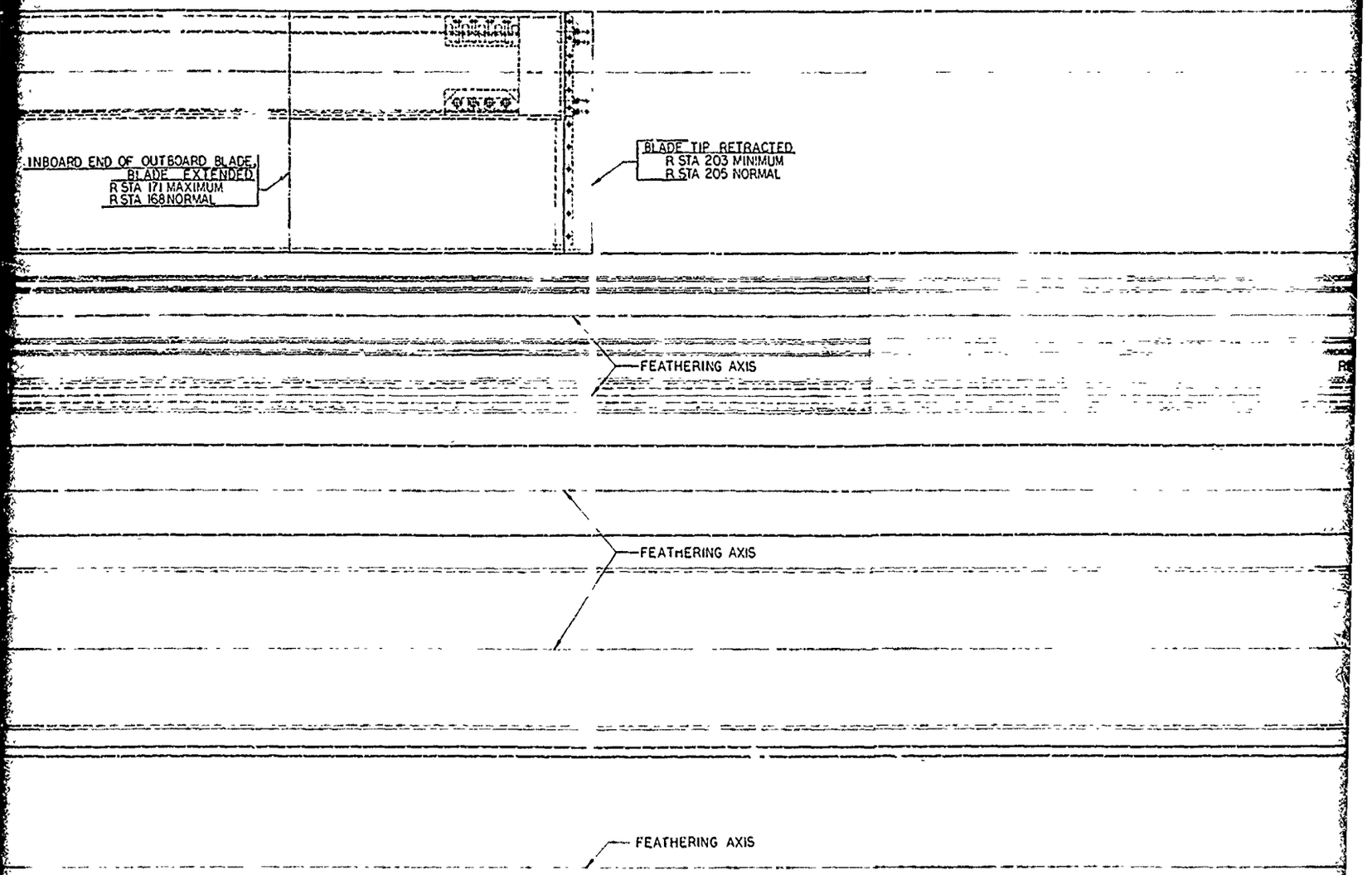
INBOARD END OF OUTBOARD BLADE
BLADE EXTENDED
R STA 171 MAXIMUM
R STA 168 NORMAL
BLADE TIP RETRACTED
R STA 203 MINIMUM
R STA 205 NORMAL
FEATHERING AXIS
FEATHERING AXIS
FEATHERING AXIS

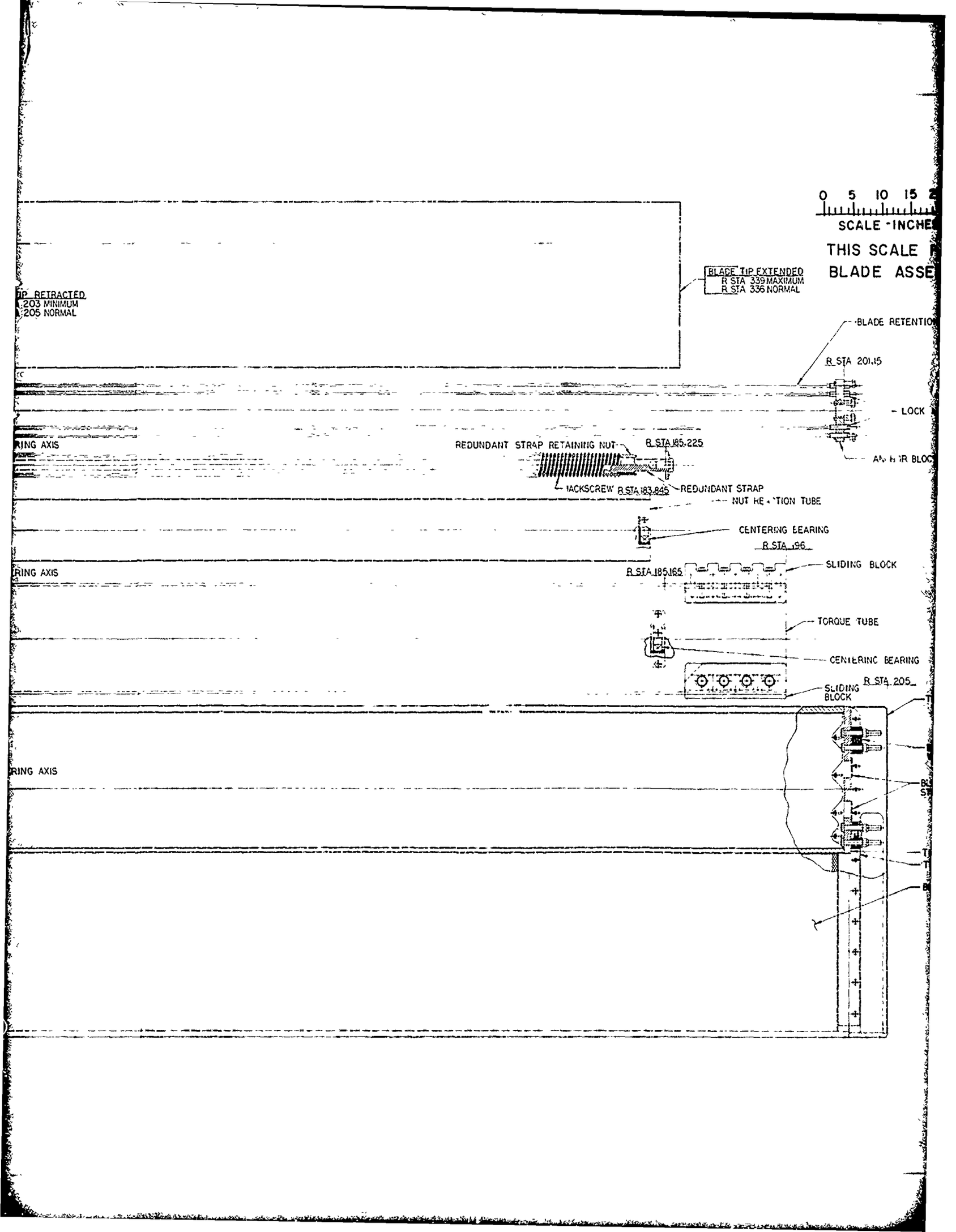
0 5 10 15
SCALE - INCHES
THIS SCALE
BLADE ASSE
BLADE TIP EXTENDED
R STA 339 MAXIMUM
R STA 336 NORMAL
IP RETRACTED
.203 MINIMUM
.205 NORMAL
BLADE RETENTION
R STA 201.45
LOCK
ANCHOR BLOCK
RING AXIS
REDUNDANT STRAP RETAINING NUT
R STA 185.225
JACKSCREW R STA 183.845
REDUNDANT STRAP
NUT RETENTION TUBE
CENTERING BEARING
R STA 196
RING AXIS
R STA 185.165
SLIDING BLOCK
TORQUE TUBE
CENTERING BEARING
R STA 205
SLIDING BLOCK
RING AXIS

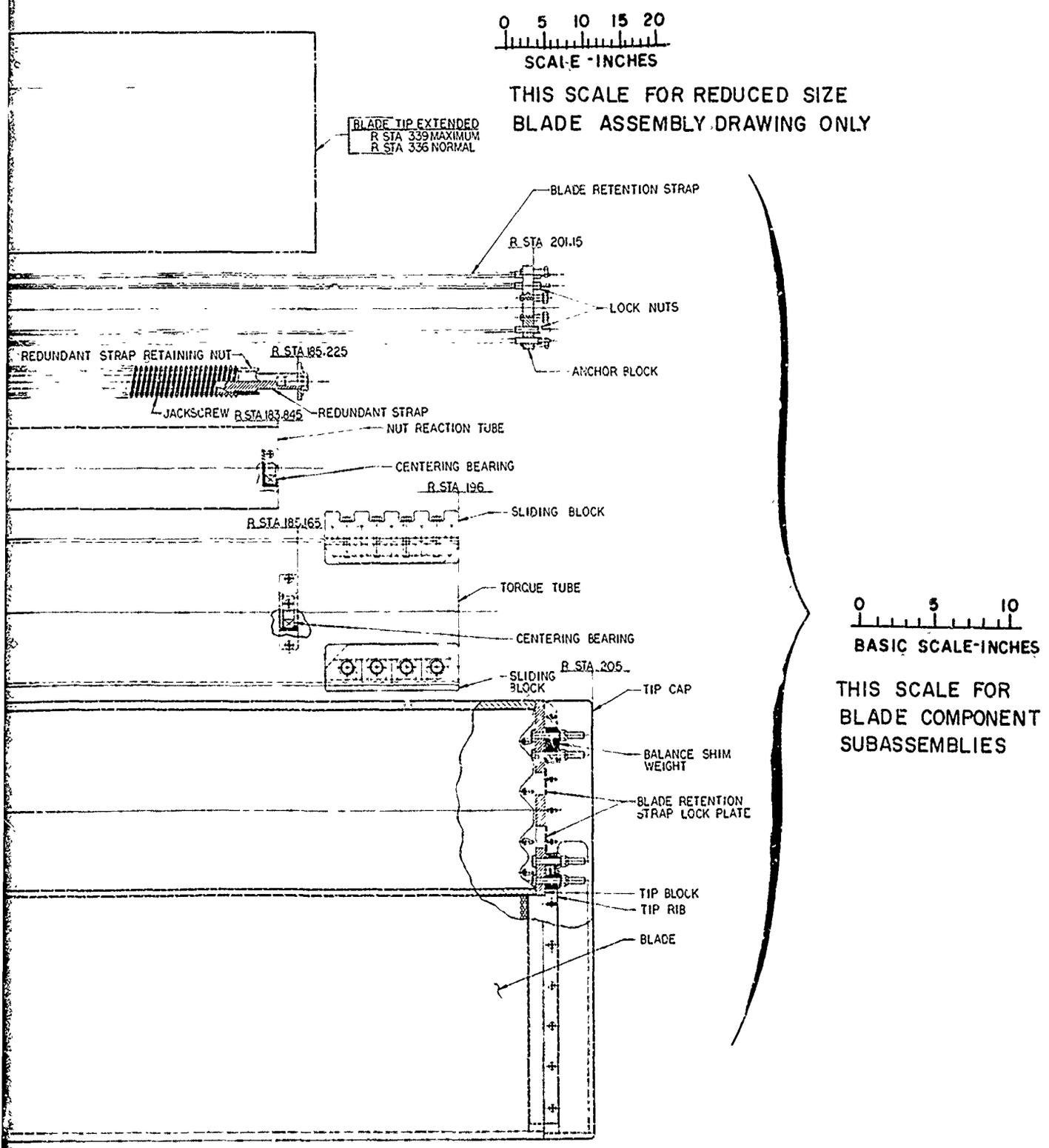
0 5 10 15 20
SCALE - INCHES
THIS SCALE FOR REDUCED SIZE
BLADE ASSEMBLY DRAWING ONLY
BLADE TIP EXTENDED
R STA 339 MAXIMUM
R STA 336 NORMAL
BLADE RETENTION STRAP
R STA 201.15
LOCK NUTS
ANCHOR BLOCK
REDUNDANT STRAP RETAINING NUT
R STA 185.225
JACKSCREW R STA 183.845
REDUNDANT STRAP
NUT REACTION TUBE
CENTERING BEARING
R STA 196
SLIDING BLOCK
R STA 185.165
TORQUE TUBE
CENTERING BEARING
R STA 205
SLIDING BLOCK
TIP CAP
BALANCE SHIM WEIGHT
BLADE RETENTION STRAP LOCK PLATE
TIP BLOCK
TIP RIB
BLADE
0 5 10
BASIC SCALE-INCHES
THIS SCALE FOR BLADE COMPONENT SUBASSEMBLIES

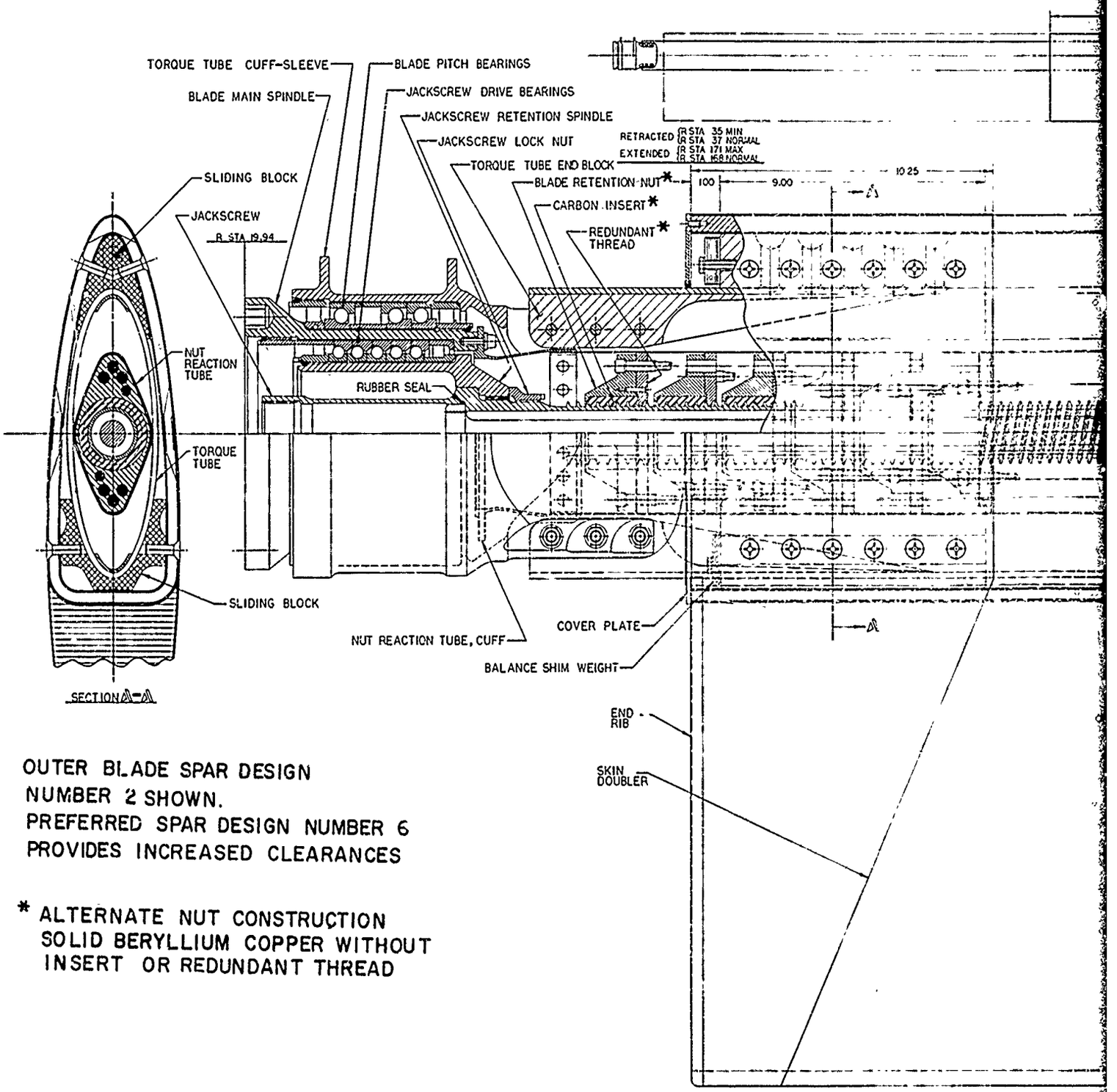

OUTER BLADE SPAR DESIGN NUMBER 2 SHOWN.
PREFERRED SPAR DESIGN NUMBER 6 PROVIDES INCREASED CLEARANCES

* ALTERNATE NUT CONSTRUCTION SOLID BERYLLIUM COPPER WITHOUT INSERT OR REDUNDANT THREAD

Figure 4. Blade Assembly Drawing.

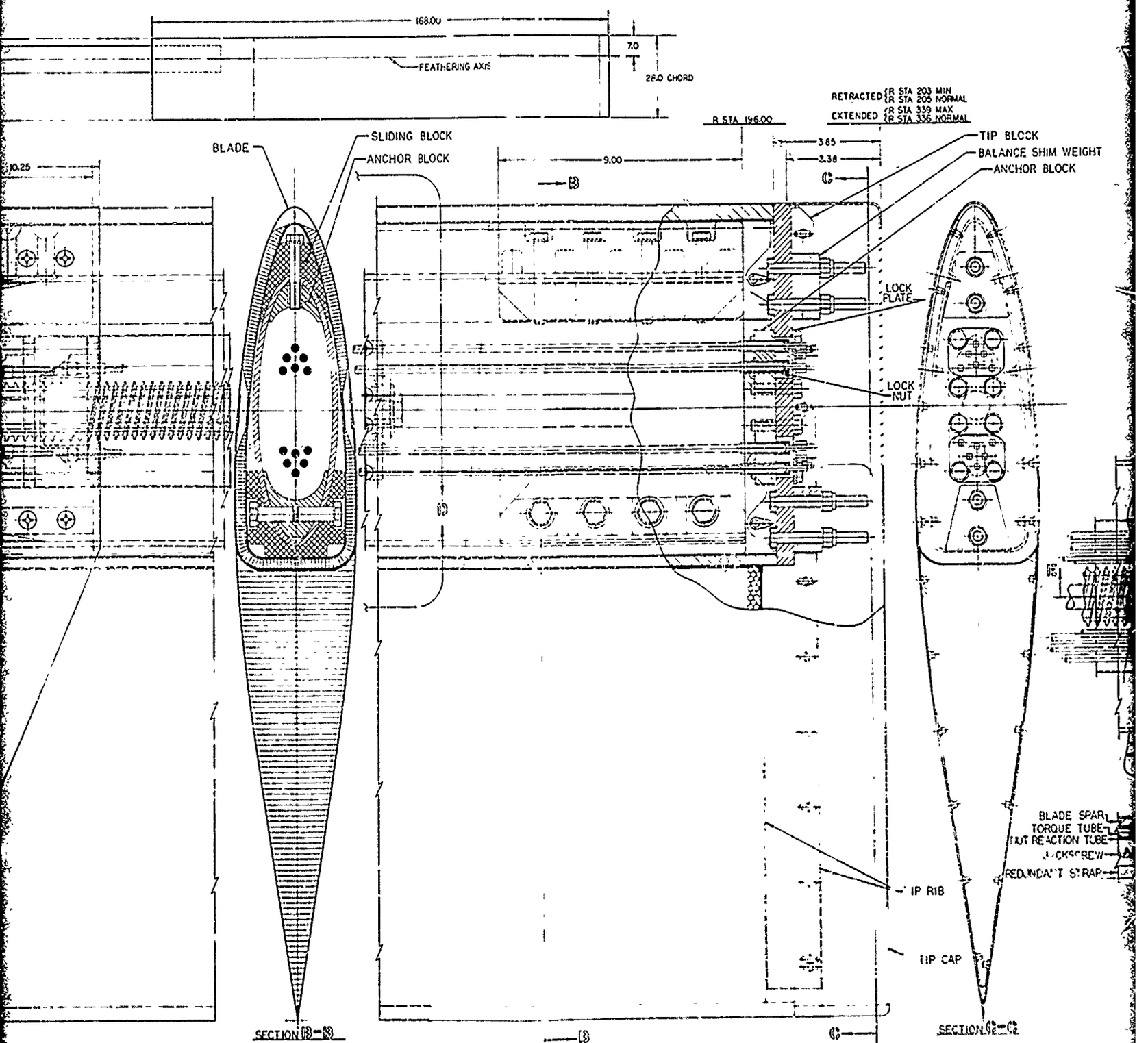
168.00
7.0
FEATHERING AXIS
28.0 CHORD
RETRACTED {R STA 203 MIN / R STA 205 NORMAL
EXTENDED {R STA 339 MAX / R STA 336 NORMAL
R STA 196.00
BLADE
SLIDING BLOCK
ANCHOR BLOCK
10.25
9.00
3.85
3.38
TIP BLOCK
BALANCE SHIM WEIGHT
ANCHOR BLOCK
LOCK PLATE
LOCK NUT
BLADE SPAR
TORQUE TUBE
NUT REACTION TUBE
LOCKSCREW
REDUNDANT STRAP
TIP RIB
TIP CAP
SECTION B-B
SECTION C-C

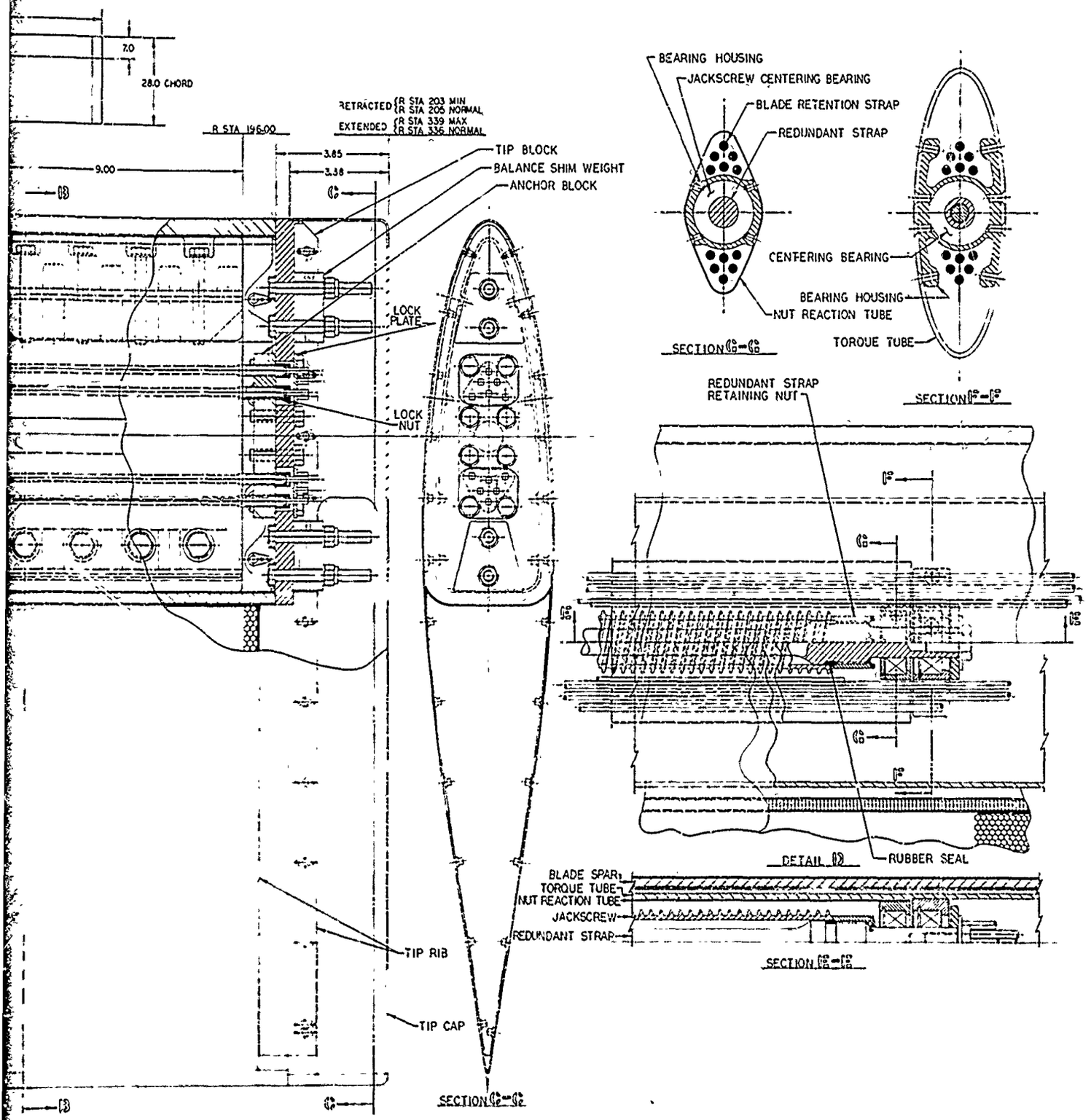
7.0
28.0 CHORD
RETRACTED {R STA 203 MIN
R STA 205 NORMAL
EXTENDED {R STA 339 MAX
R STA 336 NORMAL
R STA 196.00
3.85
3.38
9.00
TIP BLOCK
BALANCE SHIM WEIGHT
ANCHOR BLOCK
LOCK PLATE
LOCK NUT
TIP RIB
TIP CAP
SECTION
BEARING HOUSING
JACKSCREW CENTERING BEARING
BLADE RETENTION STRAP
REDUNDANT STRAP
CENTERING BEARING
BEARING HOUSING
NUT REACTION TUBE
TORQUE TUBE
SECTION
REDUNDANT STRAP RETAINING NUT
SECTION
DETAIL
RUBBER SEAL
BLADE SPAR
TORQUE TUBE
NUT REACTION TUBE
JACKSCREW
REDUNDANT STRAP
SECTION

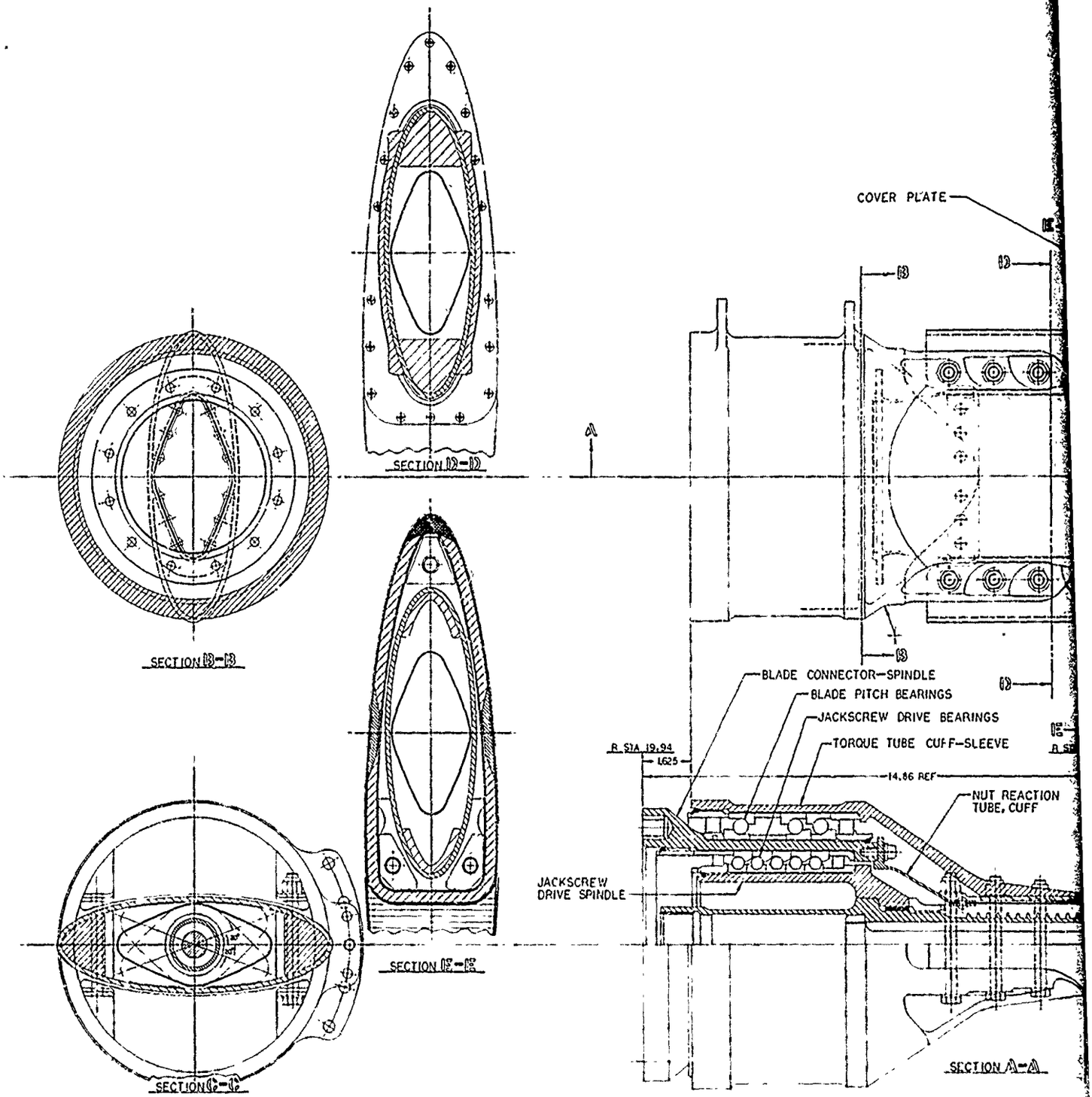

Figure 5. TRAC Rotor Blade - Root End Assembly.

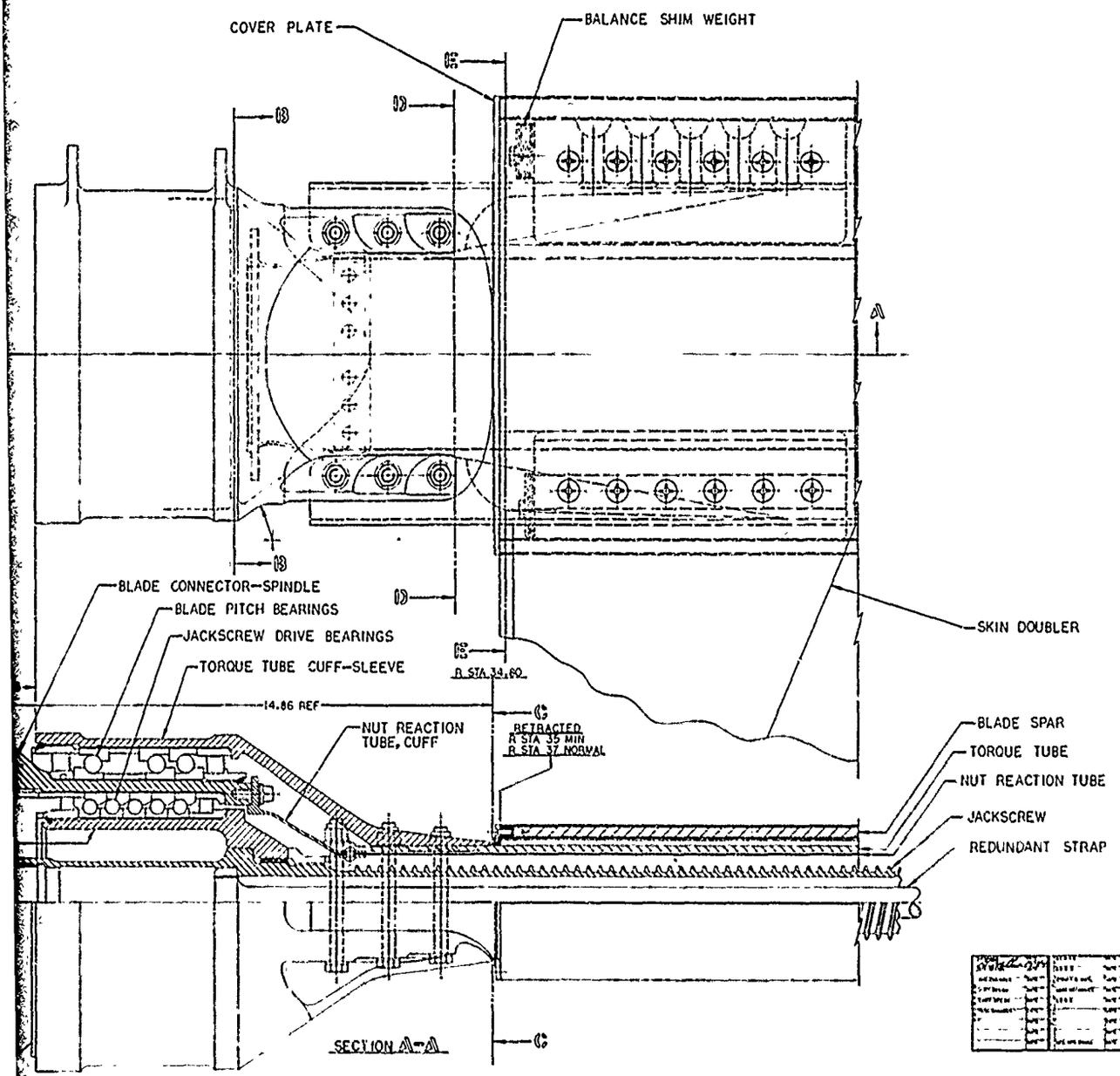

Sikorsky Aircraft

LAYOUT

TRAC ROTOR BLADE ROOT END ASSEMBLY

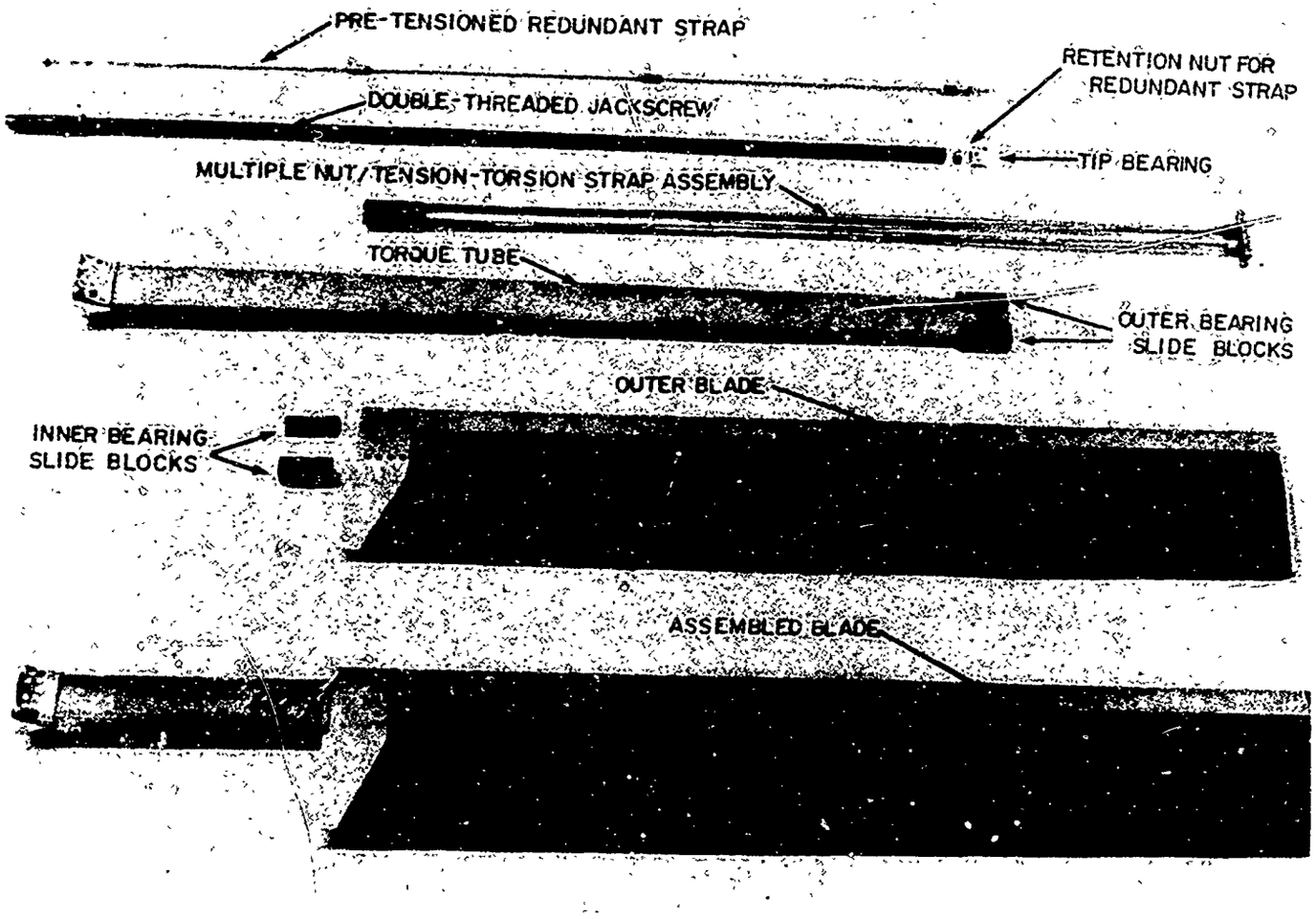

Figure 6. TRAC Dynamic Model Blade Components.

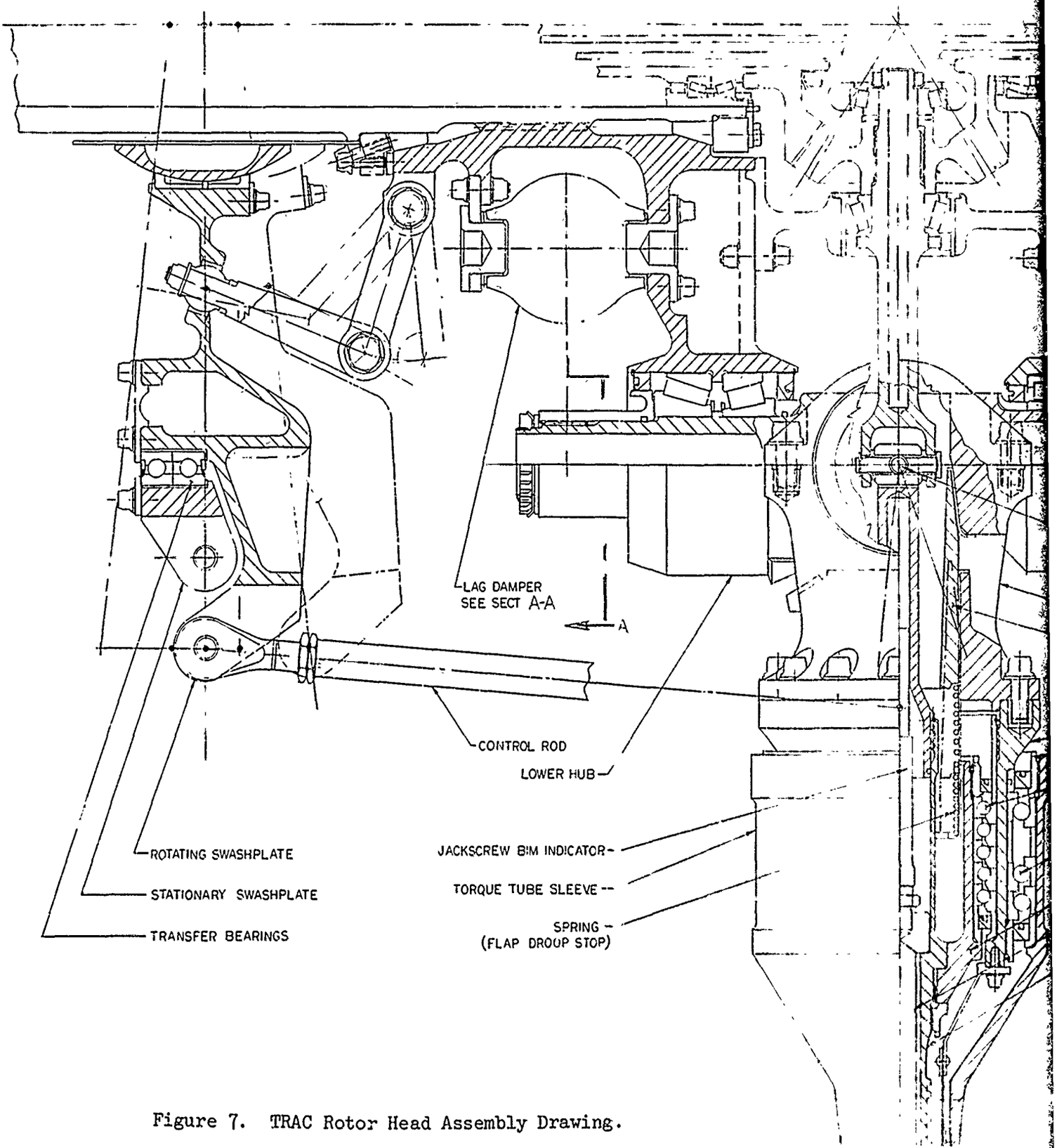

Figure 7. TRAC Rotor Head Assembly Drawing.

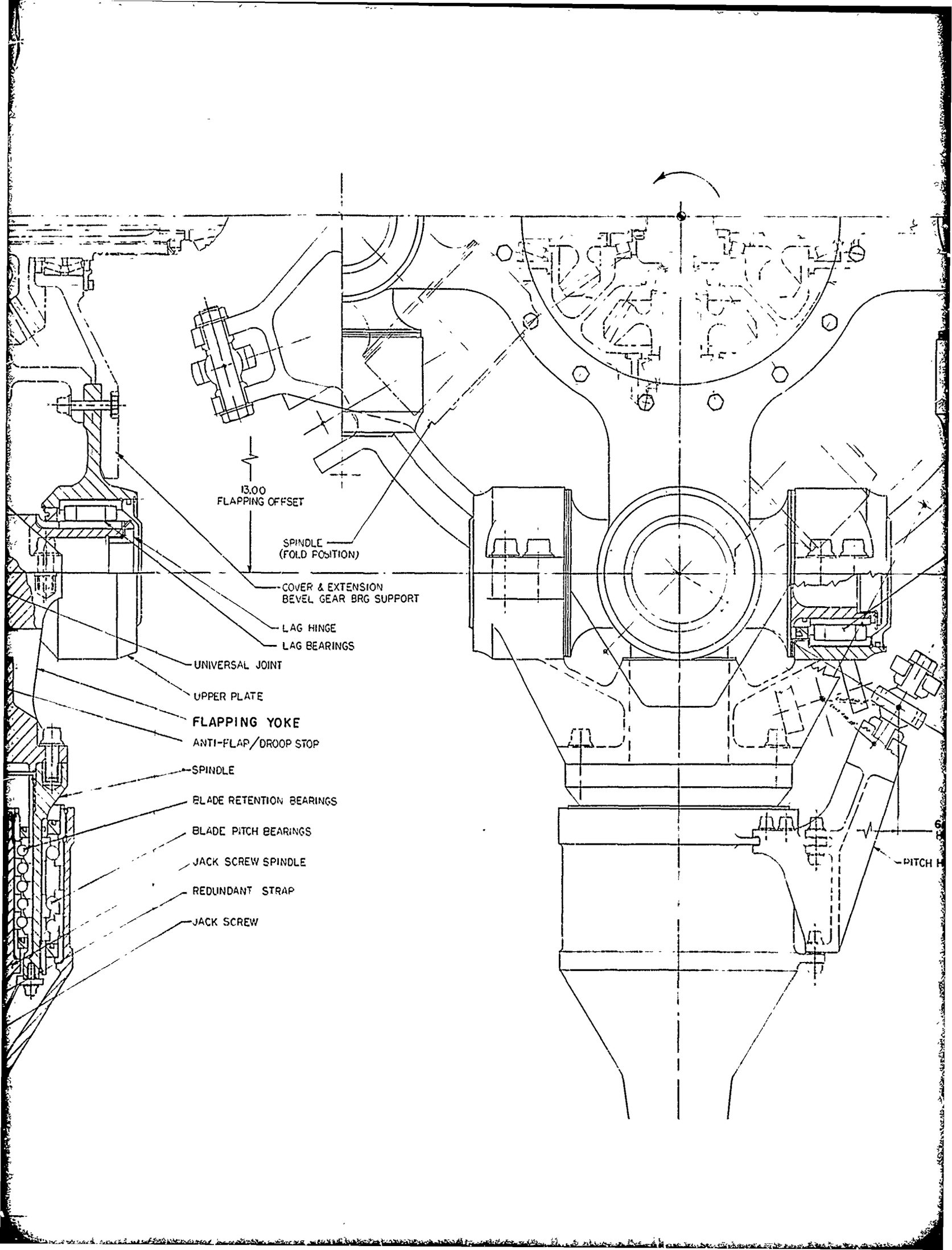
13.00
FLAPPING OFFSET
SPINDLE
(FOLD POSITION)
COVER & EXTENSION
BEVEL GEAR BRG SUPPORT
LAG HINGE
LAG BEARINGS
UNIVERSAL JOINT
UPPER PLATE
FLAPPING YOKE
ANTI-FLAP/DROOP STOP
SPINDLE
BLADE RETENTION BEARINGS
BLADE PITCH BEARINGS
JACK SCREW SPINDLE
REDUNDANT STRAP
JACK SCREW
PITCH H

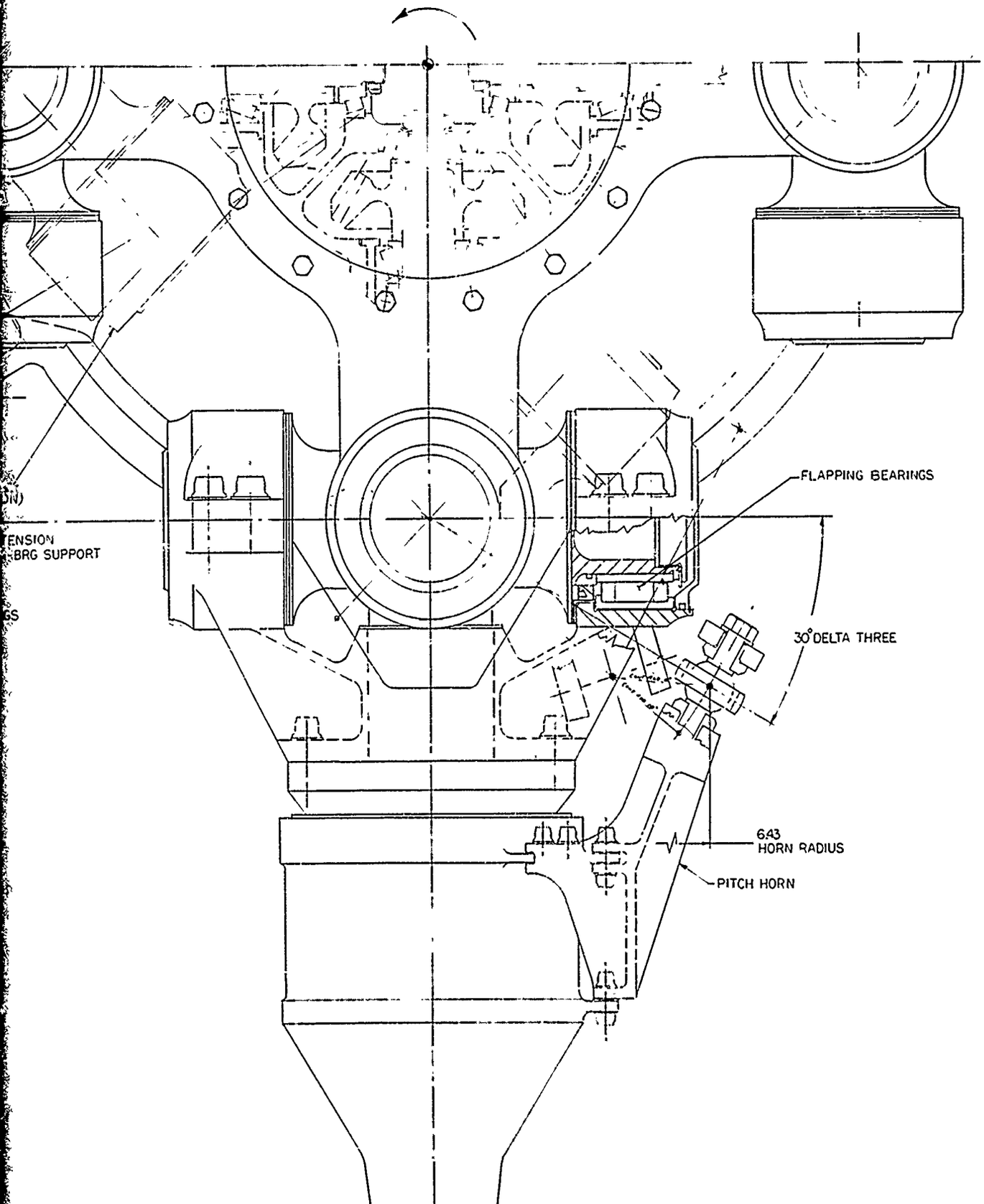
FLAPPING BEARINGS
30° DELTA THREE
6.43
HORN RADIUS
PITCH HORN

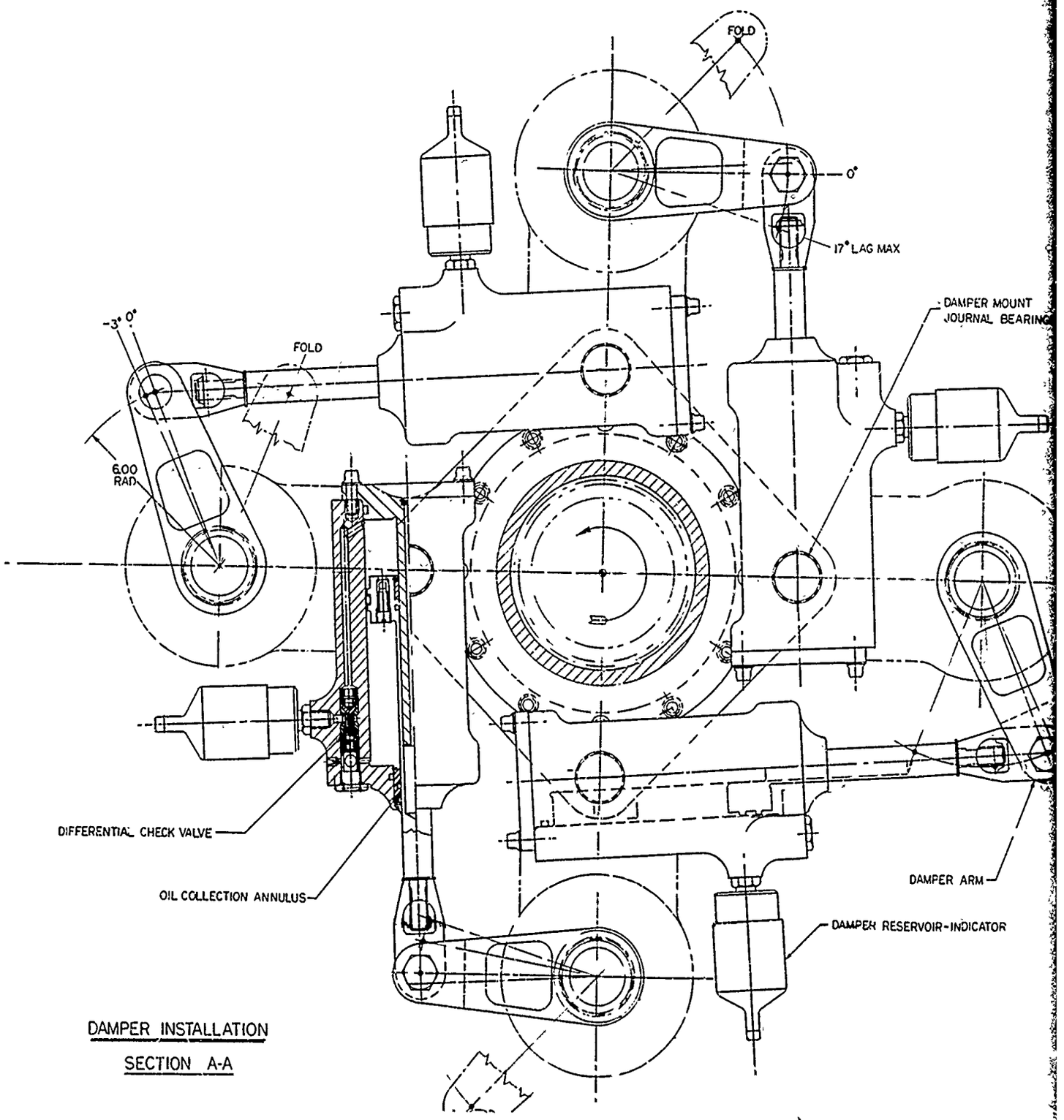

Figure 8. Lag Damper Installation.

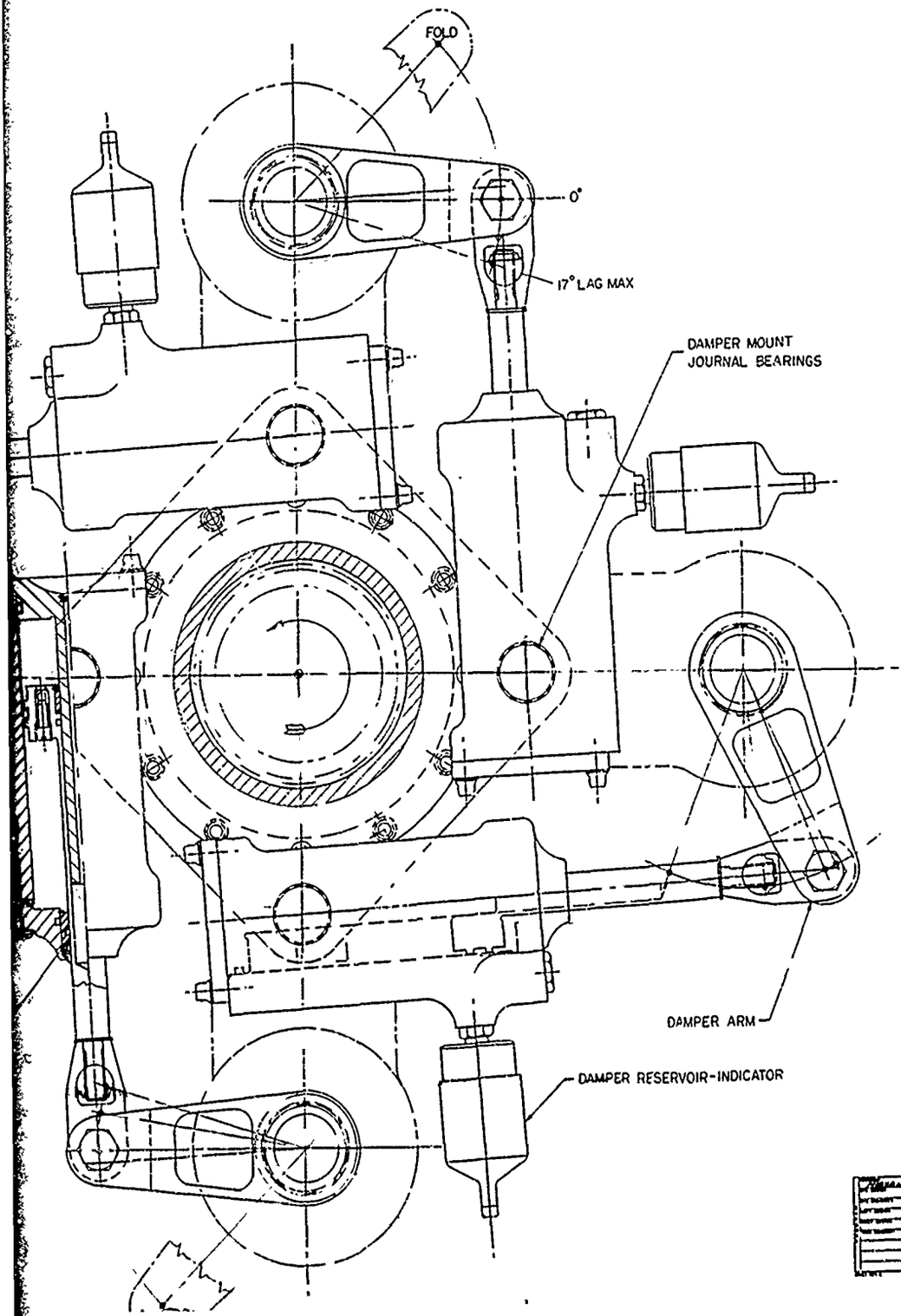

Damper Installation.

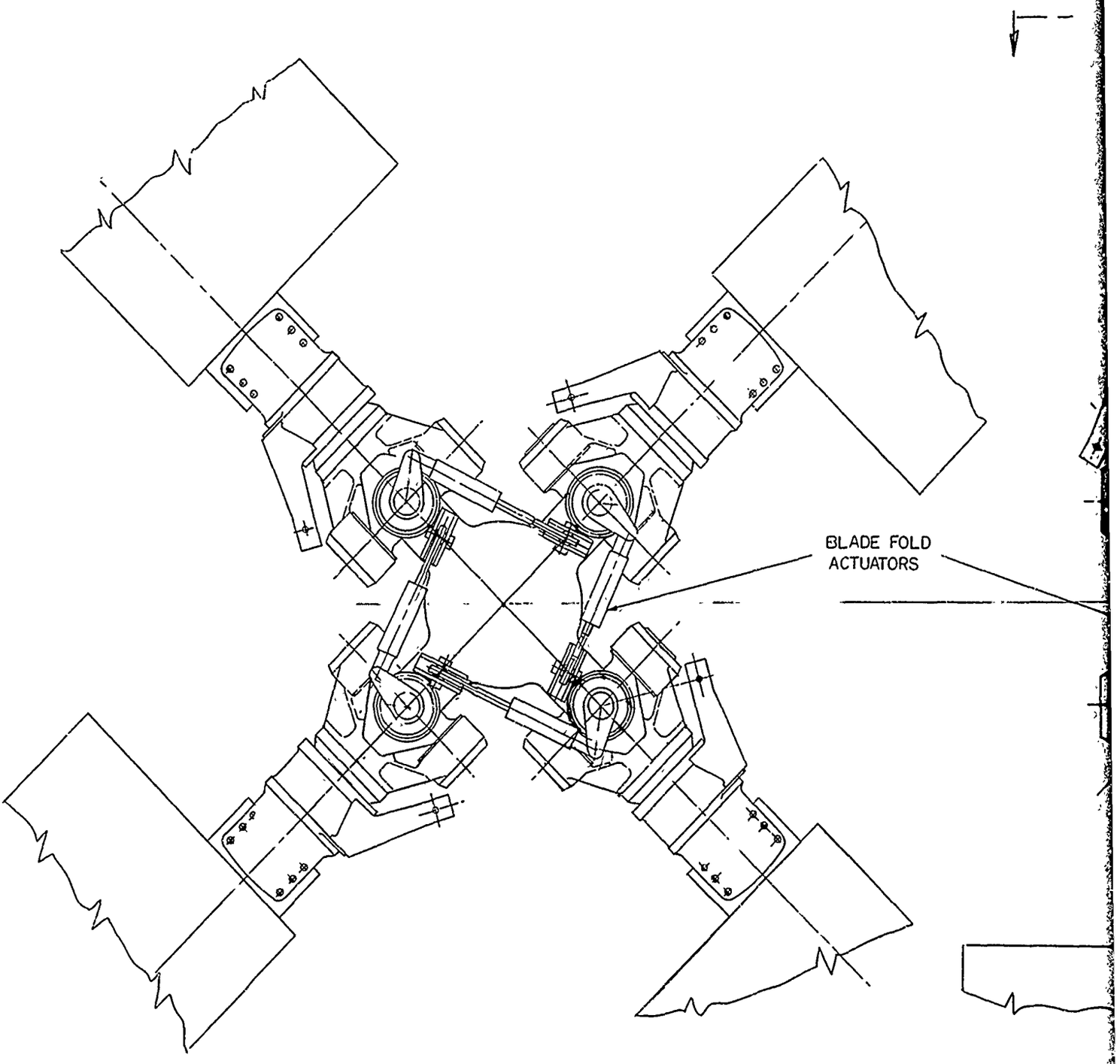

Figure 9. Blade Fold Configuration.

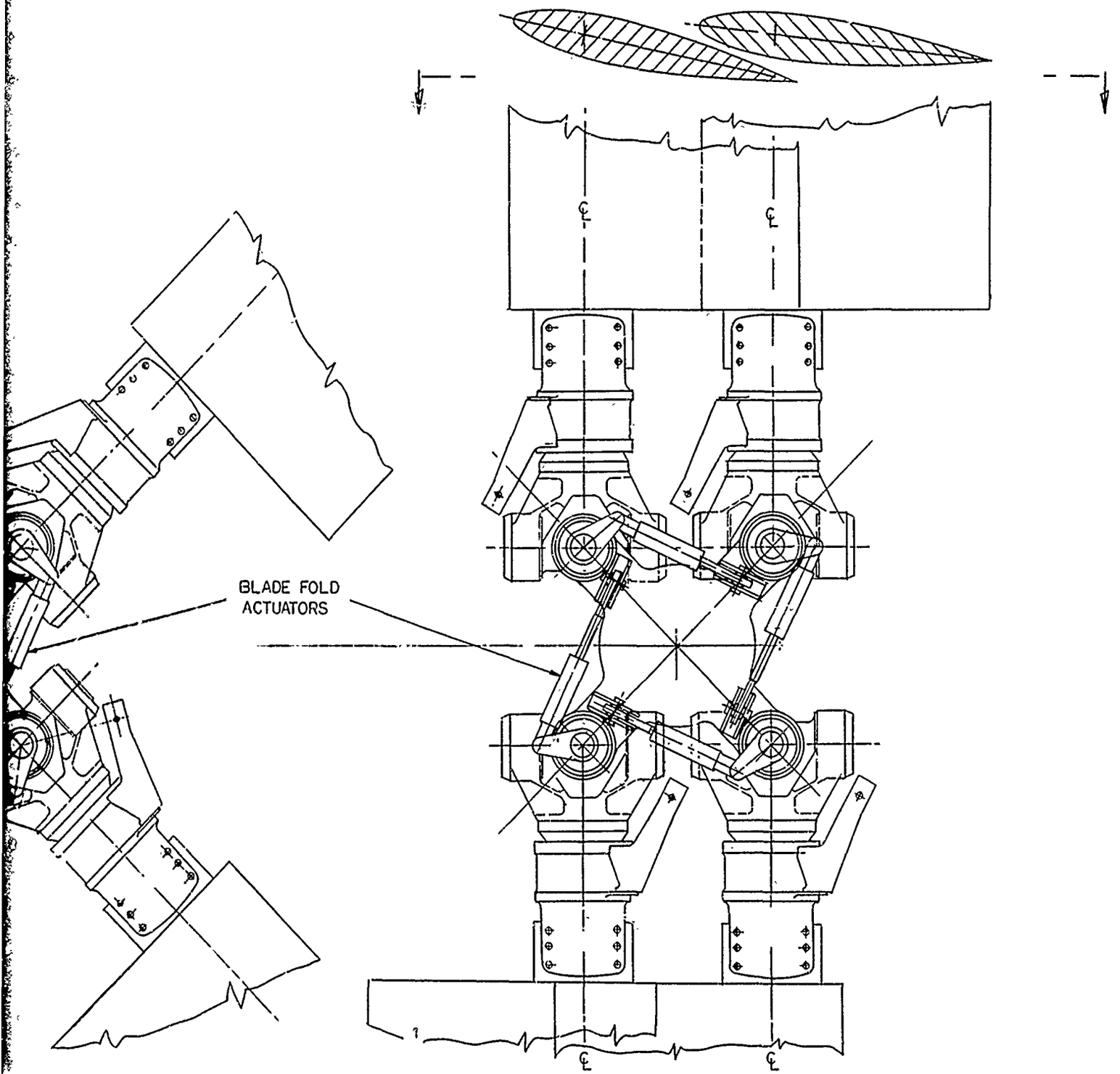

ADES

FOLDED POSITION OF BLADES

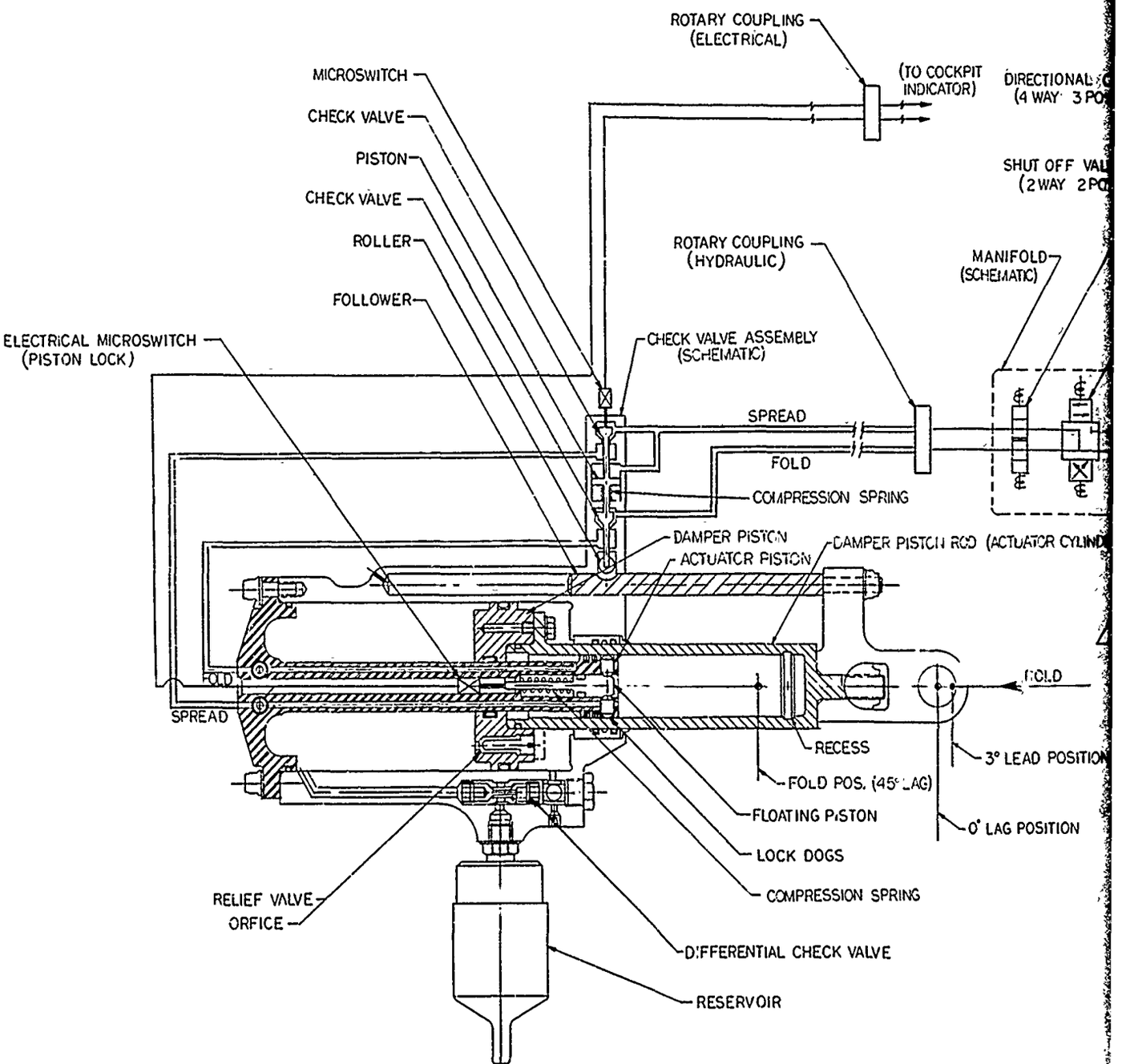

Figure 10. Integrated Lag Damper/Fold Actuator.

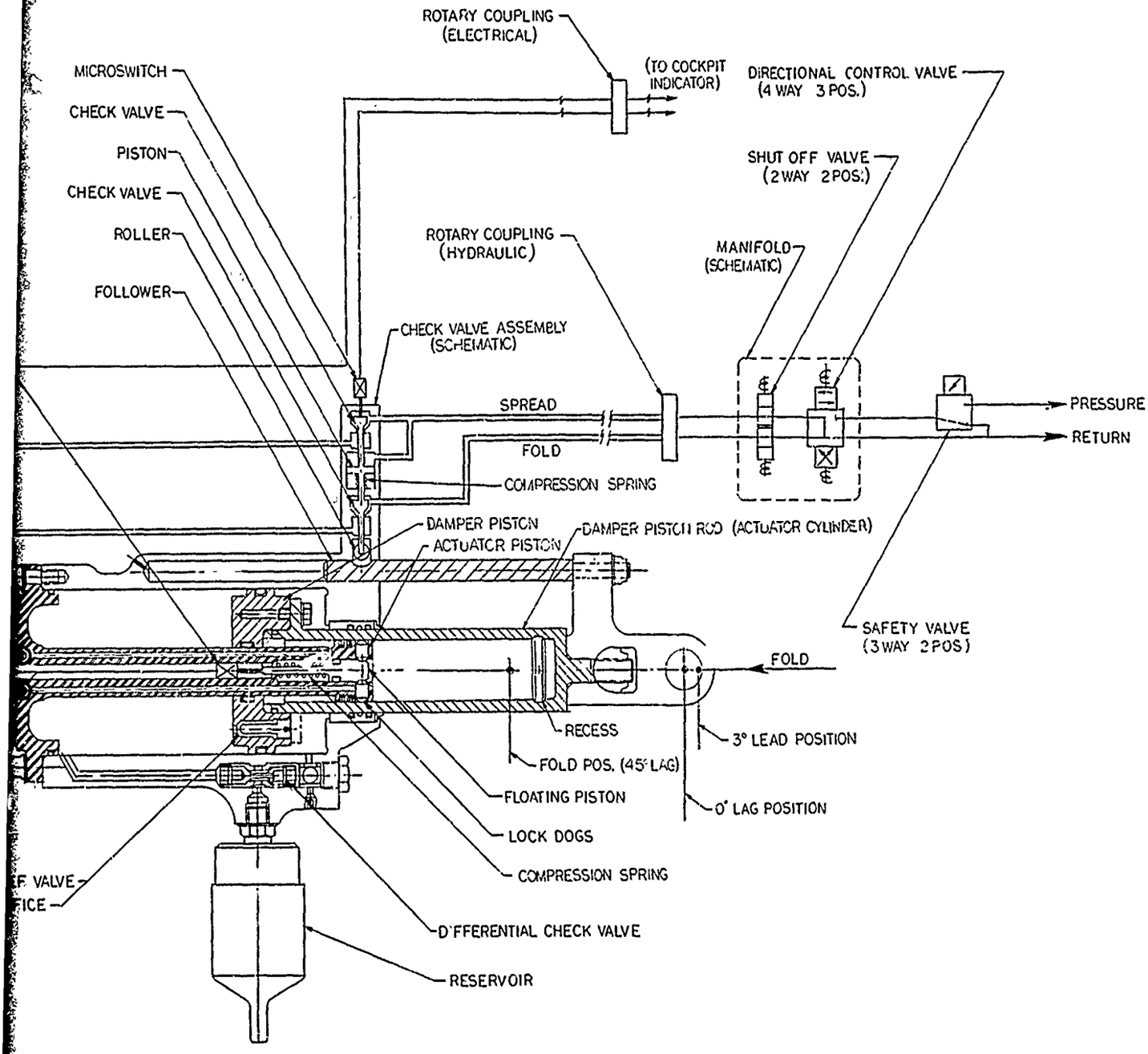

Integrated Lag Damper/Fold Actuator.

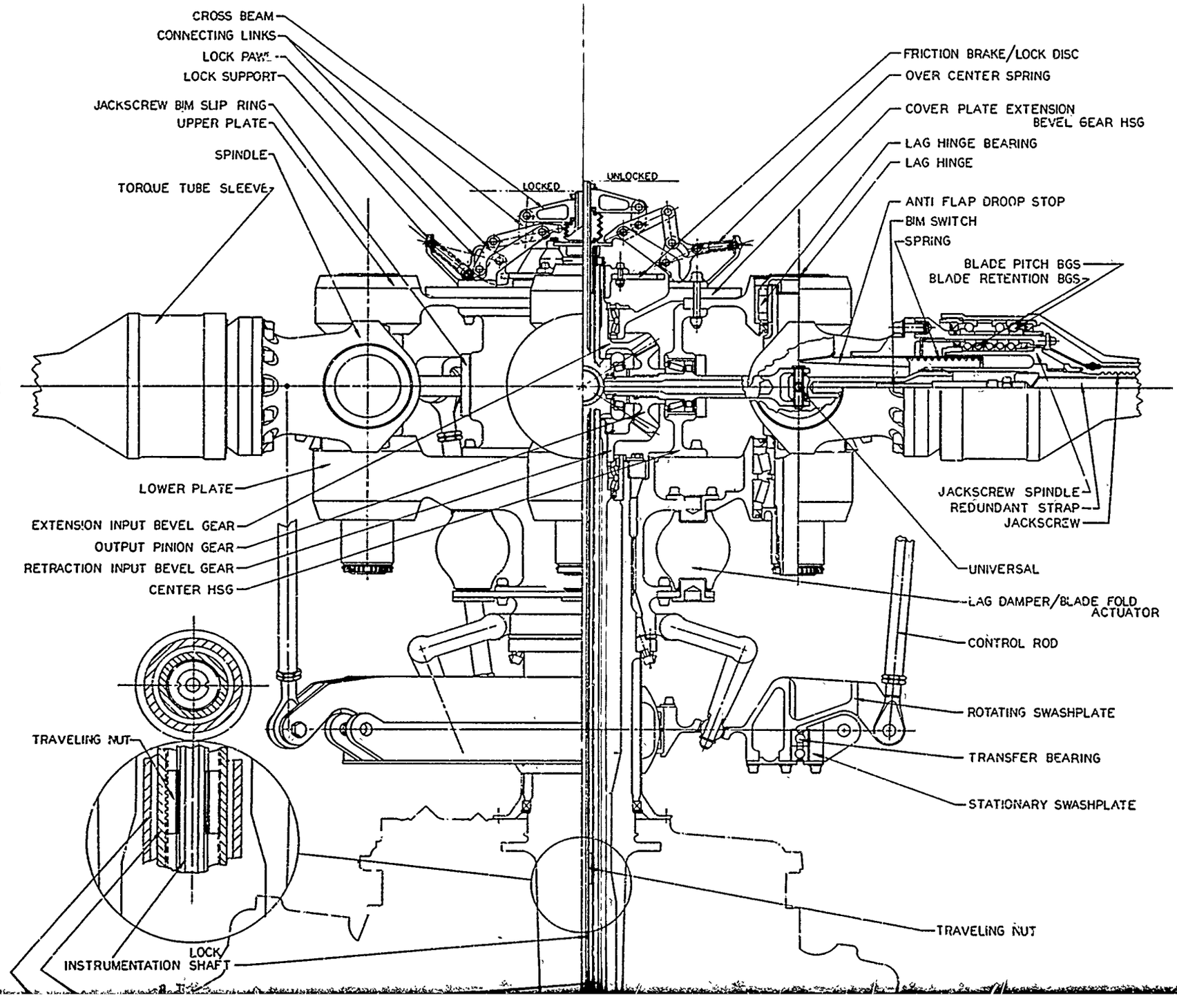
CROSS BEAM
CONNECTING LINKS
LOCK PAWL
LOCK SUPPORT
JACKSCREW BIM SLIP RING
UPPER PLATE
SPINDLE
TORQUE TUBE SLEEVE
LOCKED
UNLOCKED
FRICTION BRAKE/LOCK DISC
OVER CENTER SPRING
COVER PLATE EXTENSION
BEVEL GEAR HSG
LAG HINGE BEARING
LAG HINGE
ANTI FLAP DROOP STOP
BIM SWITCH
SPRING
BLADE PITCH BGS
BLADE RETENTION BGS
LOWER PLATE
EXTENSION INPUT BEVEL GEAR
OUTPUT PINION GEAR
RETRACTION INPUT BEVEL GEAR
CENTER HSG
JACKSCREW SPINDLE
REDUNDANT STRAP
JACKSCREW
UNIVERSAL
LAG DAMPER/BLADE FOLD
ACTUATOR
CONTROL ROD
ROTATING SWASHPLATE
TRANSFER BEARING
STATIONARY SWASHPLATE
TRAVELING NUT
TRAVELING NUT
LOCK
INSTRUMENTATION SHAFT

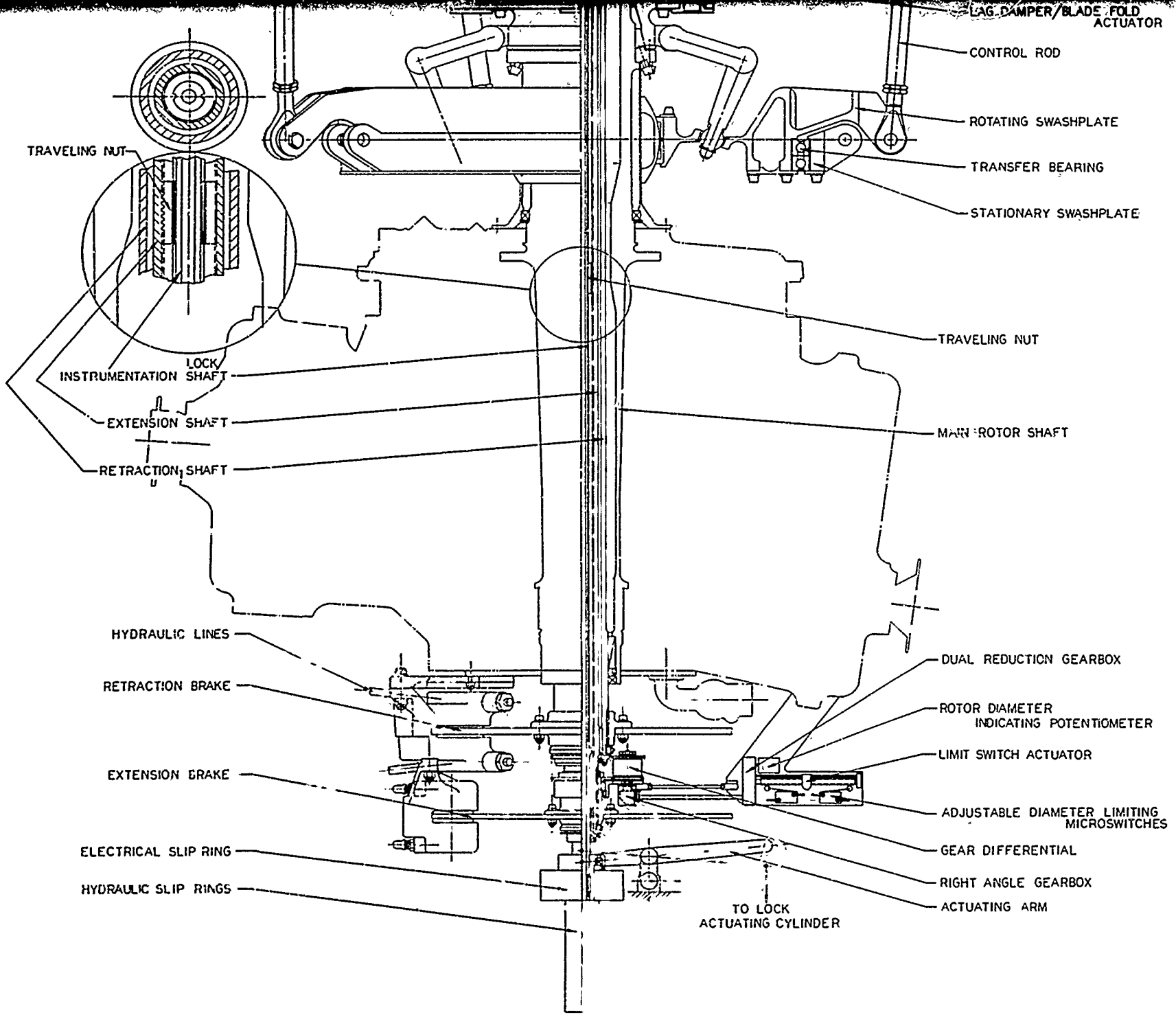

Figure 11. TRAC Rotor Retraction Mechanism Assembly.

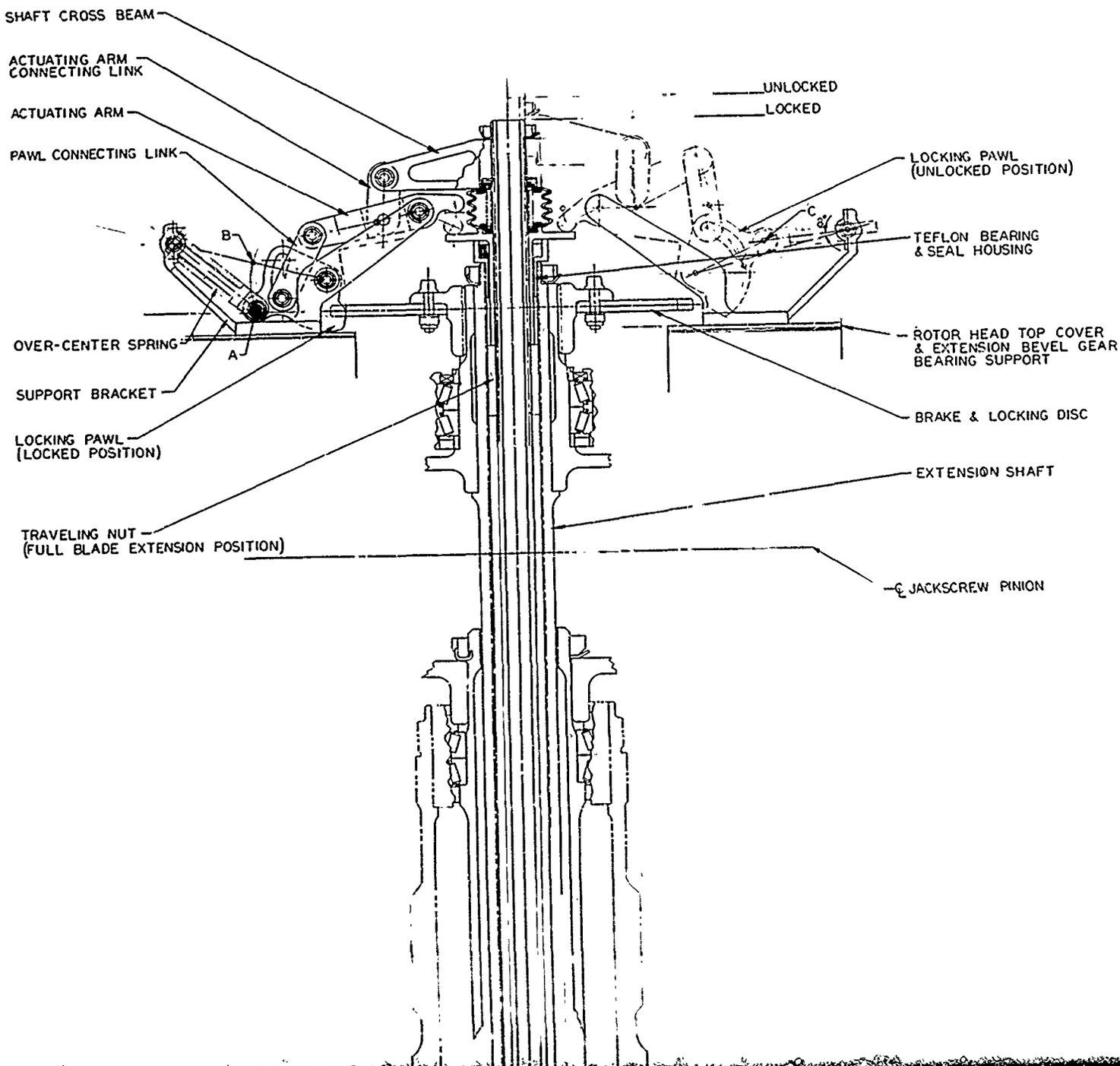
SHAFT CROSS BEAM
ACTUATING ARM CONNECTING LINK
ACTUATING ARM
PAWL CONNECTING LINK
OVER-CENTER SPRING
SUPPORT BRACKET
LOCKING PAWL (LOCKED POSITION)
TRAVELING NUT (FULL BLADE EXTENSION POSITION)
UNLOCKED
LOCKED
LOCKING PAWL (UNLOCKED POSITION)
TEFLON BEARING & SEAL HOUSING
ROTOR HEAD TOP COVER & EXTENSION BEVEL GEAR BEARING SUPPORT
BRAKE & LOCKING DISC
EXTENSION SHAFT
℄ JACKSCREW PINION
A
B
C

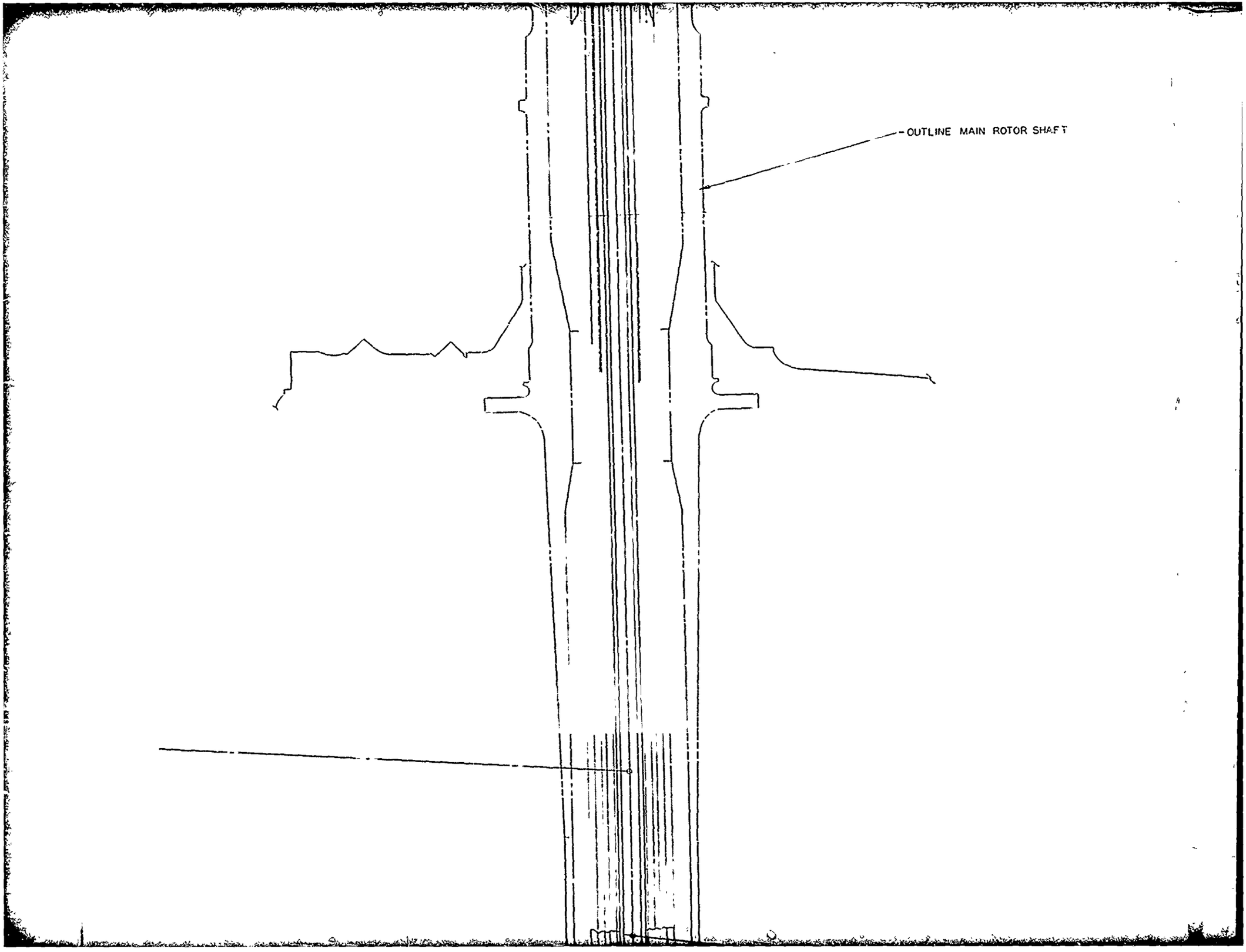
OUTLINE MAIN ROTOR SHAFT

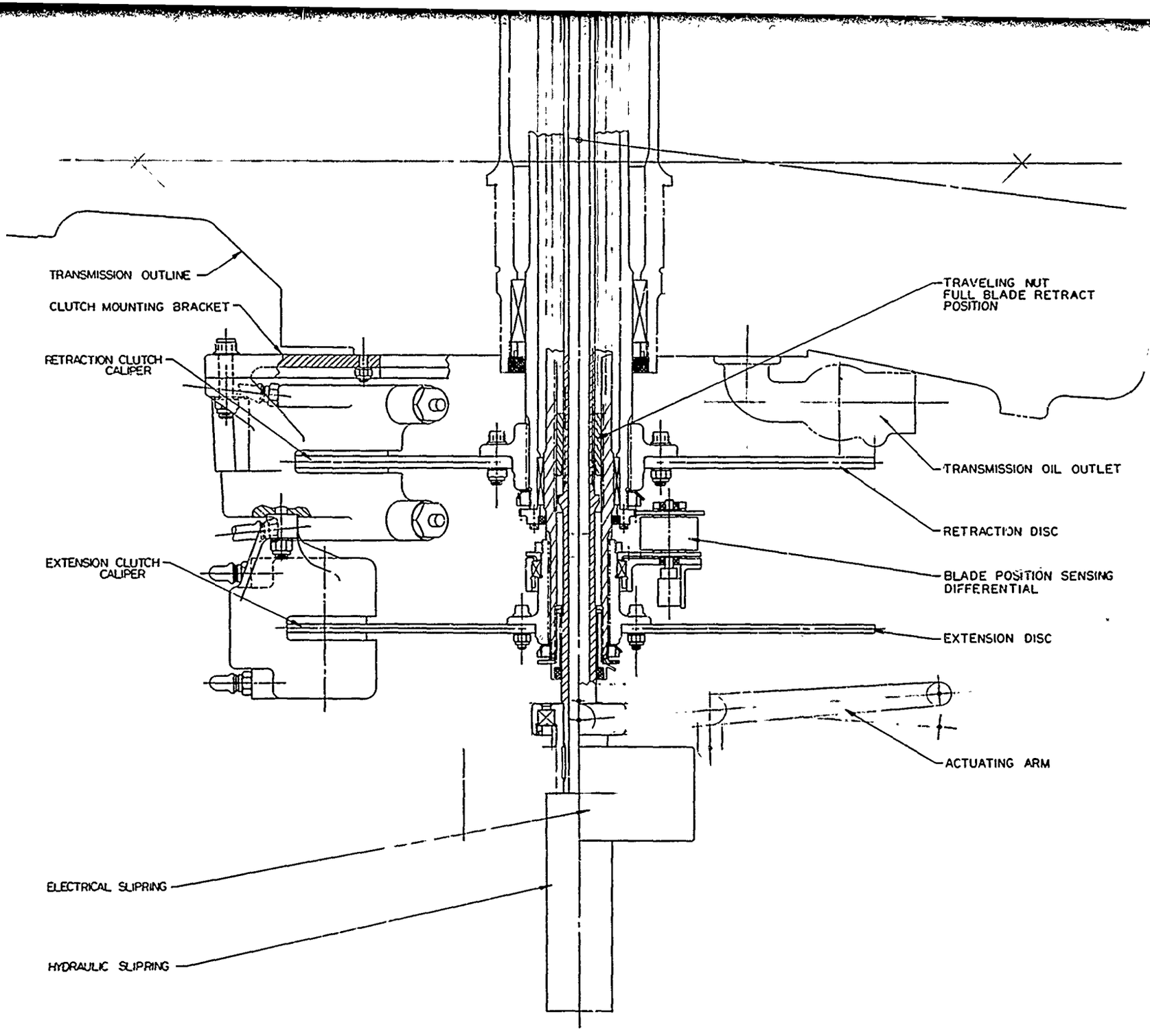

Figure 12. Diameter Control and Lock Components.

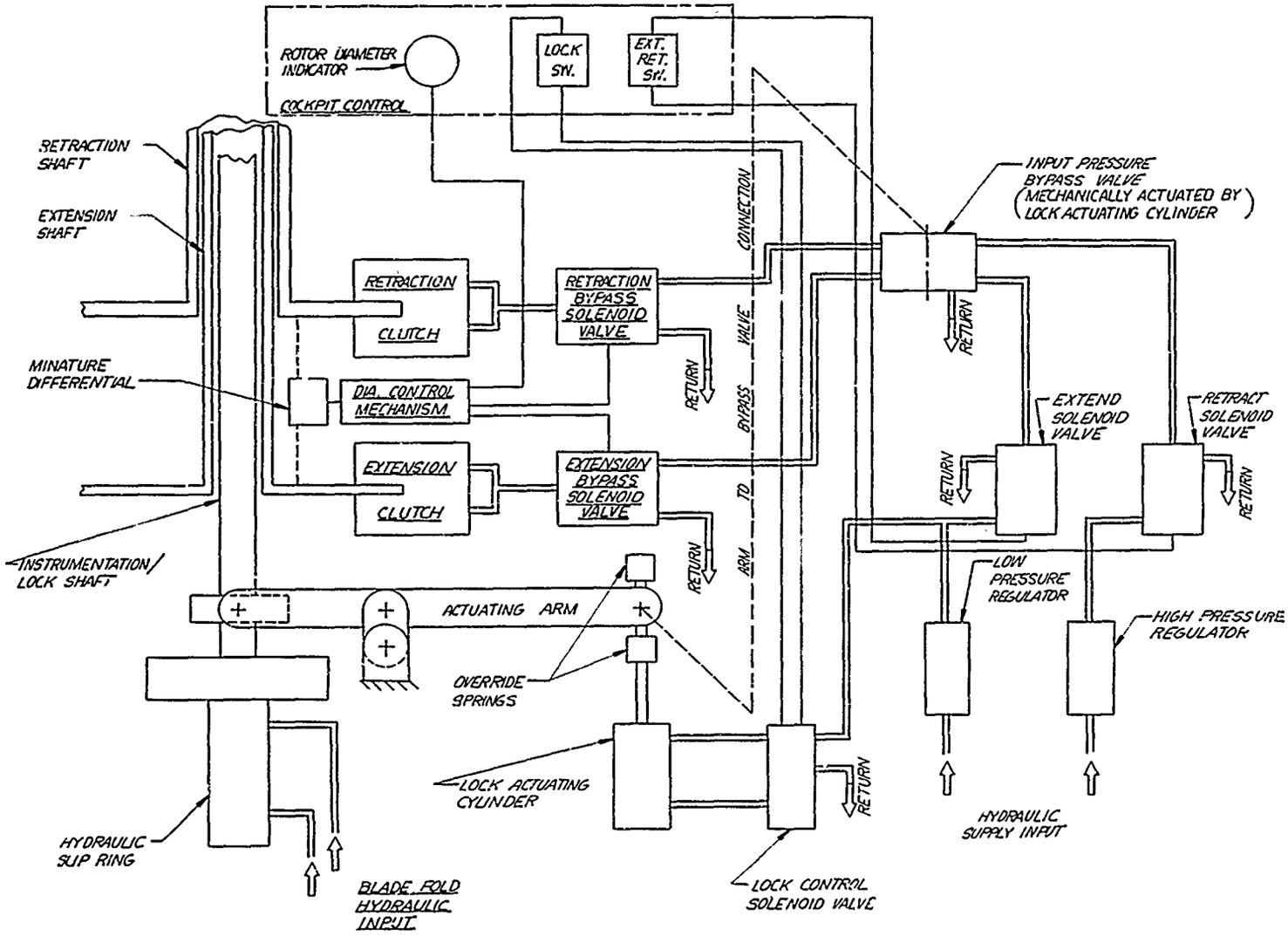

Figure 13. Schematic - Diameter Control System.

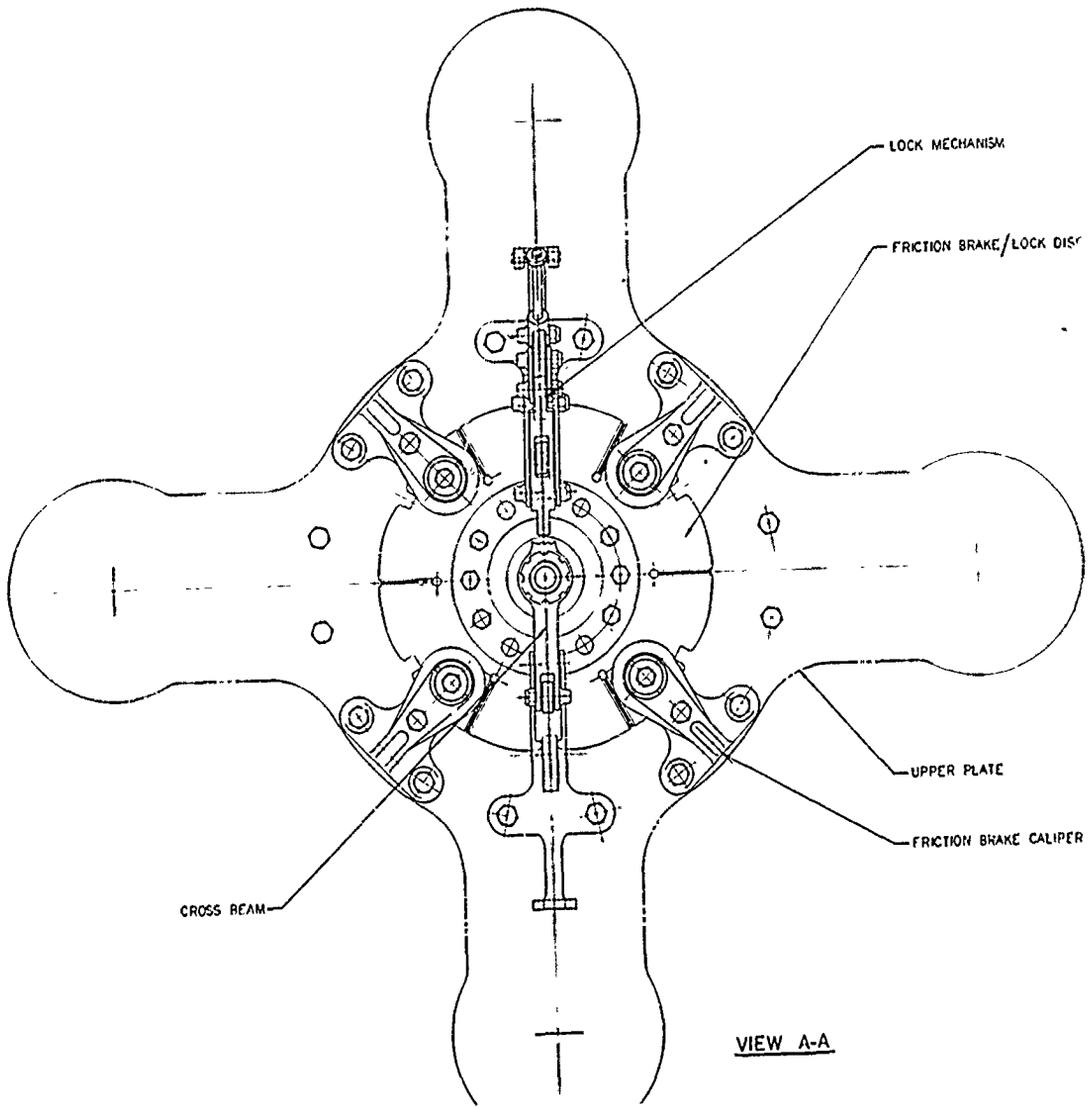

Figure 14. Friction Brake - Lock Assembly.

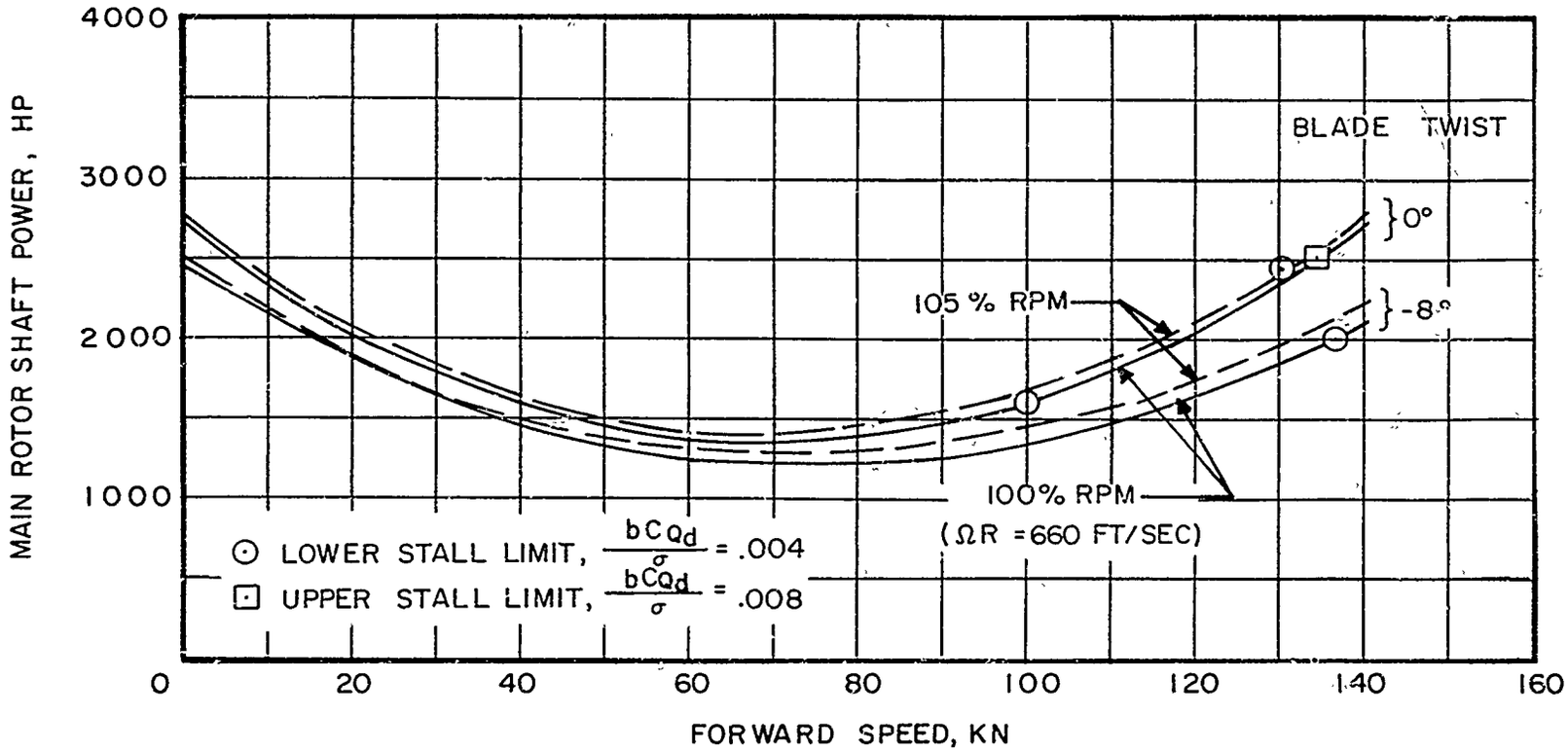

Figure 15. Performance Characteristics of Fully Extended Rotor, Sea Level Standard Conditions, Rotor Lift = 21,000 lb.

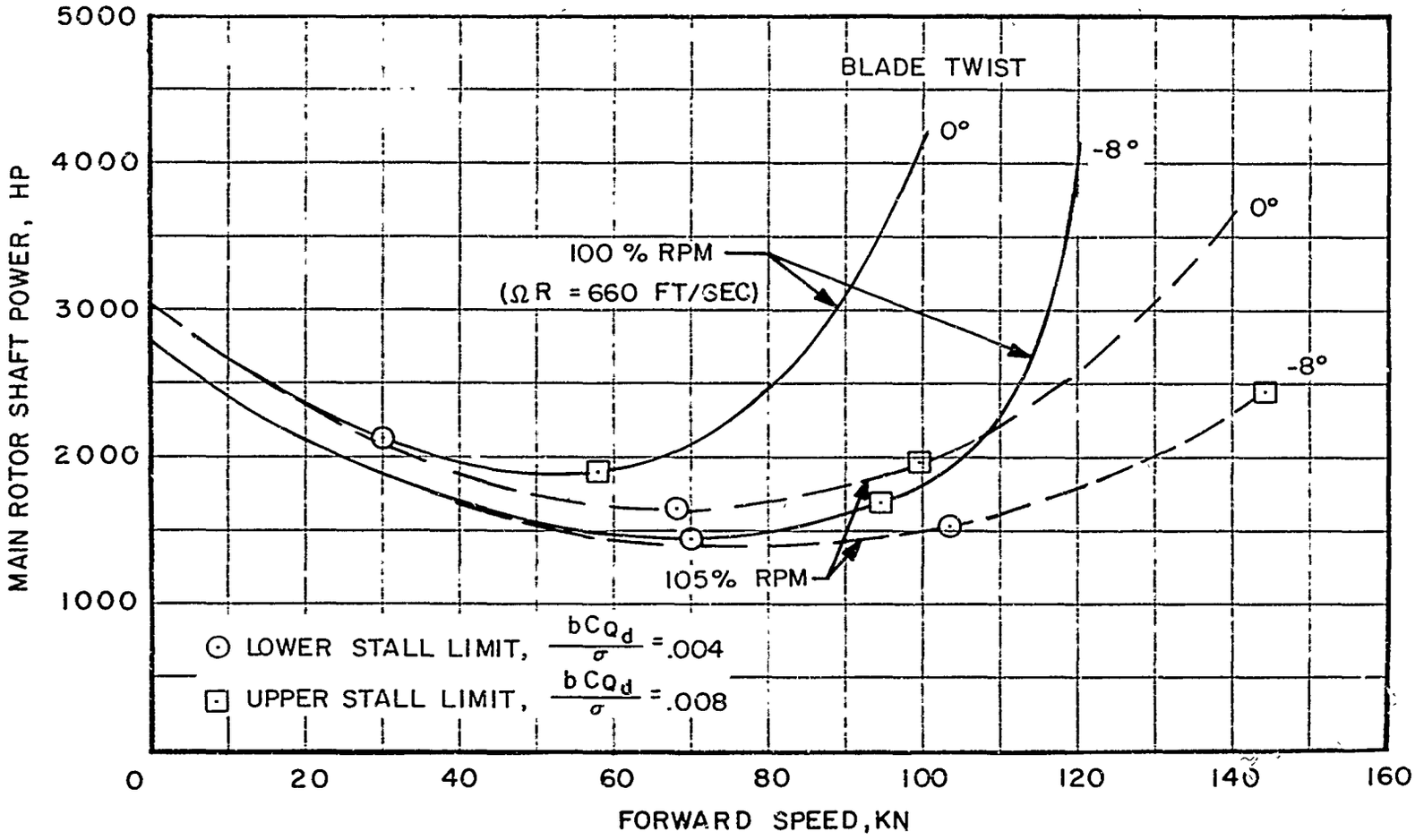

Figure 16. Performance Characteristics of Fully Extended Rotor, 4000 ft 95°F Conditions, Rotor Lift = 21,000 lb.

BLADE 1

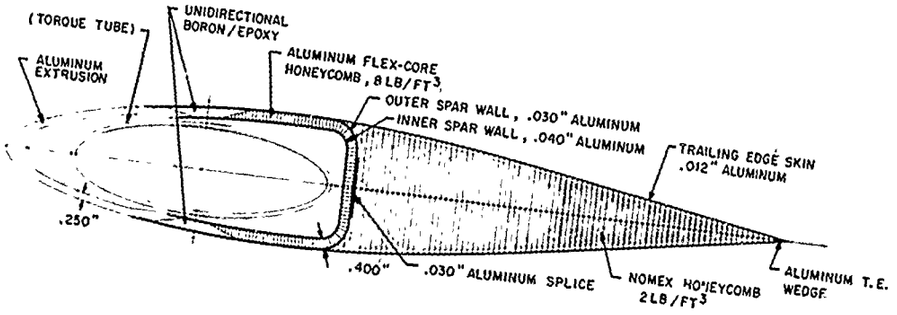

BLADE 2

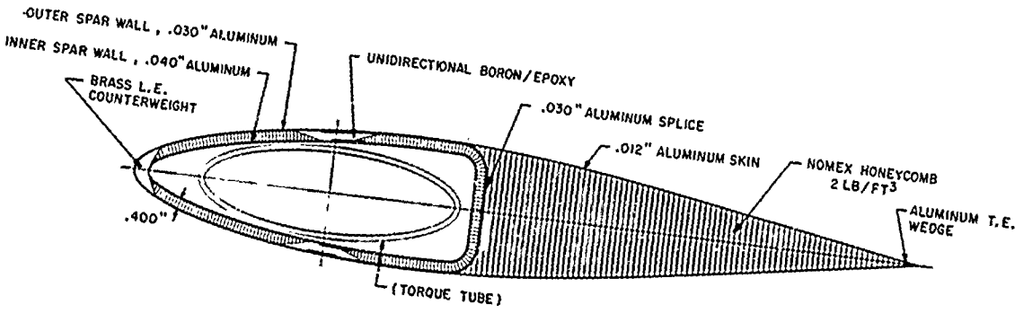

BLADE 3

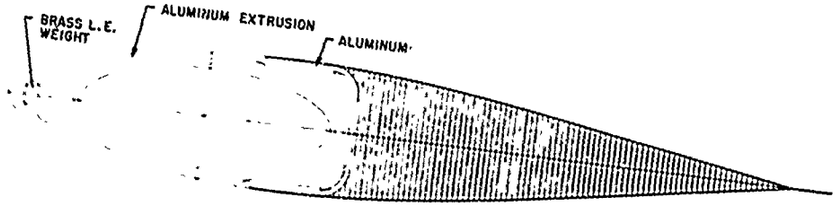

Figure 17. Outer Blade Spar Design Concepts.

BLADE 4

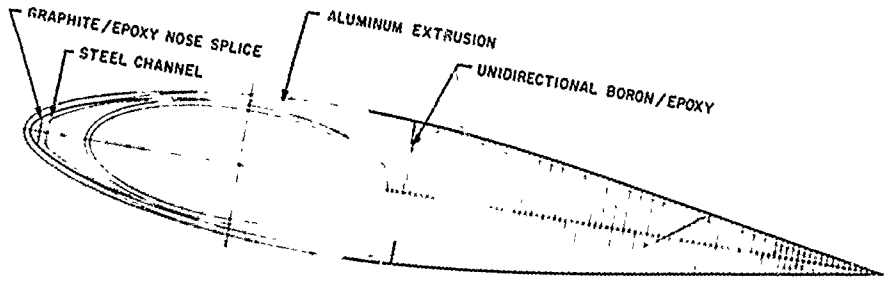

BLADE 5

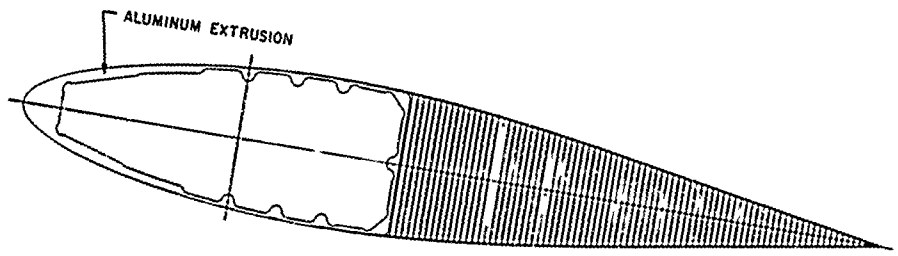

BLADE 6

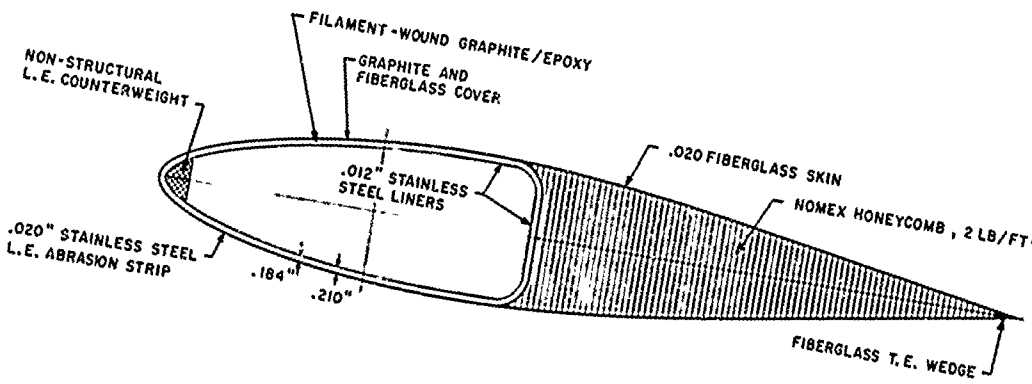

Figure 17. Continued.

BLADE 7

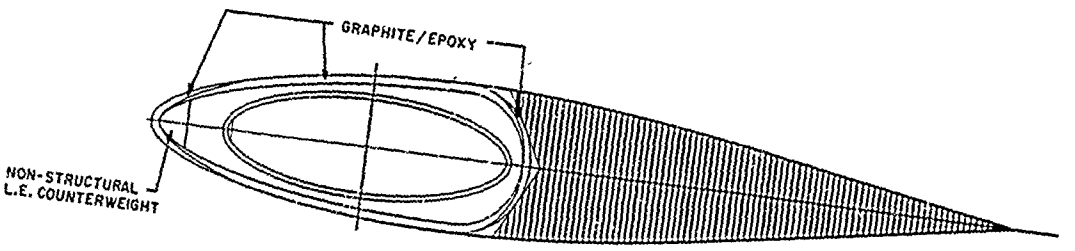

BLADE 8

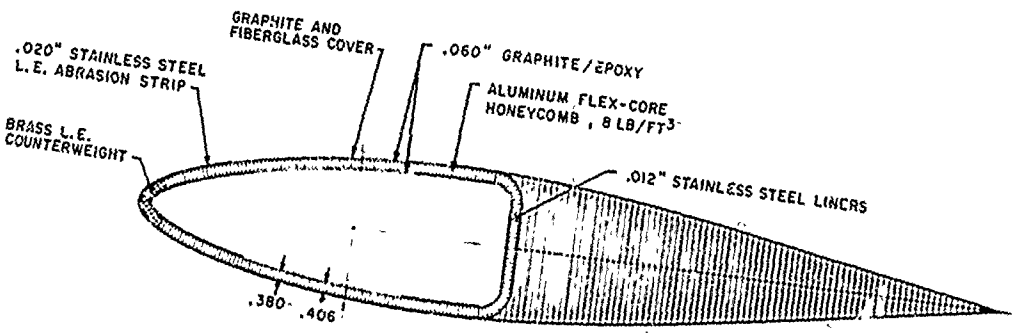

Figure 17. Concluded.

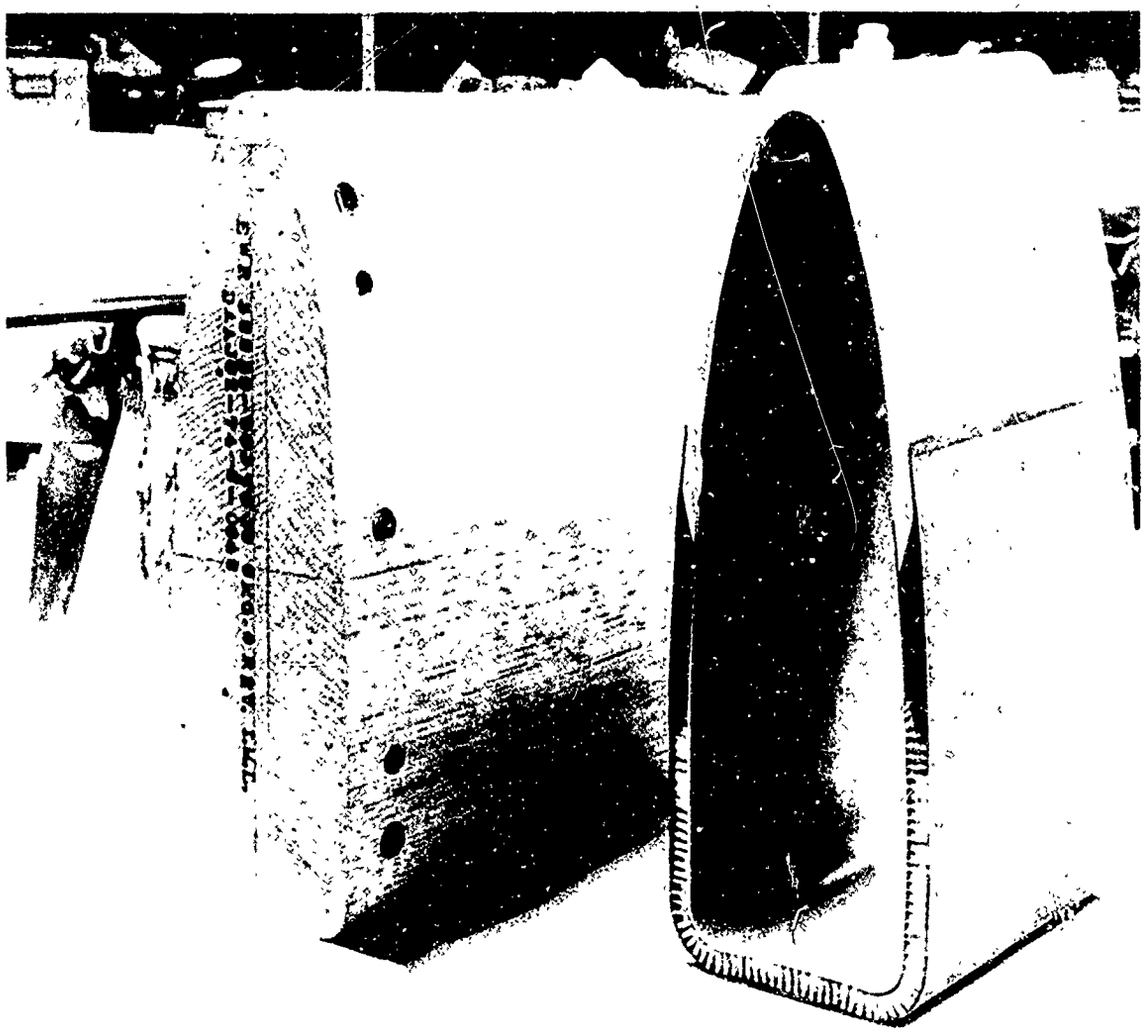

Figure 18. Sample Spar Section - Design No. 1.

(a) Completed Section

Figure 19. Sample Spar Section - Design No. 2.

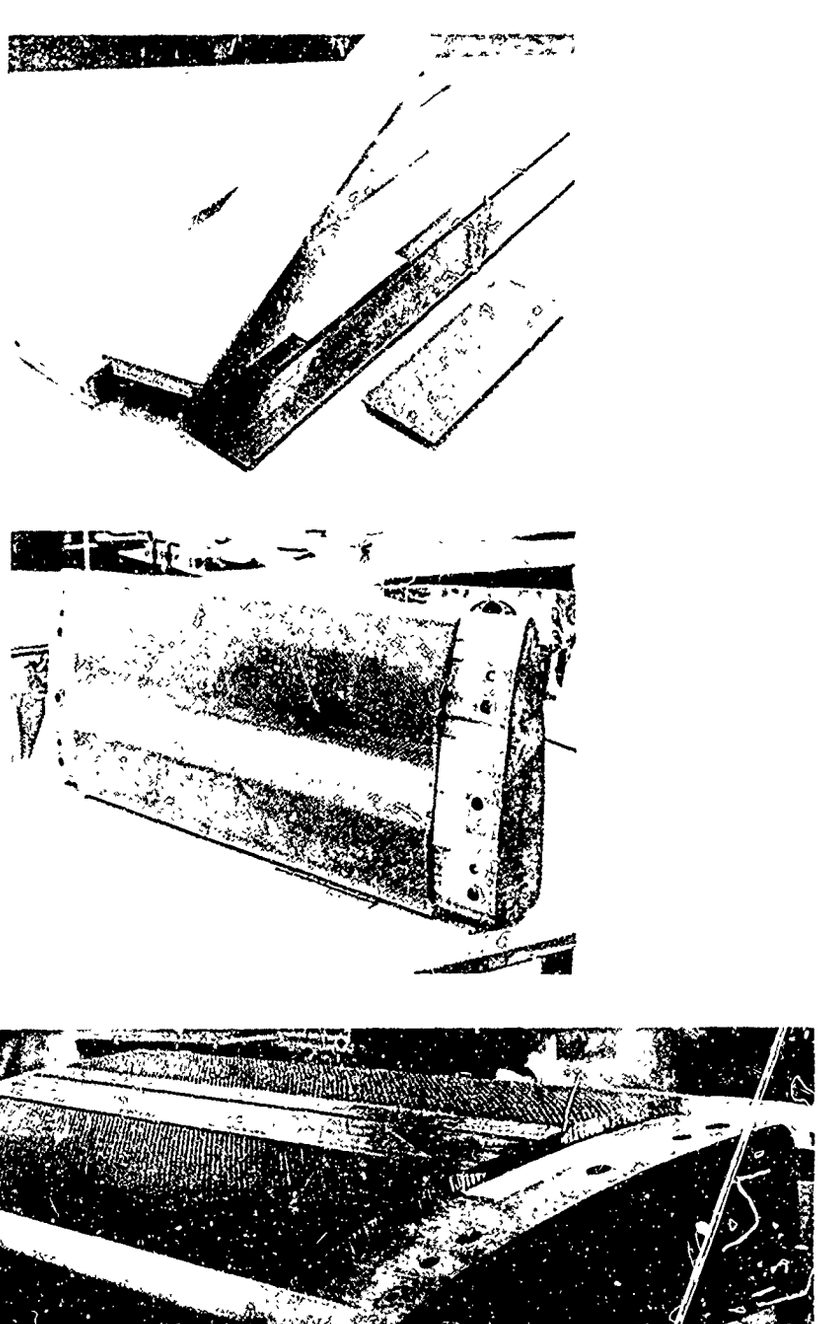

(b) Stages in Manufacture

Figure 19. Concluded.

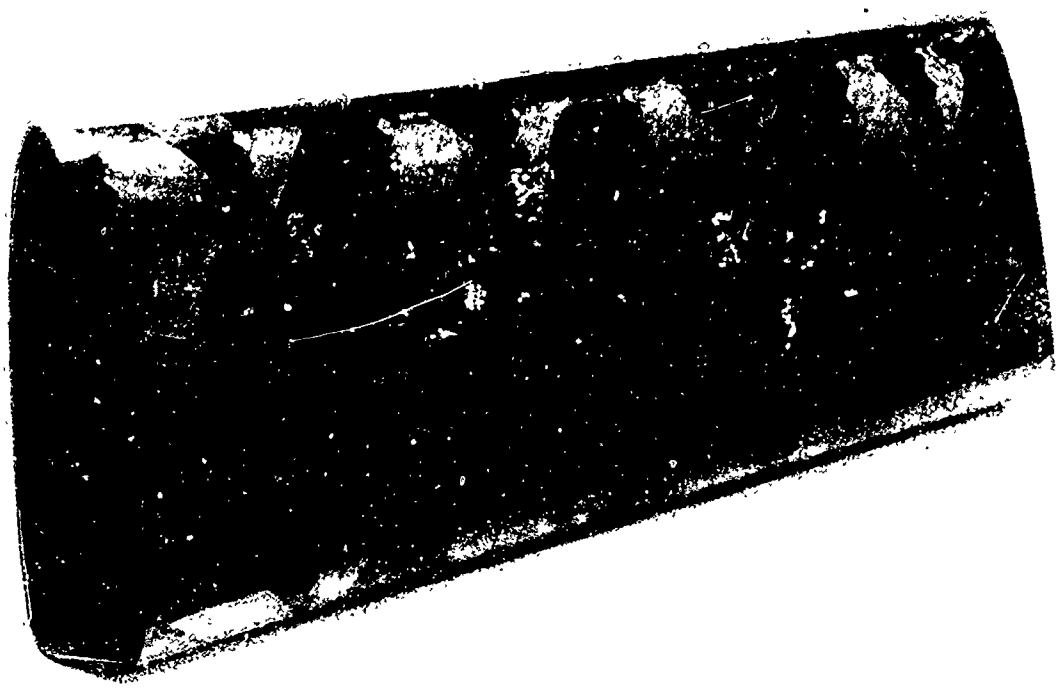

(a) Overall View

Figure 20. Sample Spar Section - Design No. 6.

(b) End and Internal Views

Figure 20. Concluded.

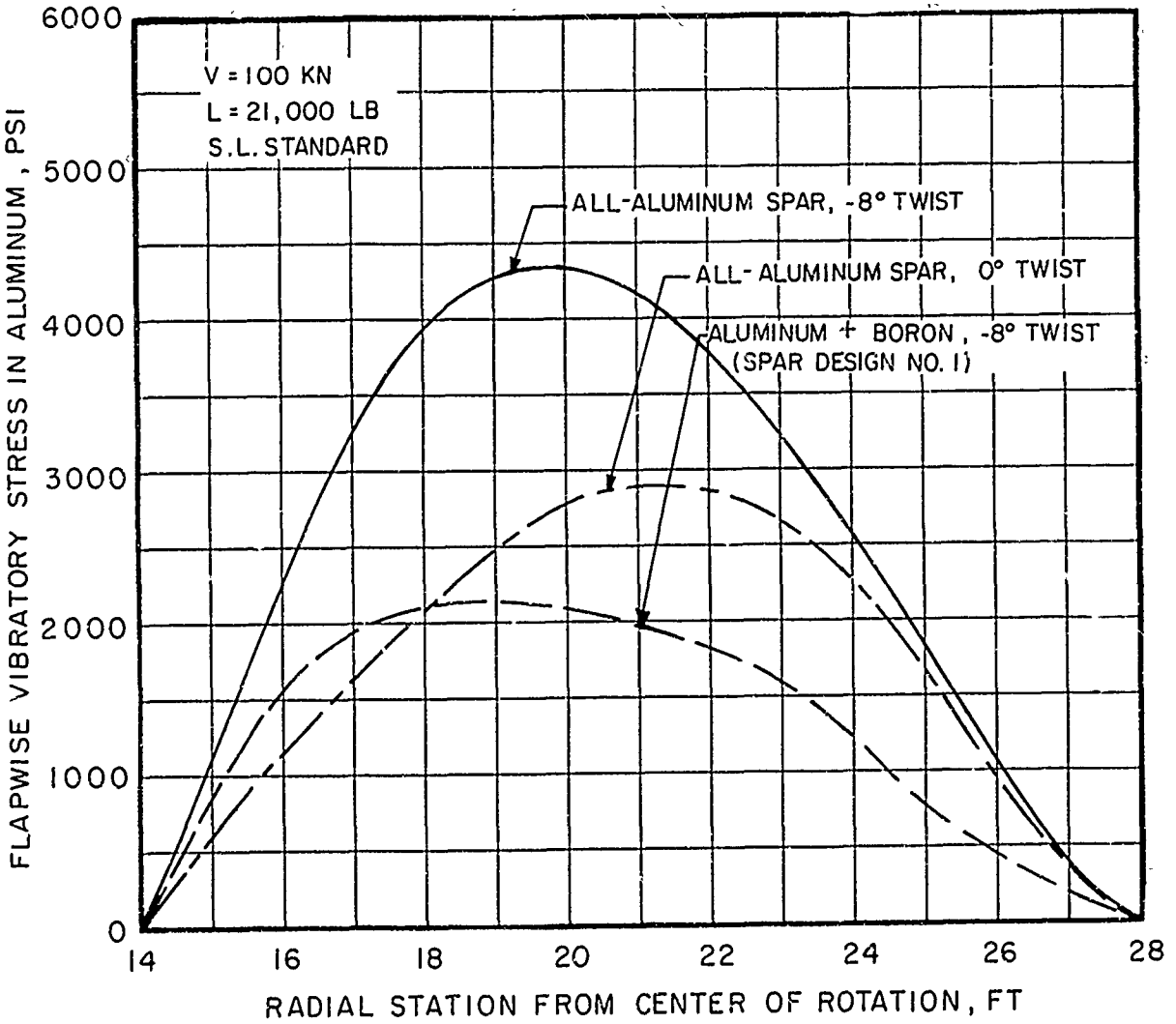

Figure 21. Effect of Twist and Spar Stiffness on Vibratory Stress of Outer Blade Spar.

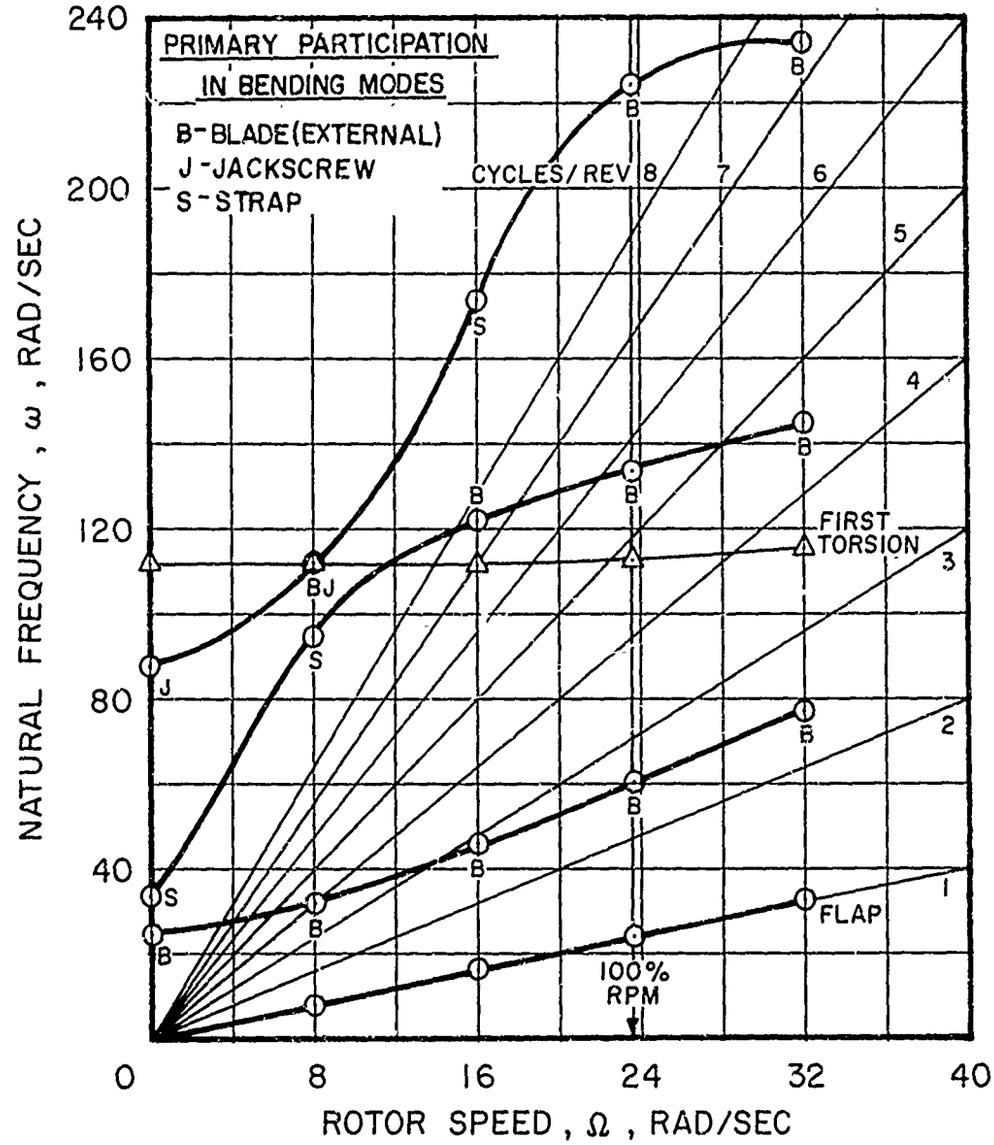

(a) Flapwise and Torsion Modes

Figure 22. Blade Natural Frequency Diagram, 100% Diameter.

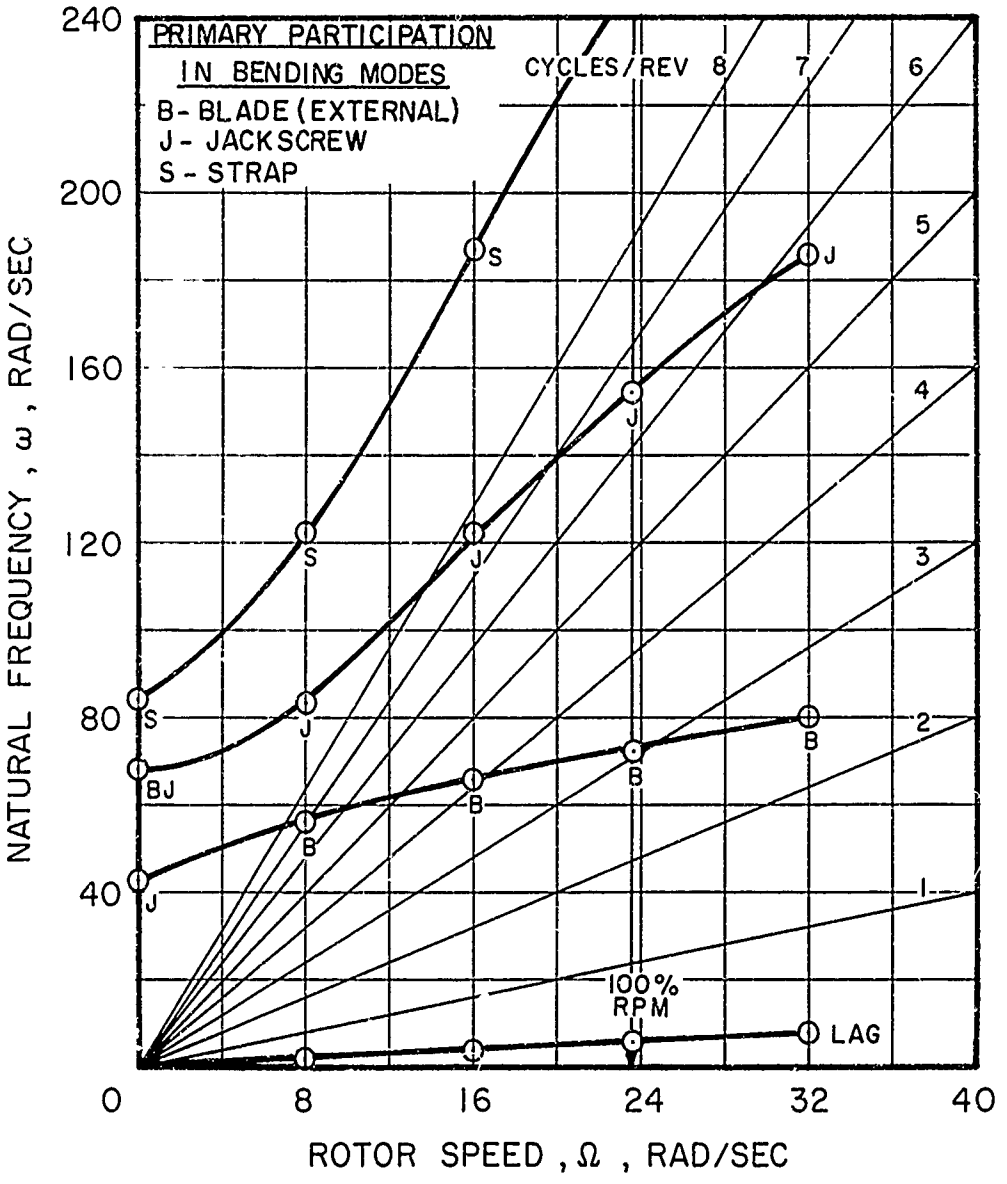

(b) Edgewise Modes

Figure 22. Concluded.

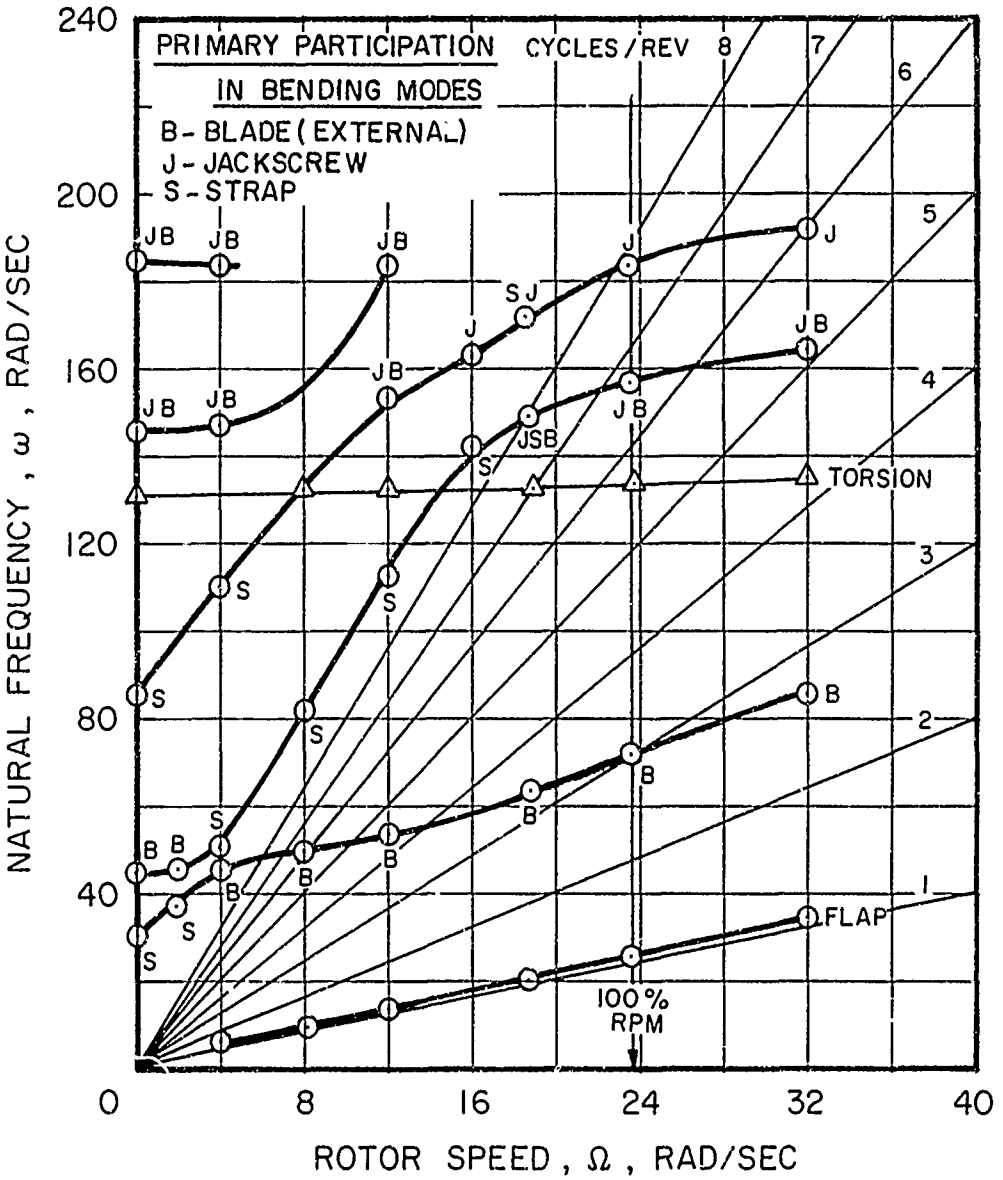

(a) Flapwise and Torsion Modes

Figure 23. Blade Natural Frequency Diagram, 80% Diameter.

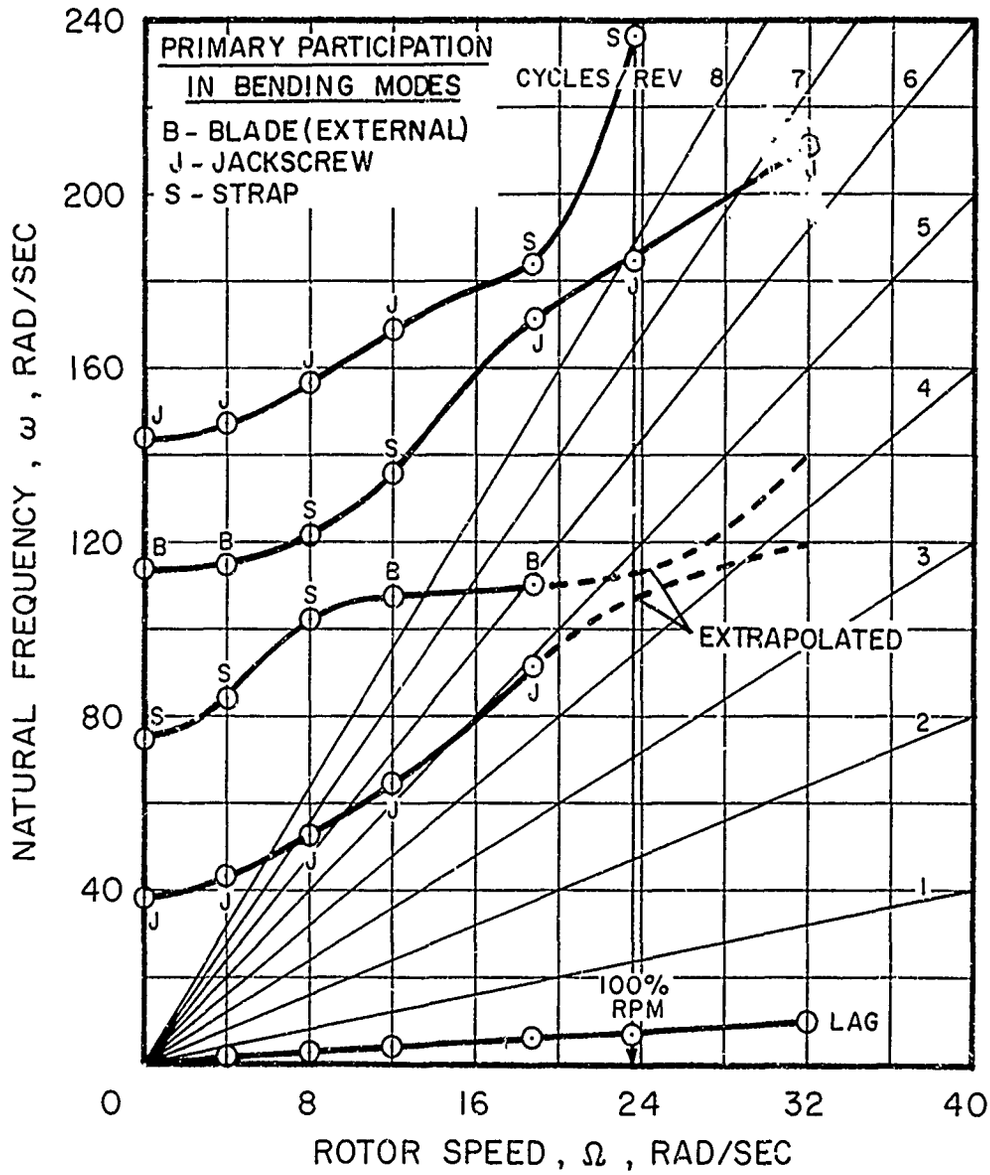

(b) Edgewise Modes

Figure 23. Concluded.

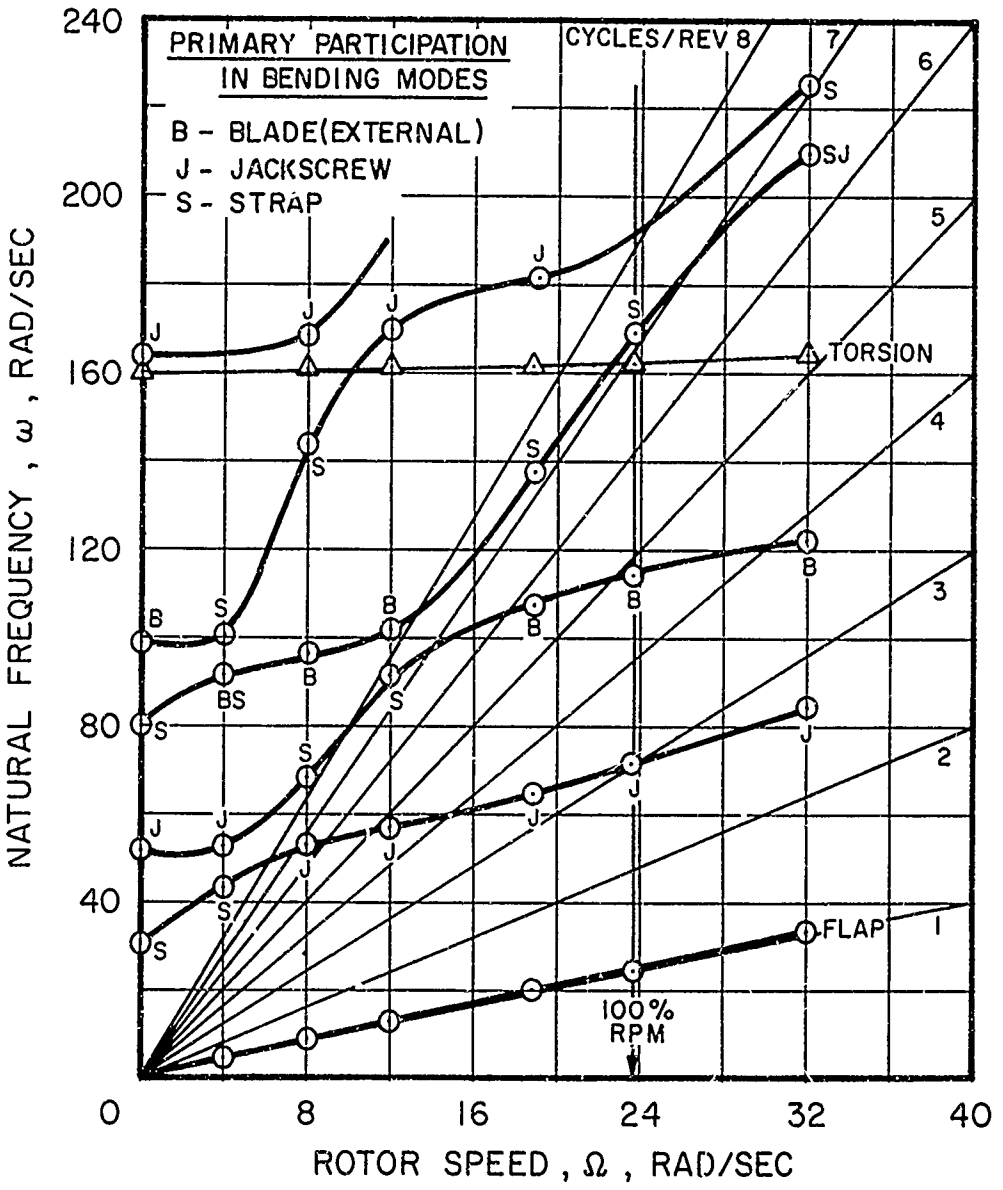

(a) Flapwise and Torsion Modes

Figure 24. Blade Natural Frequency Diagram, 60% Diameter.

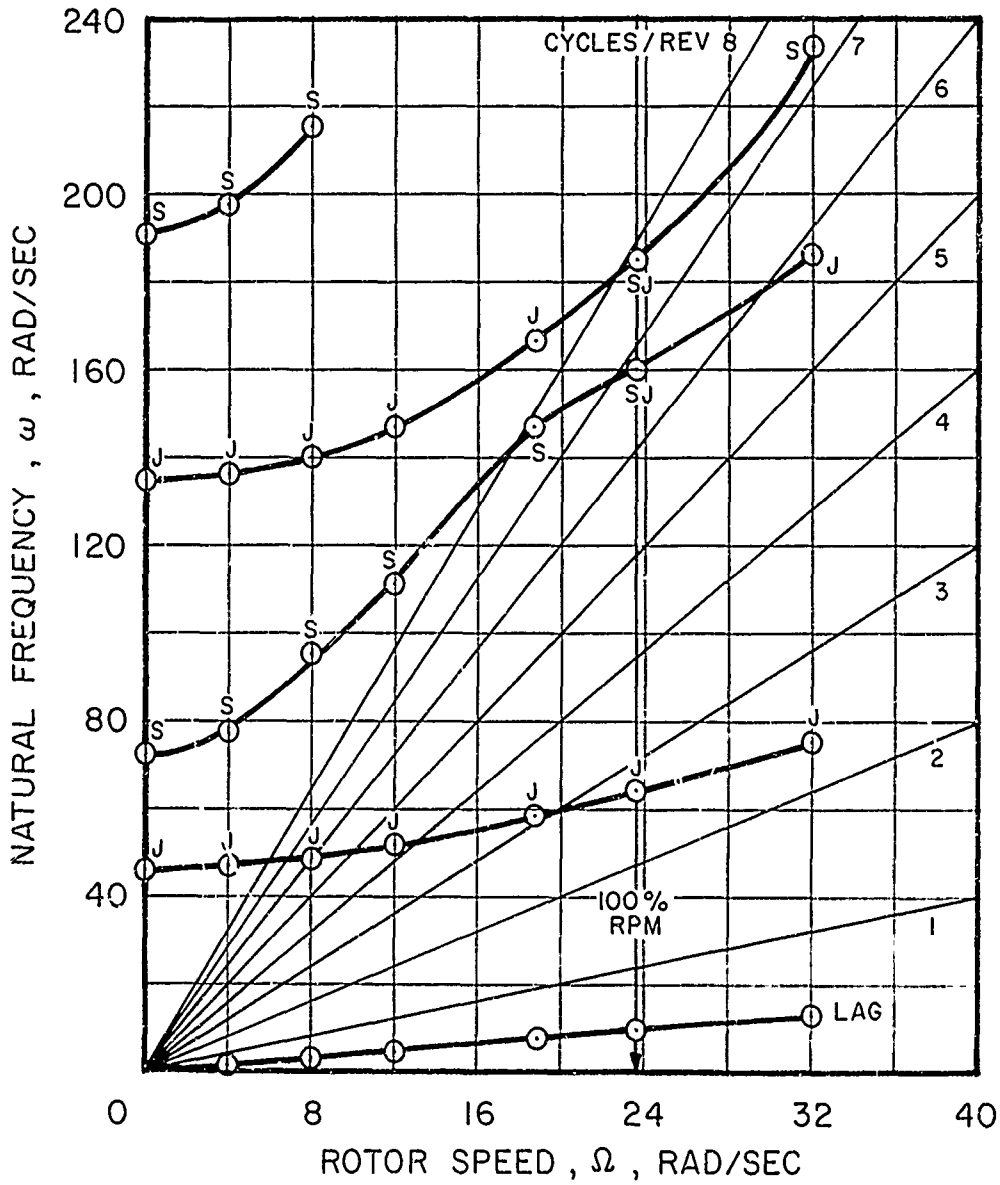

(b) Edgewise Modes

Figure 24. Concluded.

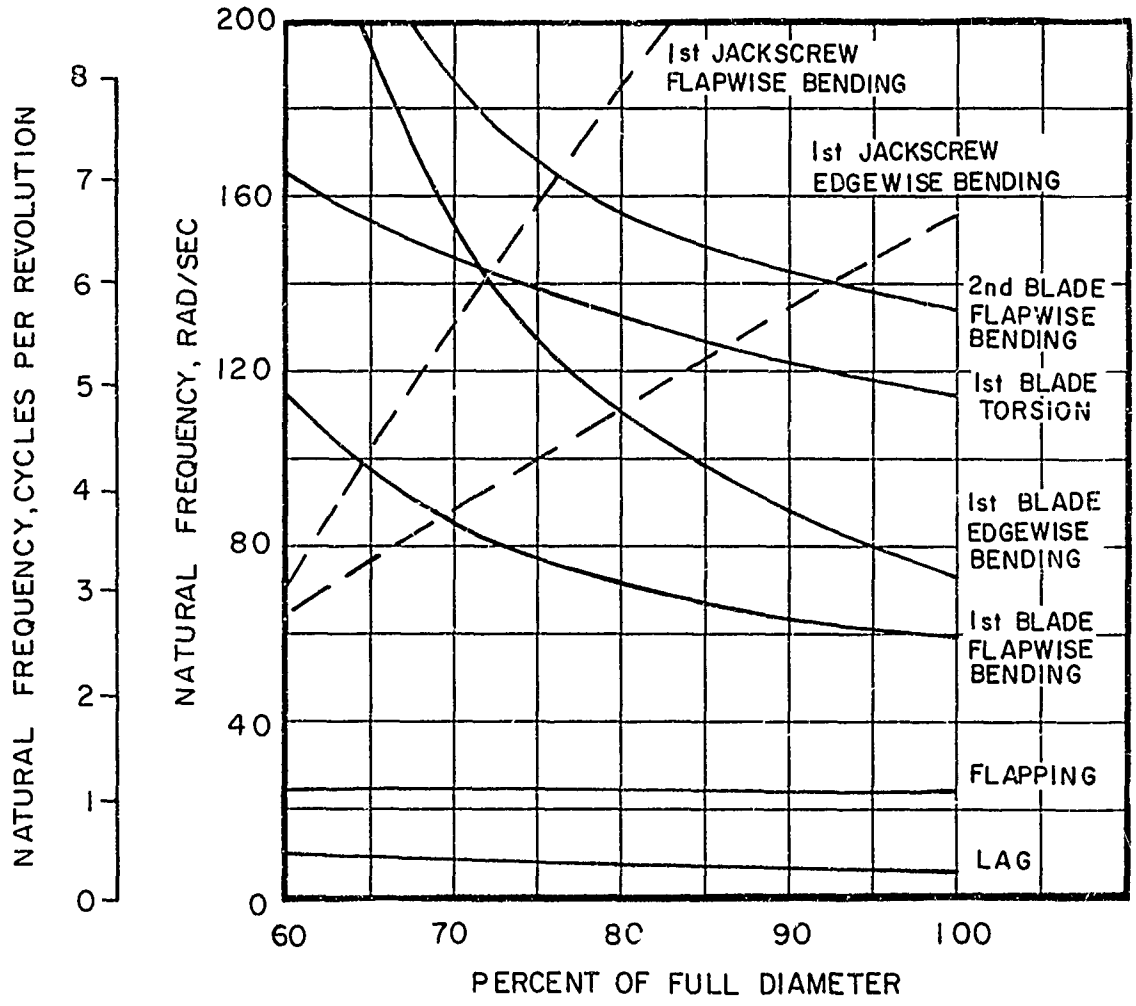

Figure 25. Variation of Blade Natural Frequencies with Diameter, 100% RPM.

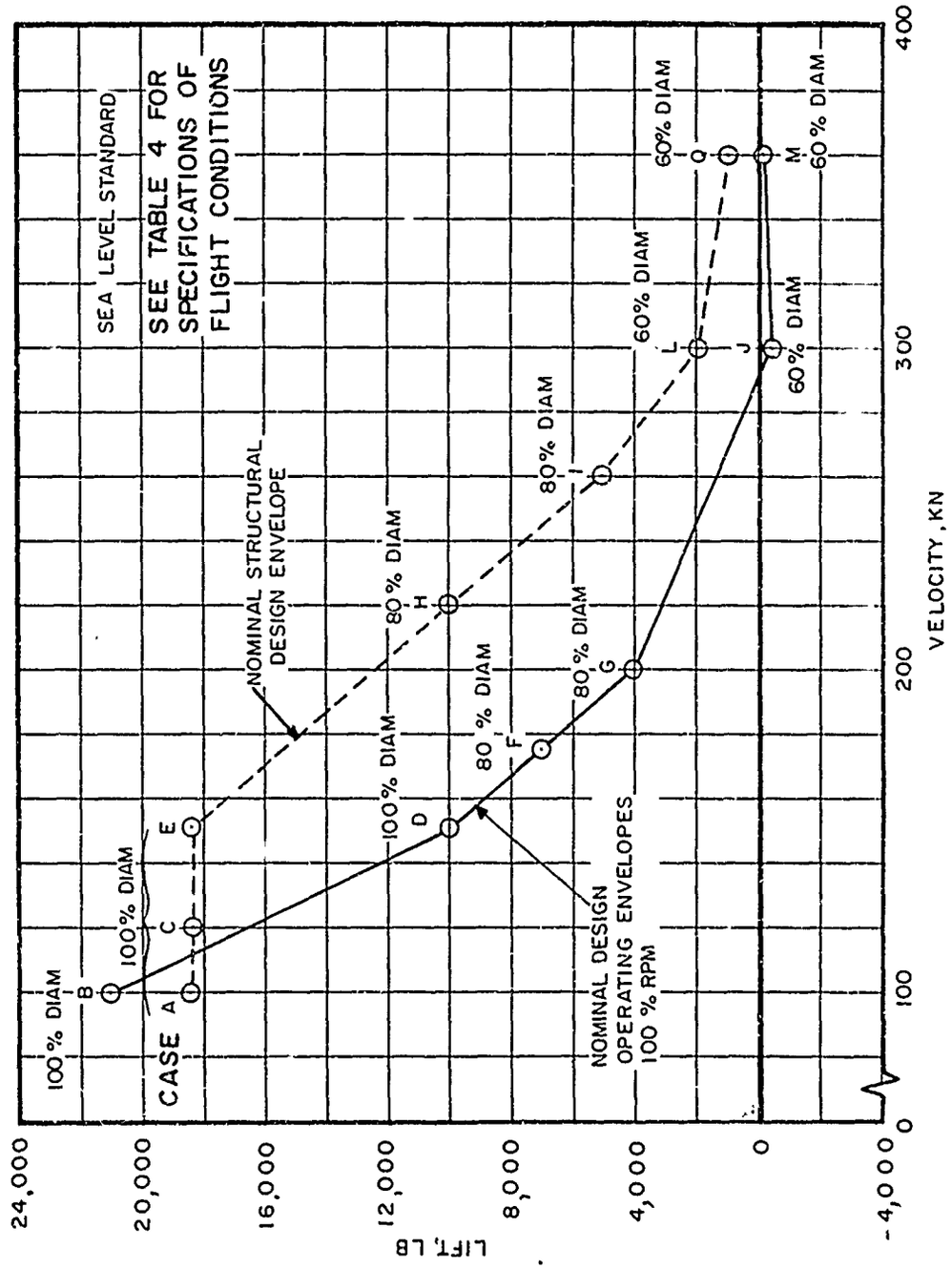

Figure 26. Variation of Rotor Lift with Forward Speed for Selected Conditions.

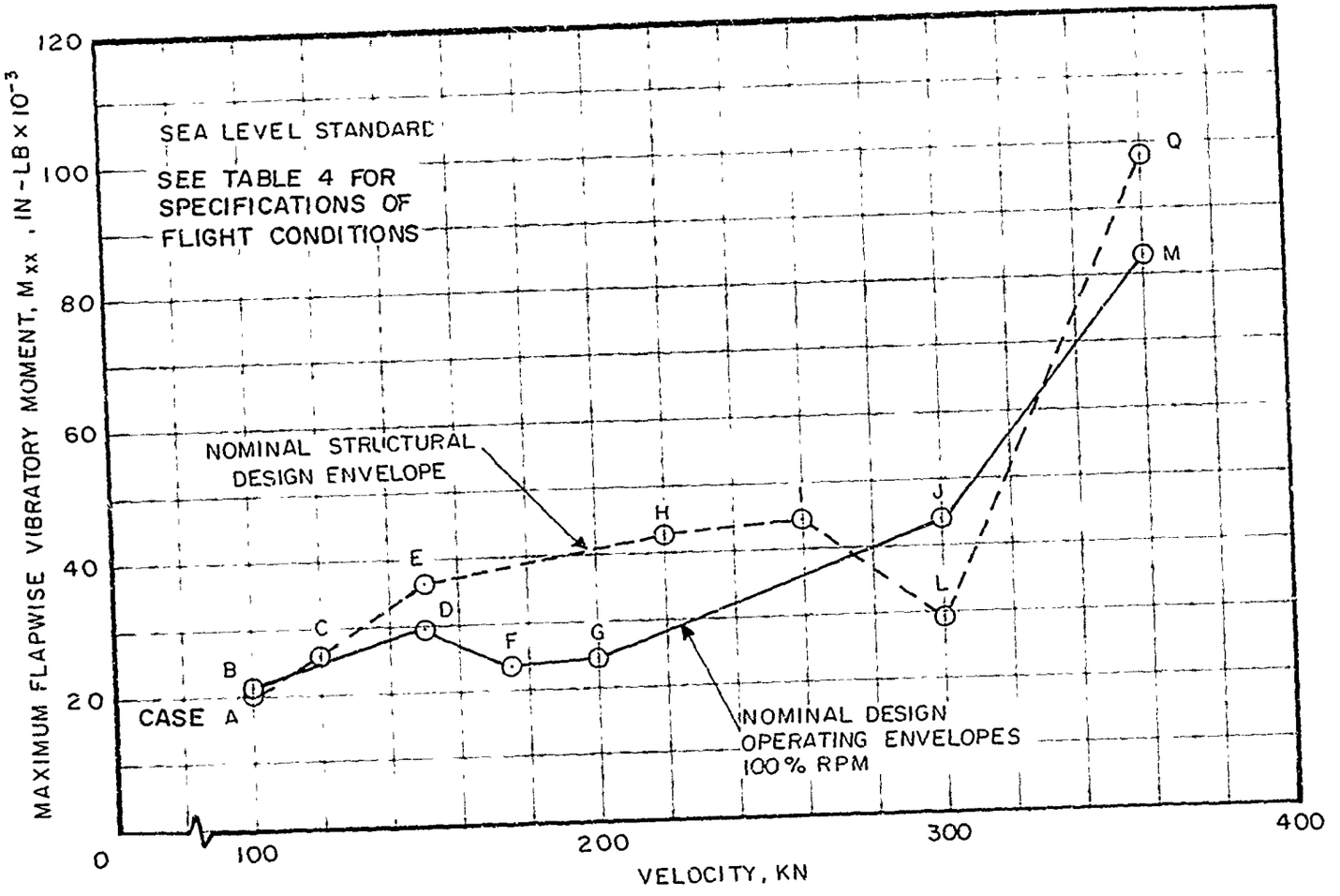

Figure 27. Variation of Flapwise Vibratory Moment with Forward Speed.

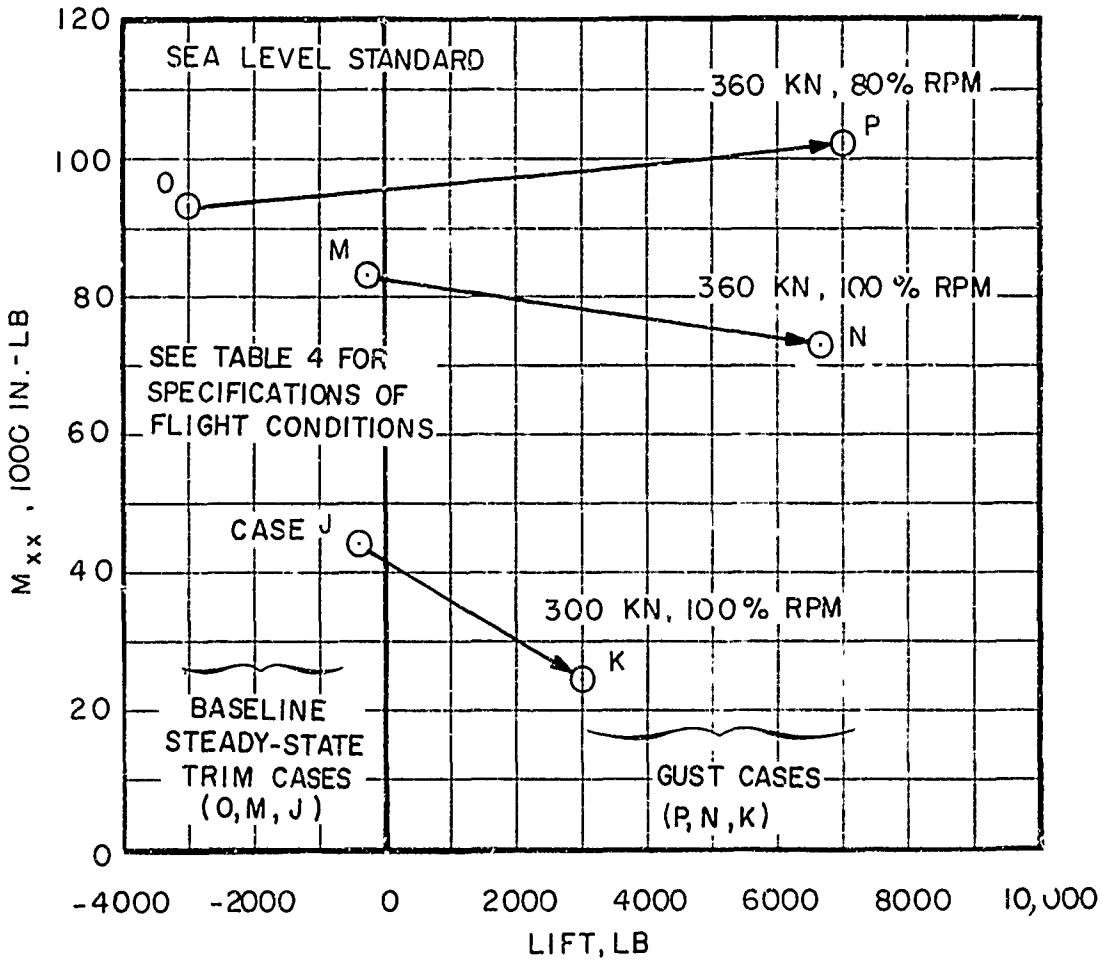

Figure 26. Effect of Vertical Gust on Rotor Loads.

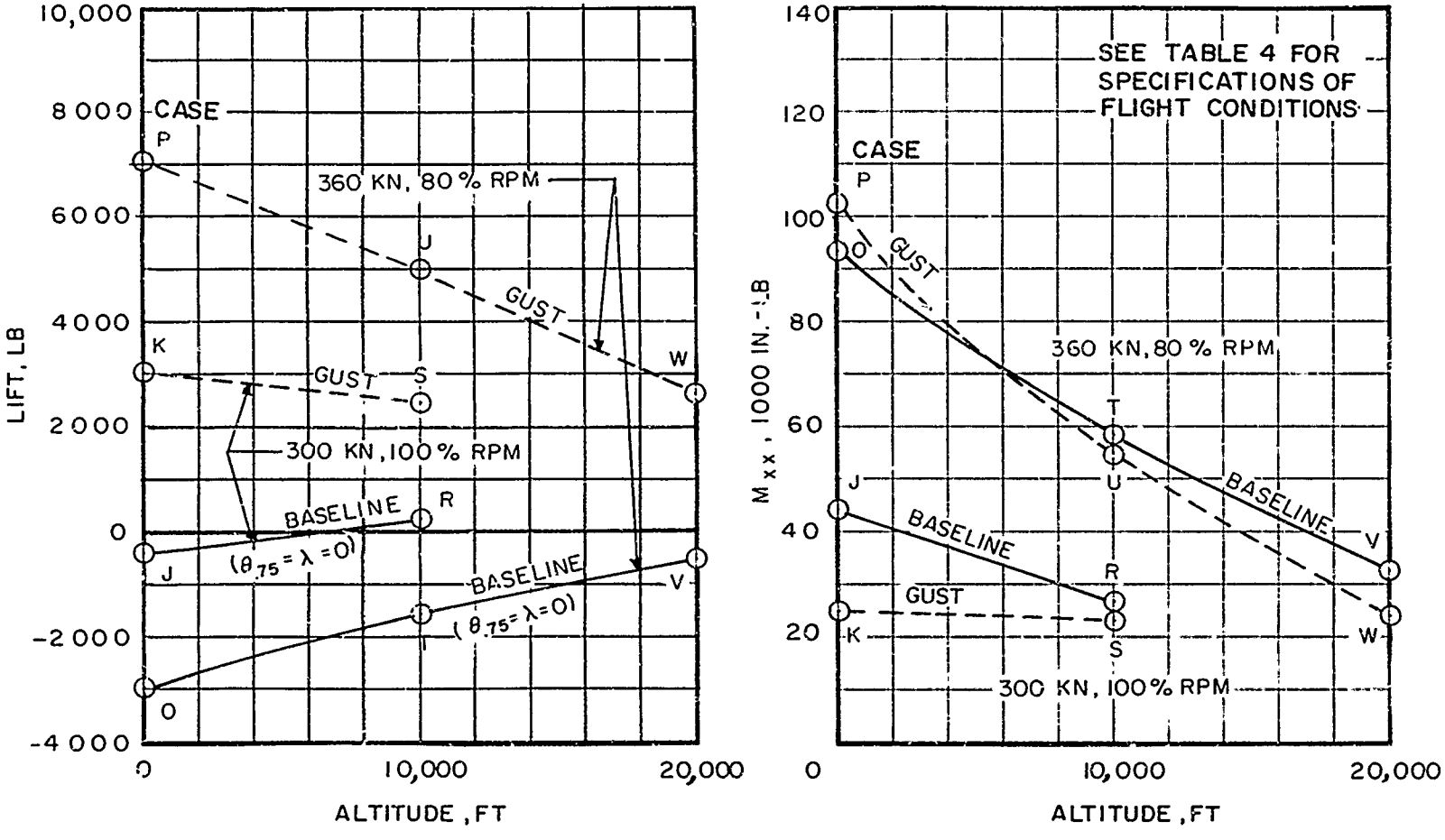

Figure 29. Effect of Altitude on Rotor Loads.

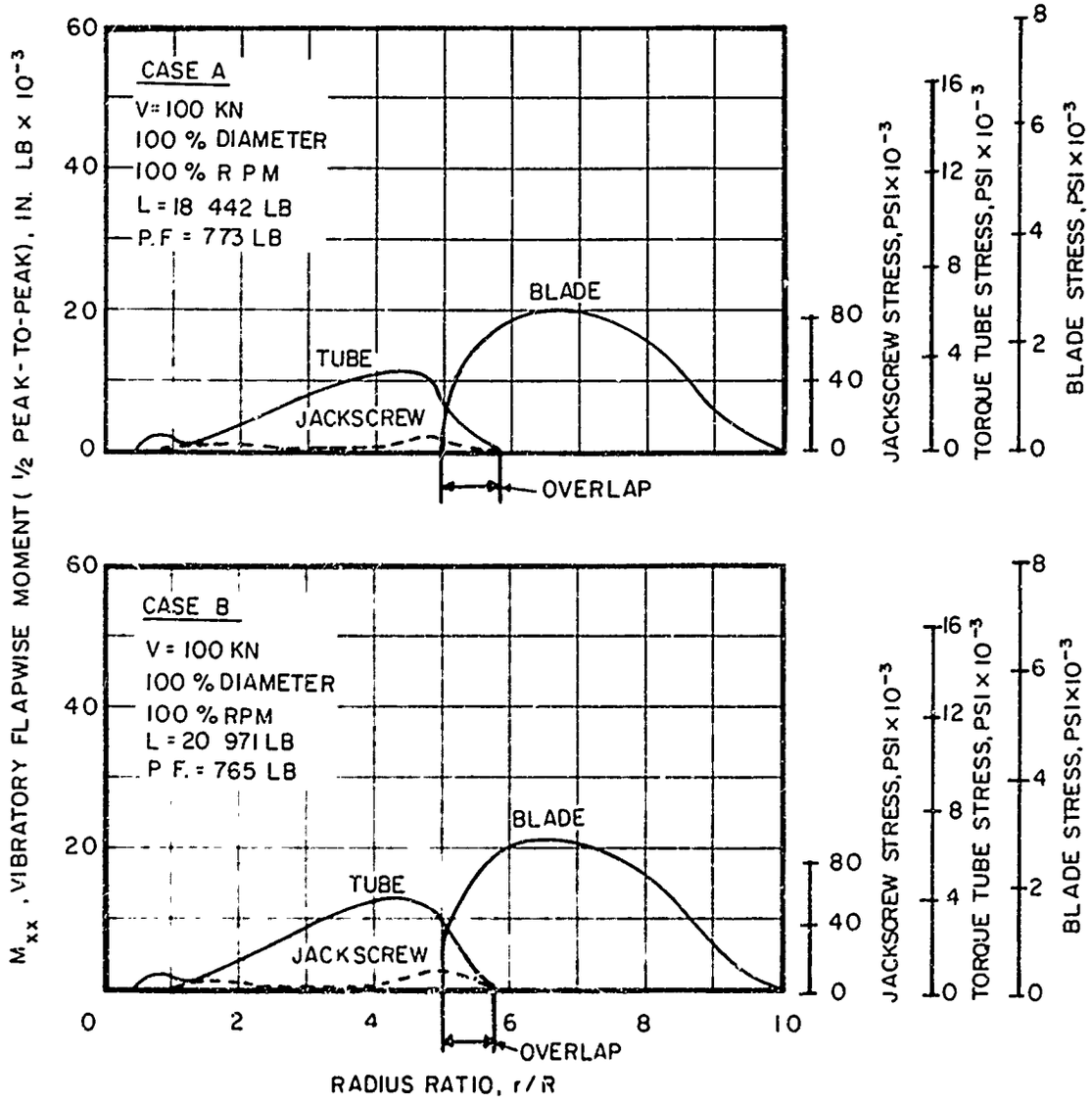

Figure 30. Radial Distribution of Flapwise Moments and Stresses.

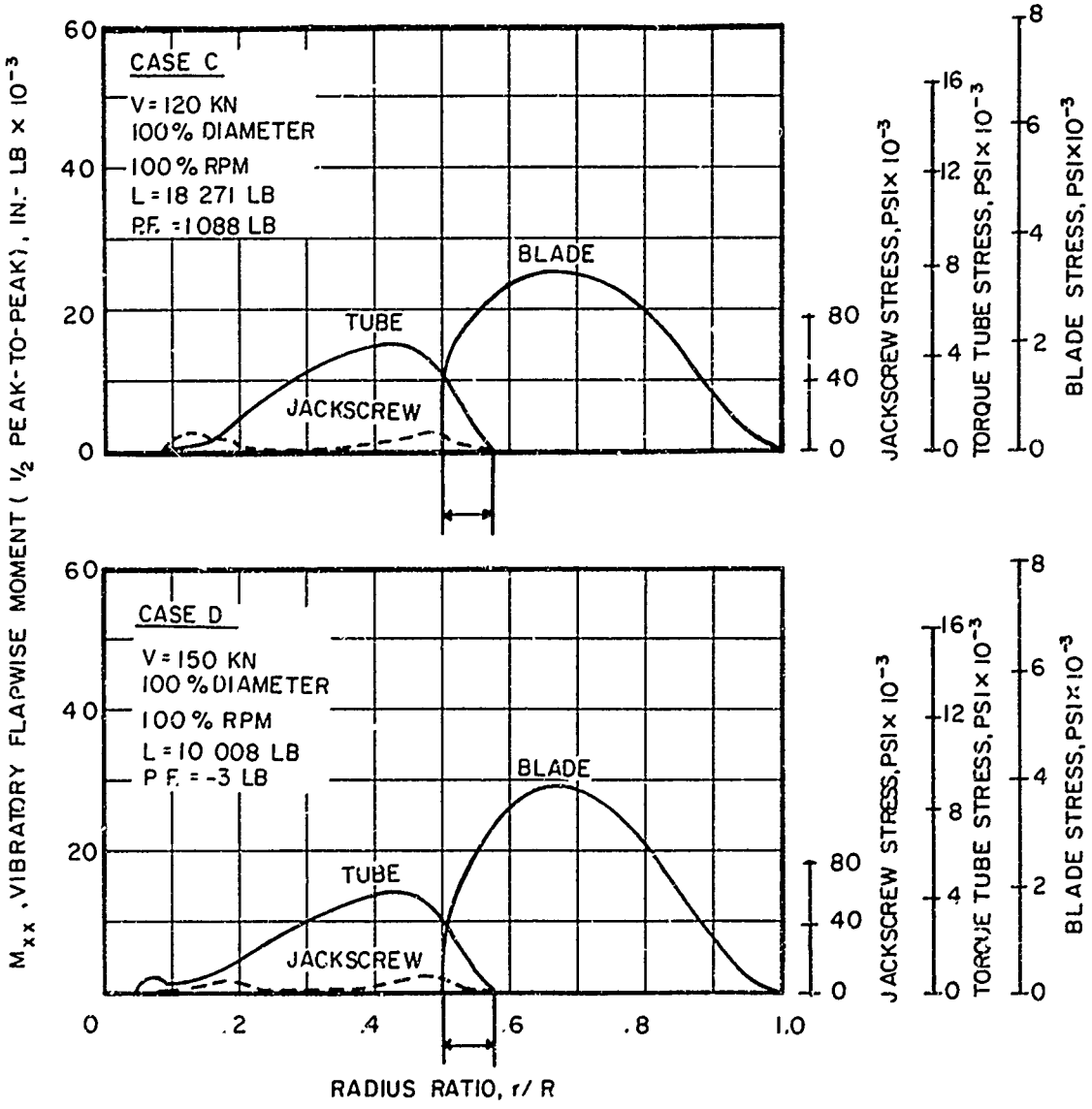

Figure 30. Continued.

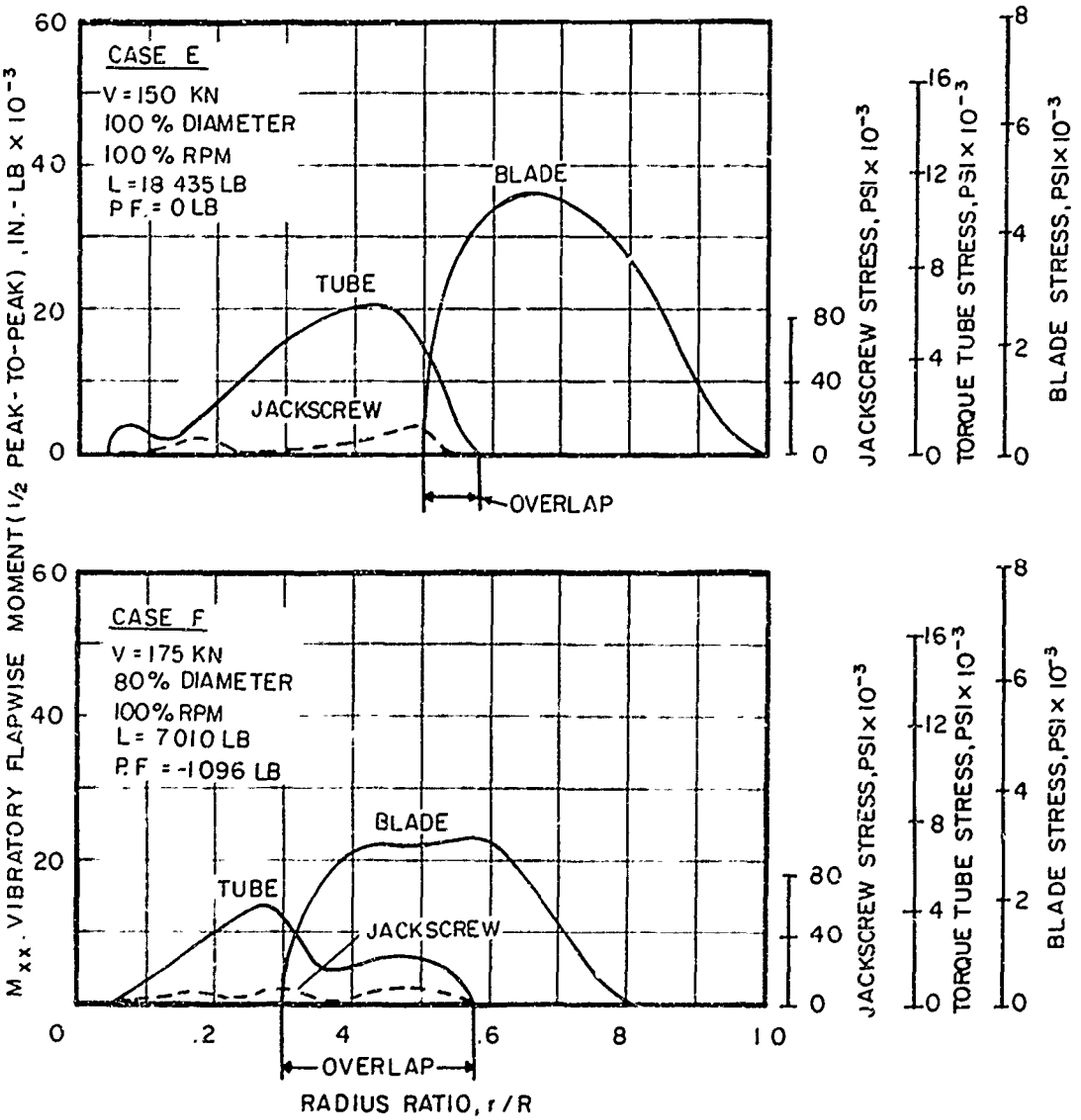

Figure 30. Continued.

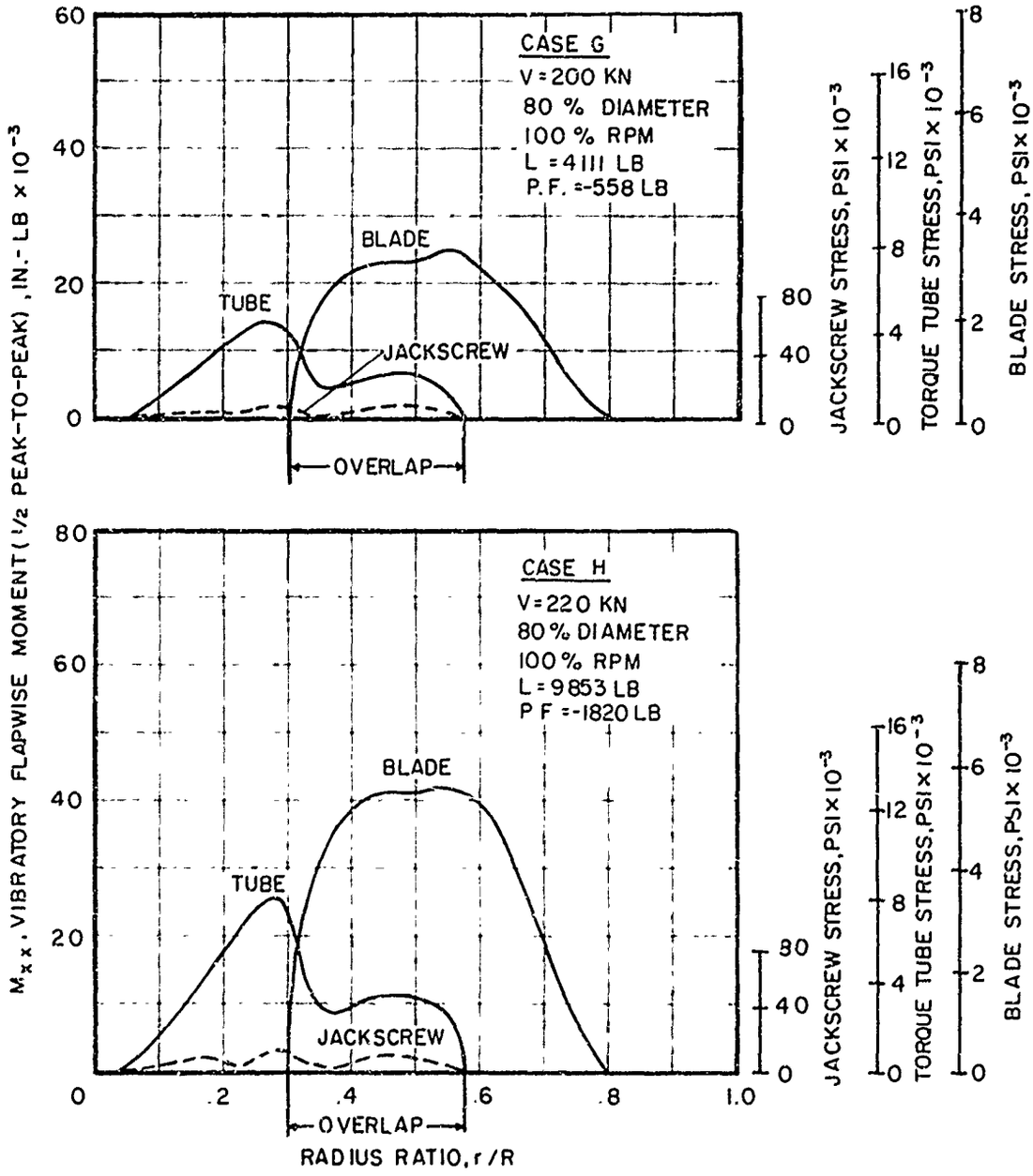

Figure 30. Continued.

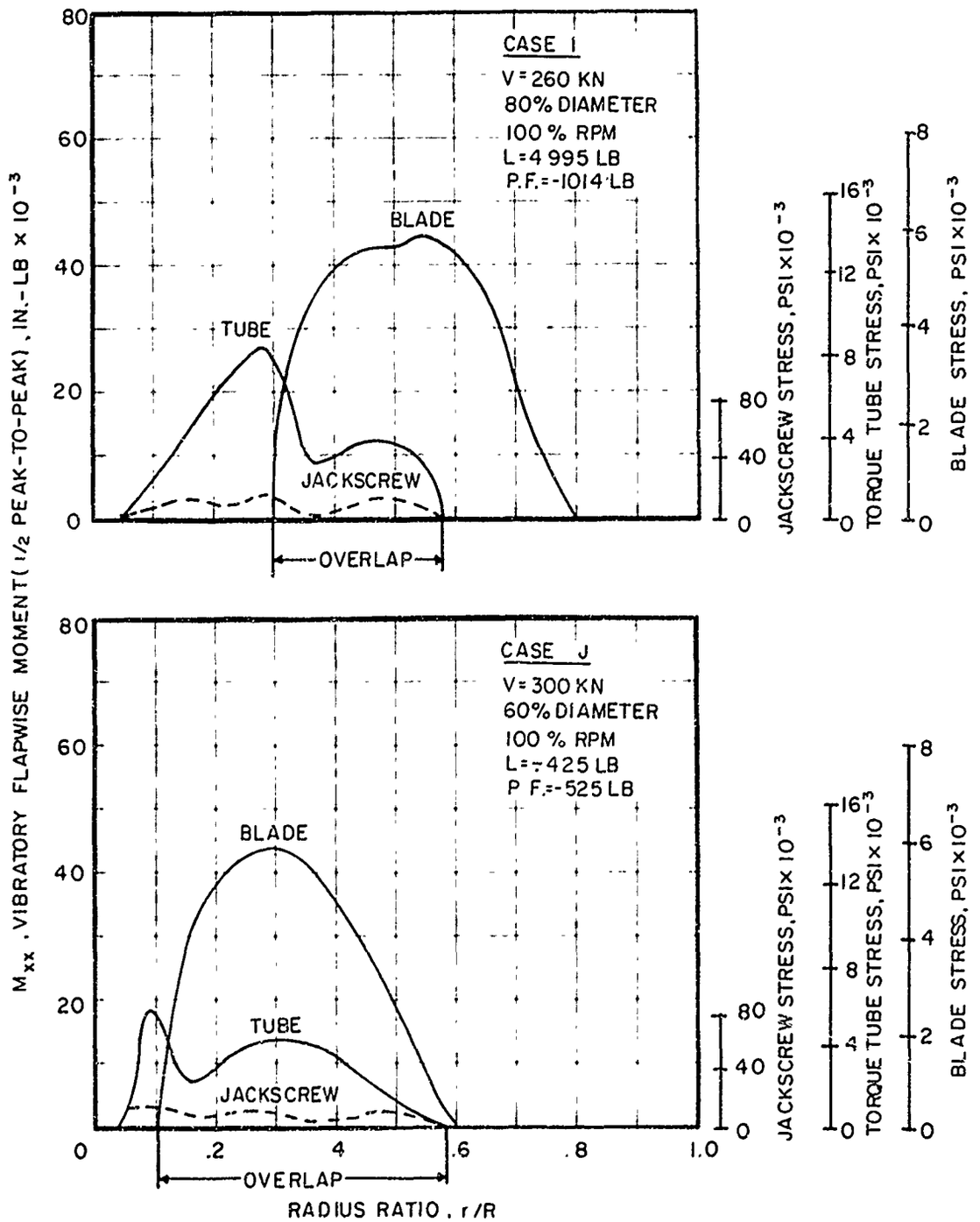

Figure 30. Continued.

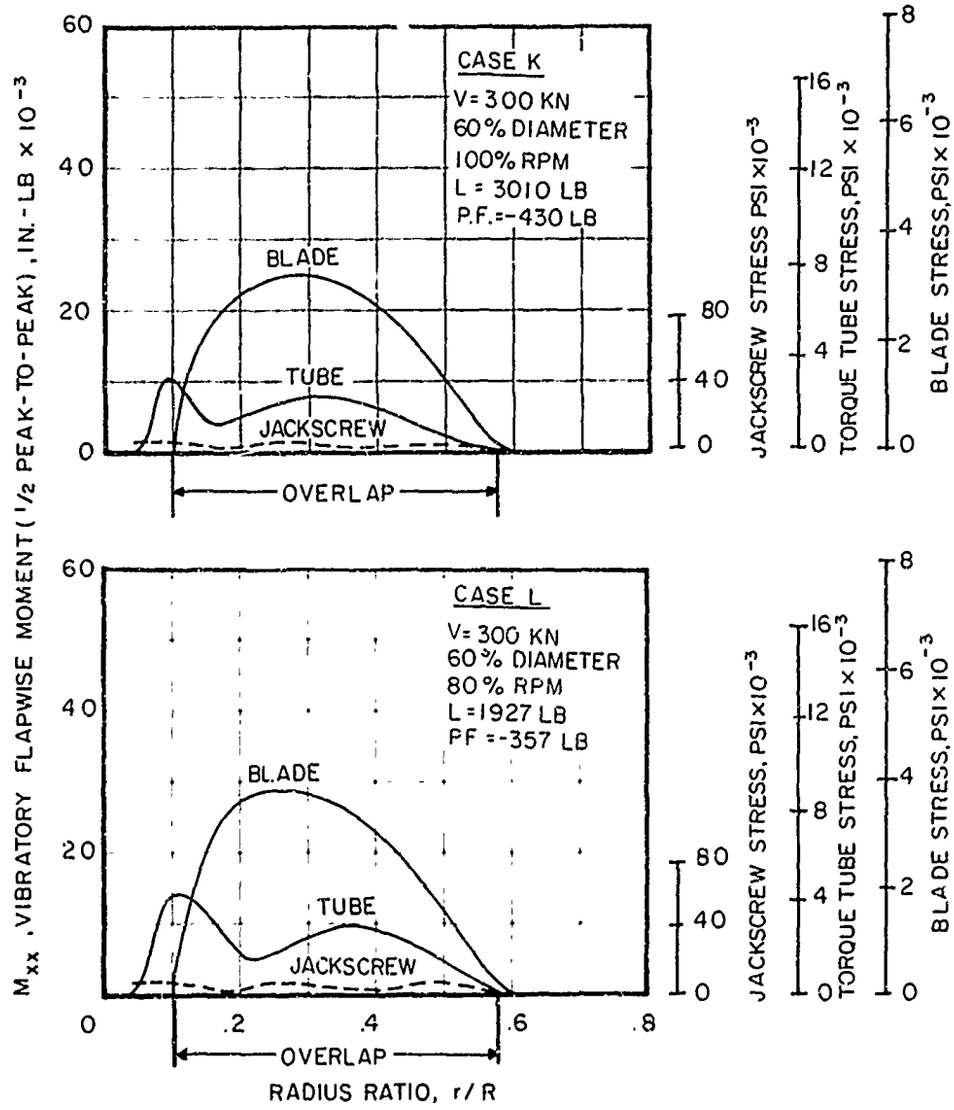

Figure 30. Continued.

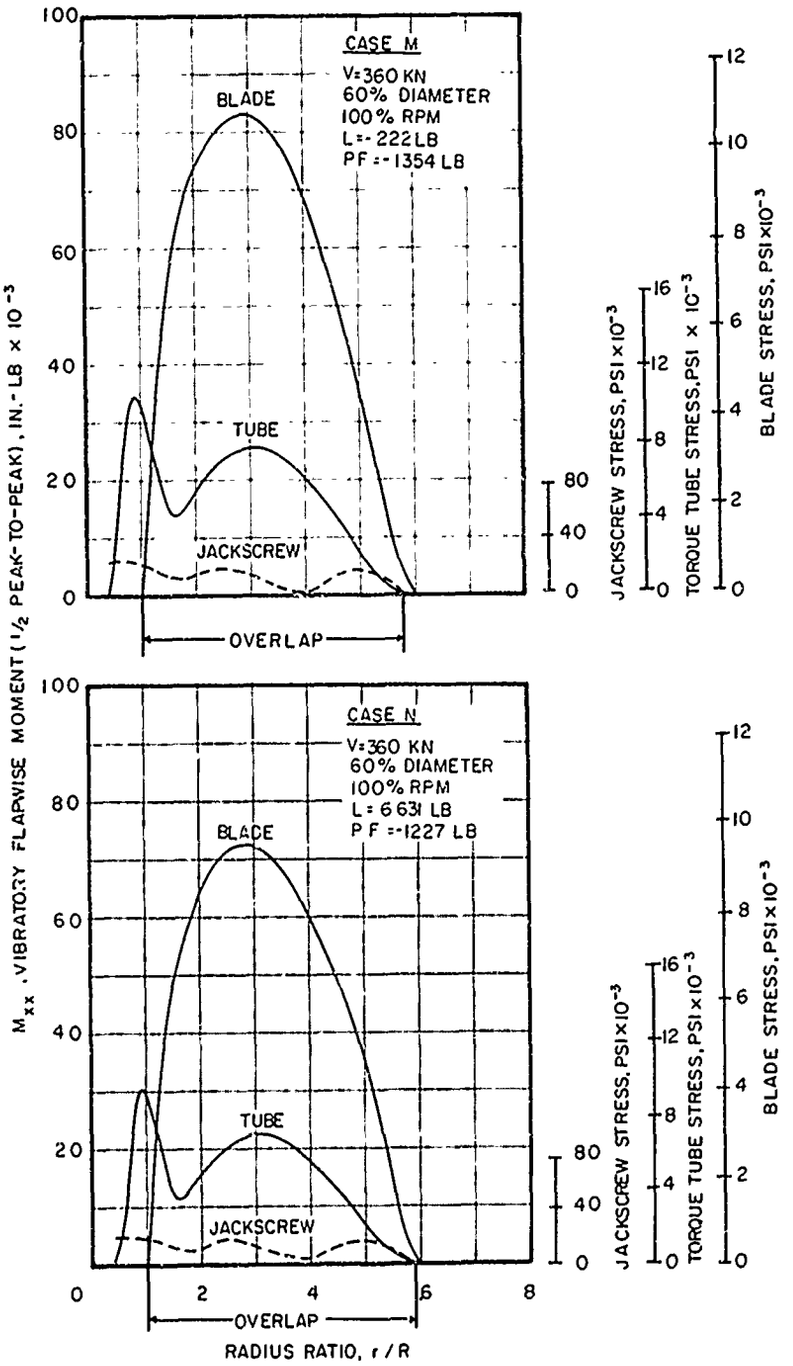

Figure 30. Continued.

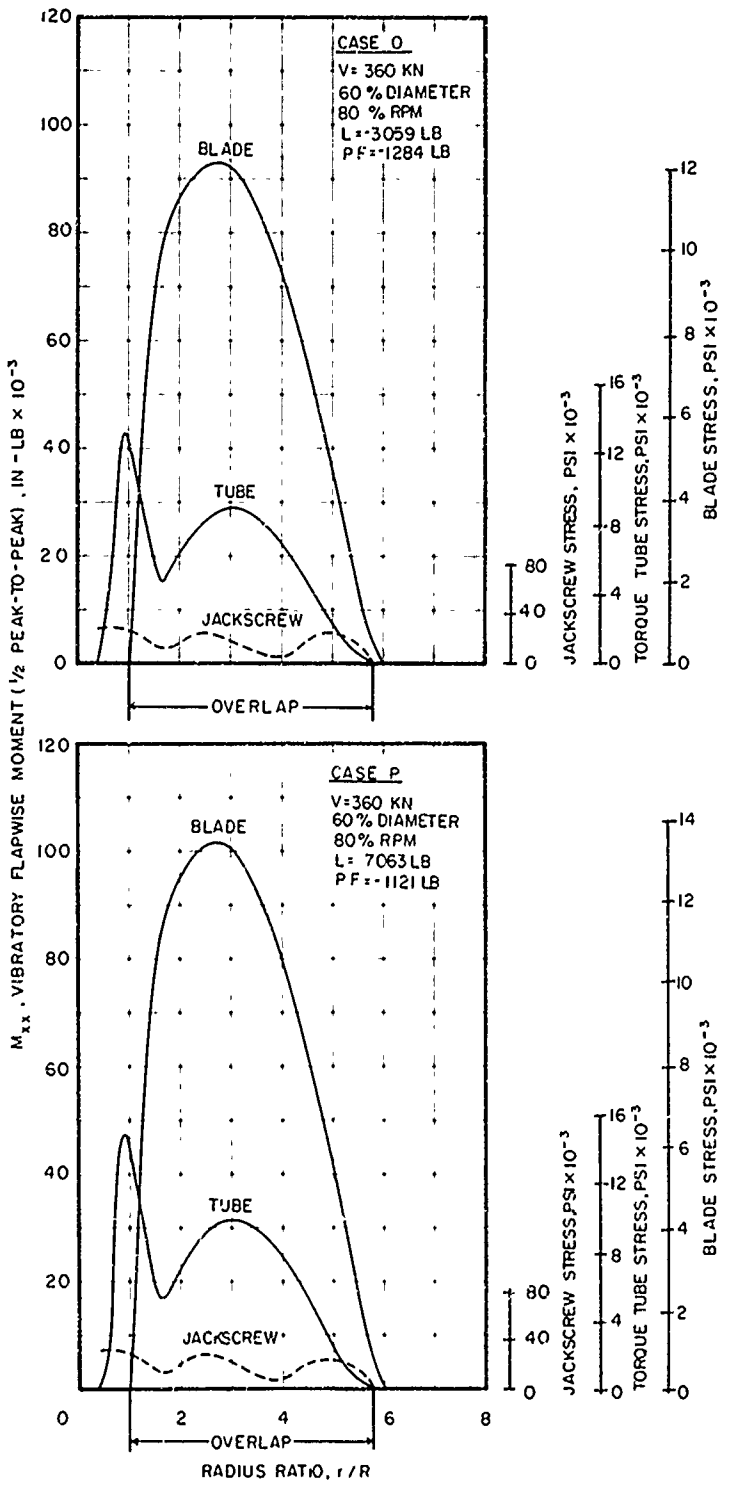

Figure 30. Continued.

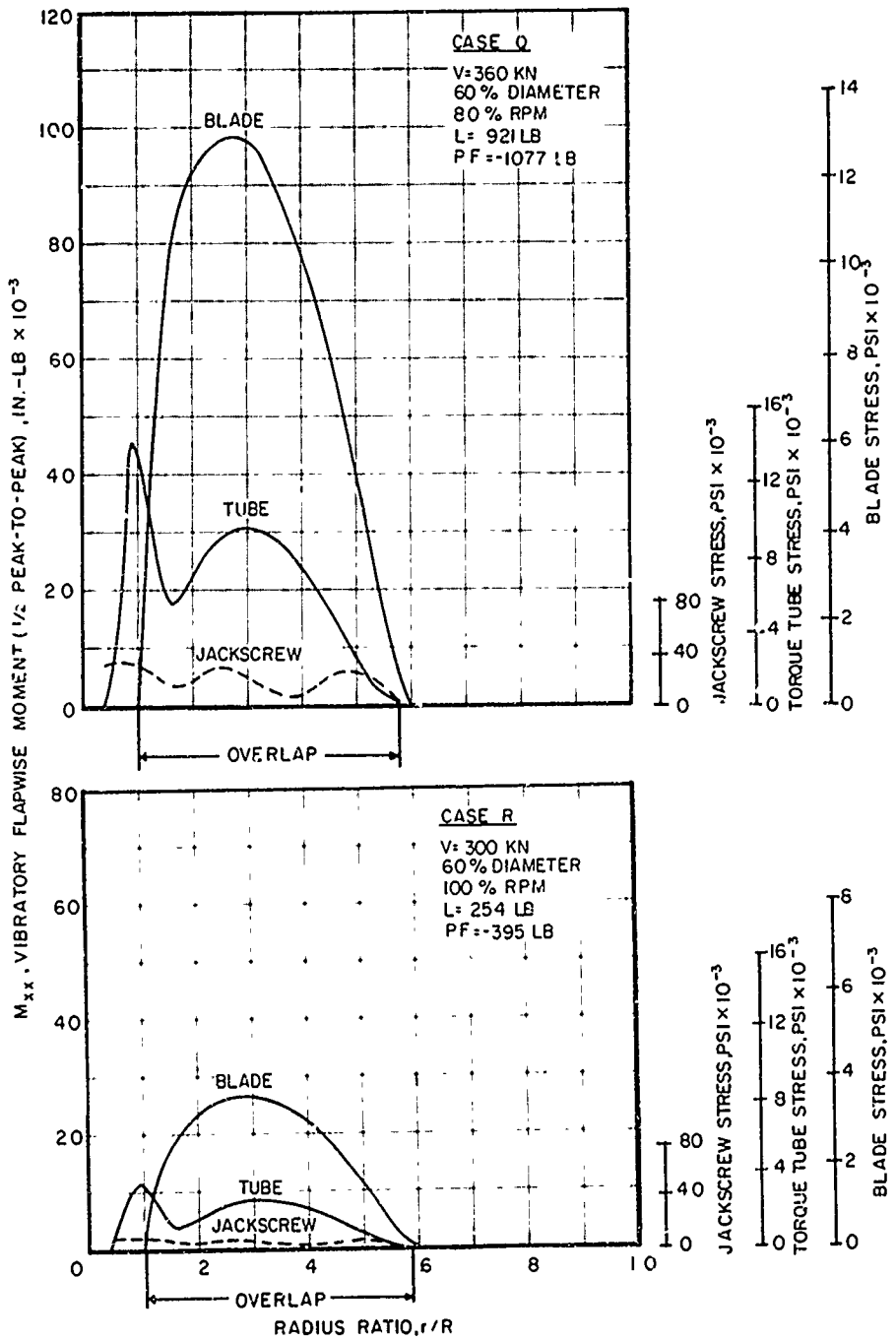

Figure 30. Continued.

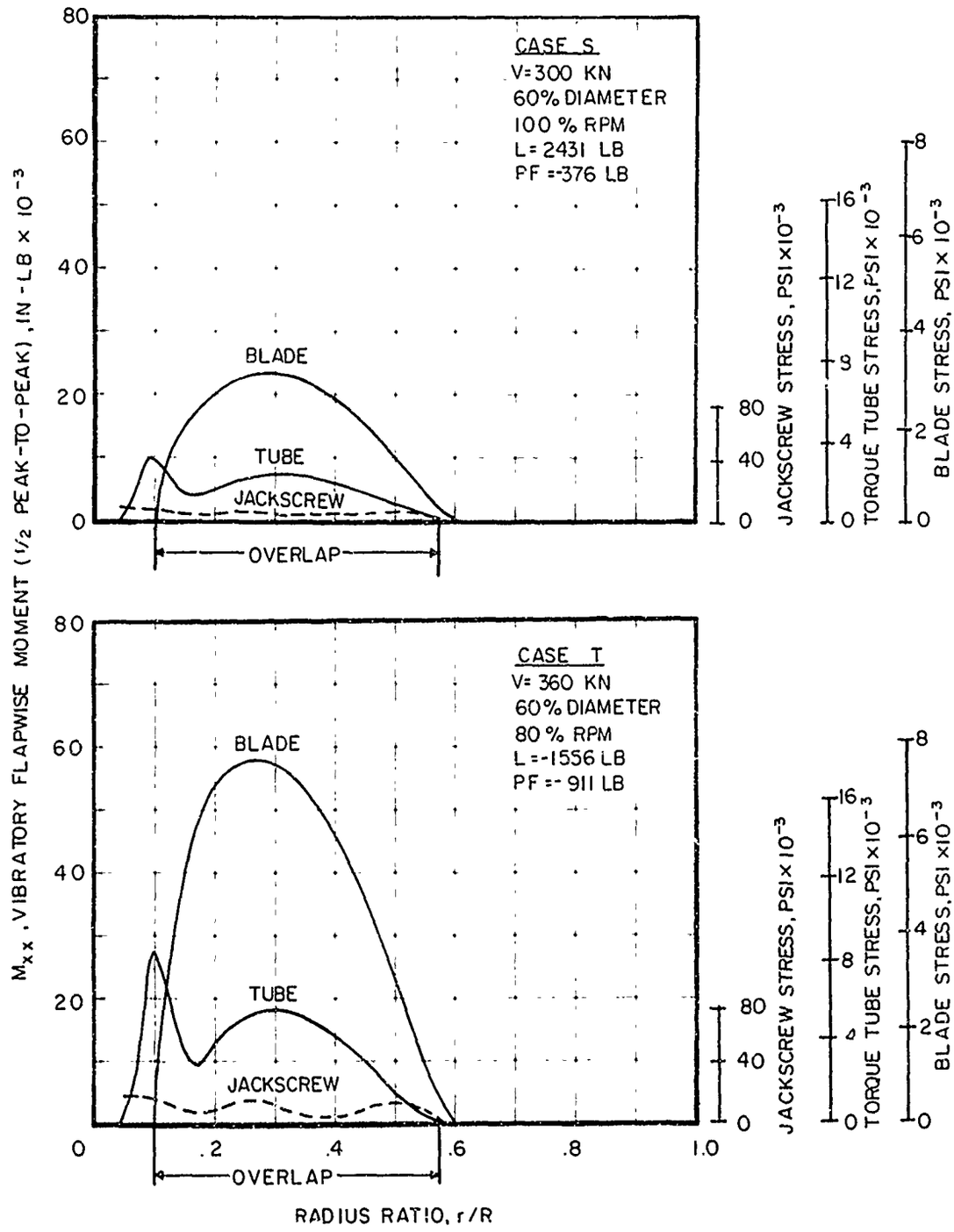

Figure 30. Continued.

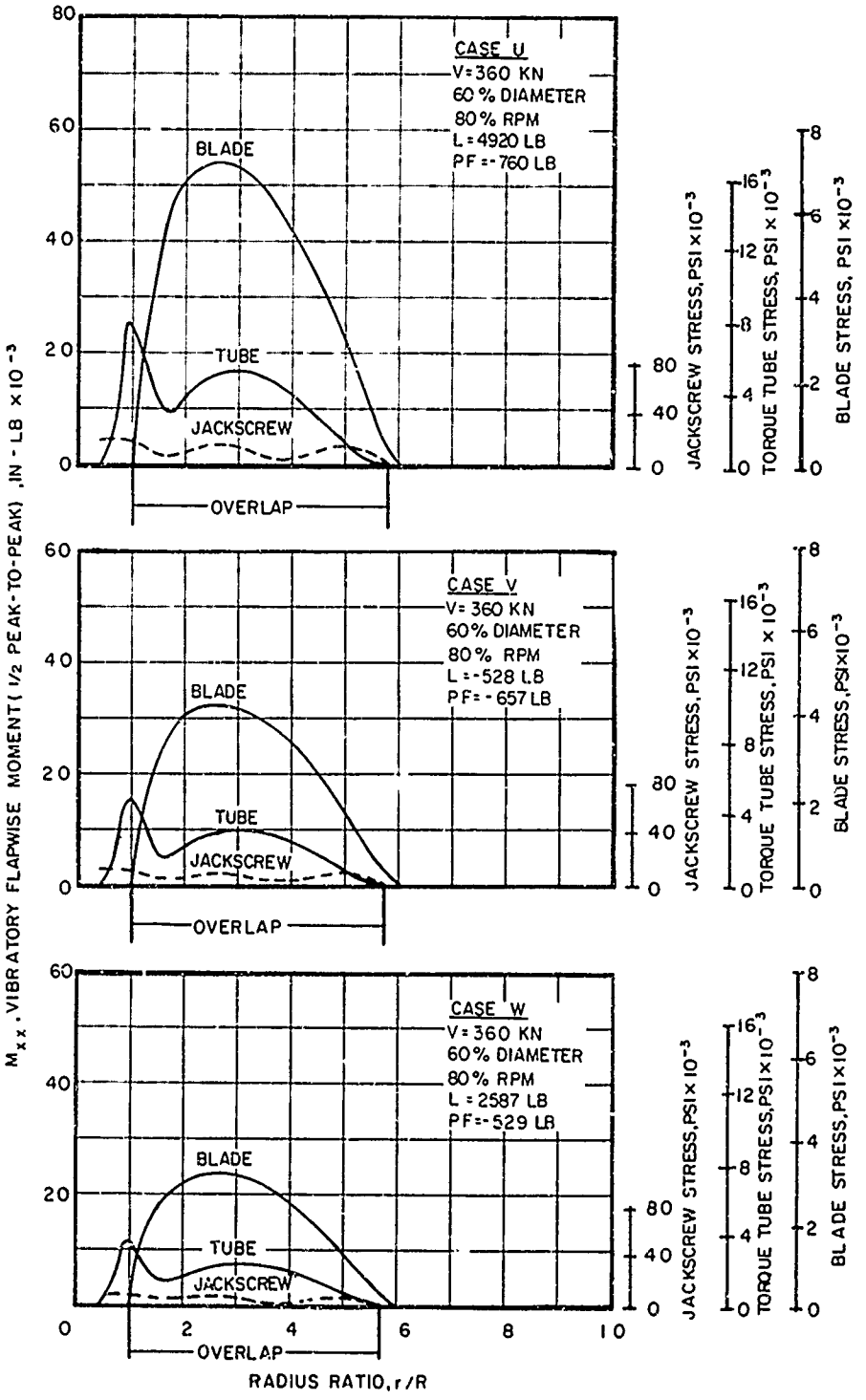

Figure 30. Concluded.

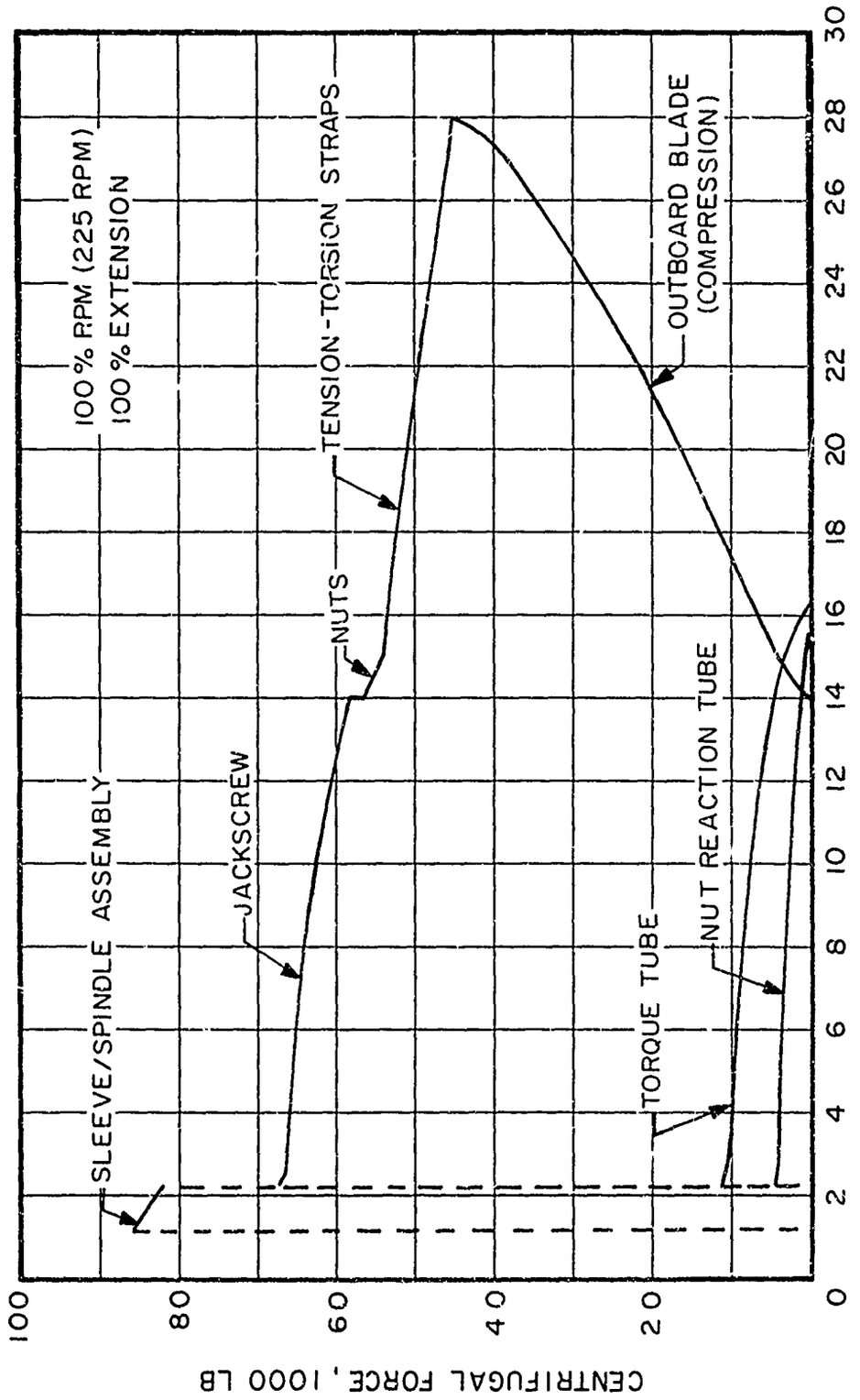

Figure 31. Centrifugal Force Distribution for Fully Extended Blade.

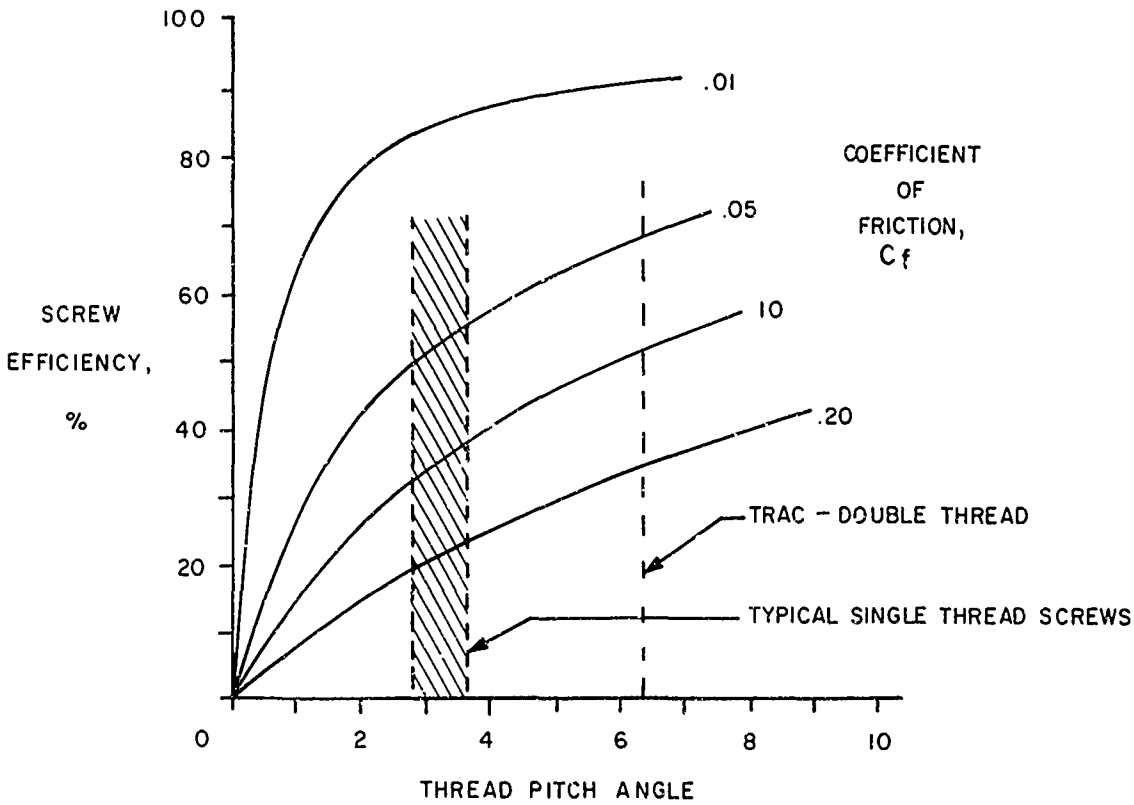

Figure 32. Effect of Thread Pitch Angle on Screw Efiiciency.

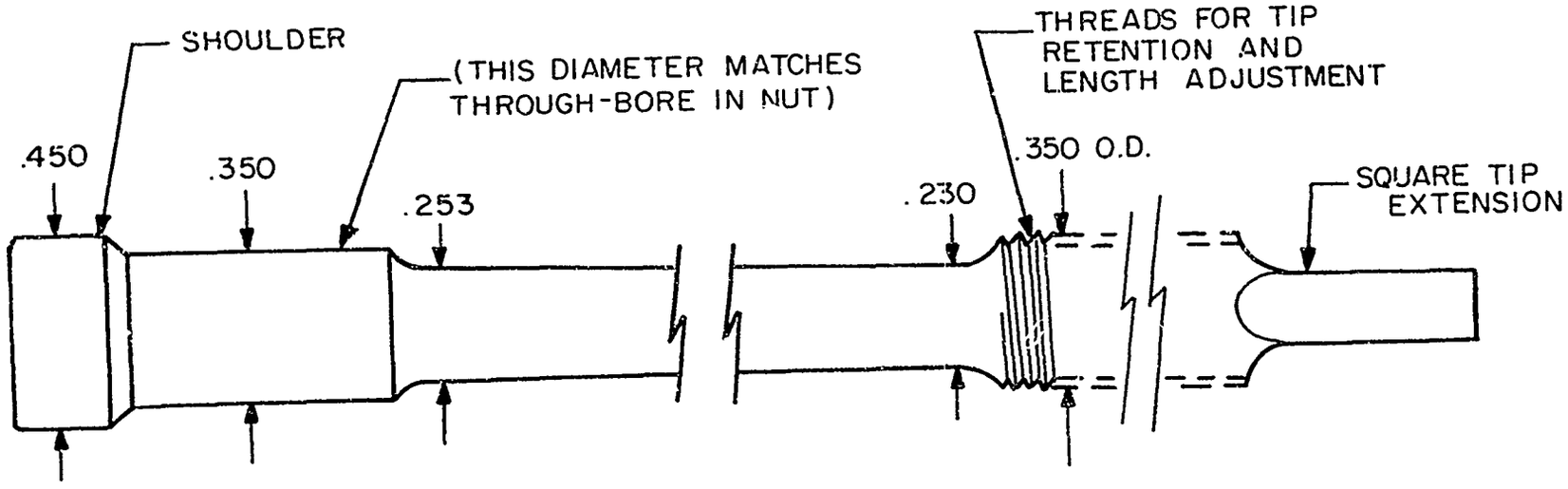

Figure 33. Tension-Torsion Strap Configuration.

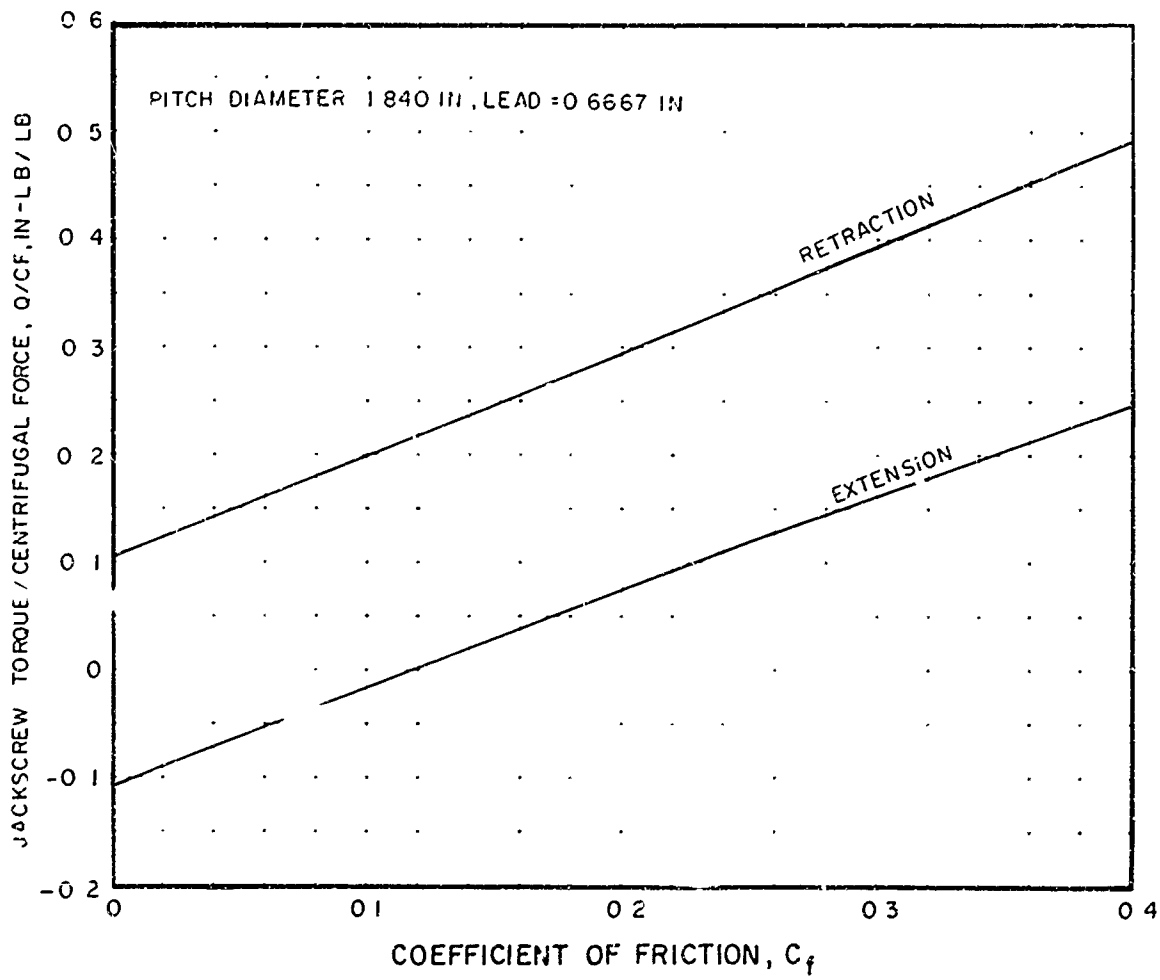

Figure 34. Torque-Friction Relationship for Jackscrew.

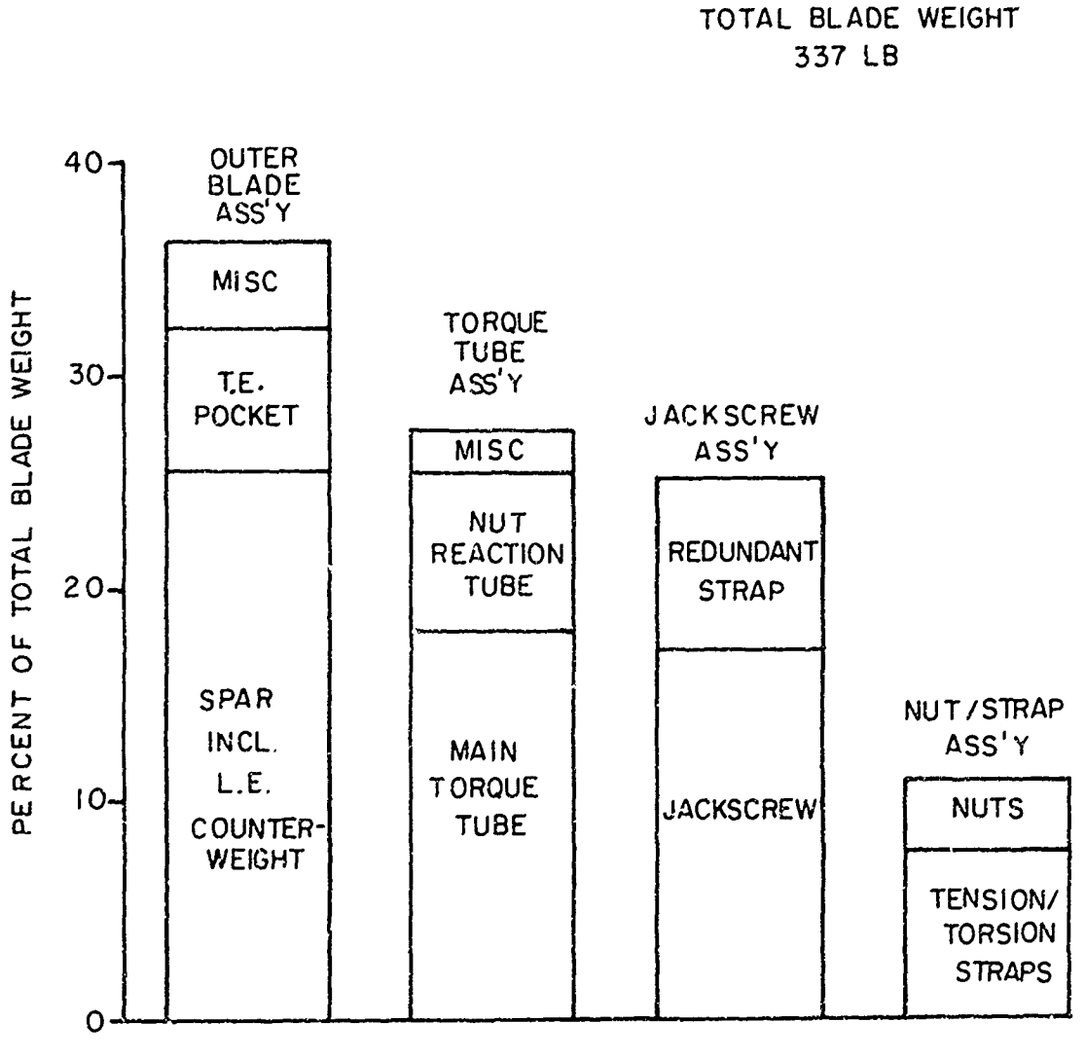

Figure 35. Relative Weight of Major Blade Components.

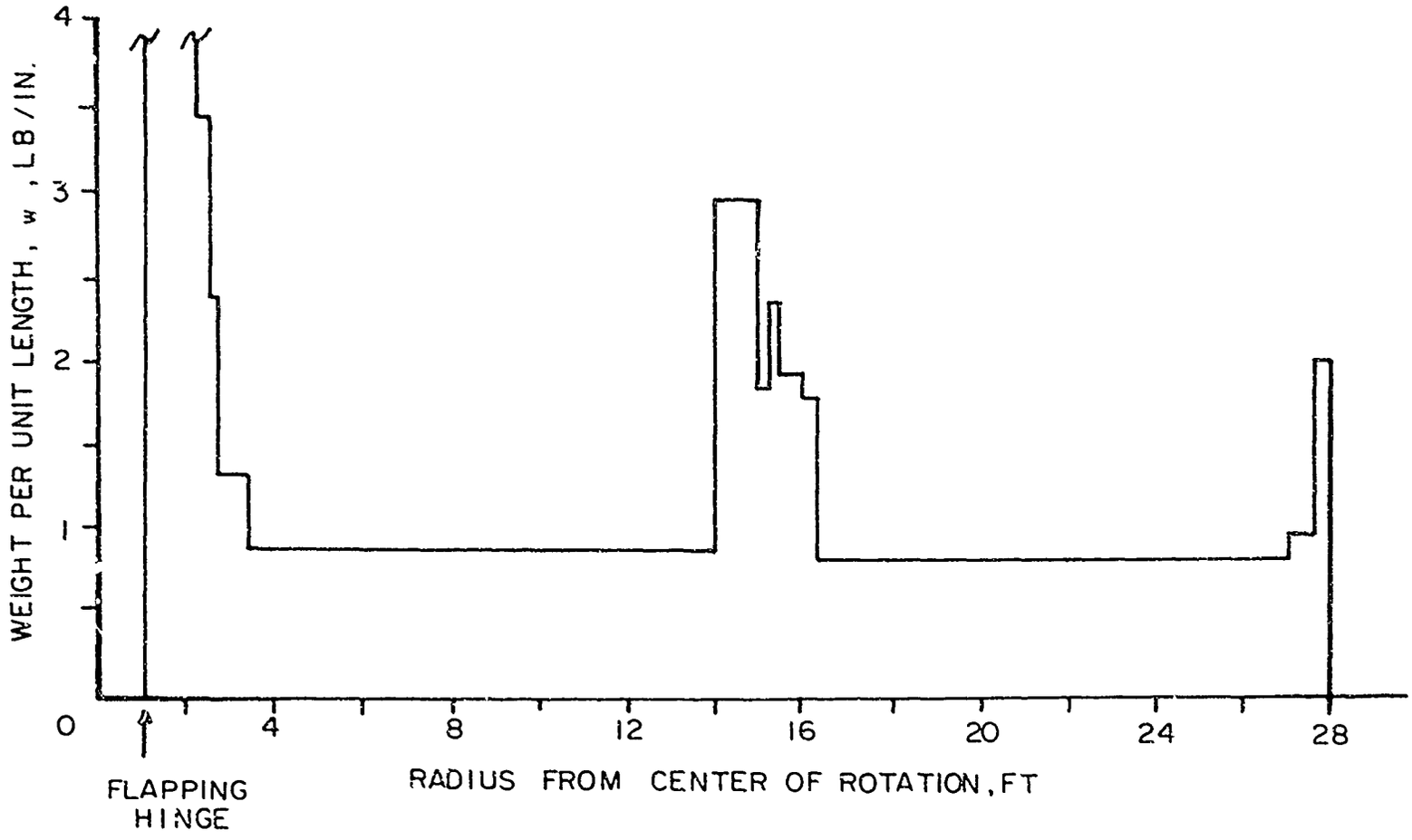

Figure 36. Spanwise Weight Distribution - Fully Extended Blade.

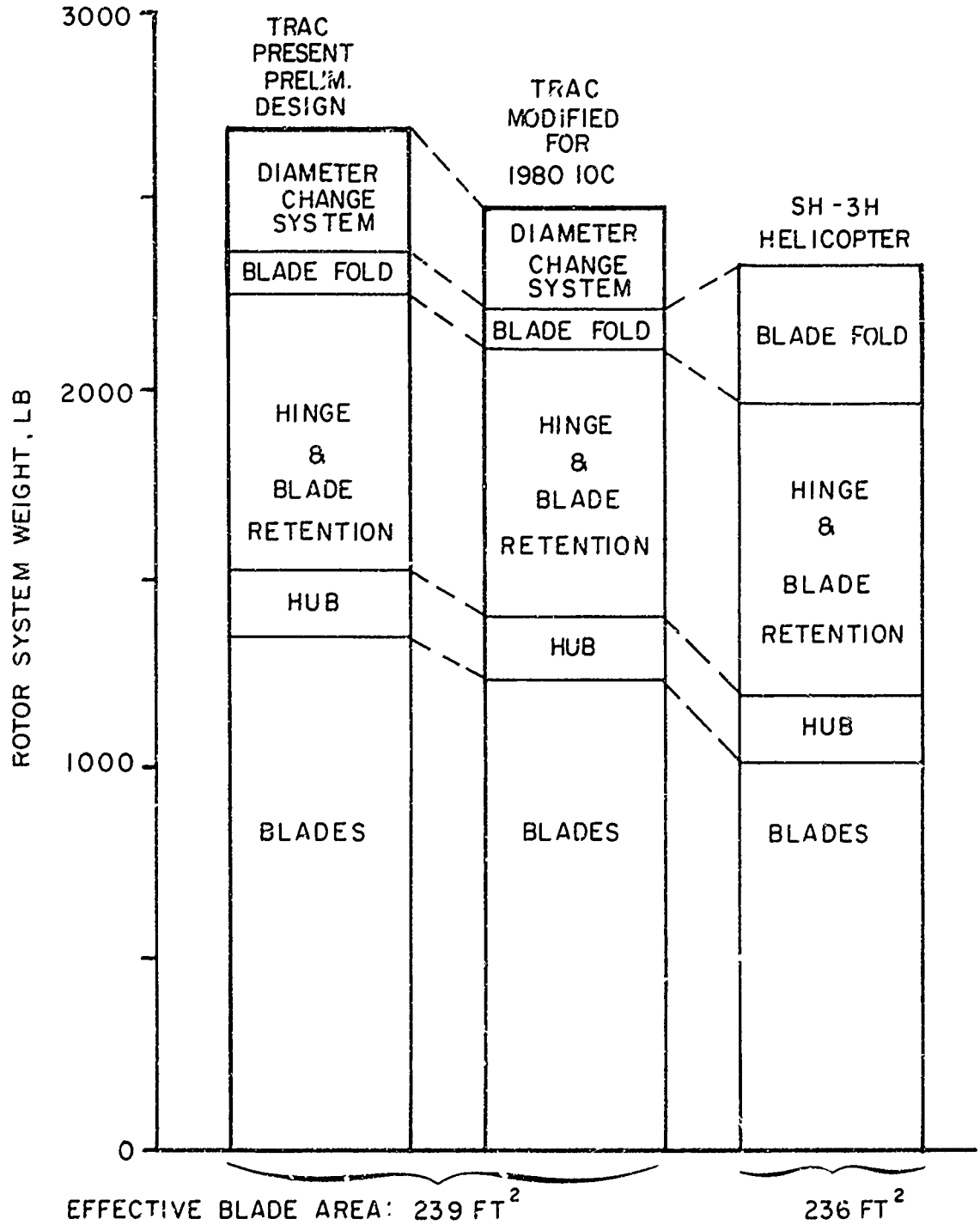

Figure 37. Rotor System Weight Comparison.

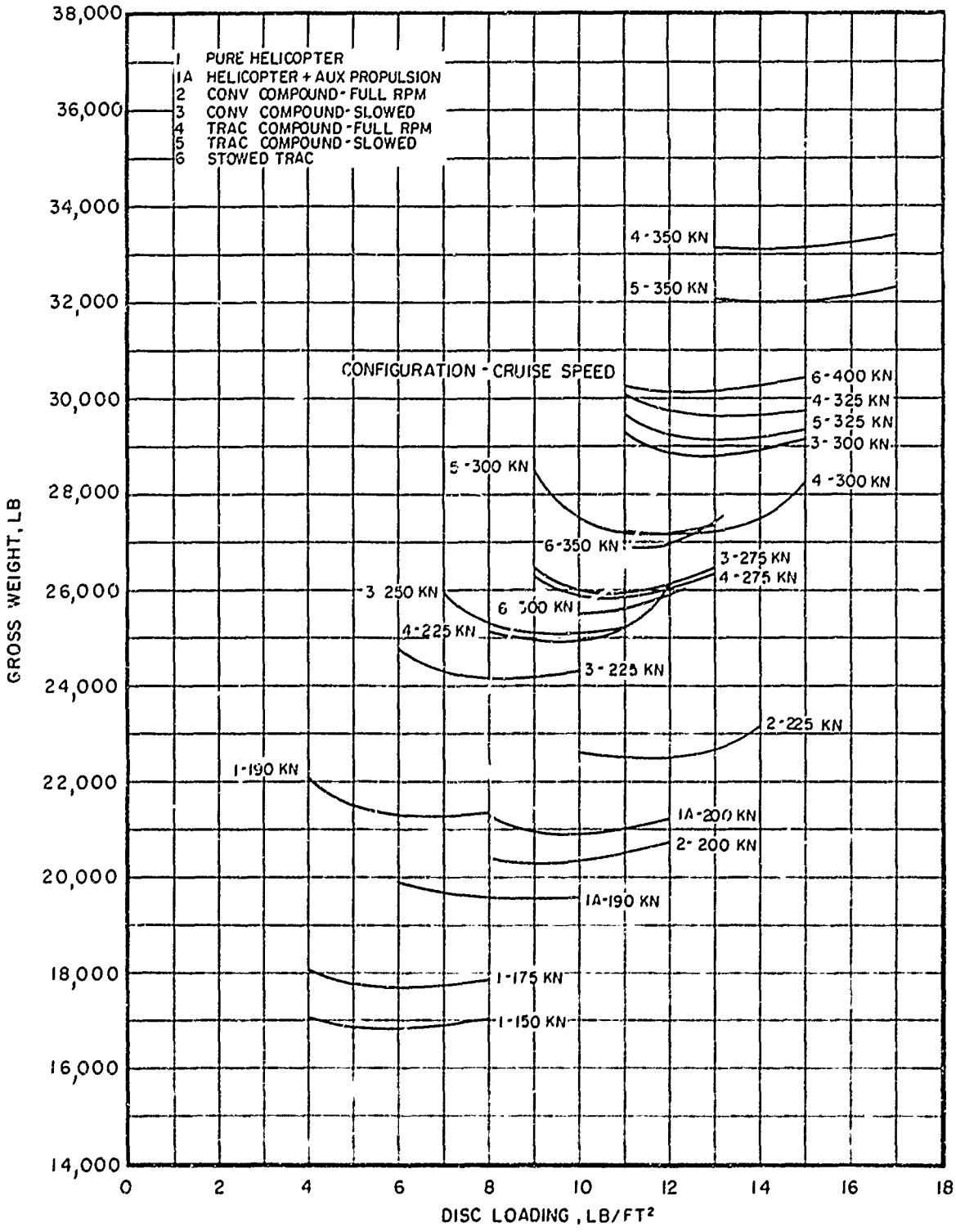

Figure 38. Disk Loading Optimization Results, 350 N.M. Range, 5000 lb Payload, 400 ft 95°F Cruise.

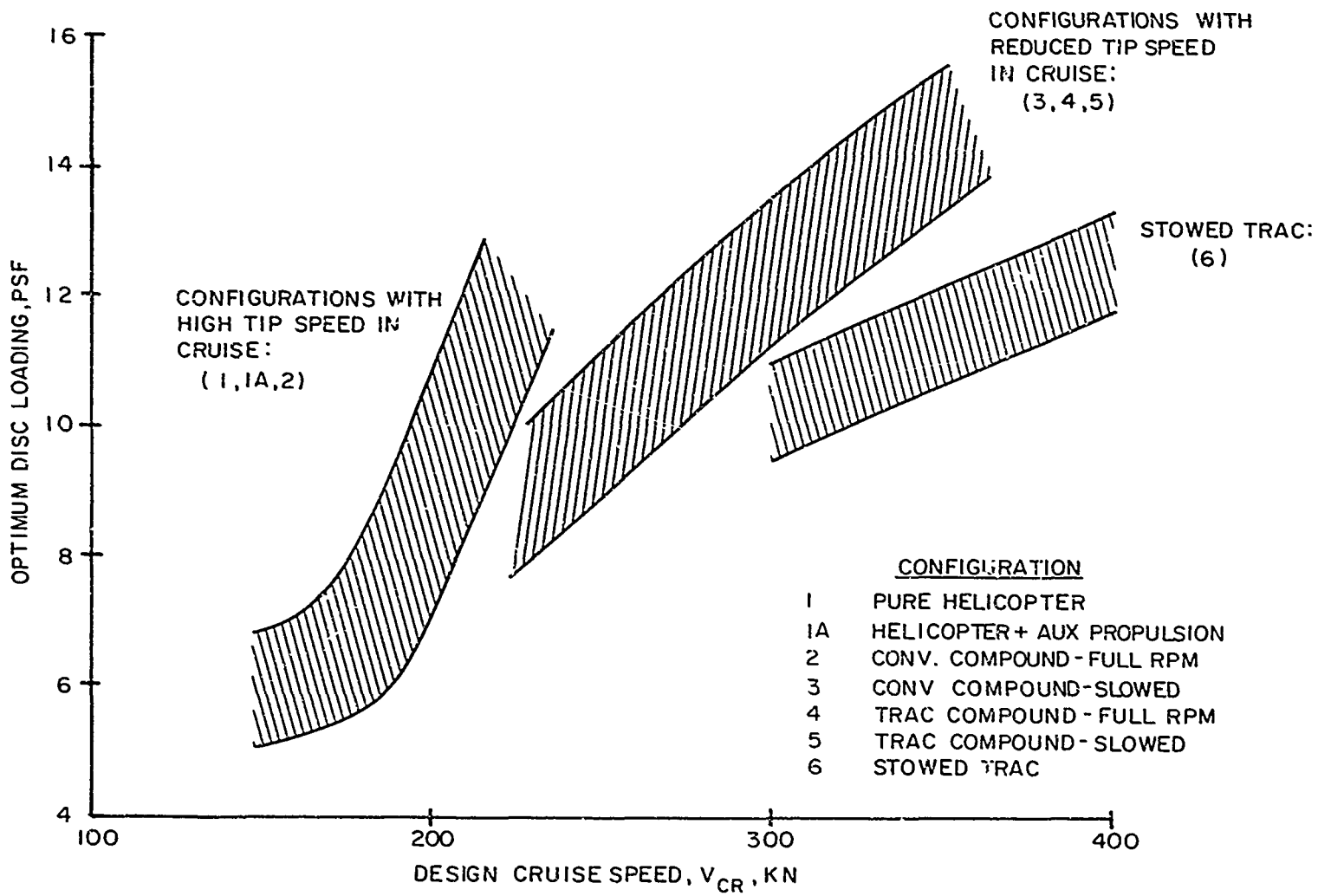

Figure 39. Optimum Disk Loading Trend with Speed.

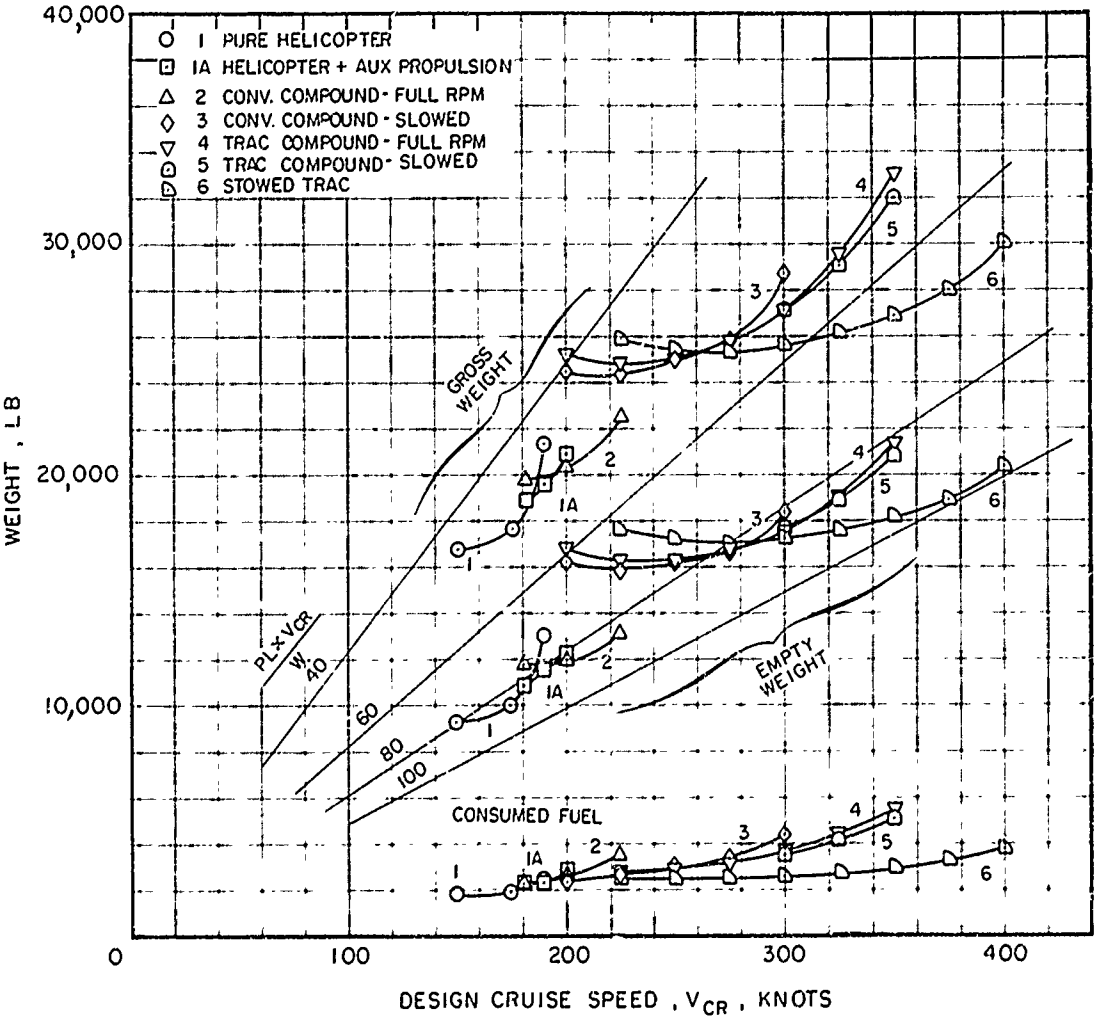

Figure 40. Aircraft Comparison Summary for 4000 ft 95°F Cruise, 5000 lb Payload, 350 N.M. Range.

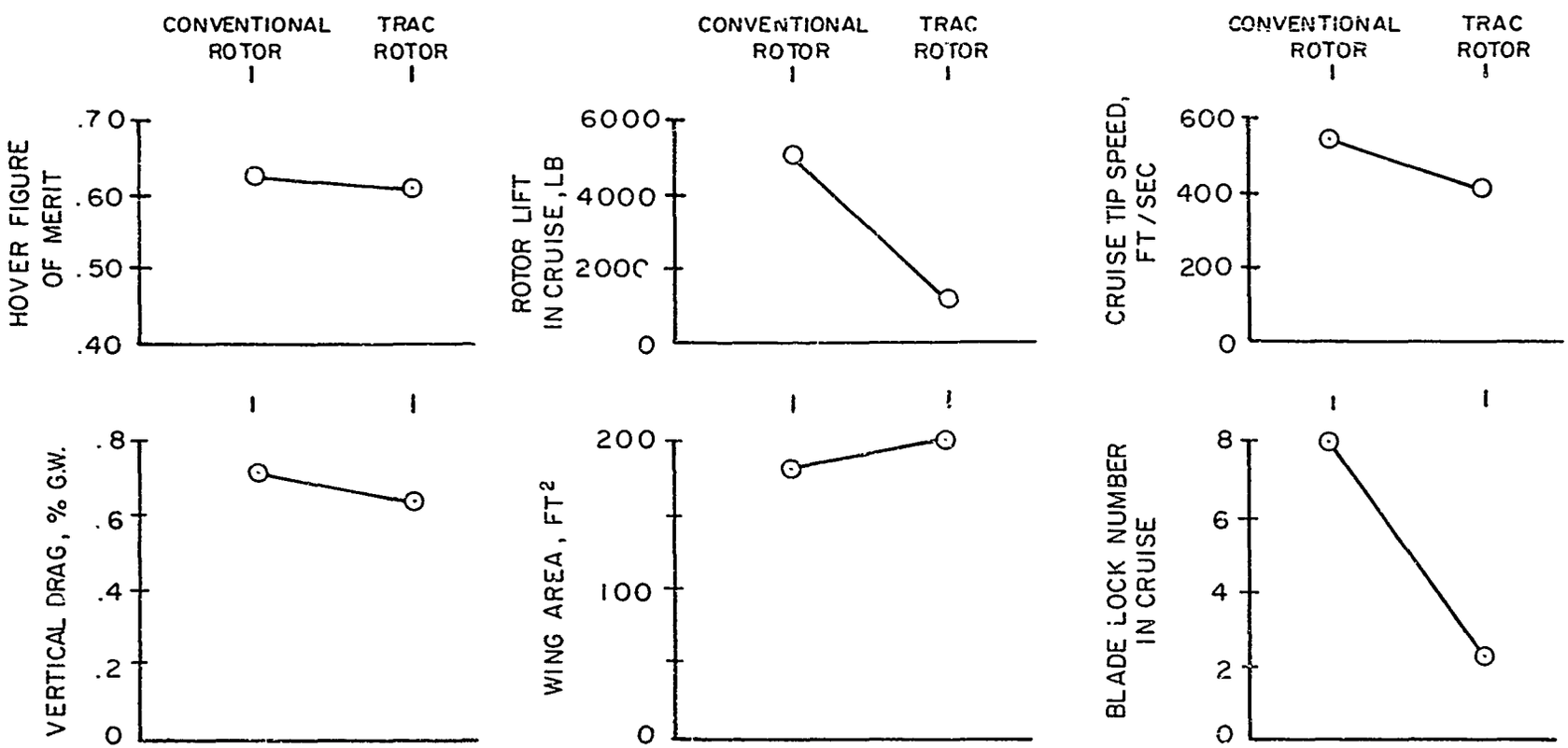

Figure 41. Performance Parameter Comparison for 300-Knot Compound Helicopters, 5000 lb Payload, 350 N.M. Range, 4000 ft 95°F Cruise.

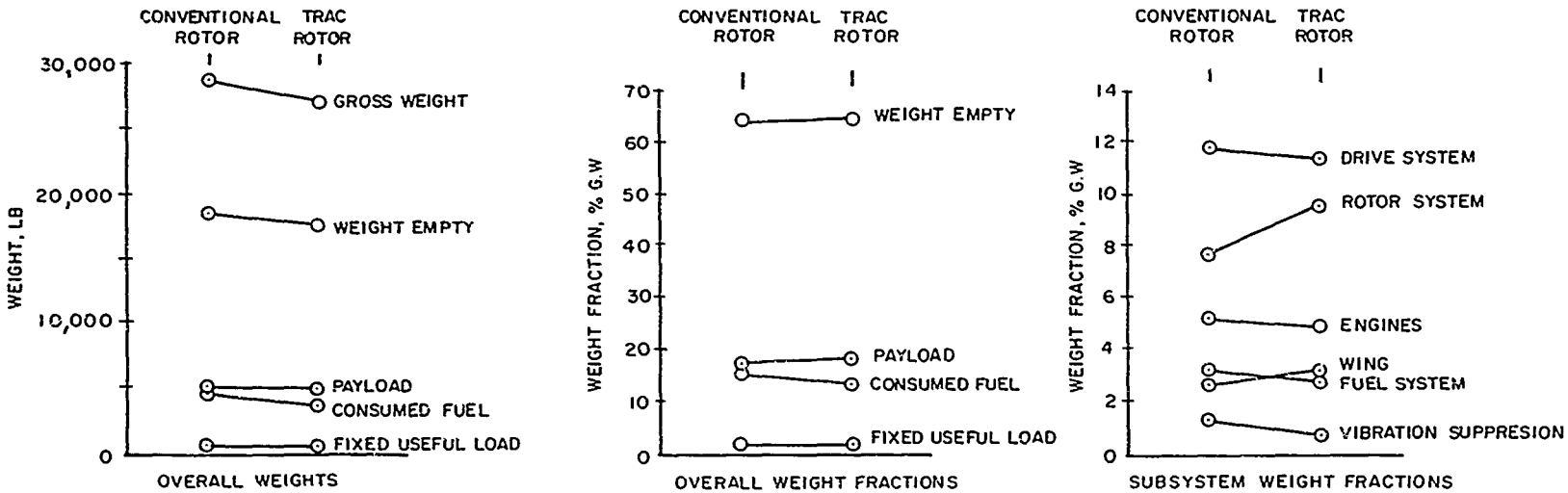

Figure 42. Weights Comparison for 300-Knot Compound Helicopters.

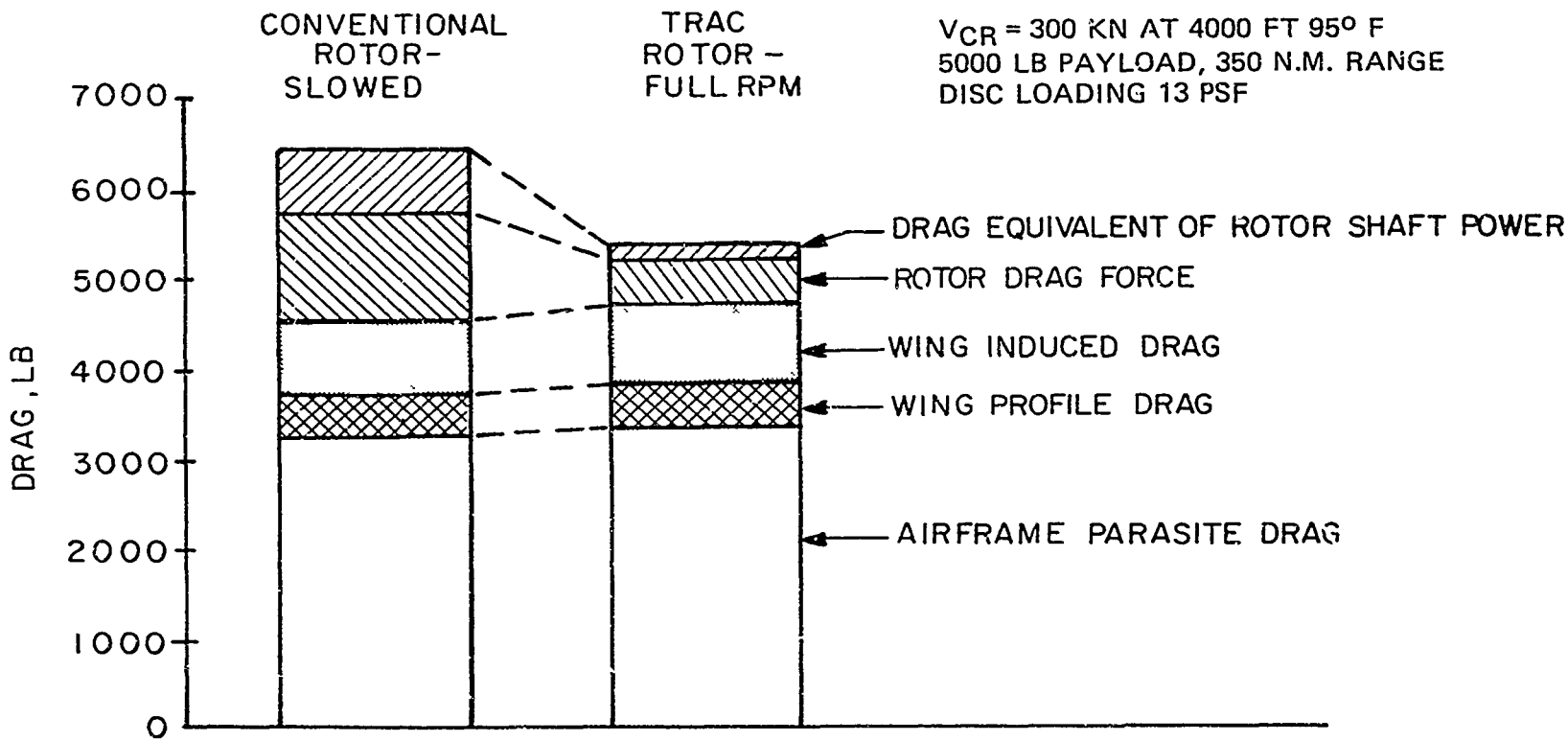

Figure 43. Drag Comparison for 300-Knot Compound Helicopters.

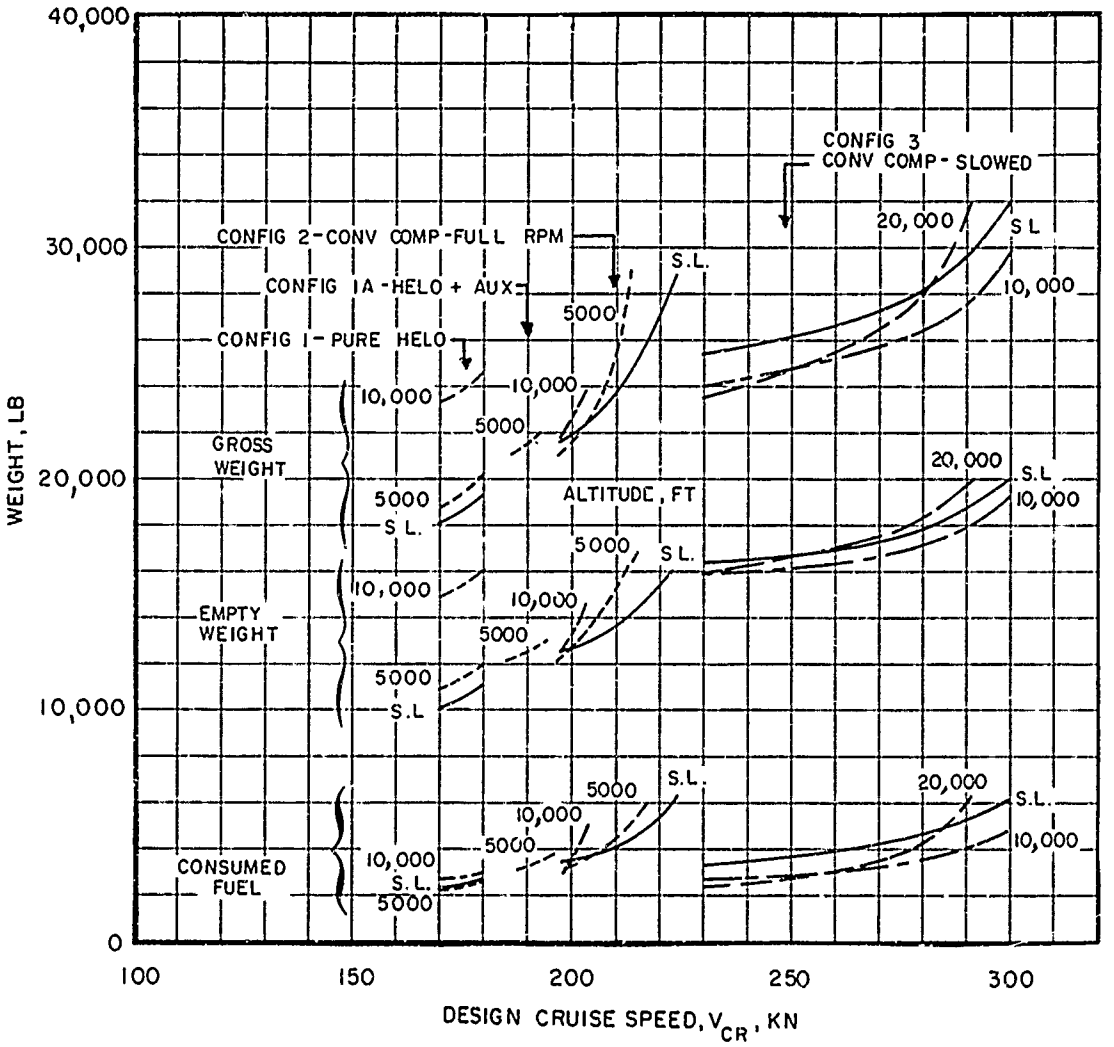

(a) Conventional Rotor Configurations

Figure 44. Aircraft Comparison Summary - Effect of Altitude for Standard Day Cruise, Hover Capability OGE at 4000 ft 95°F, 5000 lb Payload, 350 N.M. Range.

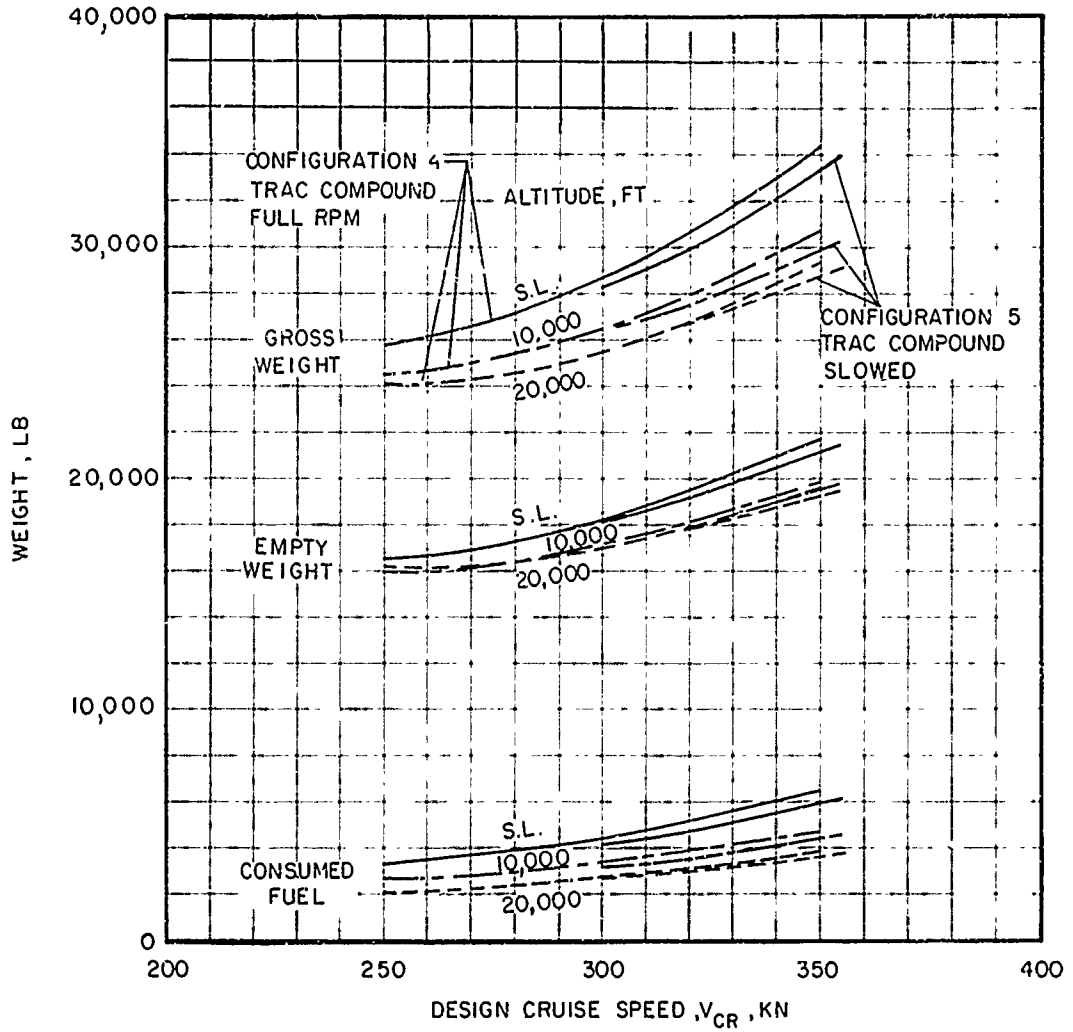

(b) TRAC Rotor Compound Helicopters

Figure 44. Continued.

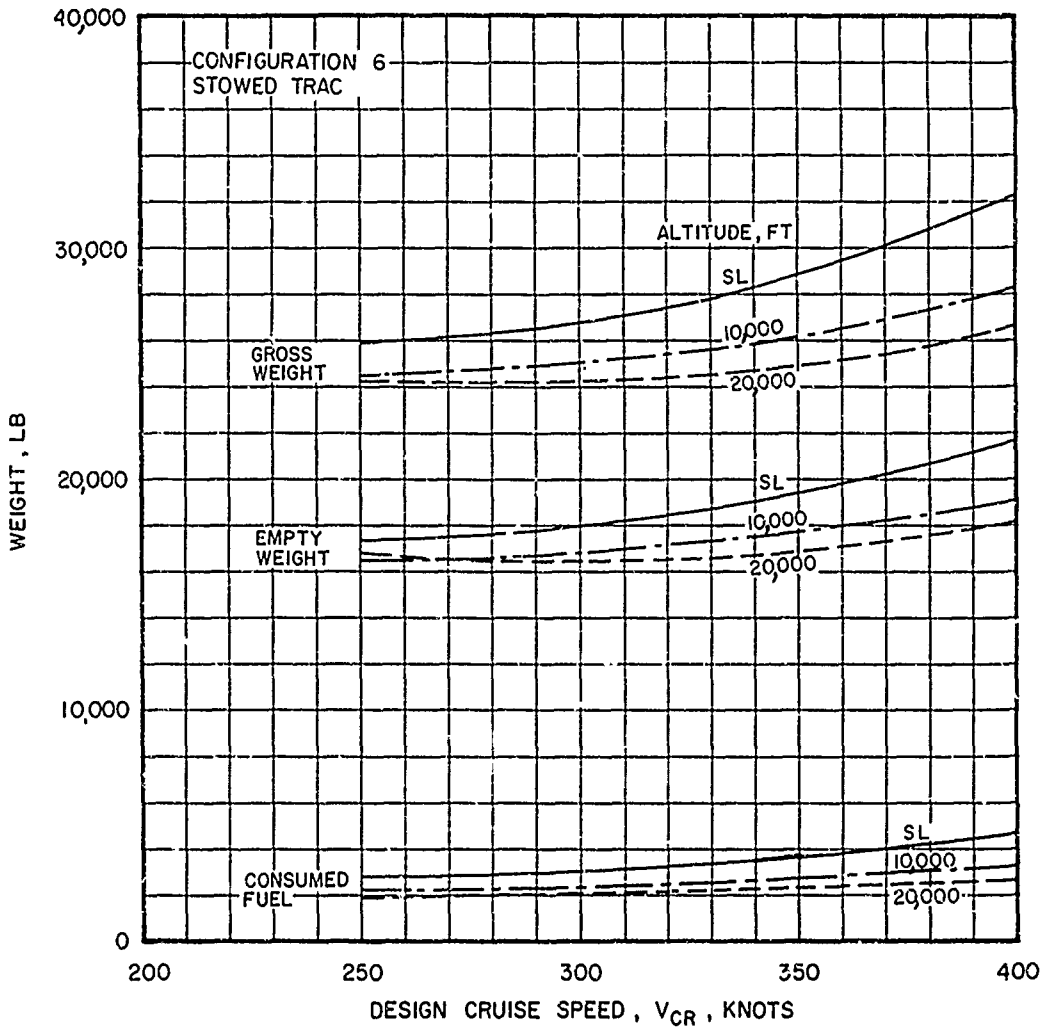

(c) Stowed TRAC Rotor

Figure 44. Concluded.

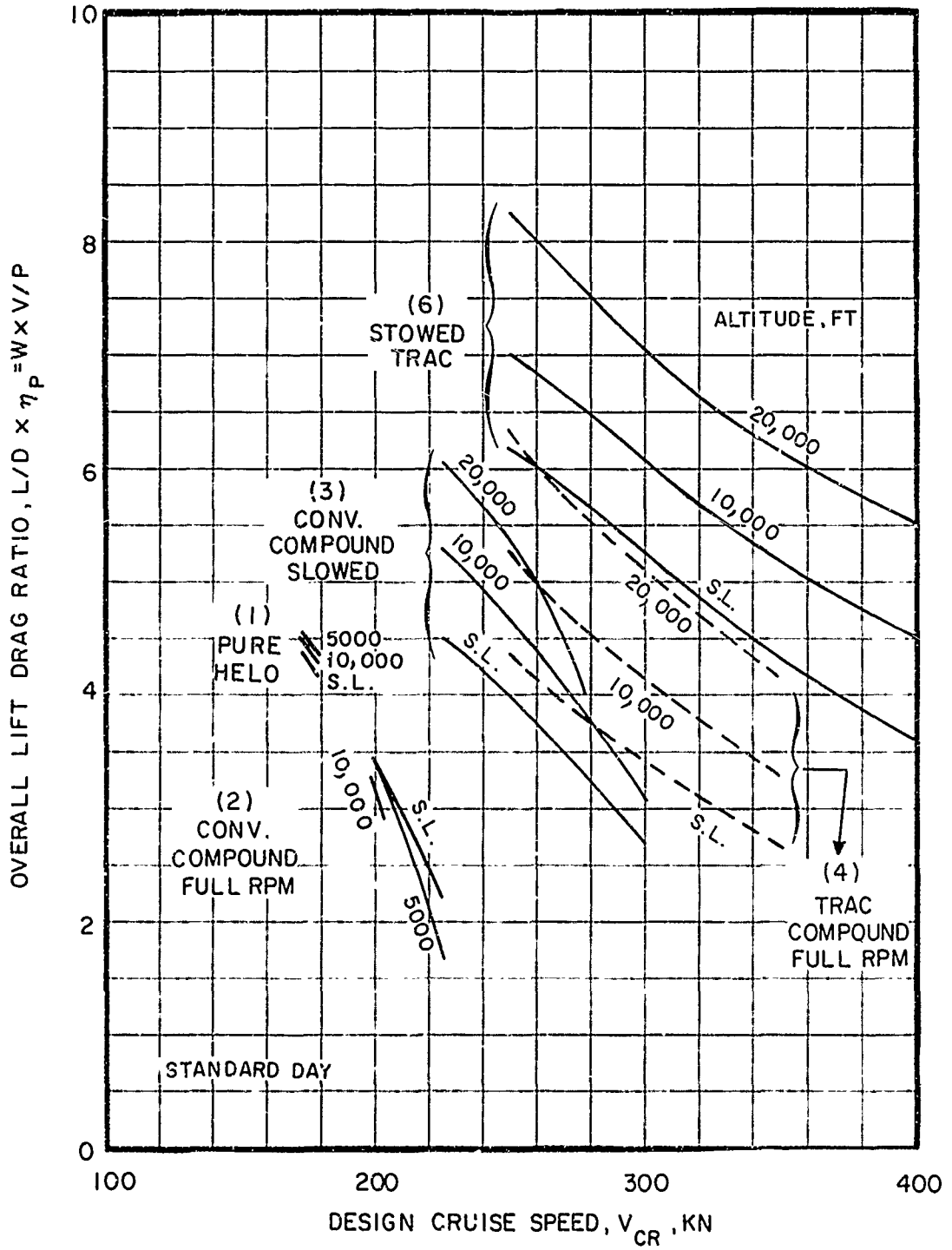

Figure 45. Comparison of Overall Equivalent Lift Drag Ratios.

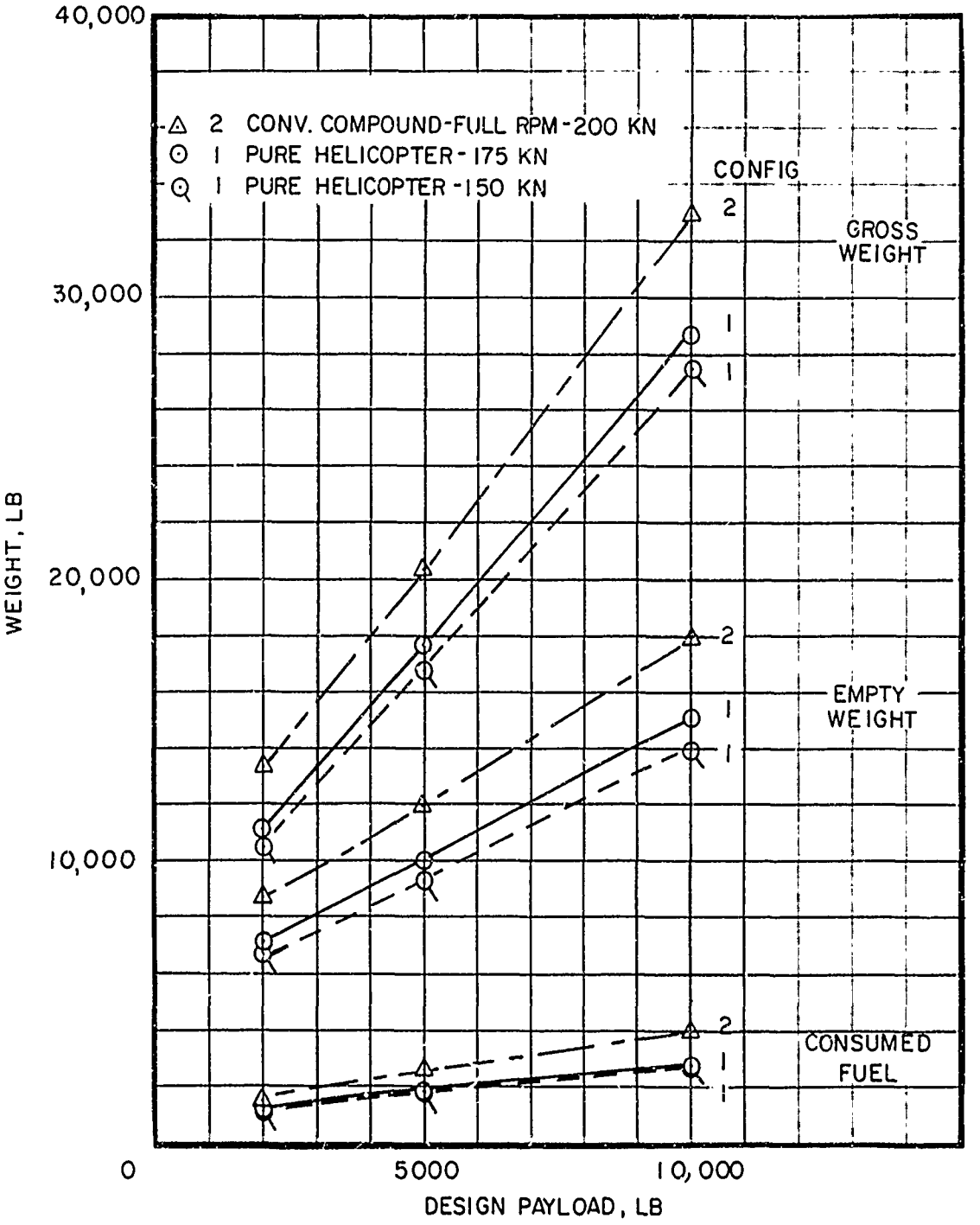

(a) Design Cruise Speed 150 - 200 Knots.

Figure 46. Effect of Design Payload on Weights, Design Range 350 N.M., 4000 ft 95°F Cruise.

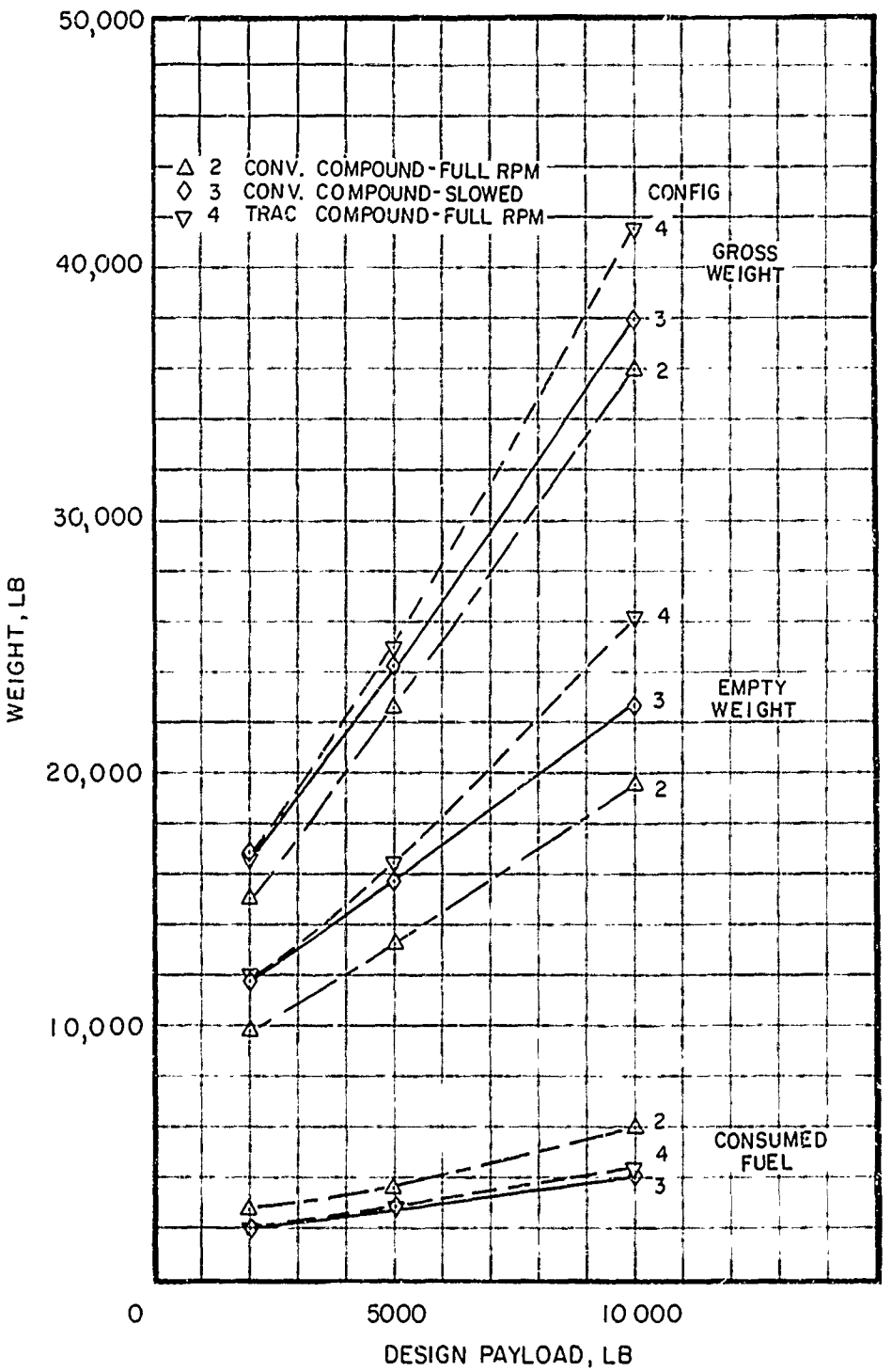

(b) Design Cruise Speed 225 Knots.

Figure 46. Continued.

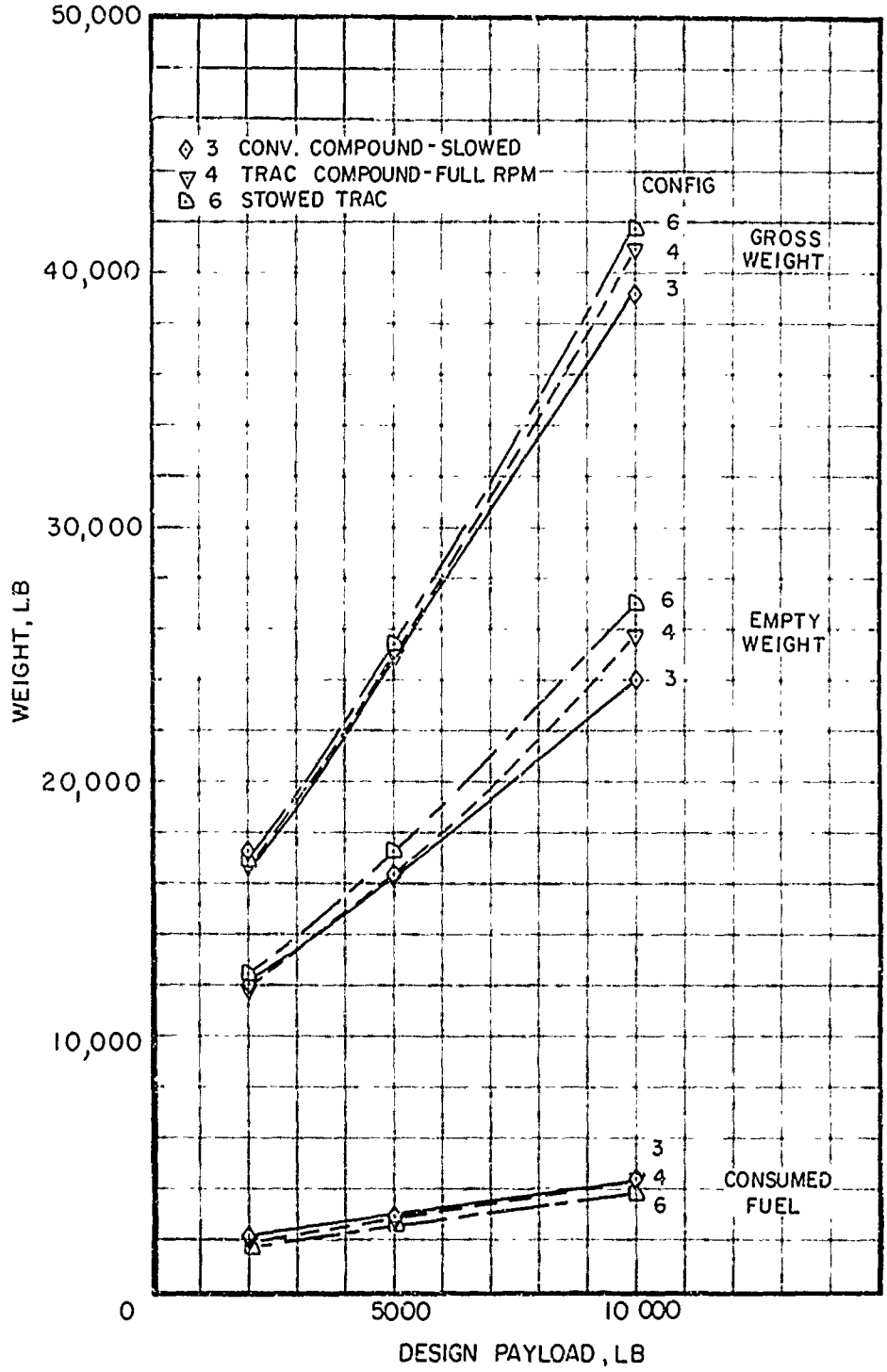

(c) Design Cruise Speed 250 Knots.

Figure 46. Continued.

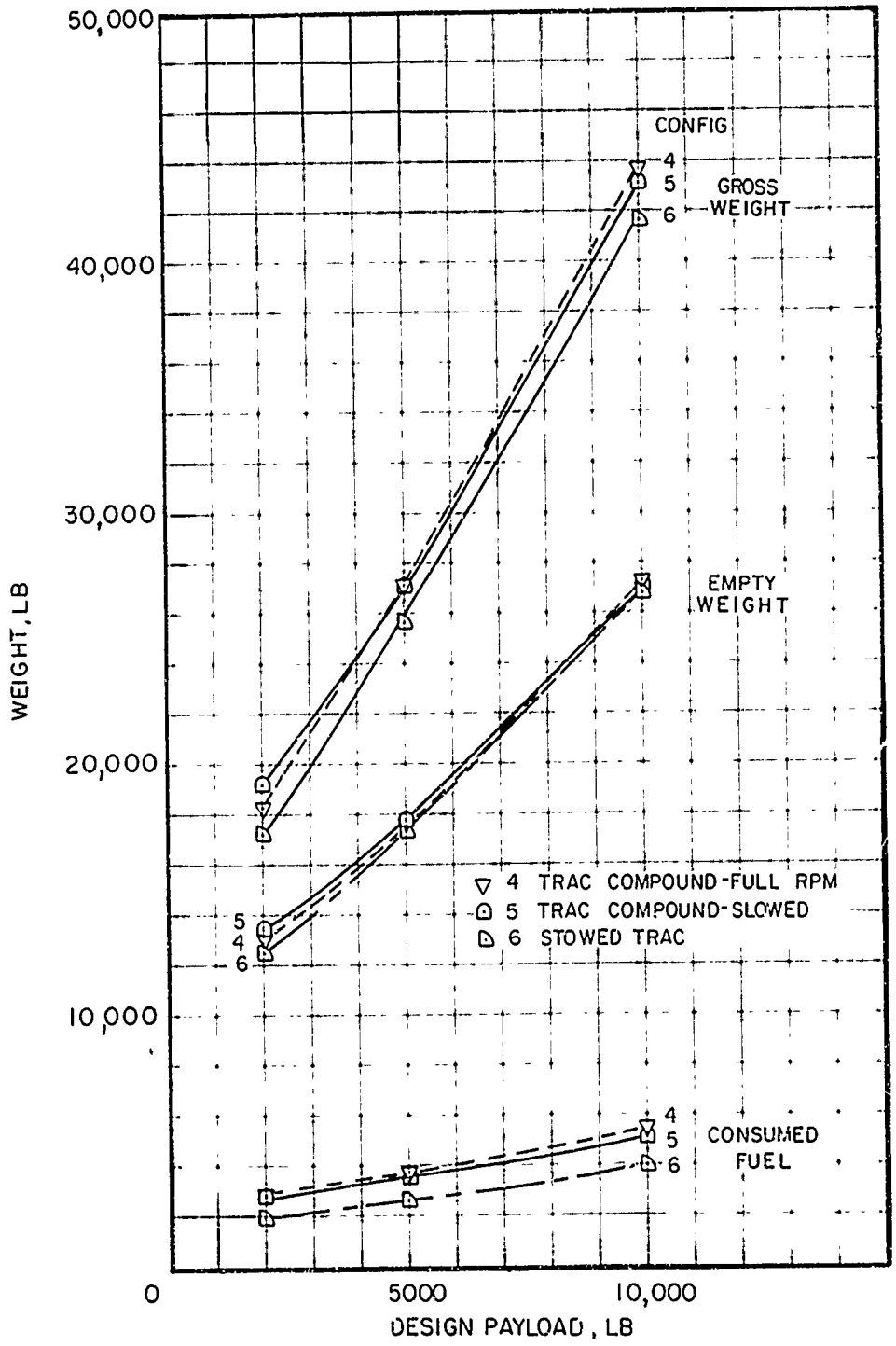

(d) Design Cruise Speed 300 Knots.

Figure 46. Continued.

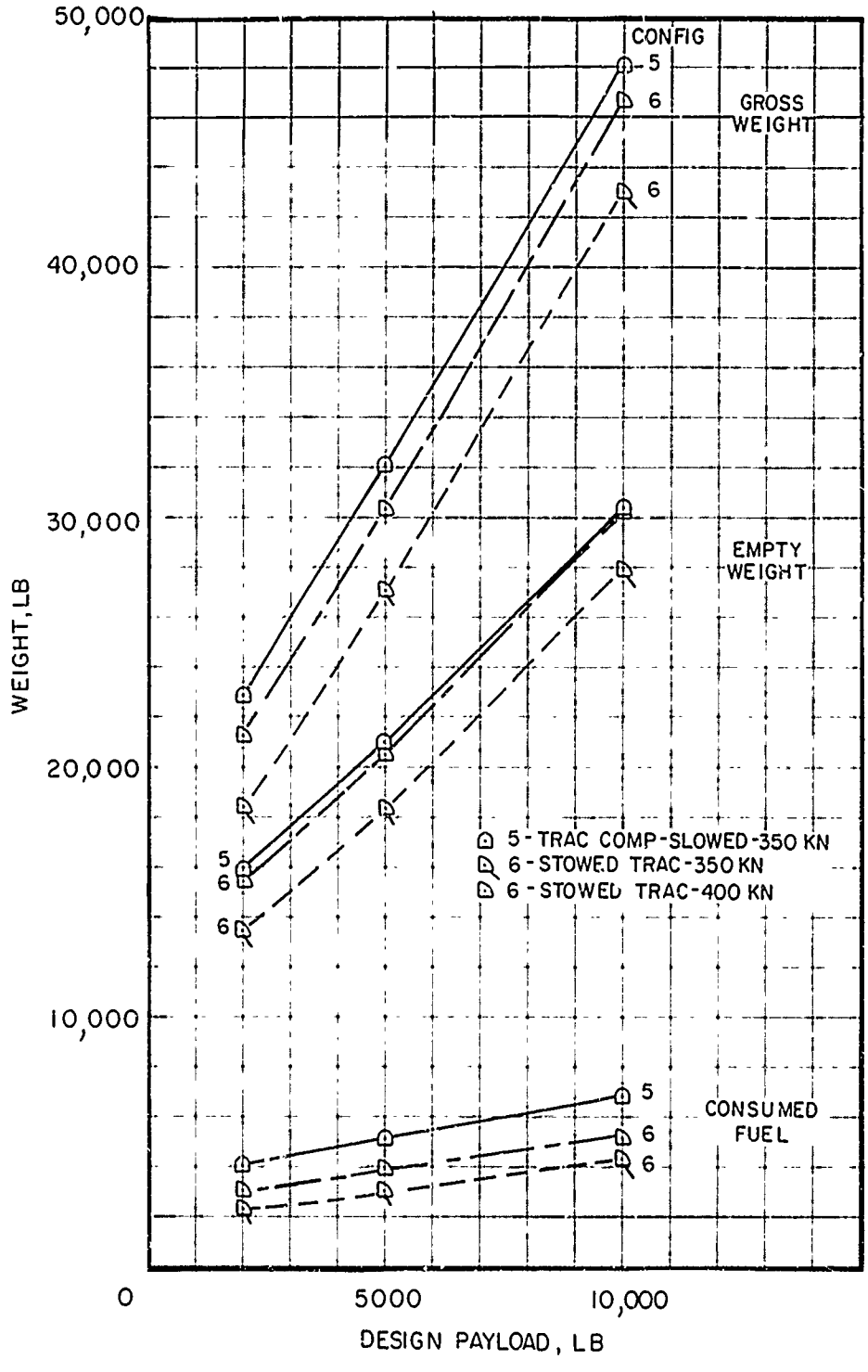

(e) Design Cruise Speed 350 - 400 Knots.

Figure 46. Concluded.

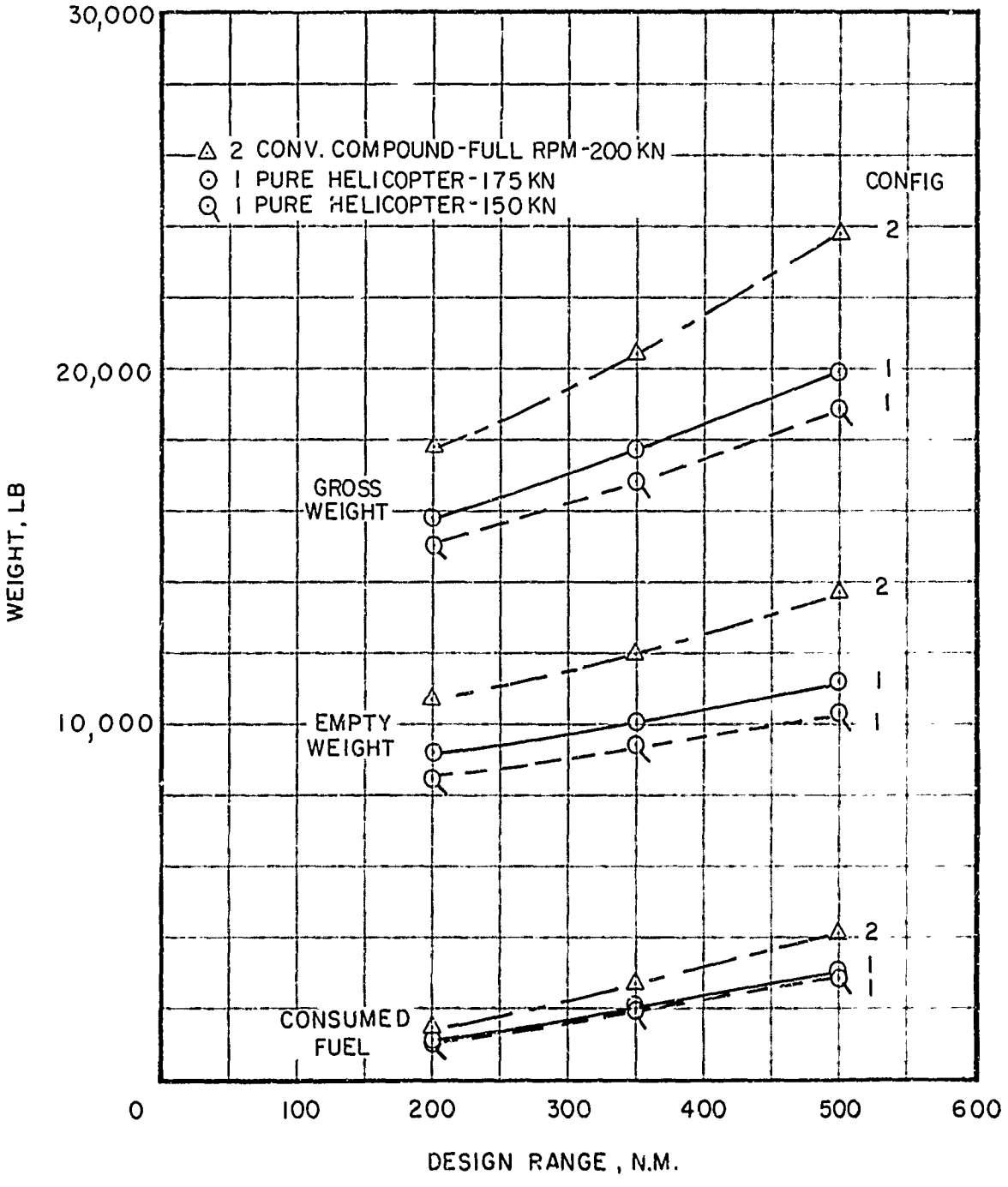

(a) Design Cruise Speed 150 - 200 Knots.

Figure 47. Effect of Design Range on Weights, Design Payload 5000 lb, 4000 ft 95°F Cruise.

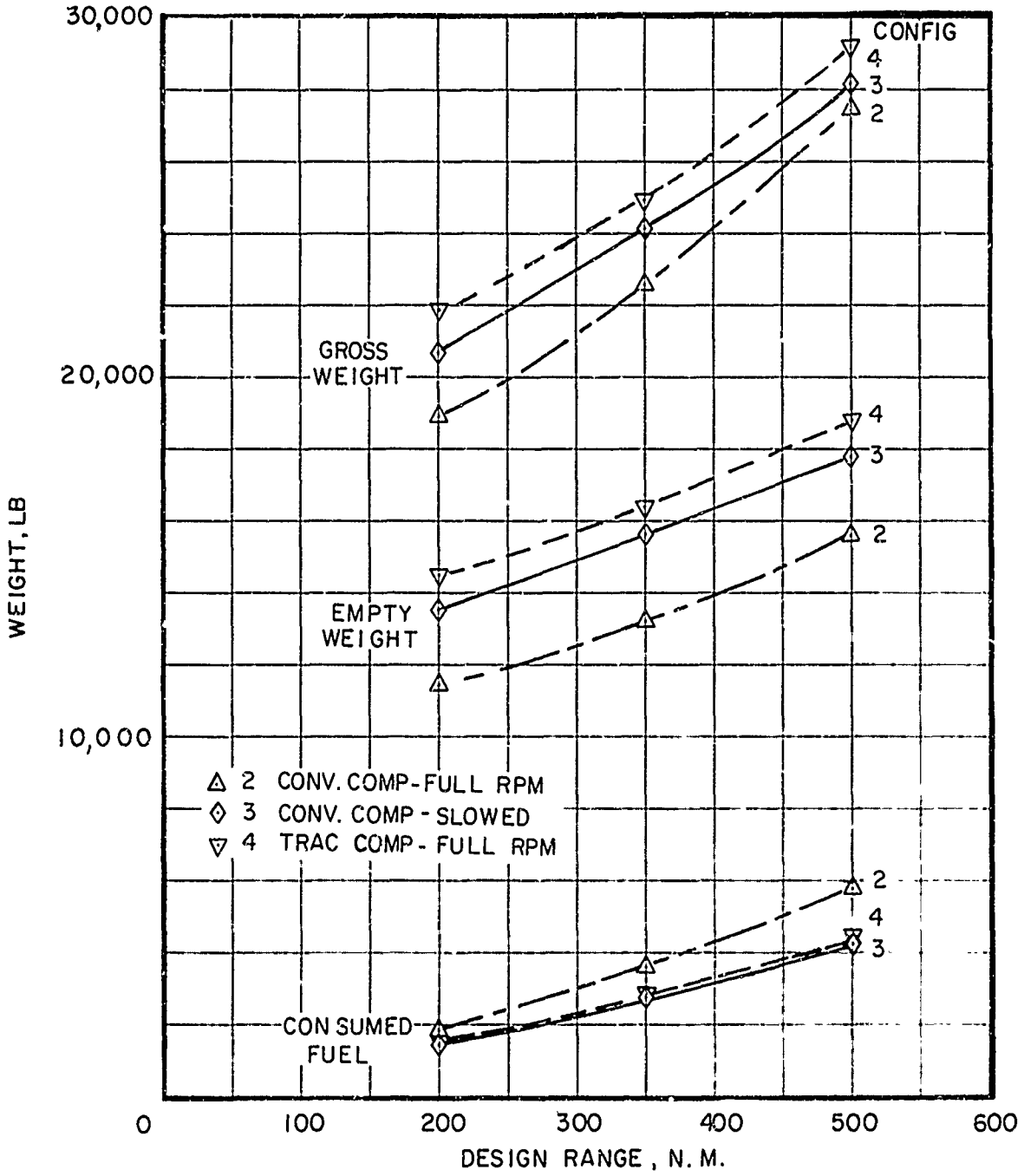

(b) Design Cruise Speed 225 Knots.

Figure 47. Continued.

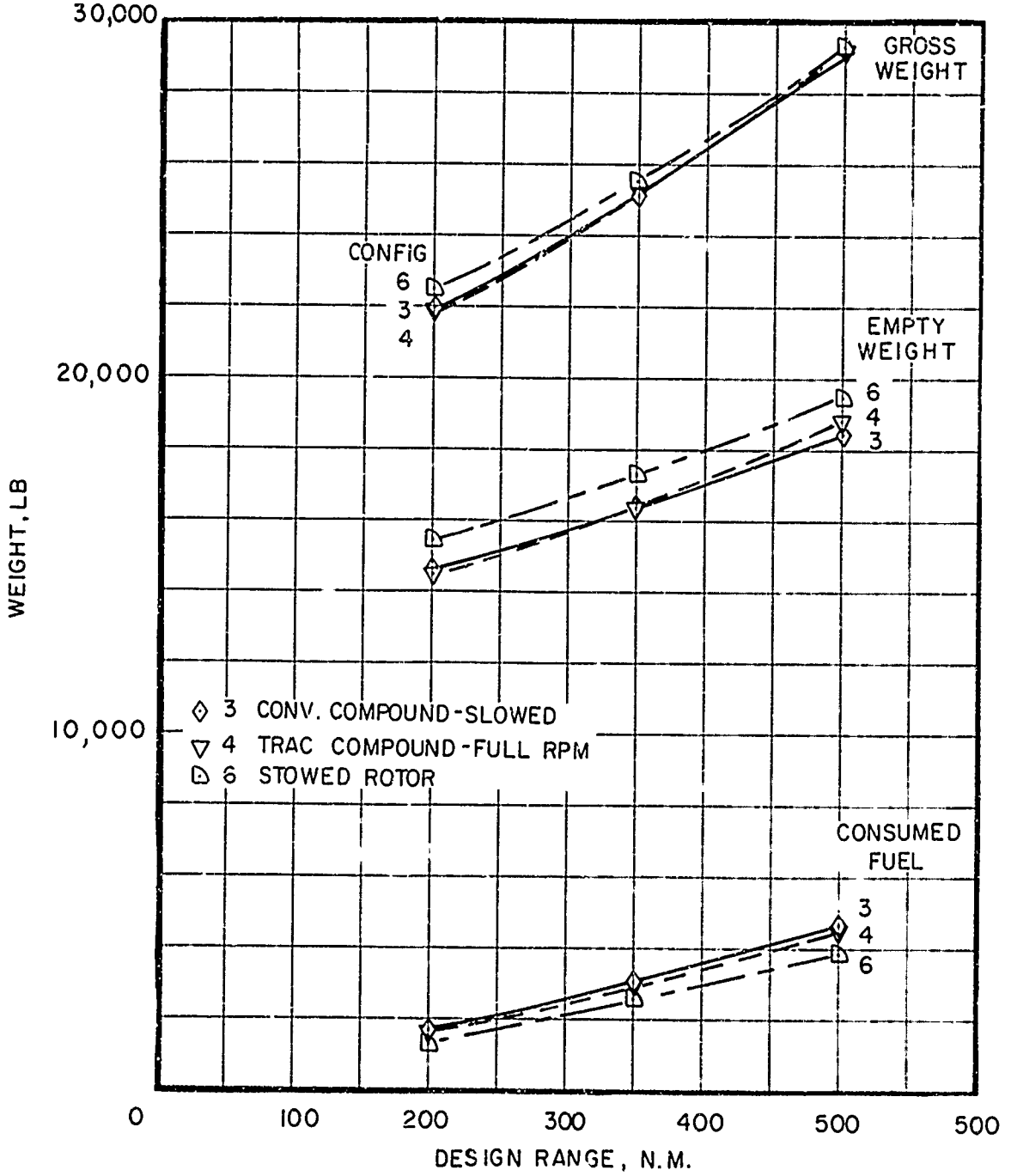

(c) Design Cruise Speed 250 Knots.

Figure 47. Continued.

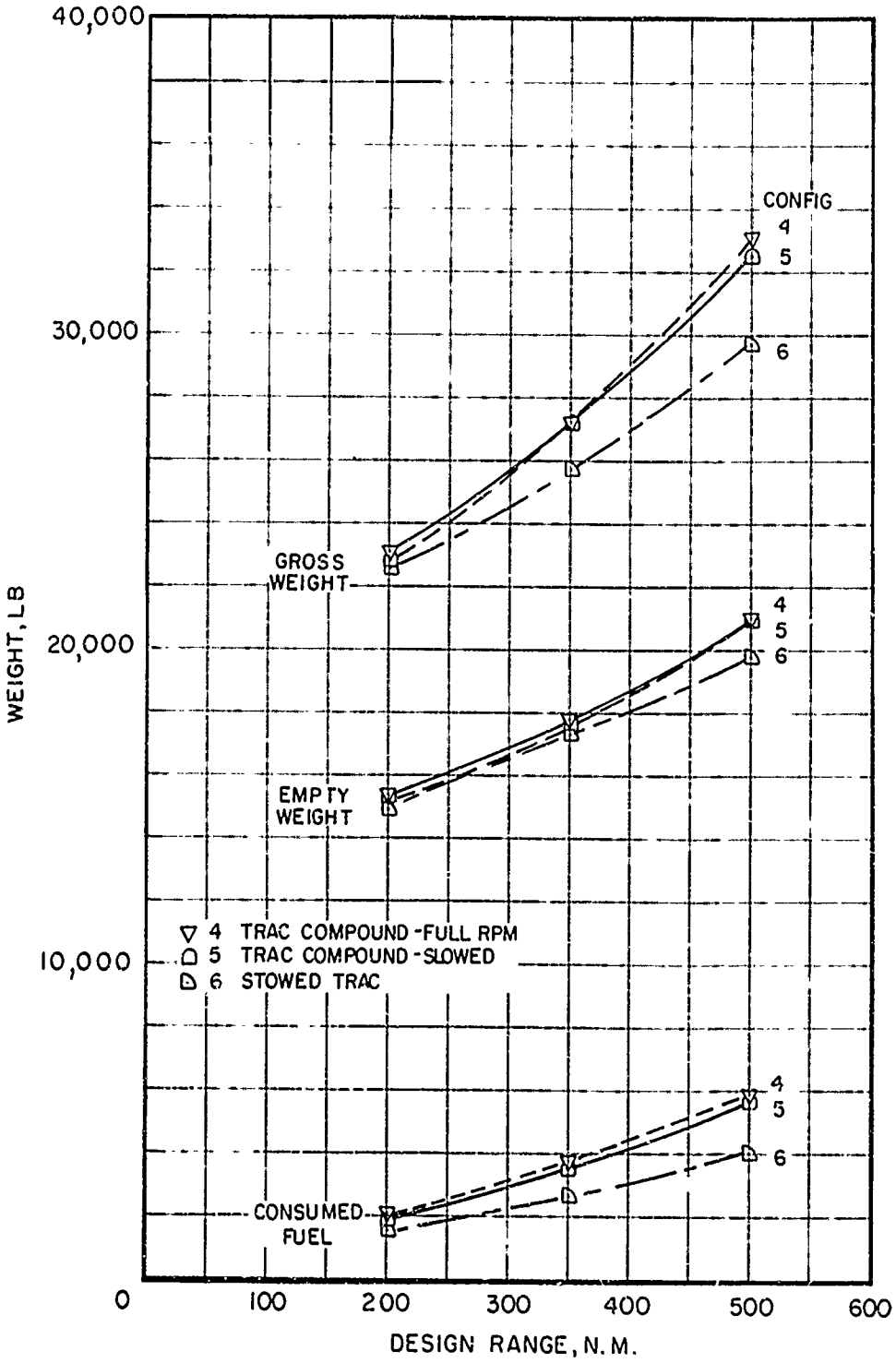

(d) Design Cruise Speed 300 Knots.

Figure 47. Continued.

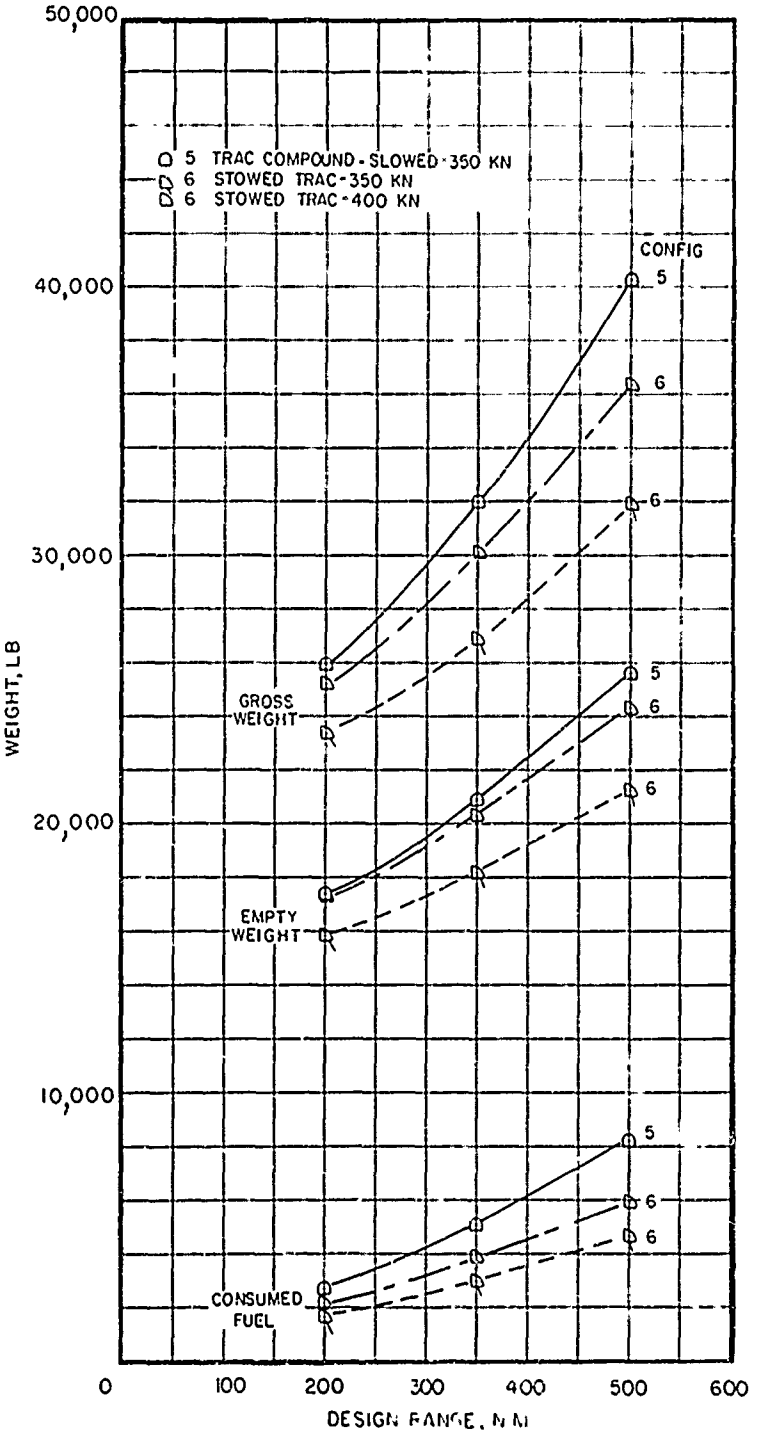

(e) Design Cruise Speed 350 - 400 Knots.

Figure 47. Concluded.

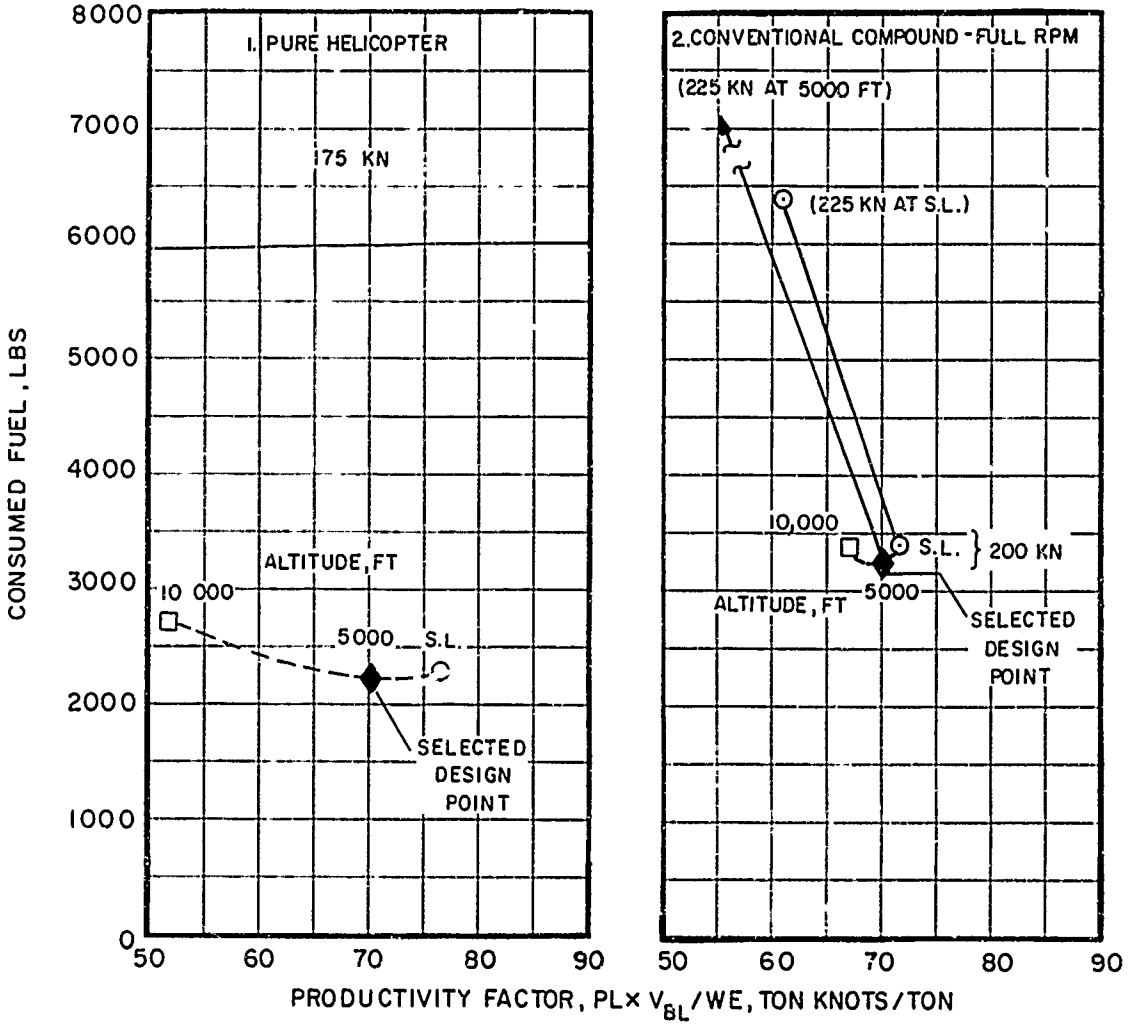

(a) Helicopter and Full RPM Conventional Rotor Compound

Figure 48. Effect of Design Cruise Speed and Altitude on Productivity and Consumed Fuel, Standard Day Cruise, 5000 lb Payload, 350 N.M. Range.

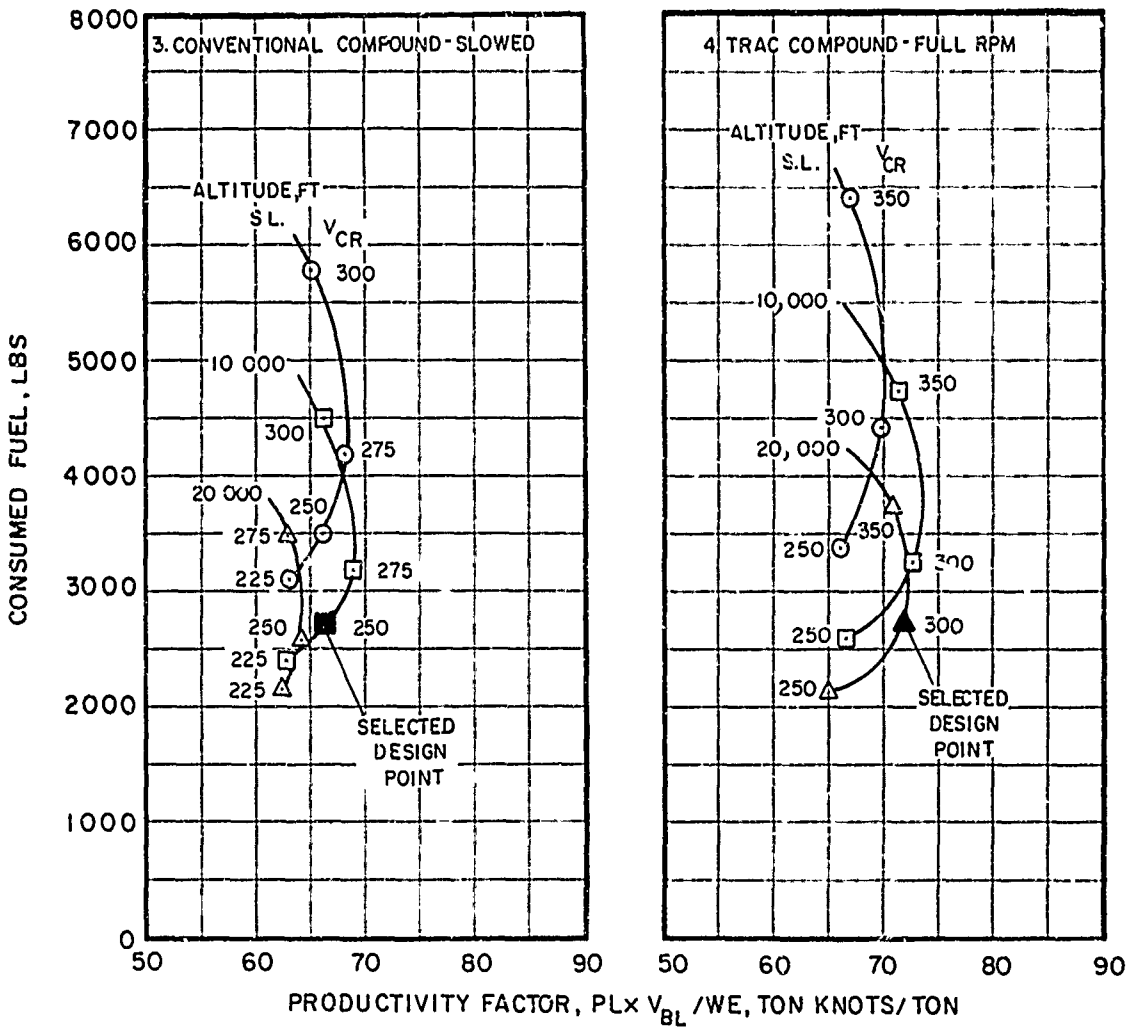

(b) Conventional Rotor Compound-Slowed, and Full RPM TRAC Compound

Figure 48. Continued.

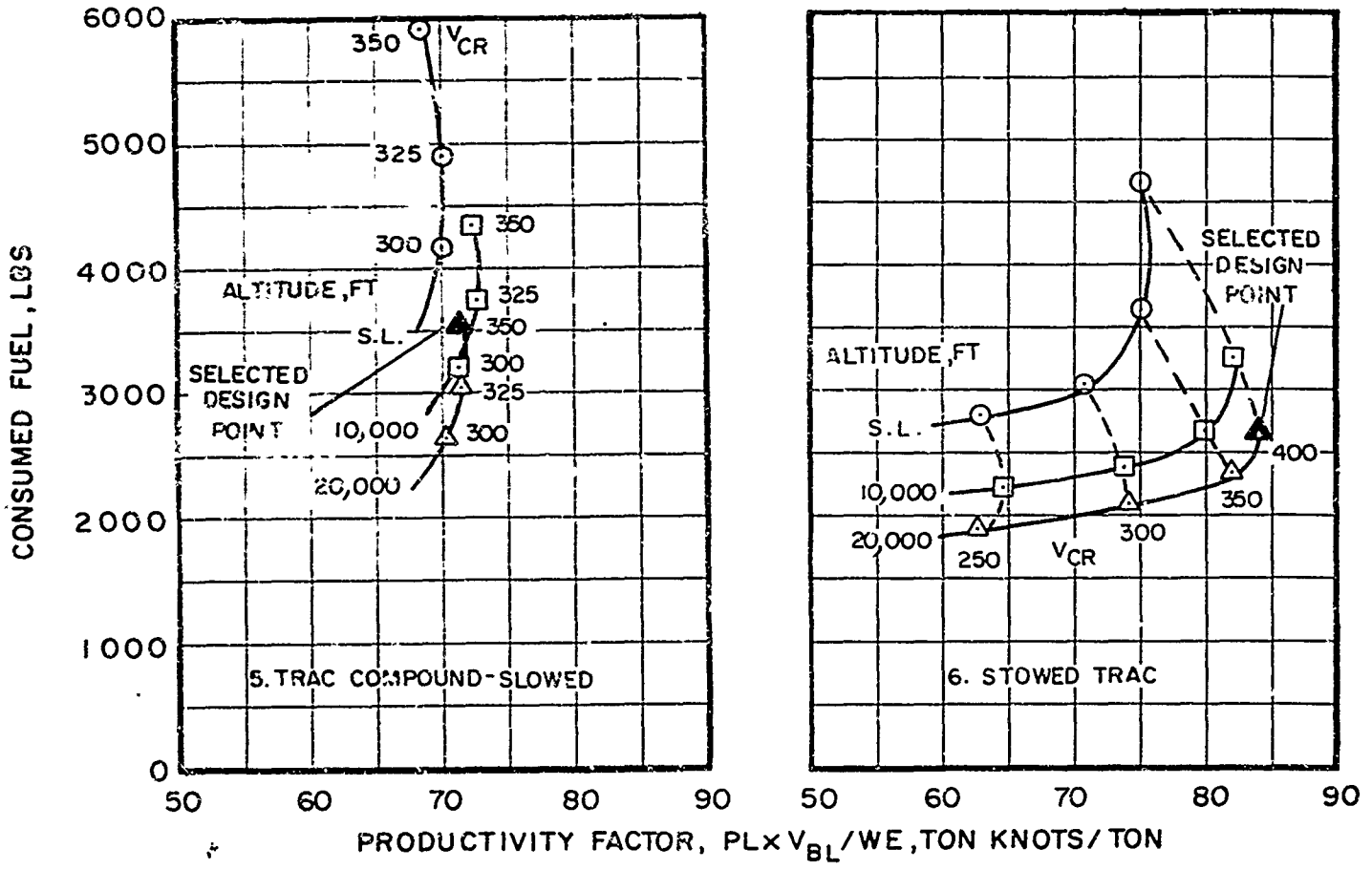

(c) Slowed TRAC Compound and Stowed TRAC

Figure 48. Concluded.

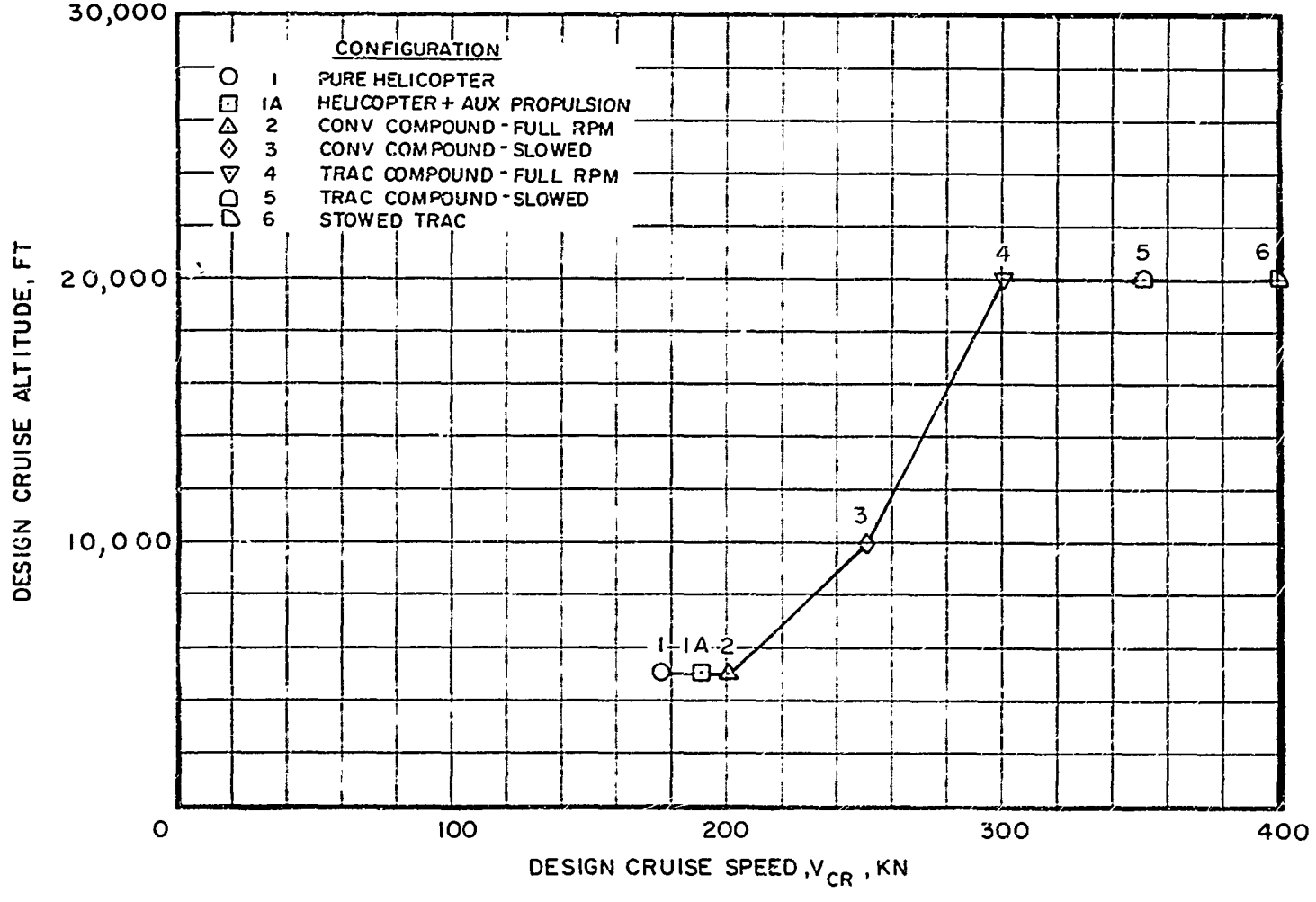

Figure 49. Cruise Speed and Altitude for Selected Point Design Aircraft, Standard Day Cruise, 5000 lb Payload, 350 N.M. Range.

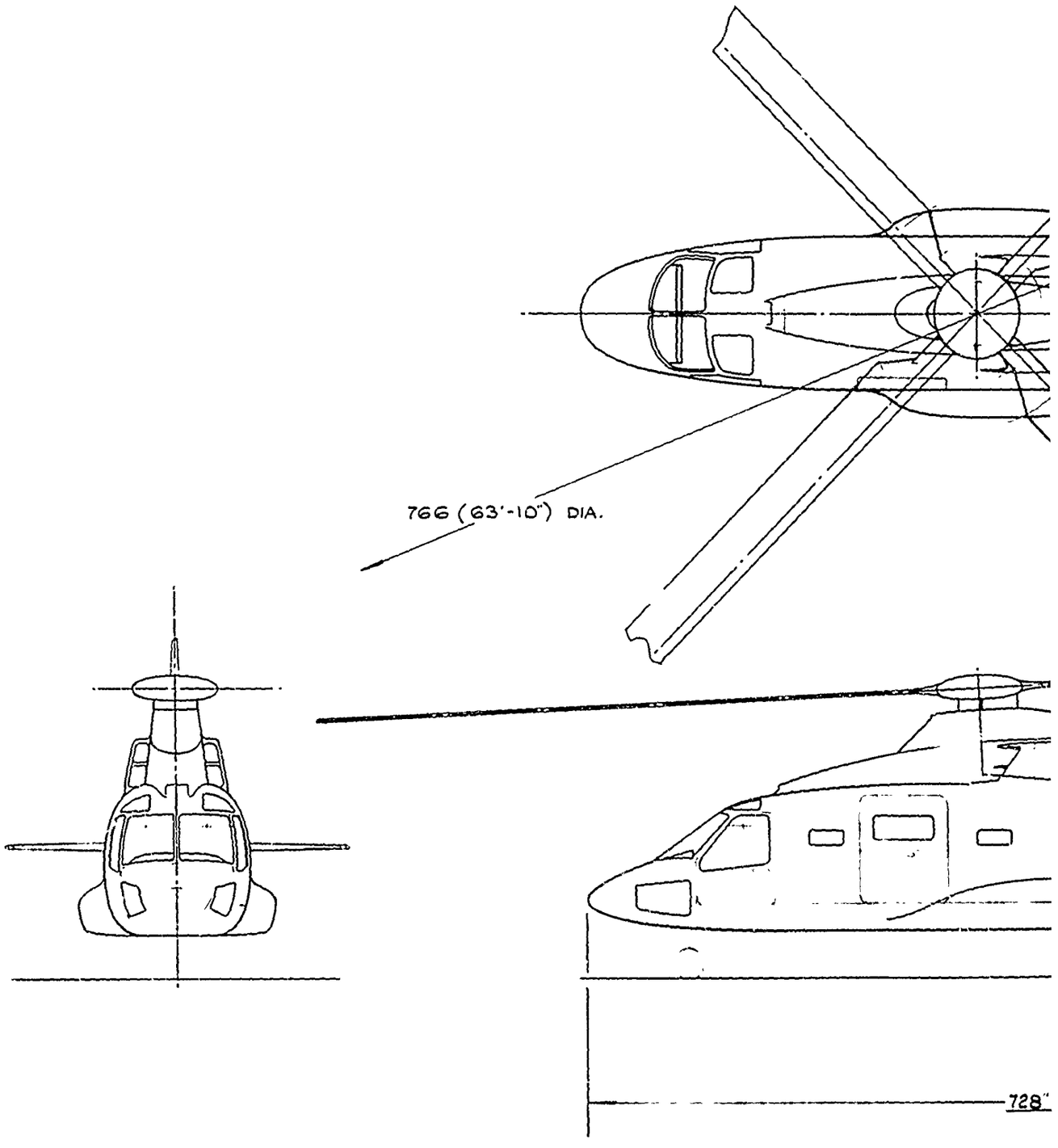

Figure 50. Three-View Drawing, Configuration 1, 175-Knot Pure Helicopter.

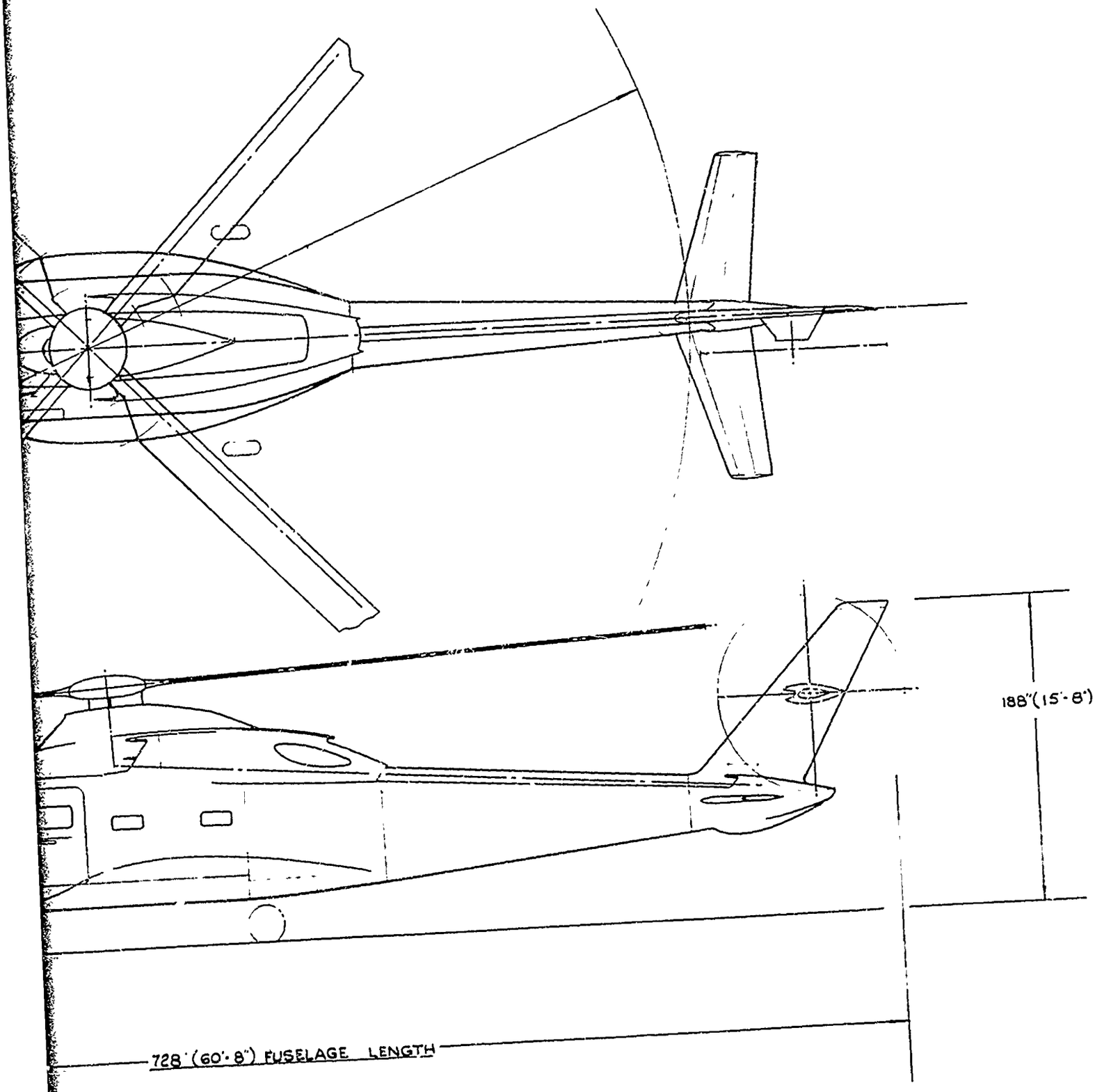
188" (15'-8")
728" (60'-8") FUSELAGE LENGTH

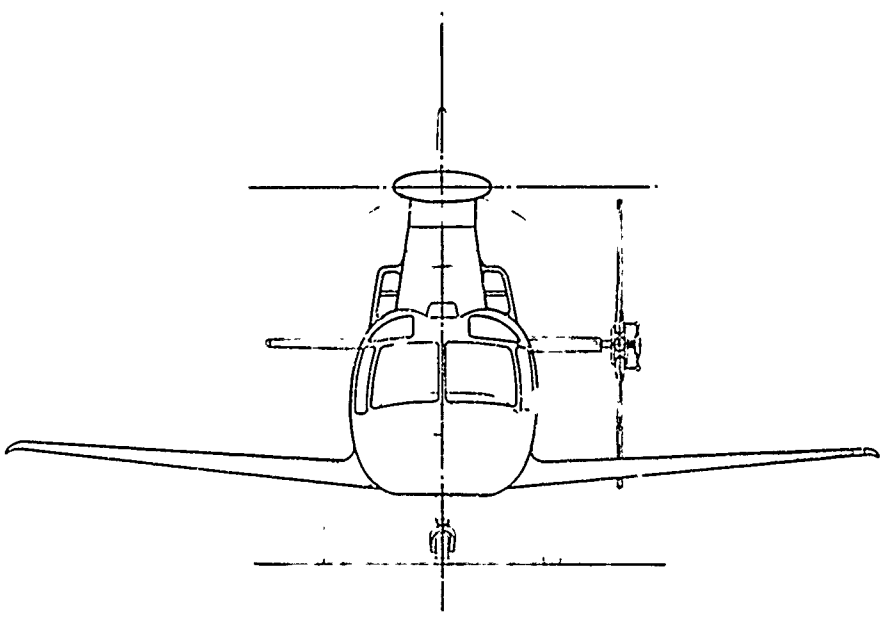

Figure 51. Three-View Drawing, Configuration 2, 200-Knot Full RPM Conventional Rotor Compound.

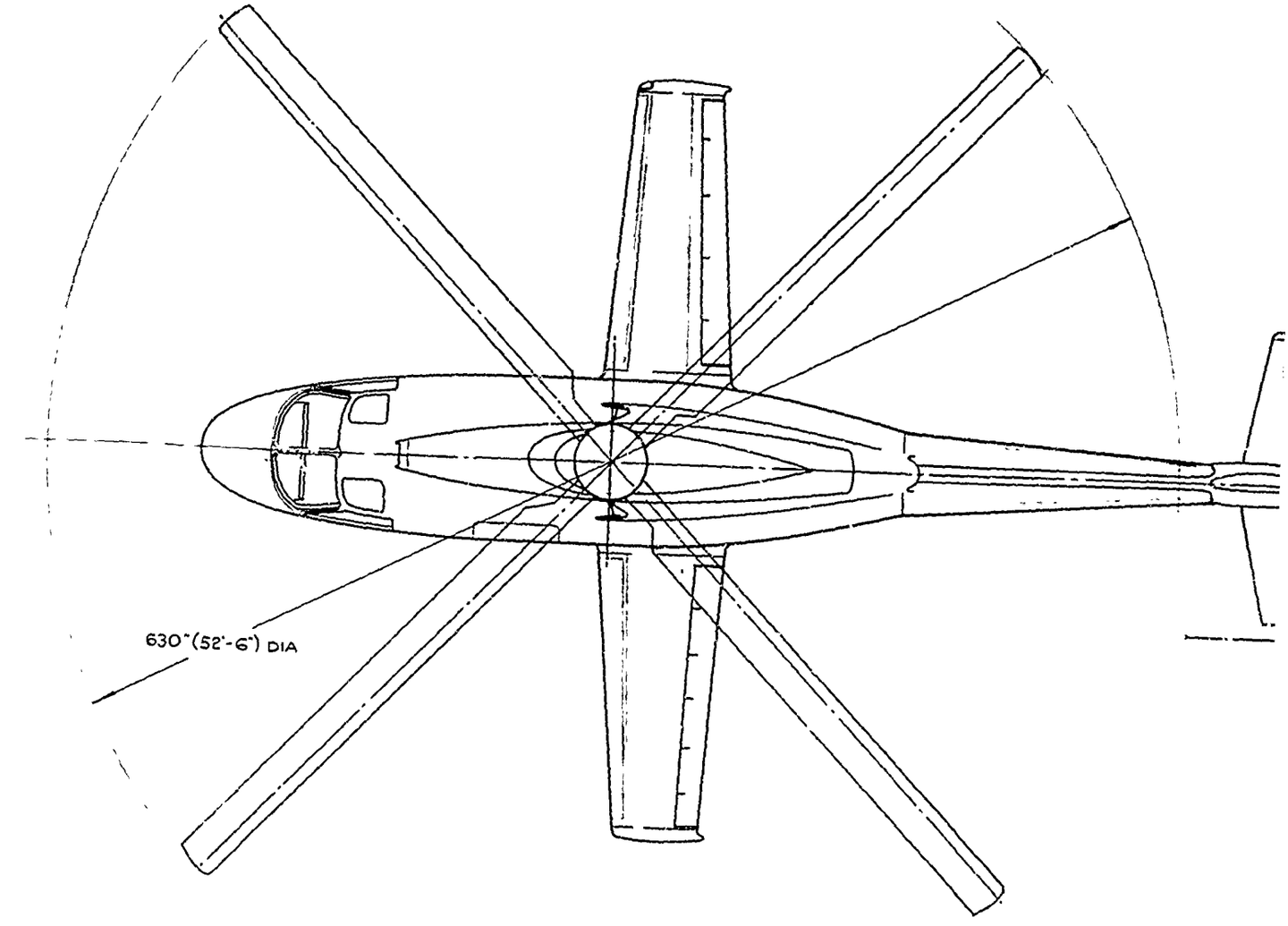

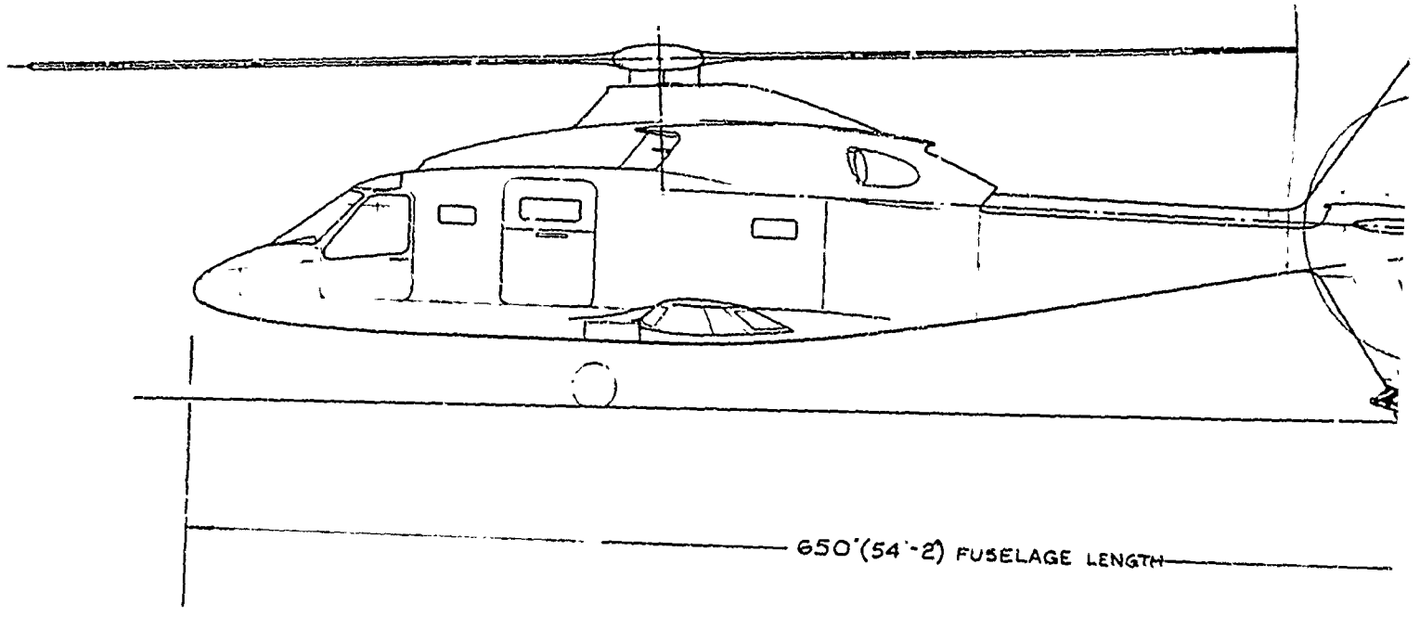

Full RPM

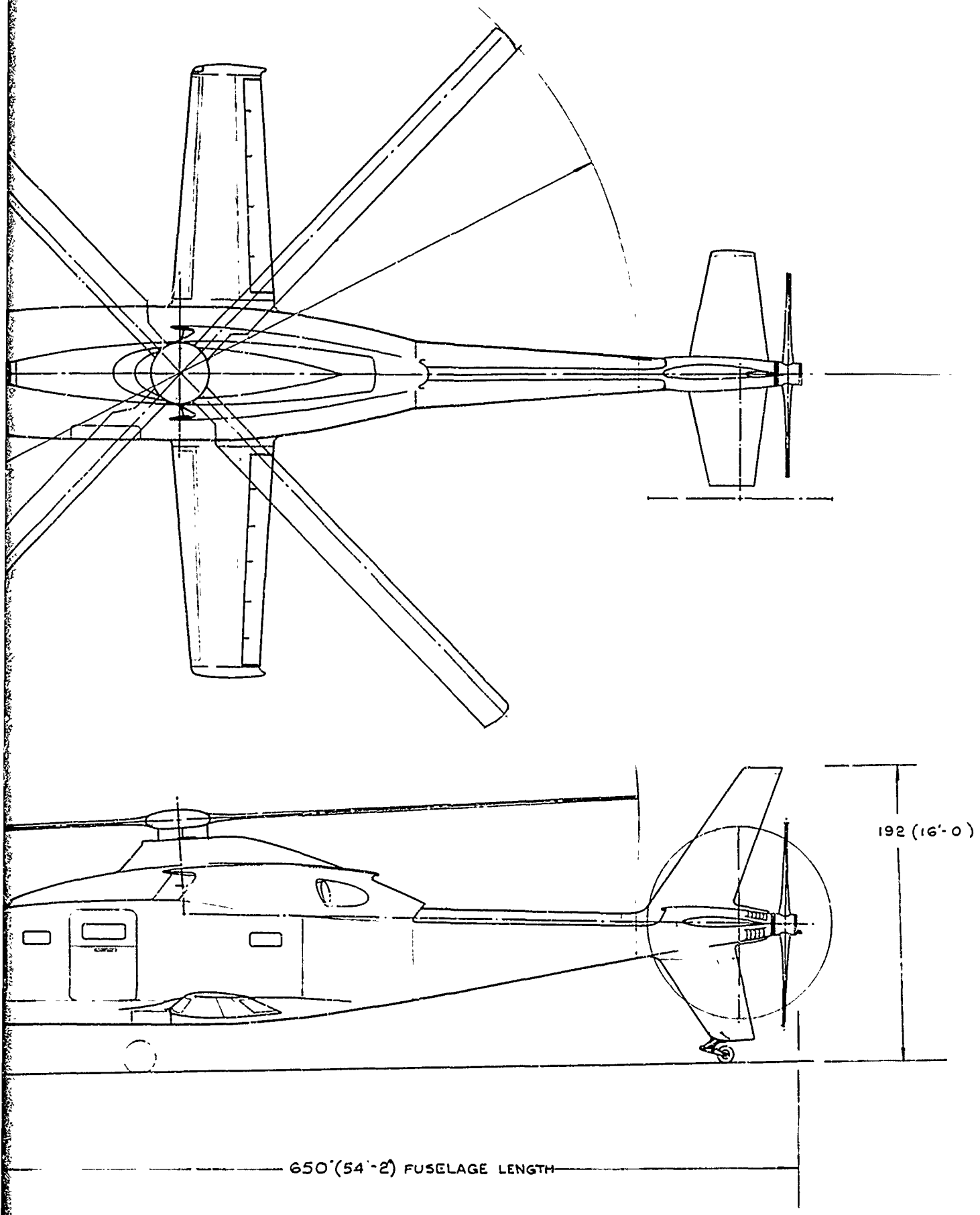
192 (16'-0)
650"(54'-2) FUSELAGE LENGTH

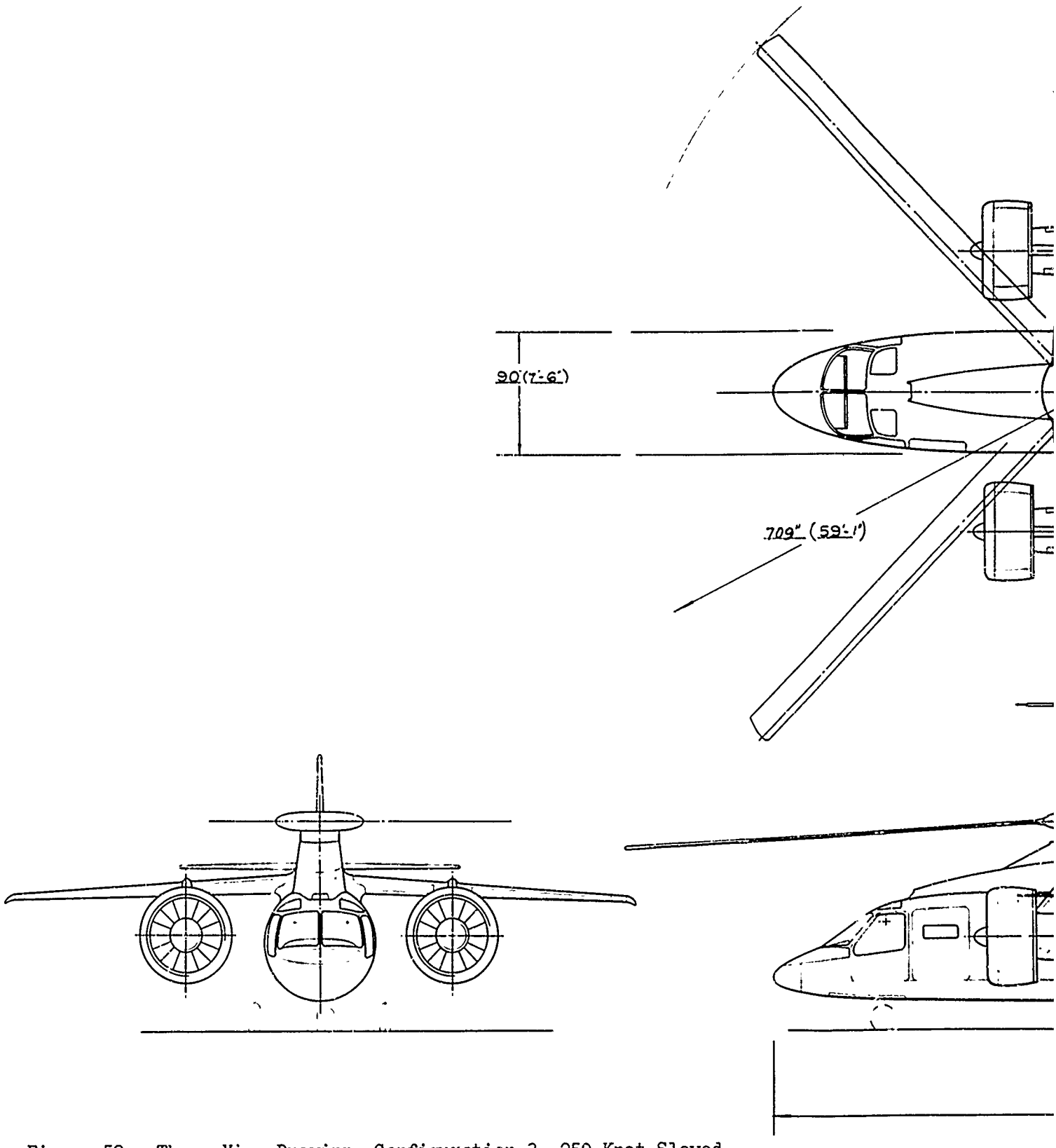

Figure 52. Three-View Drawing, Configuration 3, 250-Knot Slowed Conventional Rotor Compound.

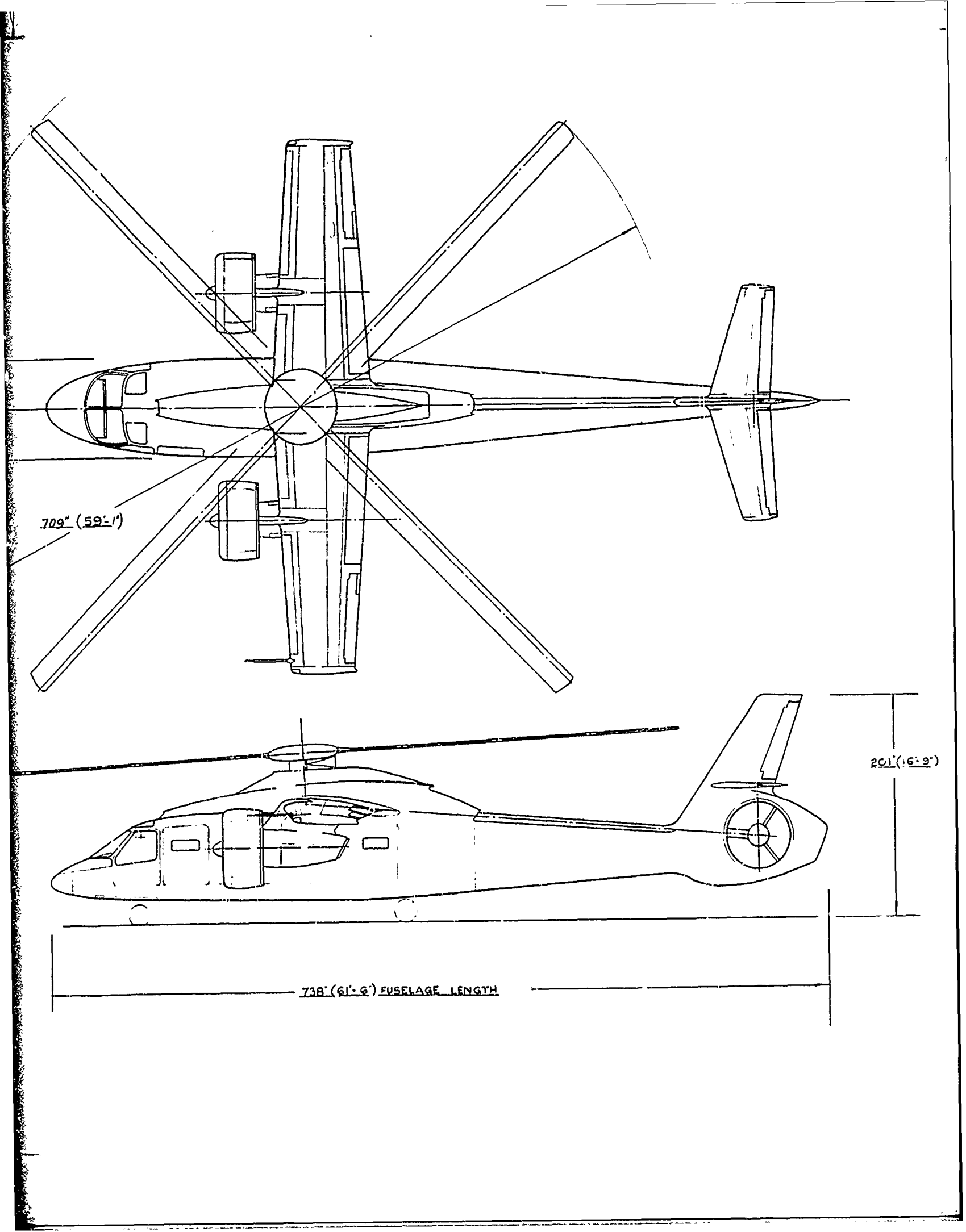
709" (59'-1")
201" (16'-9")
738" (61'-6") FUSELAGE LENGTH

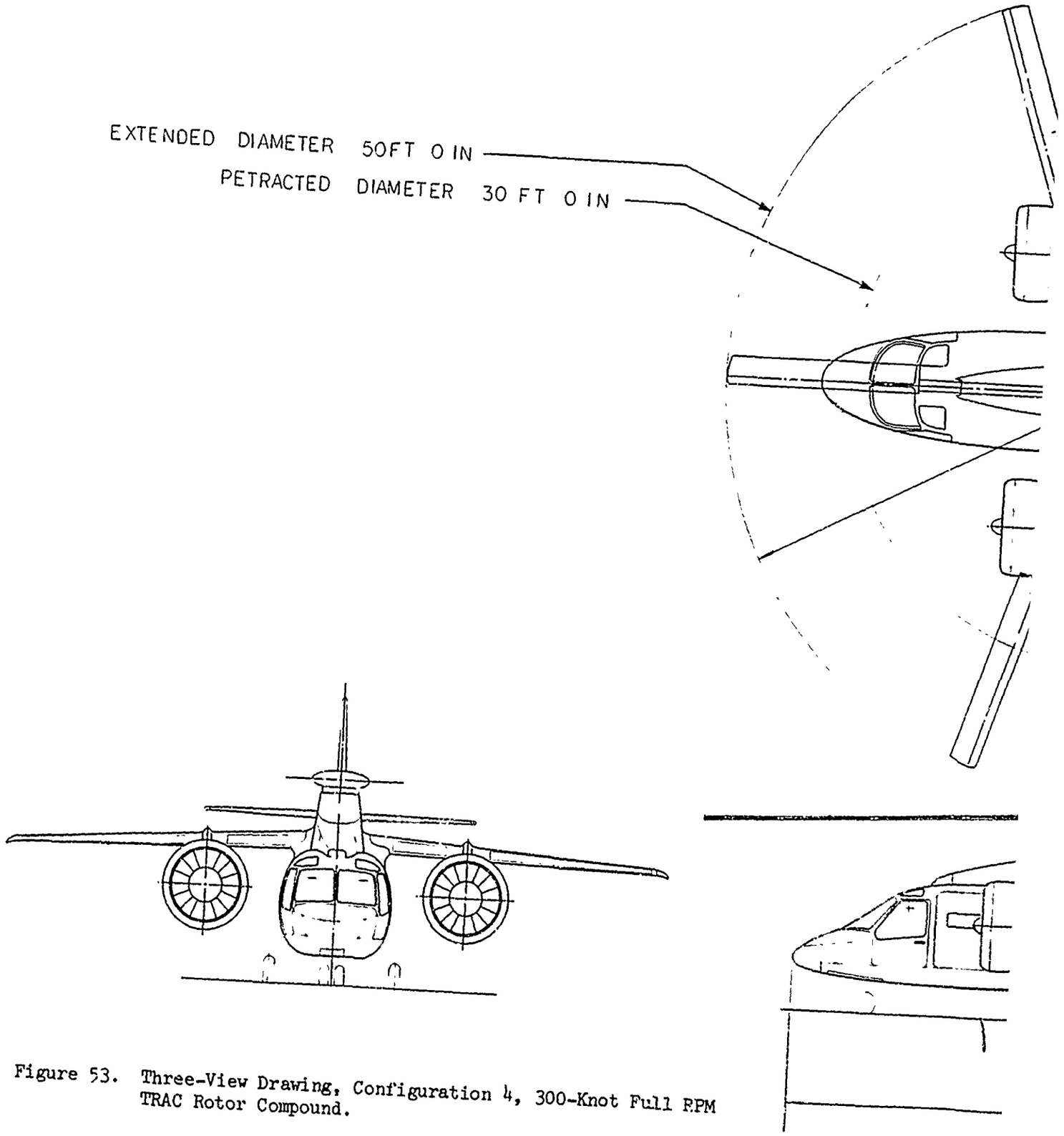

Figure 53. Three-View Drawing, Configuration 4, 300-Knot Full RPM TRAC Rotor Compound.

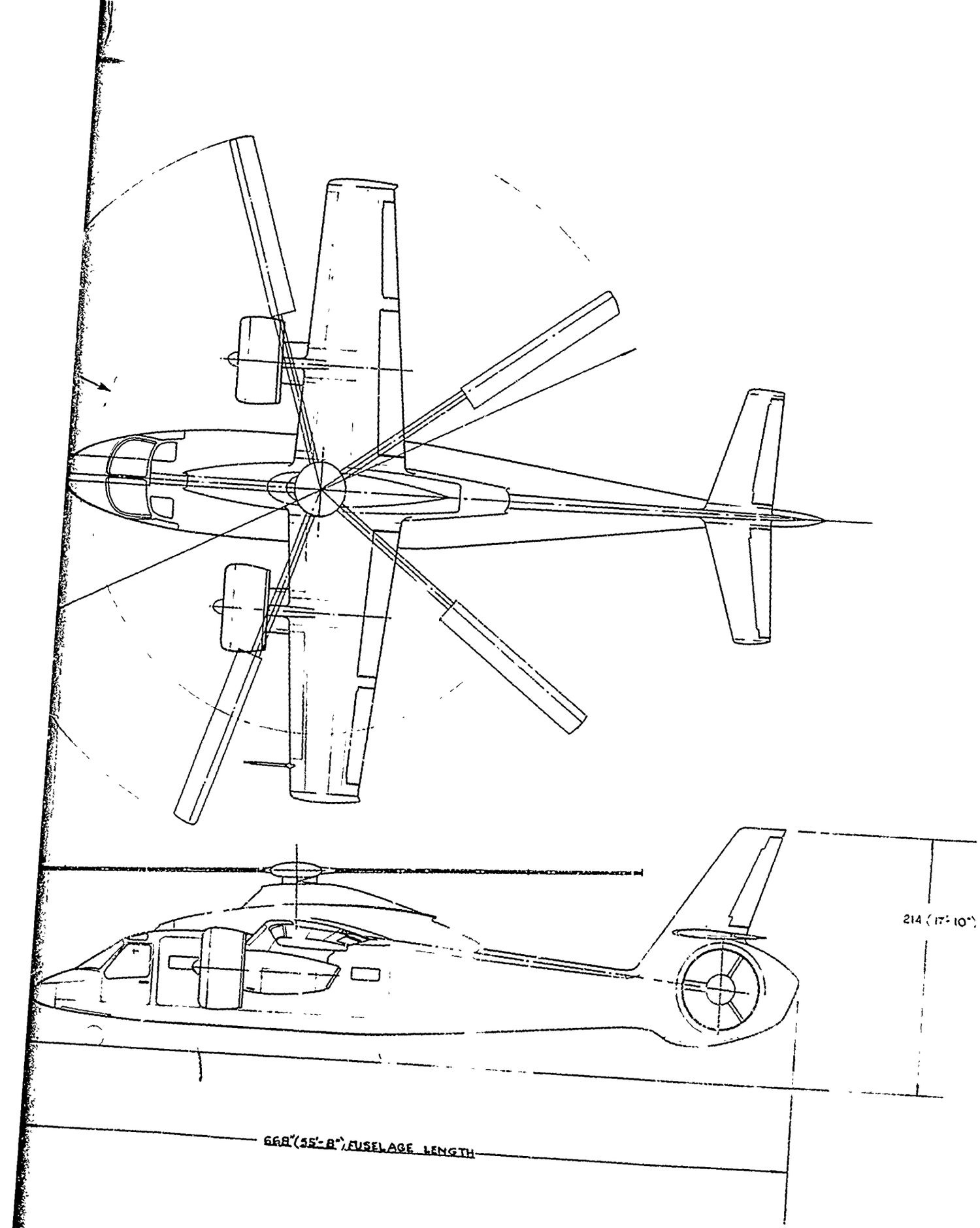
214 (17'-10")
668" (55'-8") FUSELAGE LENGTH

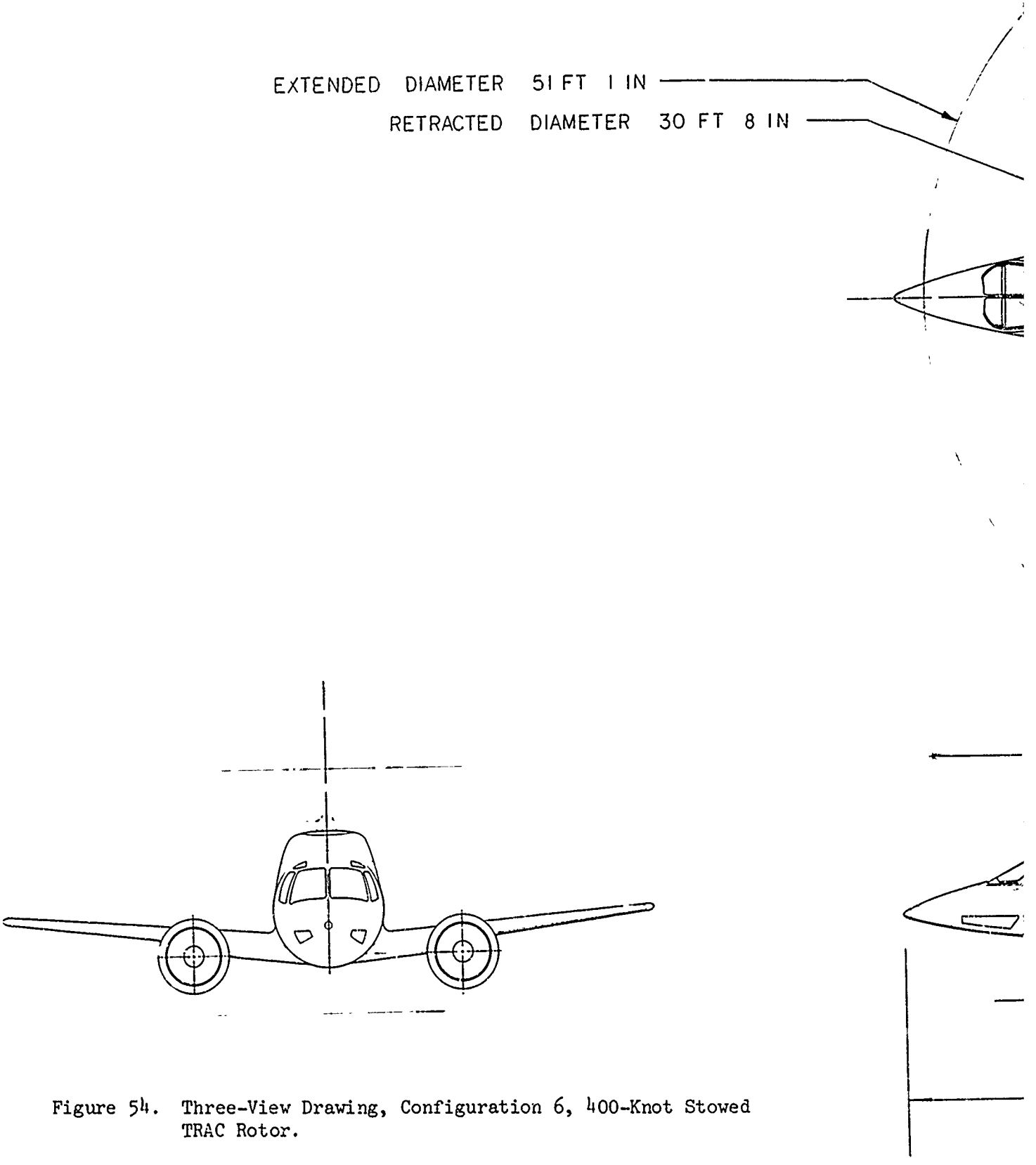

Figure 54. Three-View Drawing, Configuration 6, 400-Knot Stowed TRAC Rotor.

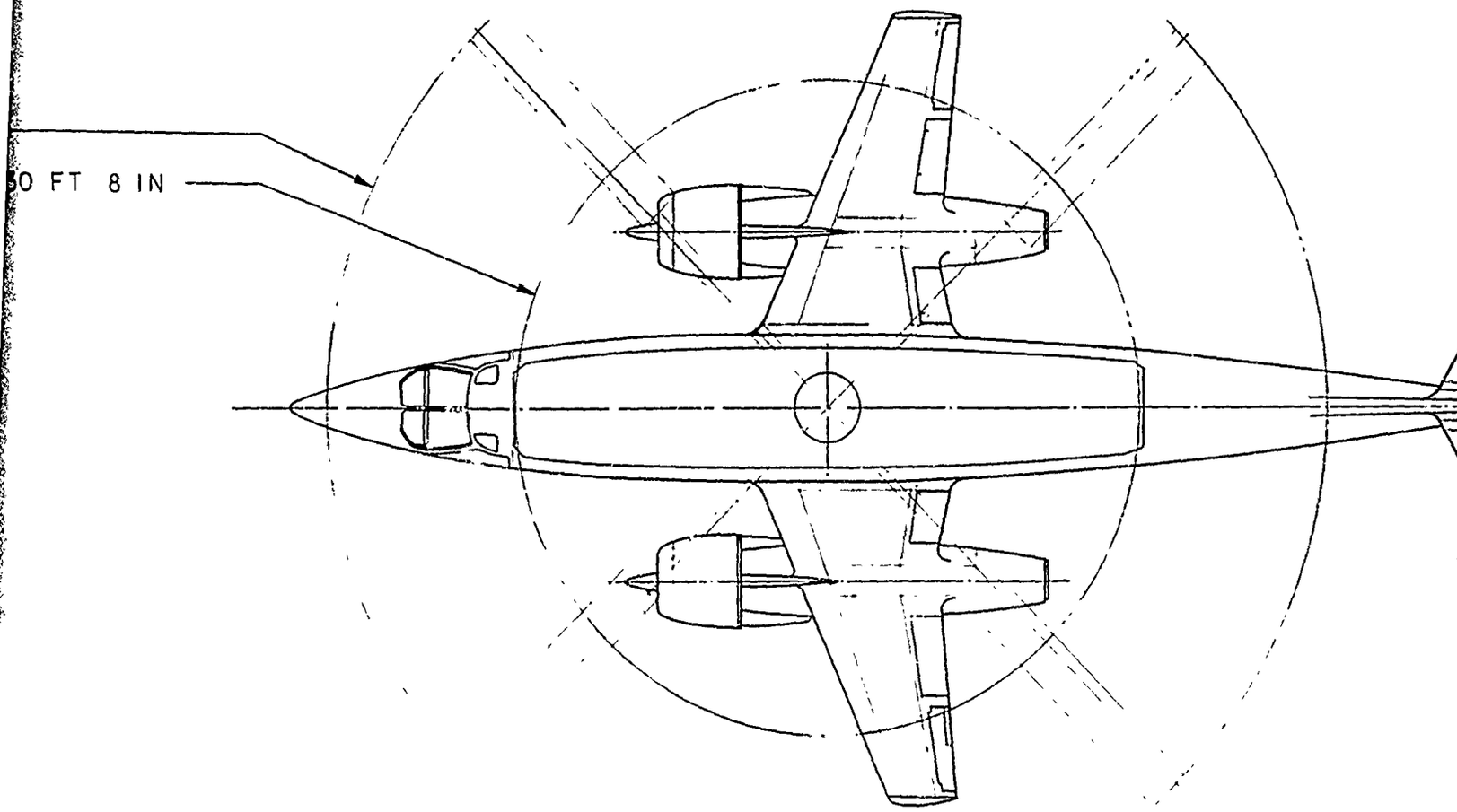

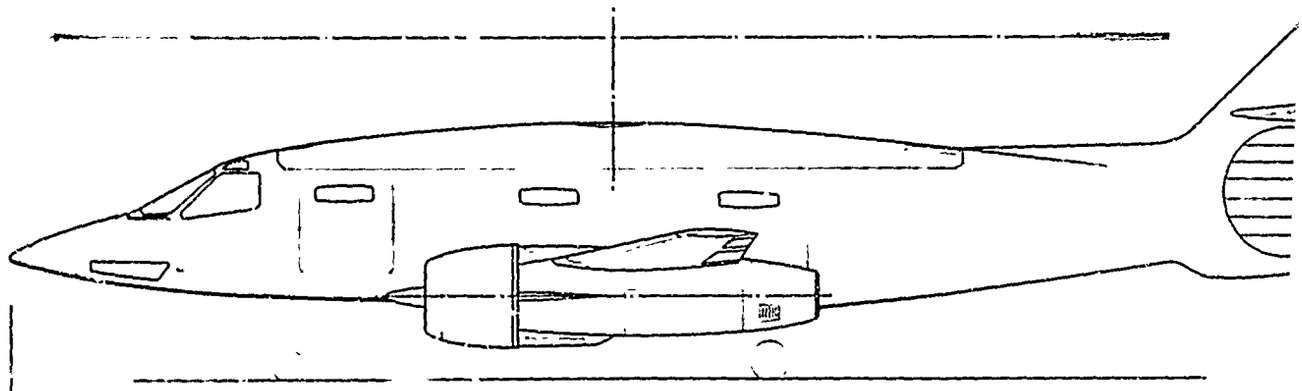

t Stowed

815" (67'-11") FUSELAGE LENGTH

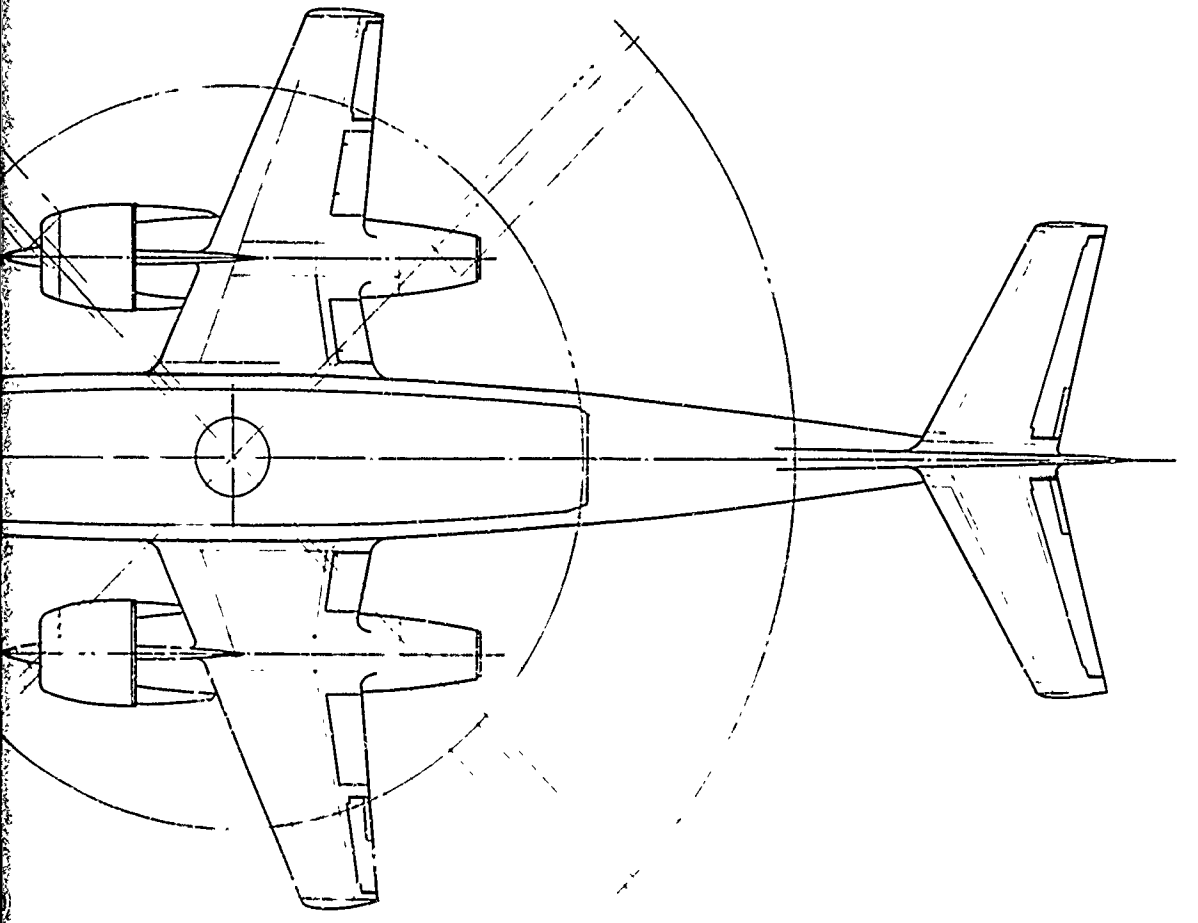

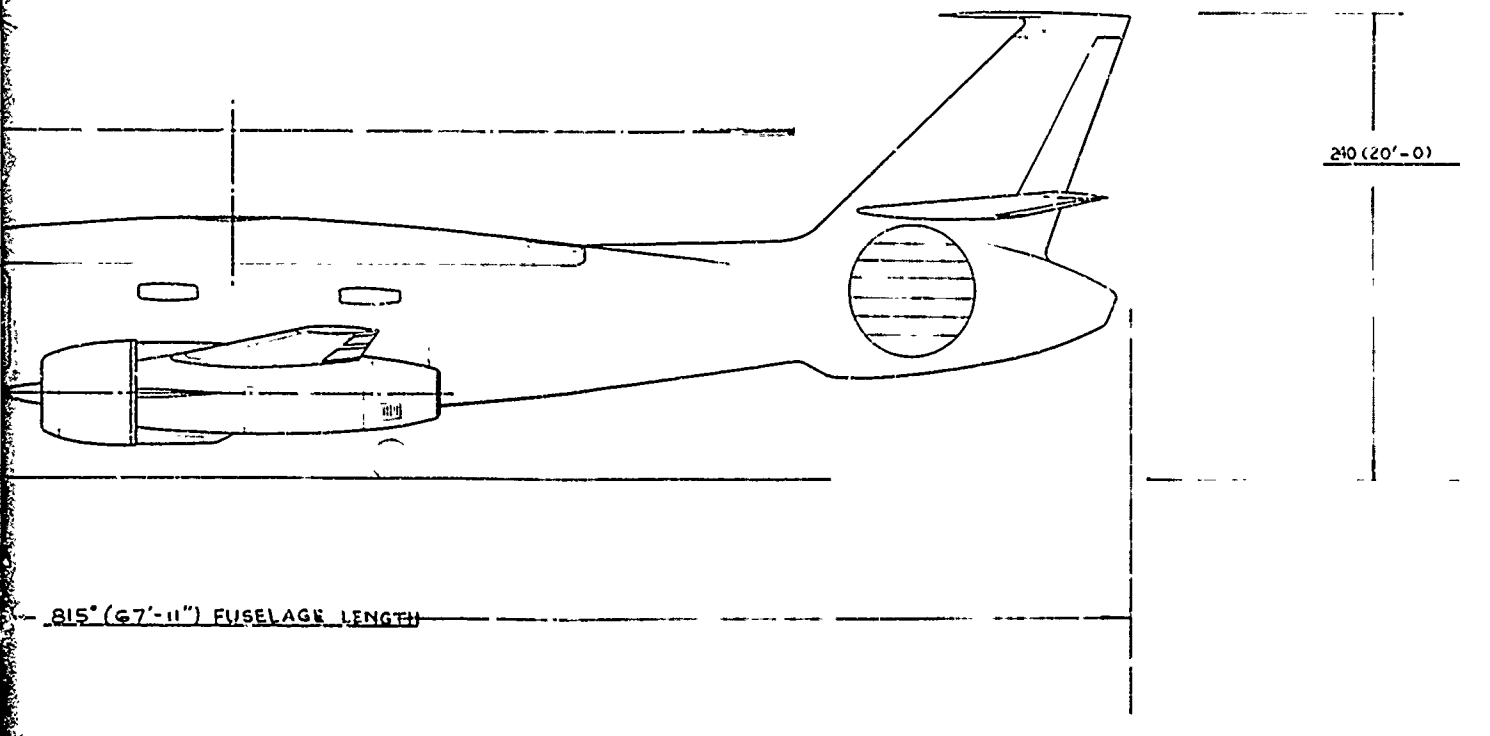
240 (20'-0)
815" (67'-11") FUSELAGE LENGTH

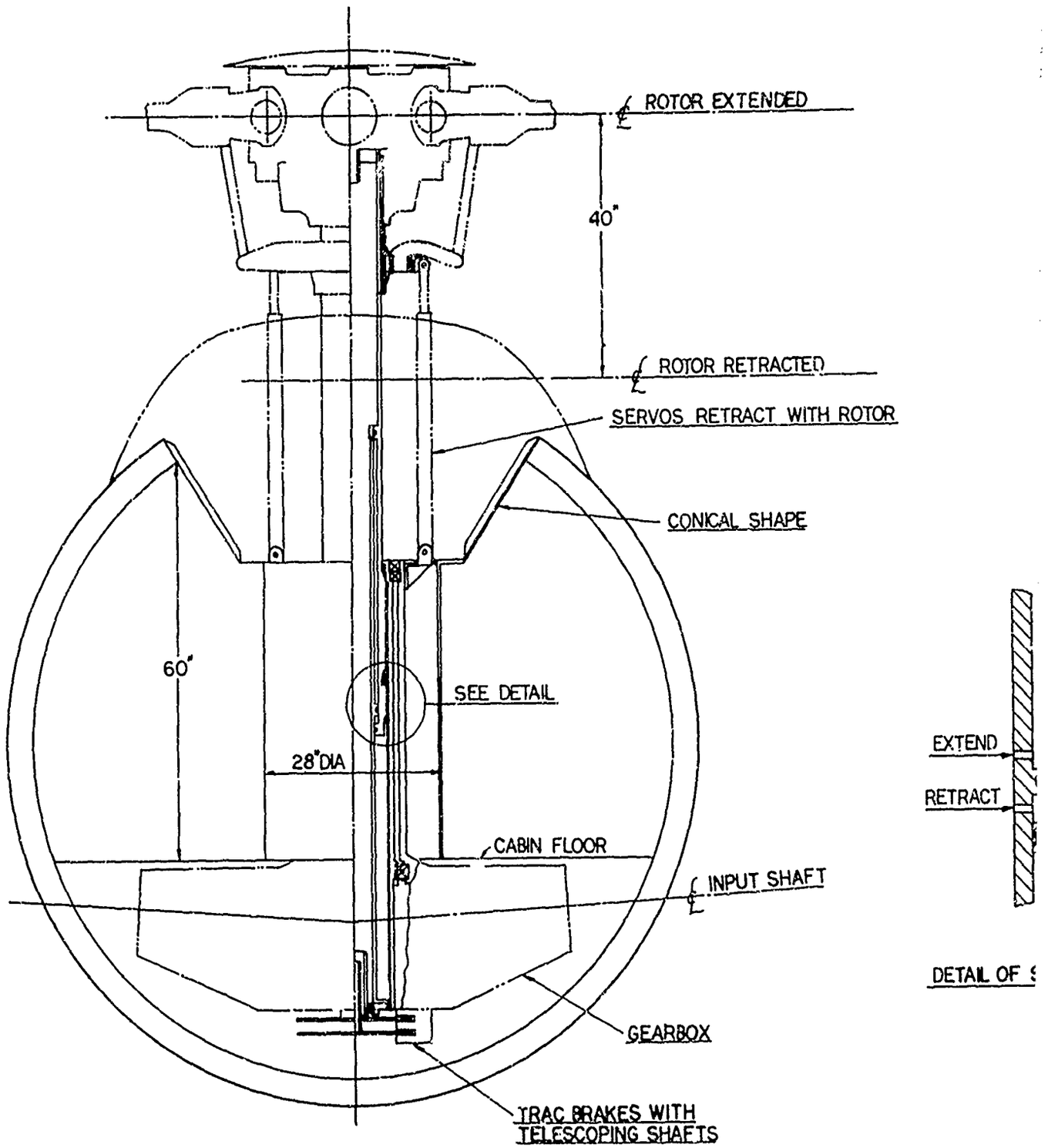

TELESCOPING ROTOR SHAFT LAYOUT

Figure 55. Extensible Shaft Layout.

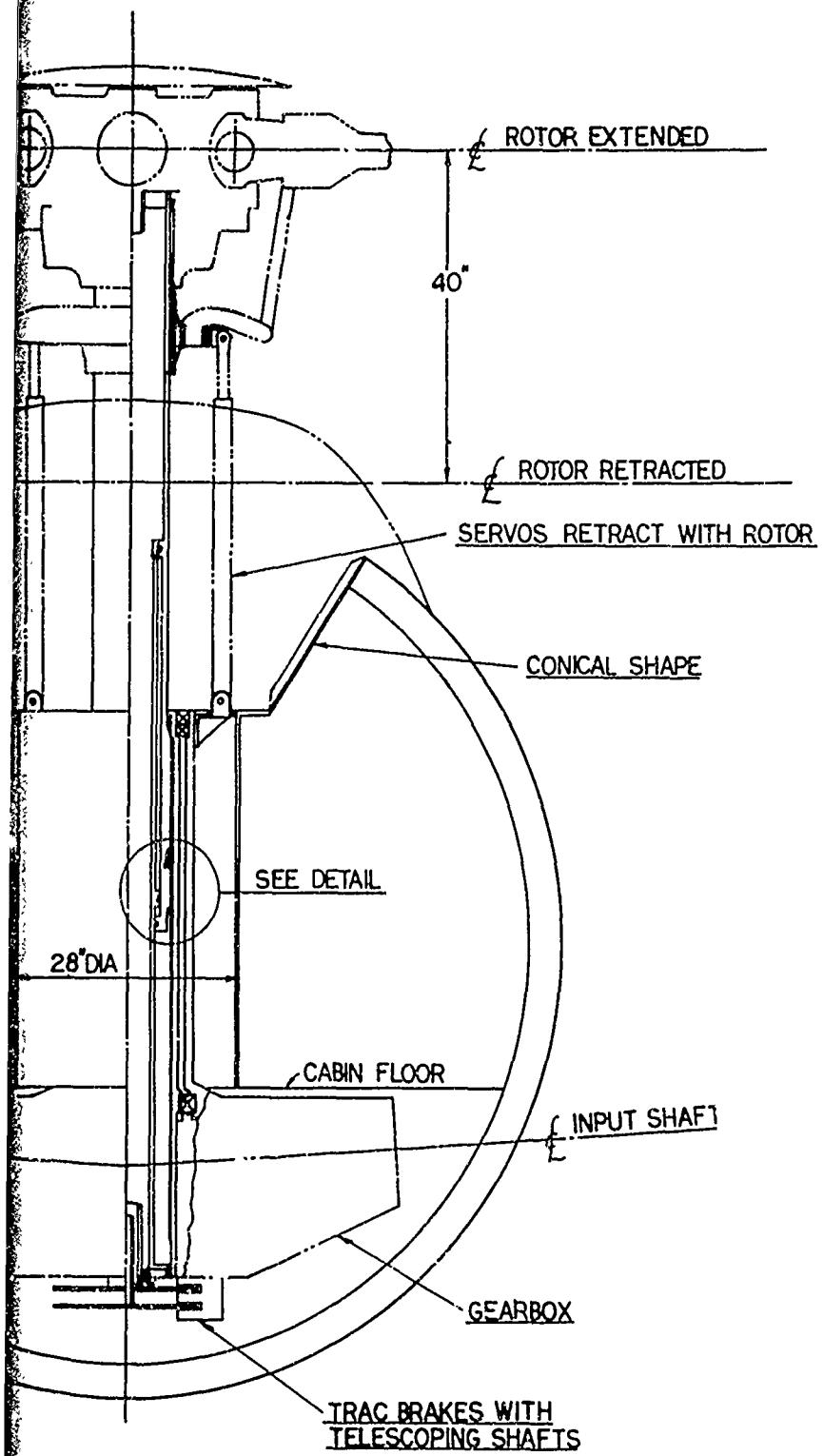

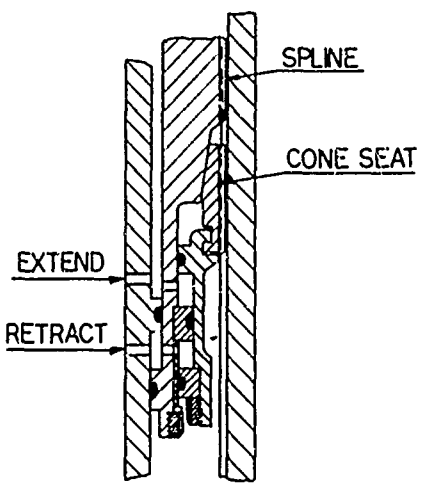

DETAIL OF SHAFT LOCK SYSTEM

NG ROTOR SHAFT LAYOUT

55. Extensible Shaft Layout.

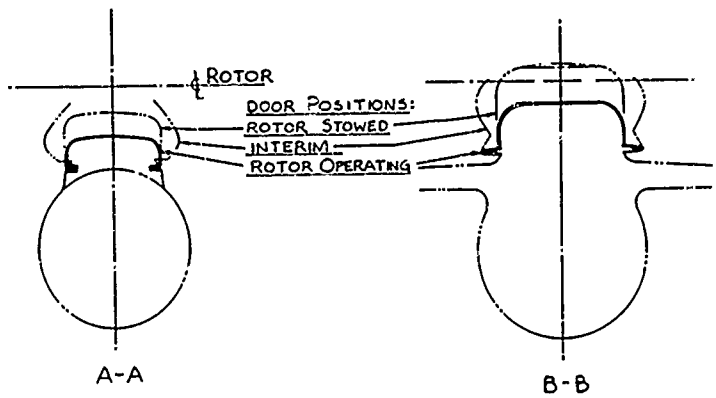

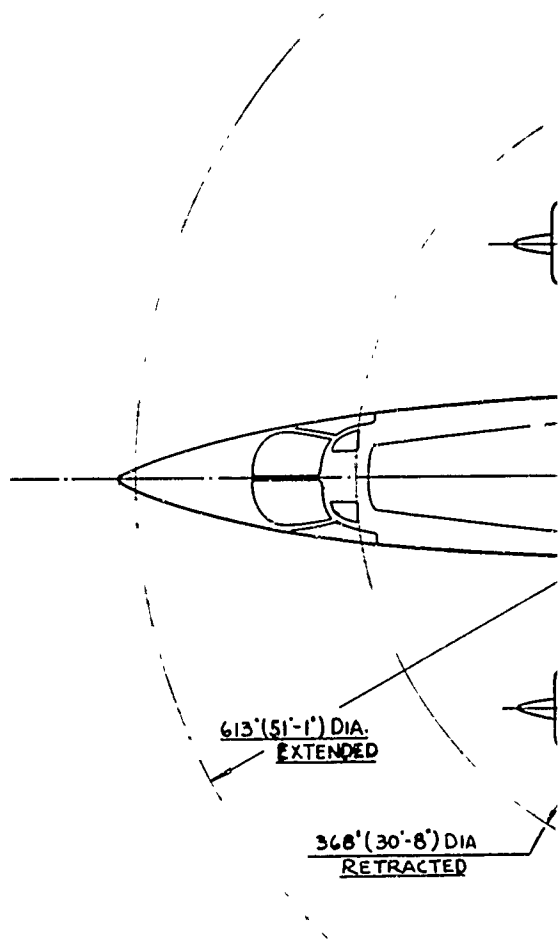

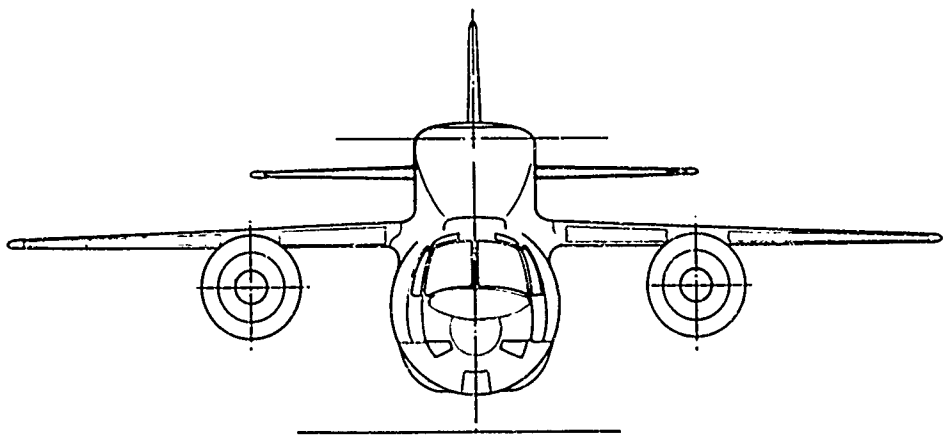

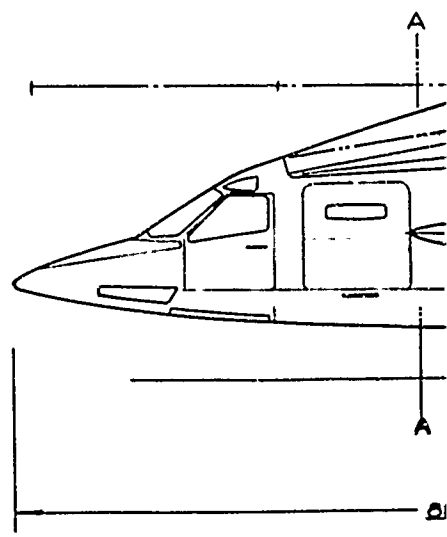

Figure 56. Three-View Drawing, Configuration 6, 400-Knot Stowed TRAC Rotor Alternate Design.

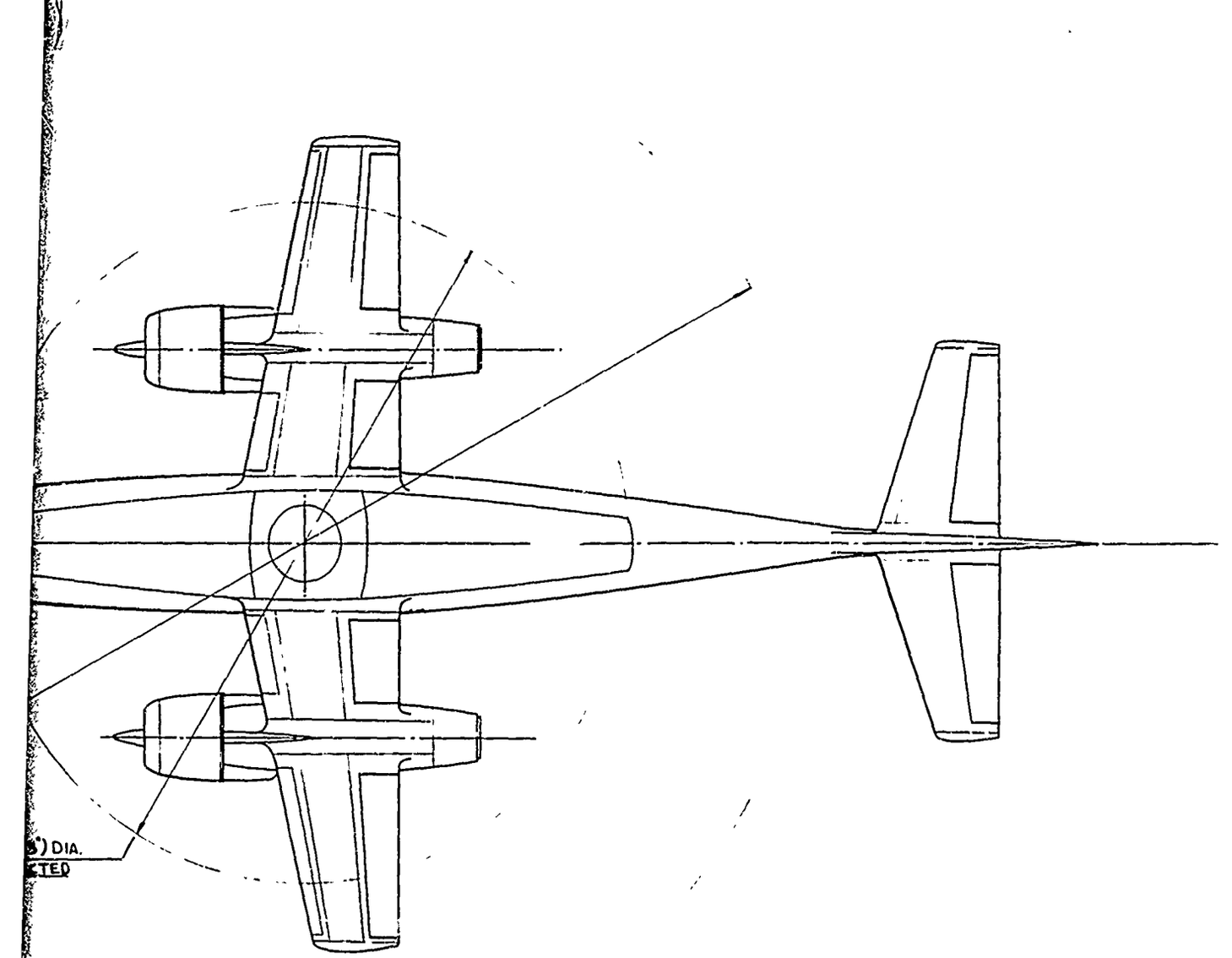
) DIA.
TED

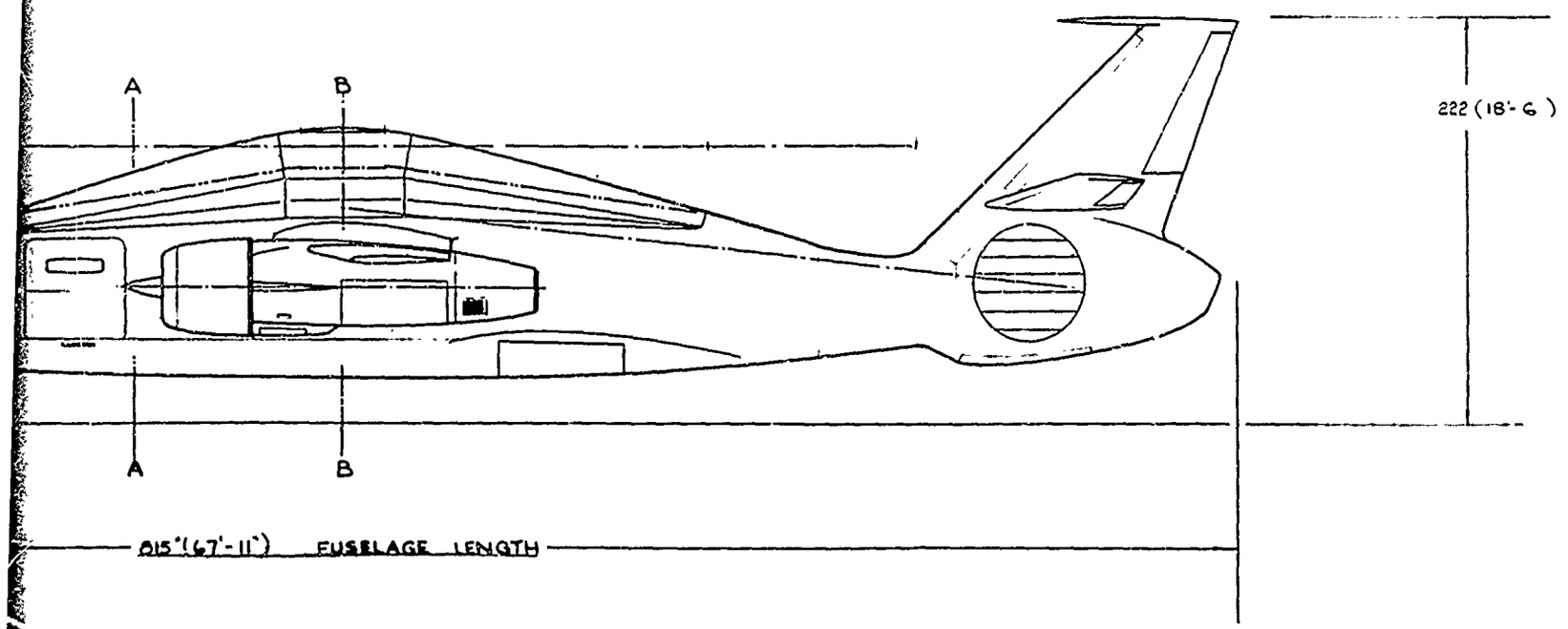
A
B
222 (18'-6")
A
B
815"(67'-11") FUSELAGE LENGTH

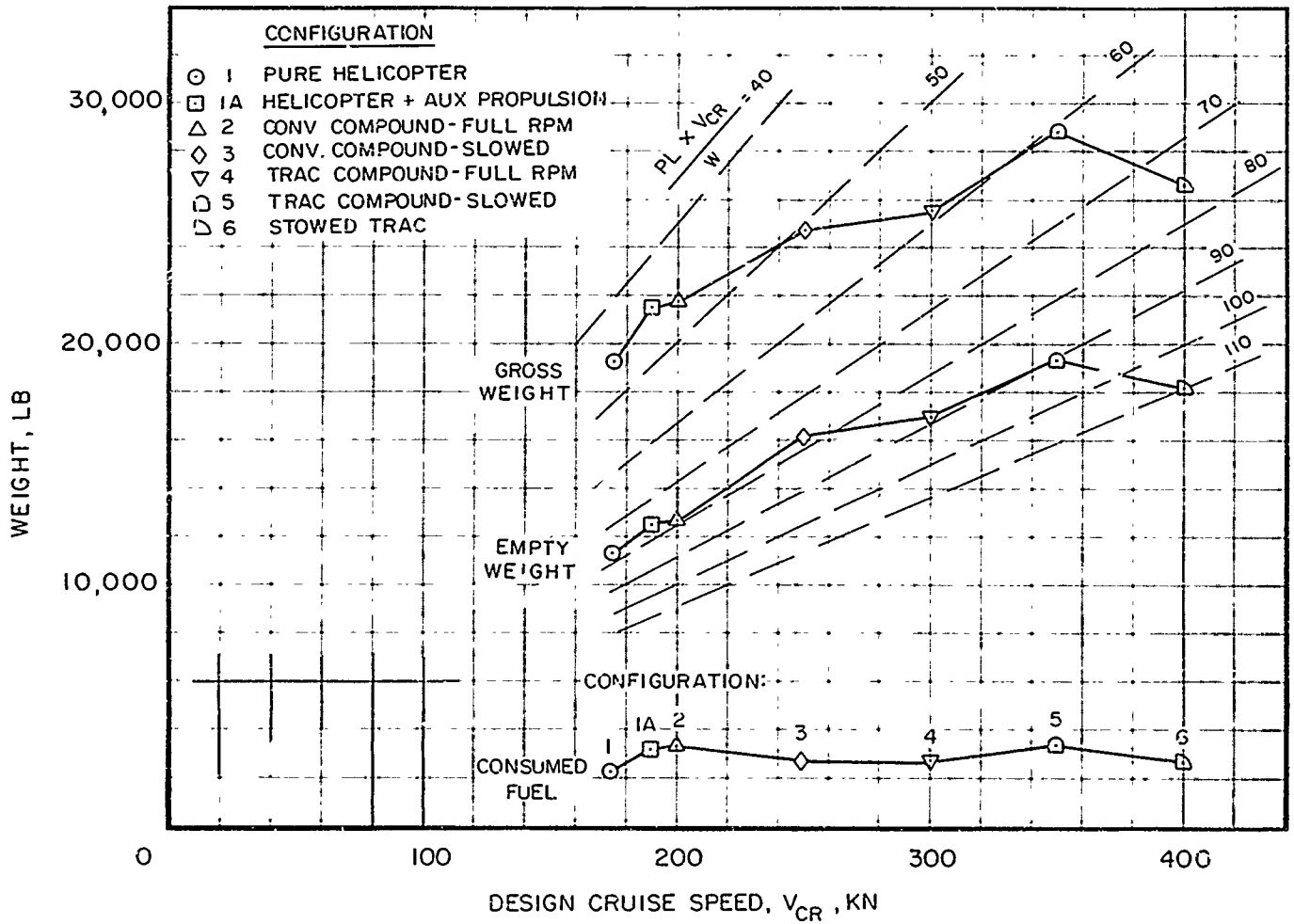

Figure 57. Comparison Summary for Point Design Aircraft, 5000 lb Payload, 350 N.M. Range.

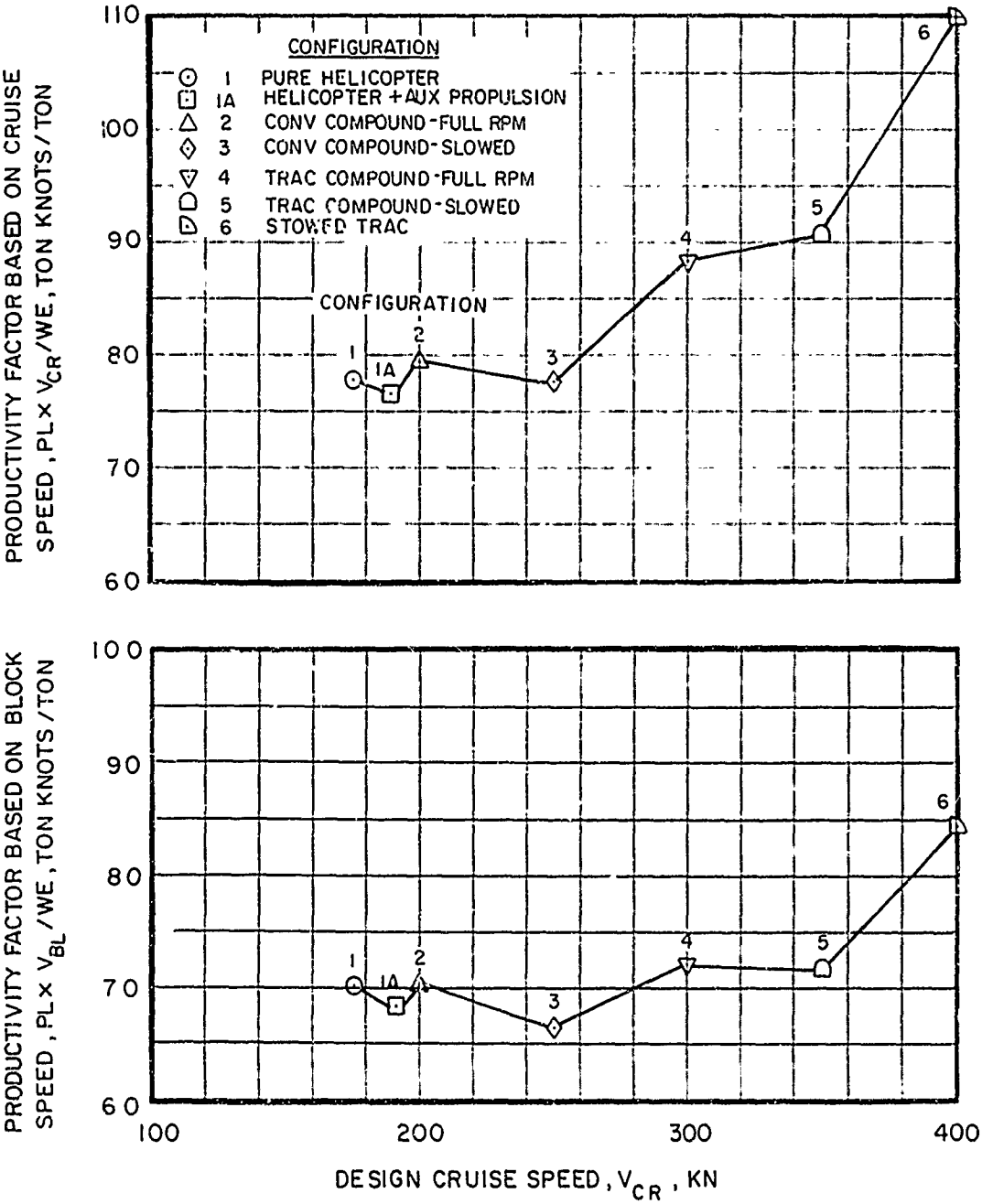

Figure 58. Aircraft Productivity Comparison, 5000 lb Payload, 350 N.M. Range.

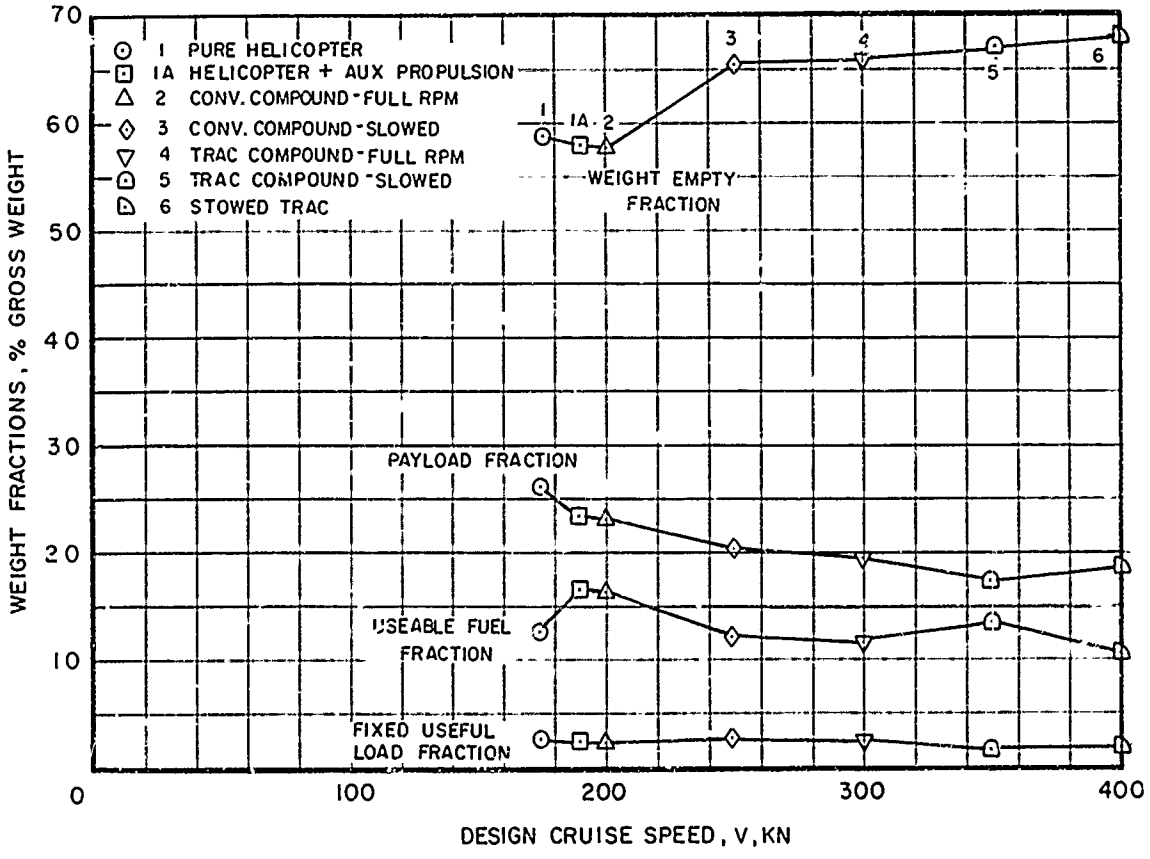

Figure 59. Overall Weight Fraction Comparison.

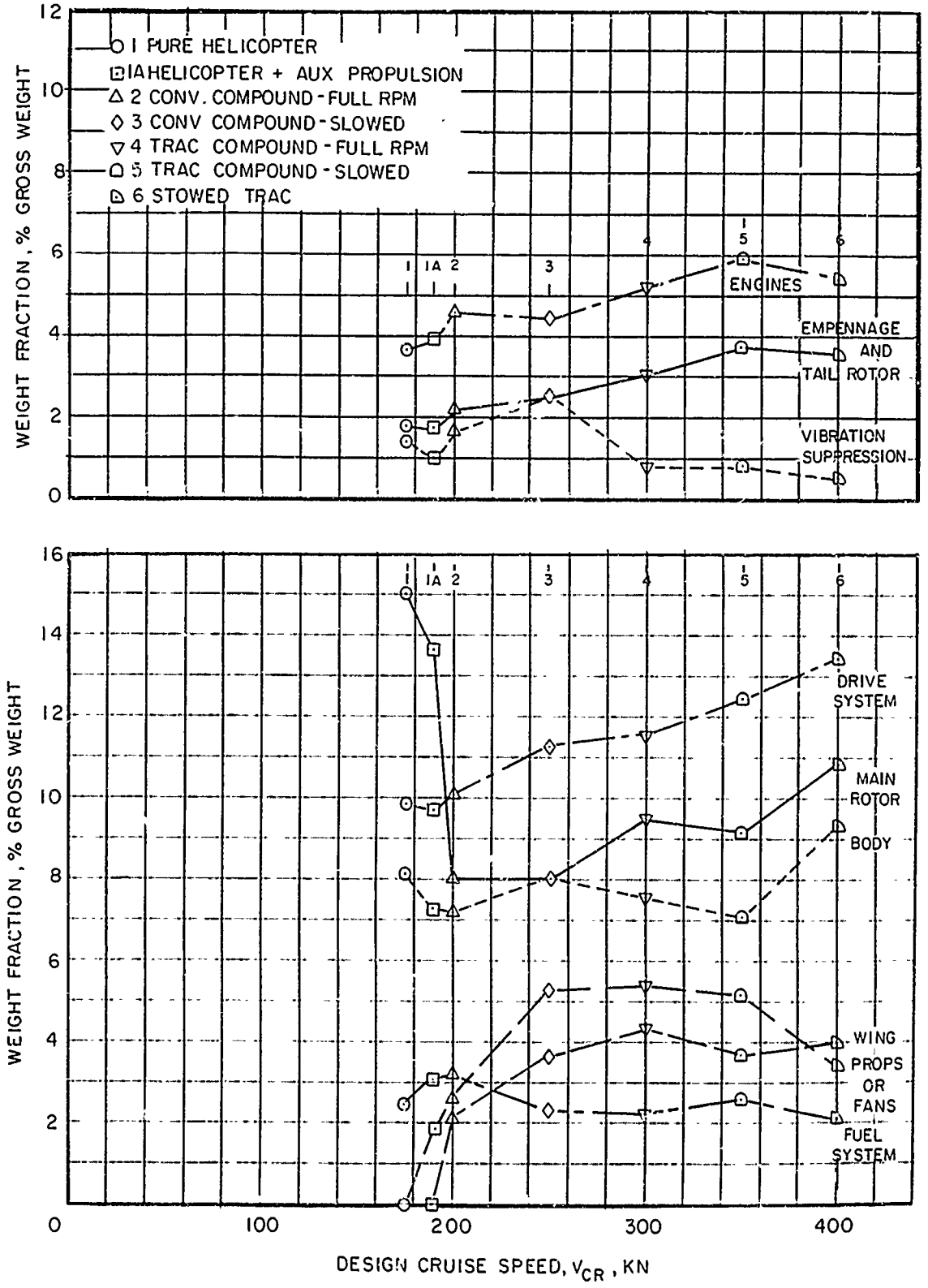

Figure 60. Subsystem Weight Fraction Comparison.

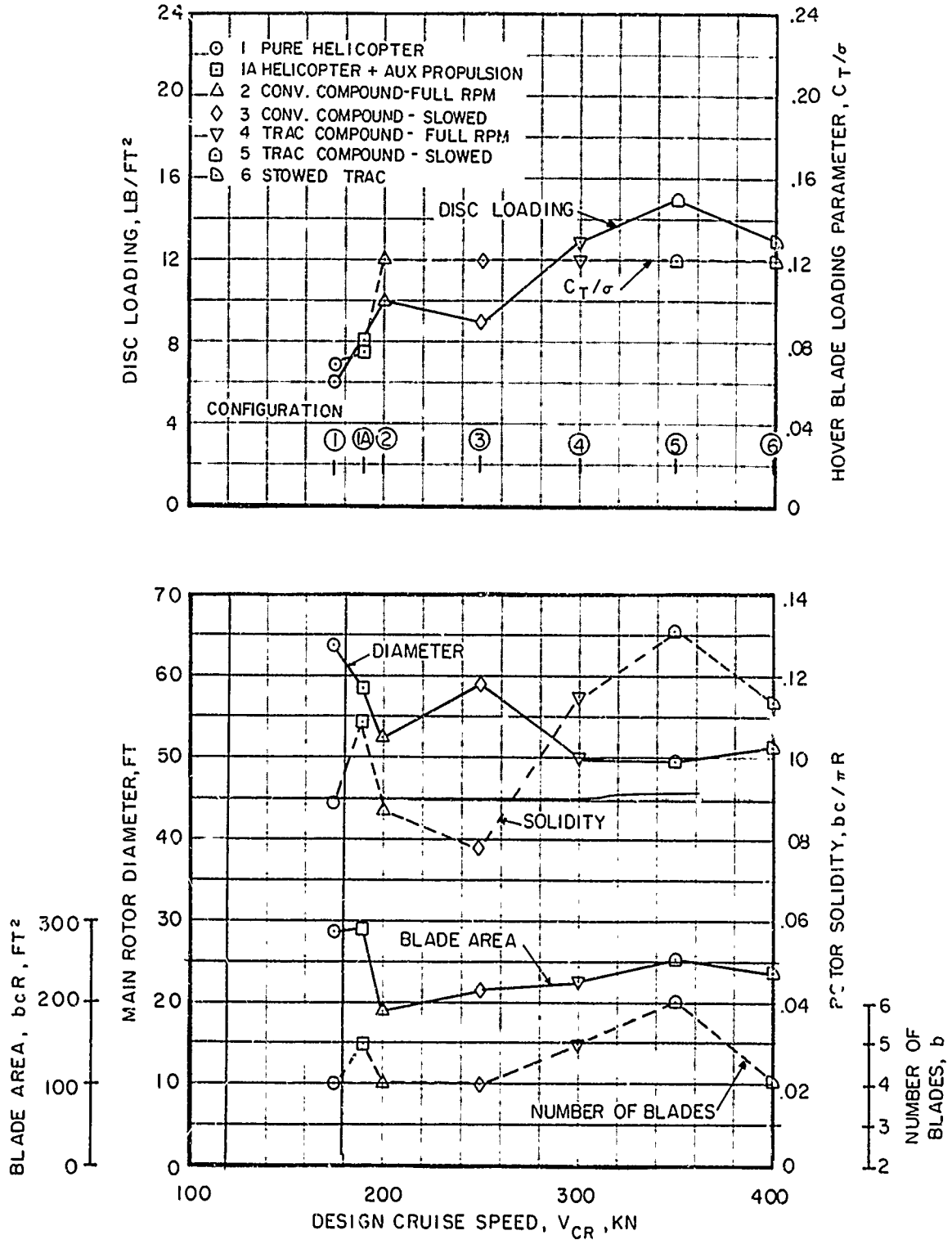

Figure 61. Comparisons of Main Rotor Aerodynamic Design Parameters.

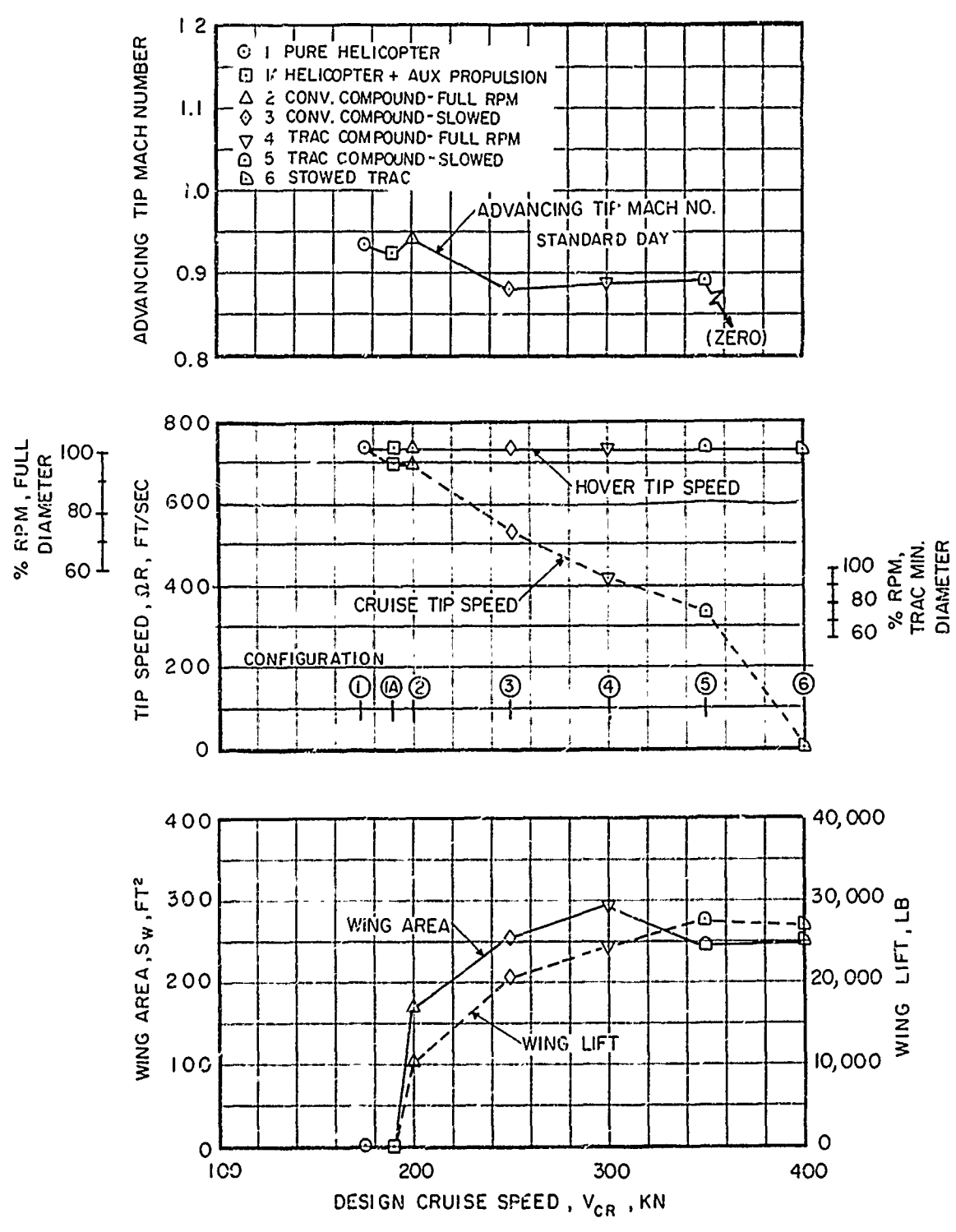

Figure 62. Comparison of Rotor and Wing Aerodynamic Design Parameters.

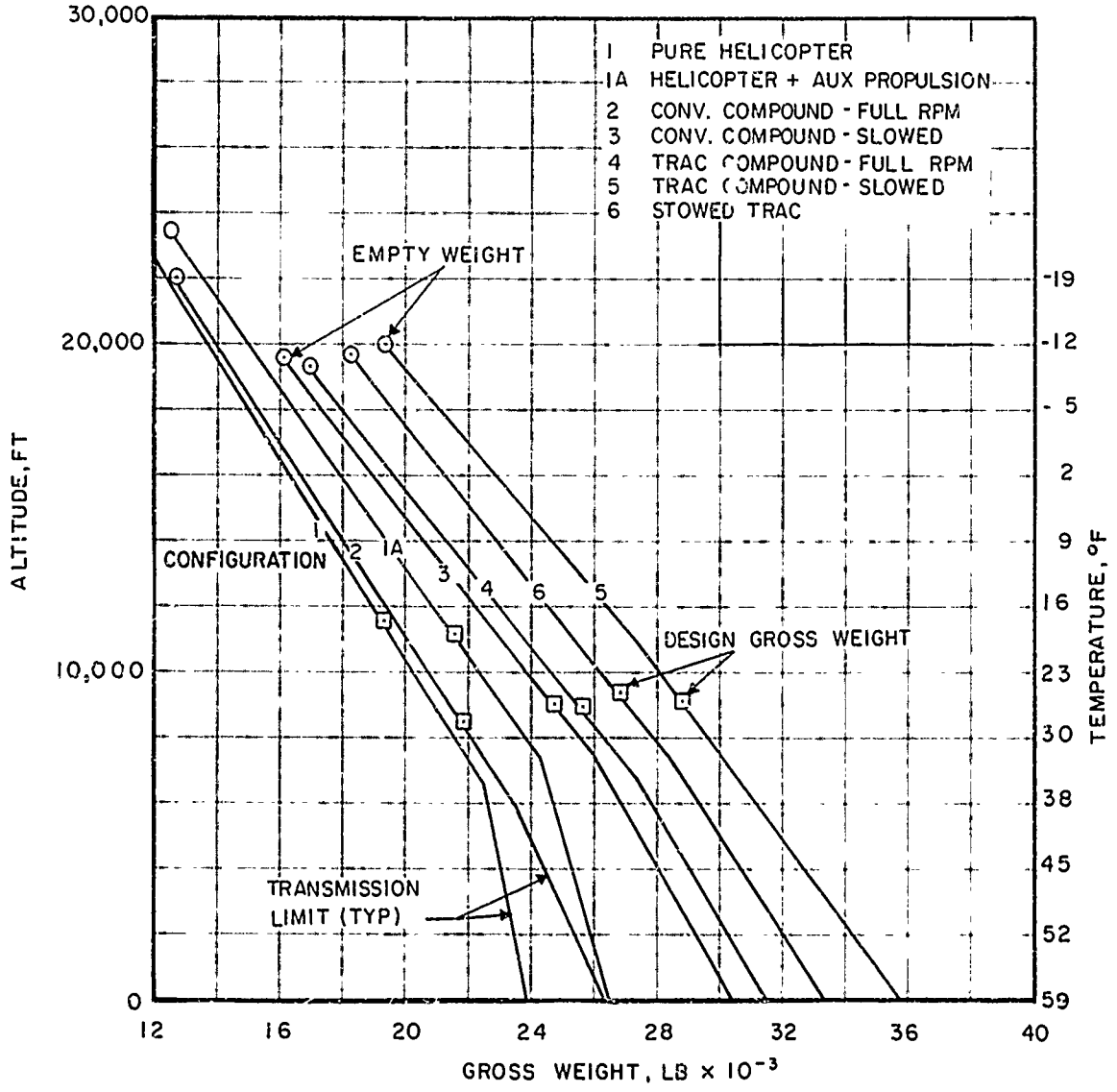

(a) Standard Day

Figure 63. Effect of Altitude on Out-of-Ground Effect Hover Capability, IRP Engine Rating.

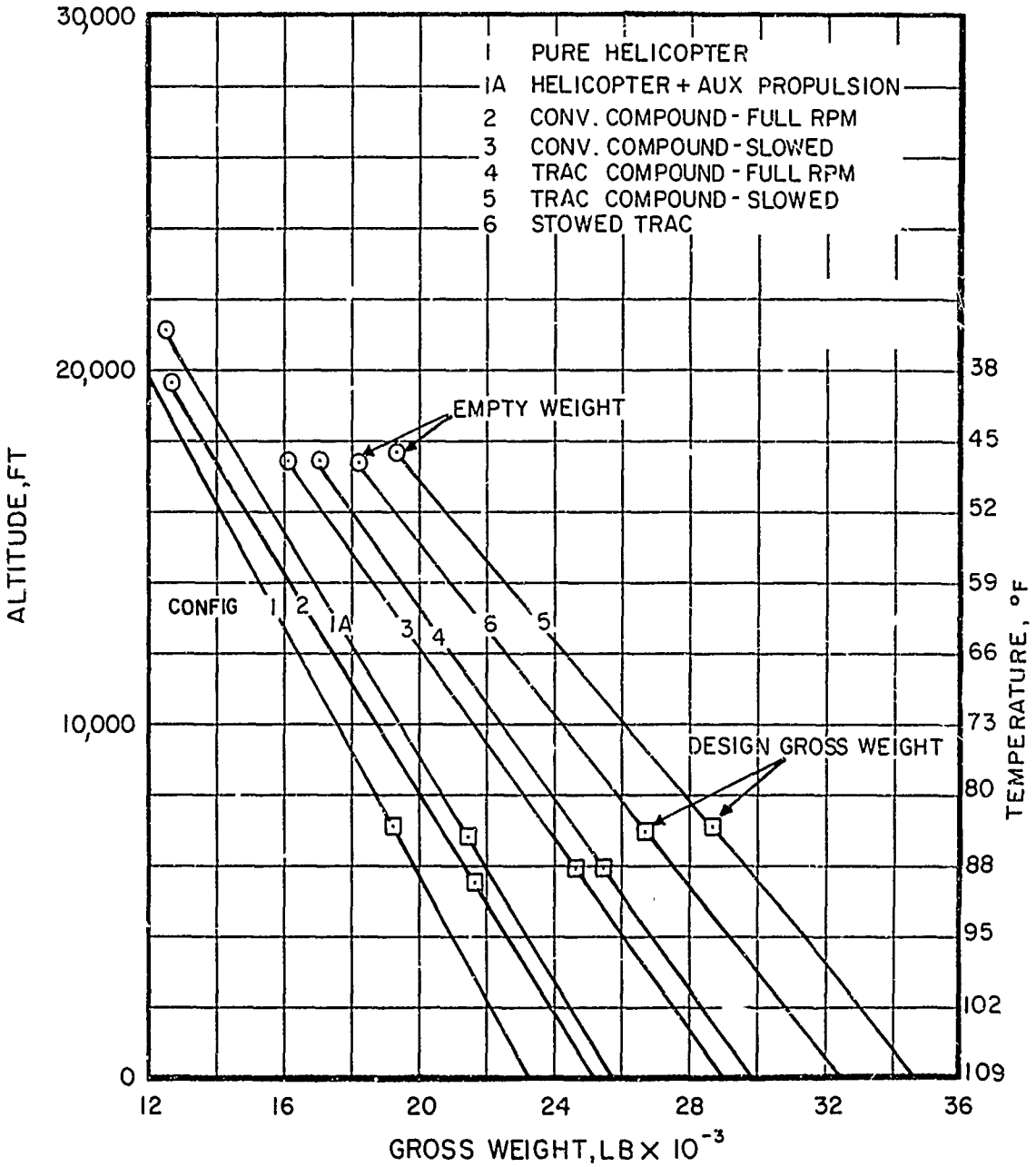

(b) Hot Day

Figure 63. Concluded.

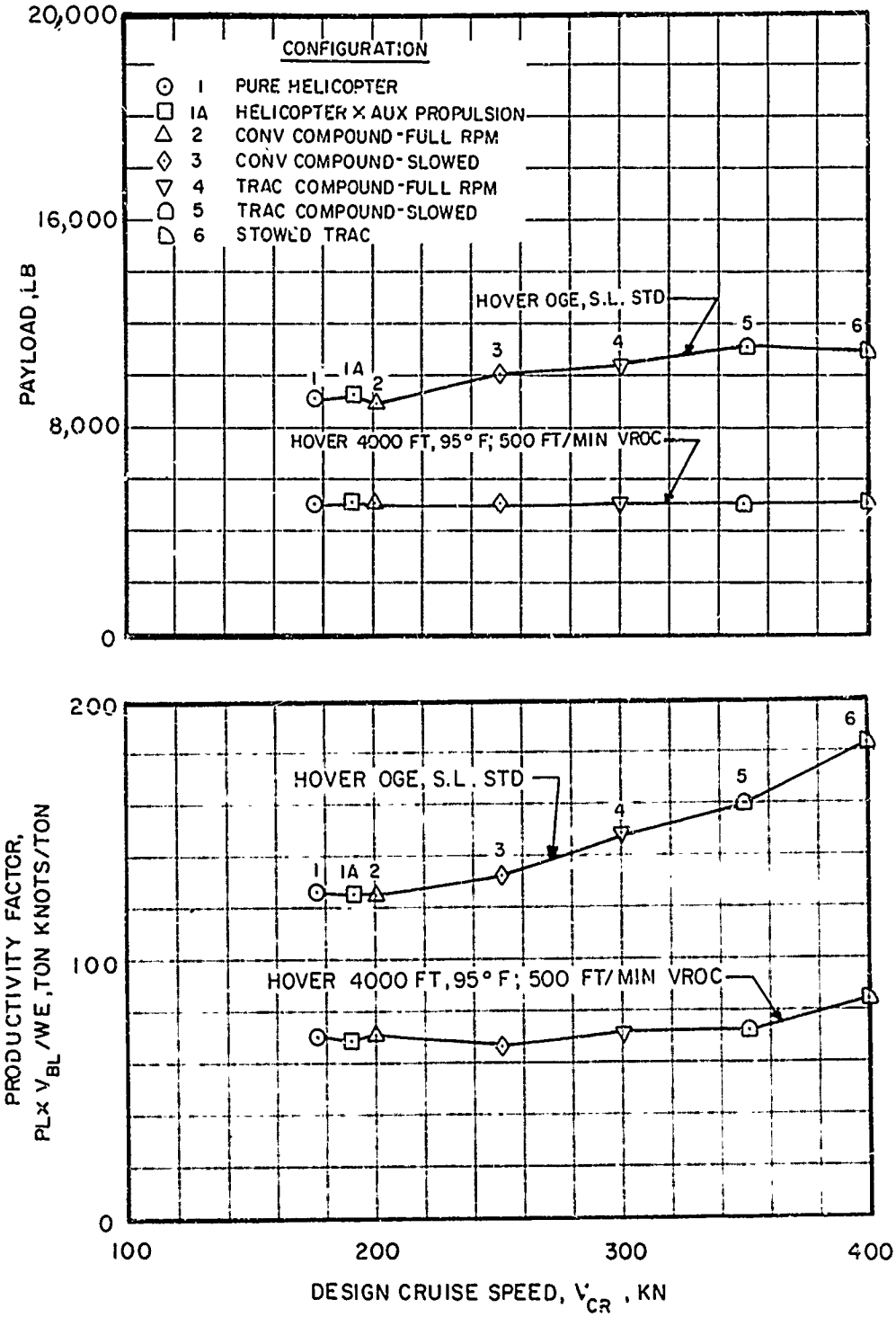

Figure 64. Effect of Hover Requirements on Payload and Productivity for 350 N.M. Range.

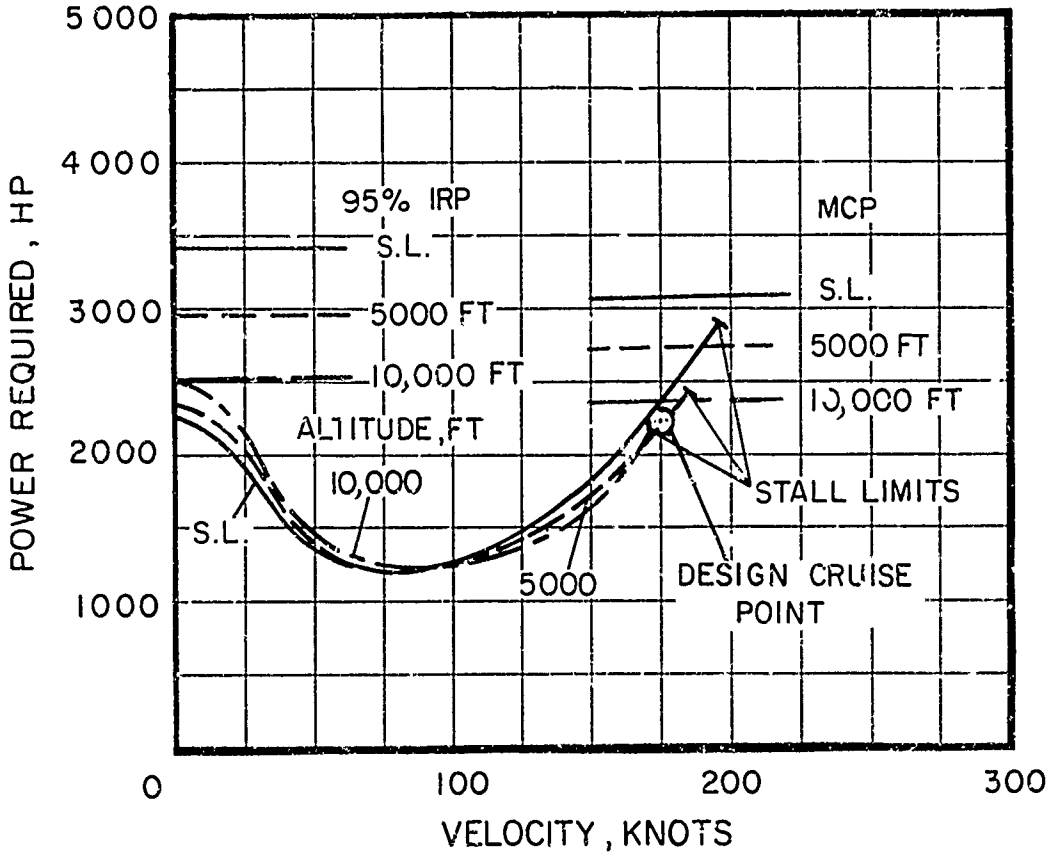

(a) Configuration 1, 175-Knot Pure Helicopter

Figure 65. Power Required Versus Forward Speed.

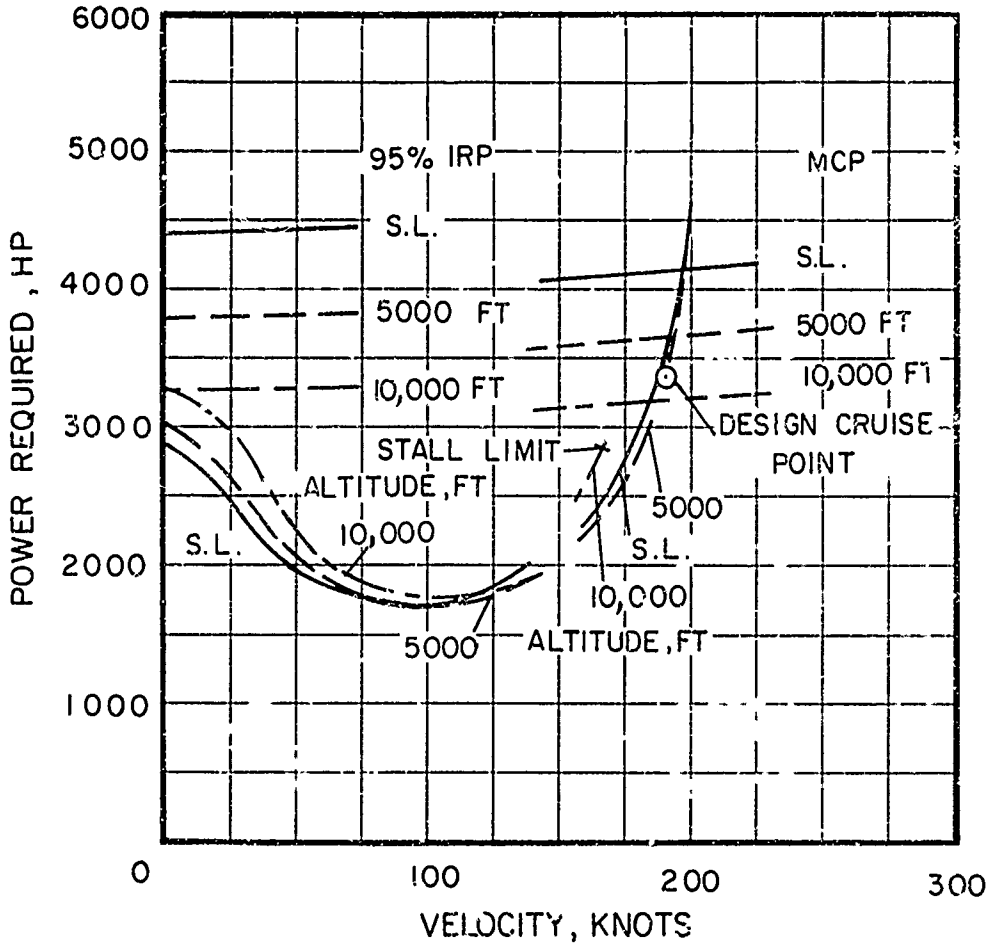

(b) Configuration 1A, 190-Knot Helicopter Plus Auxiliary Propulsion

Figure 65. Continued.

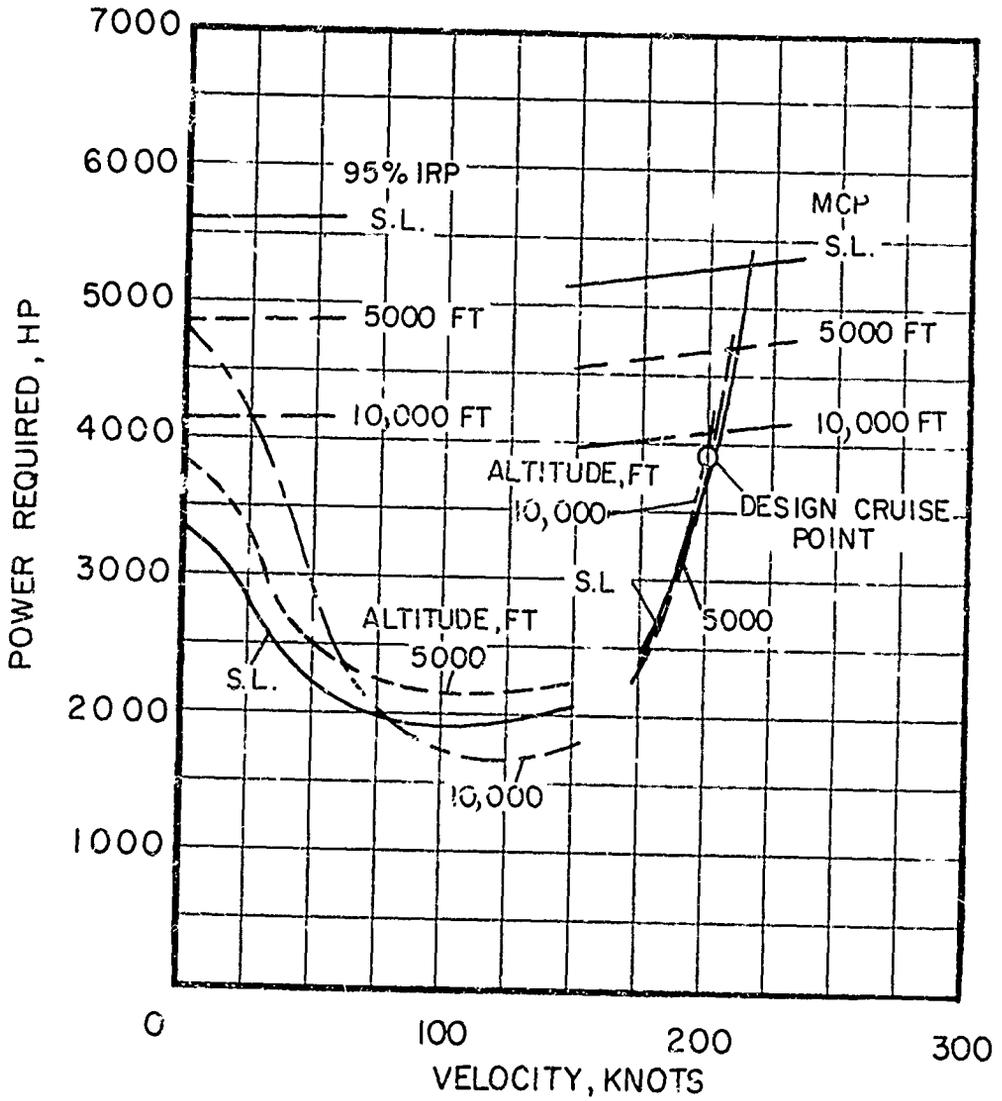

(c) Configuration 2, 200-Knot Full RPM Conventional Rotor Compound

Figure 65. Continued.

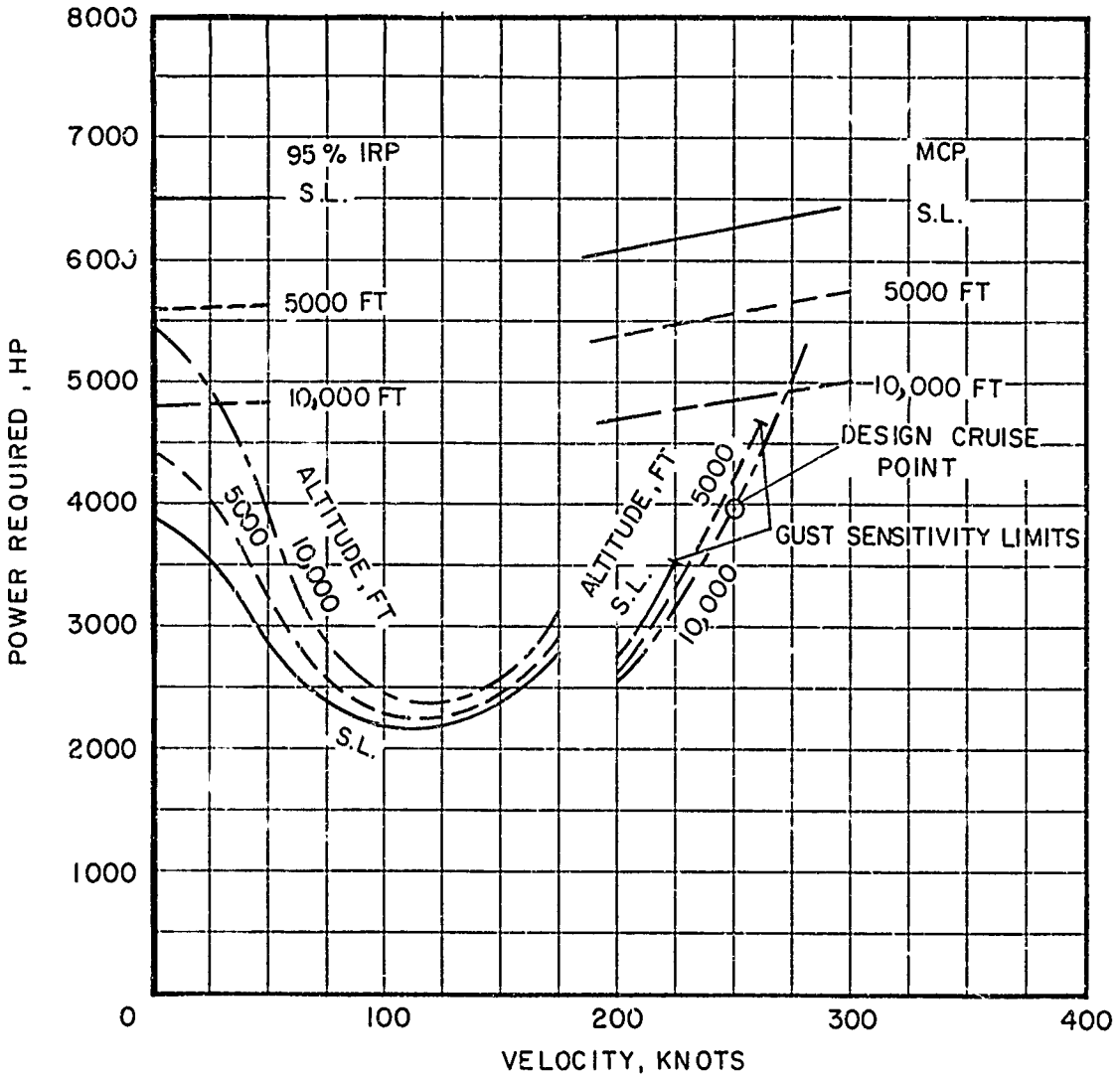

(d) Configuration 3, 250-Knot Slowed Conventional Rotor Compound

Figure 65. Continued.

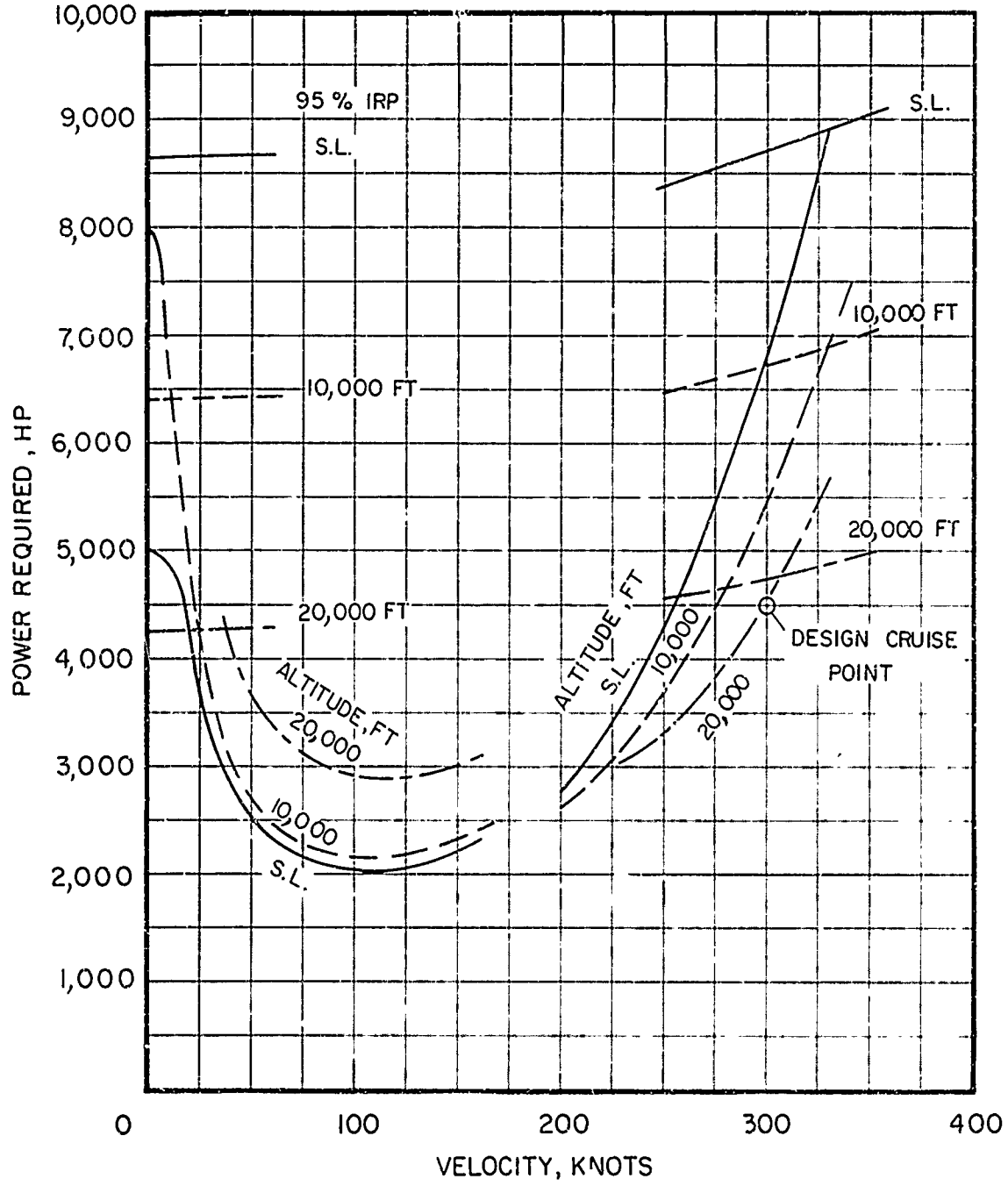

(e) Configuration 4, 300-Knot Full RPM TRAC Rotor Compound

Figure 65. Continued.

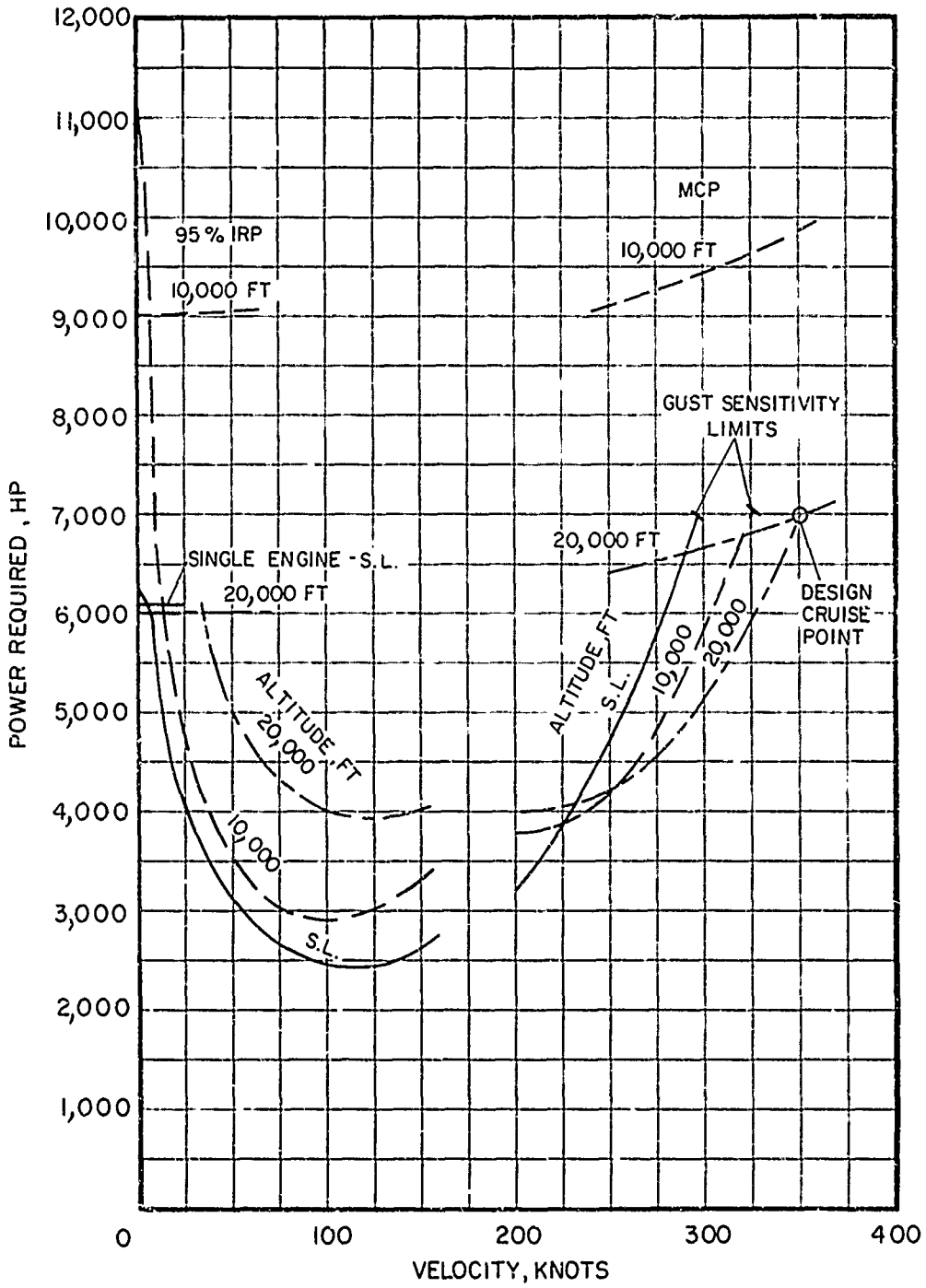

(f) Configuration 5, 350-Knot Slowed TRAC Rotor Compound

Figure 65. Continued.

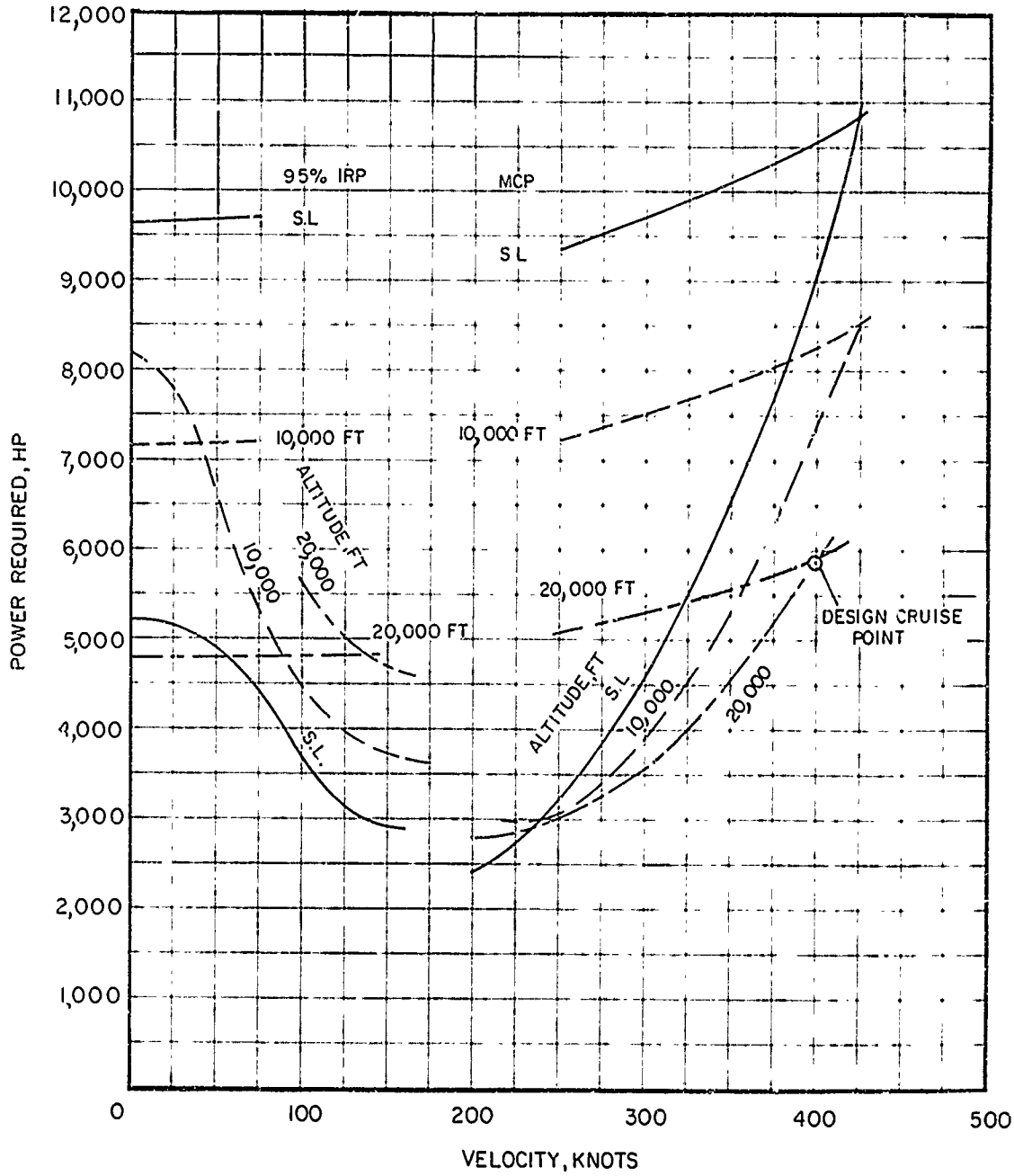

(g) Configuration 6, 400-Knot Stowed TRAC Rotor

Figure 65. Concluded.

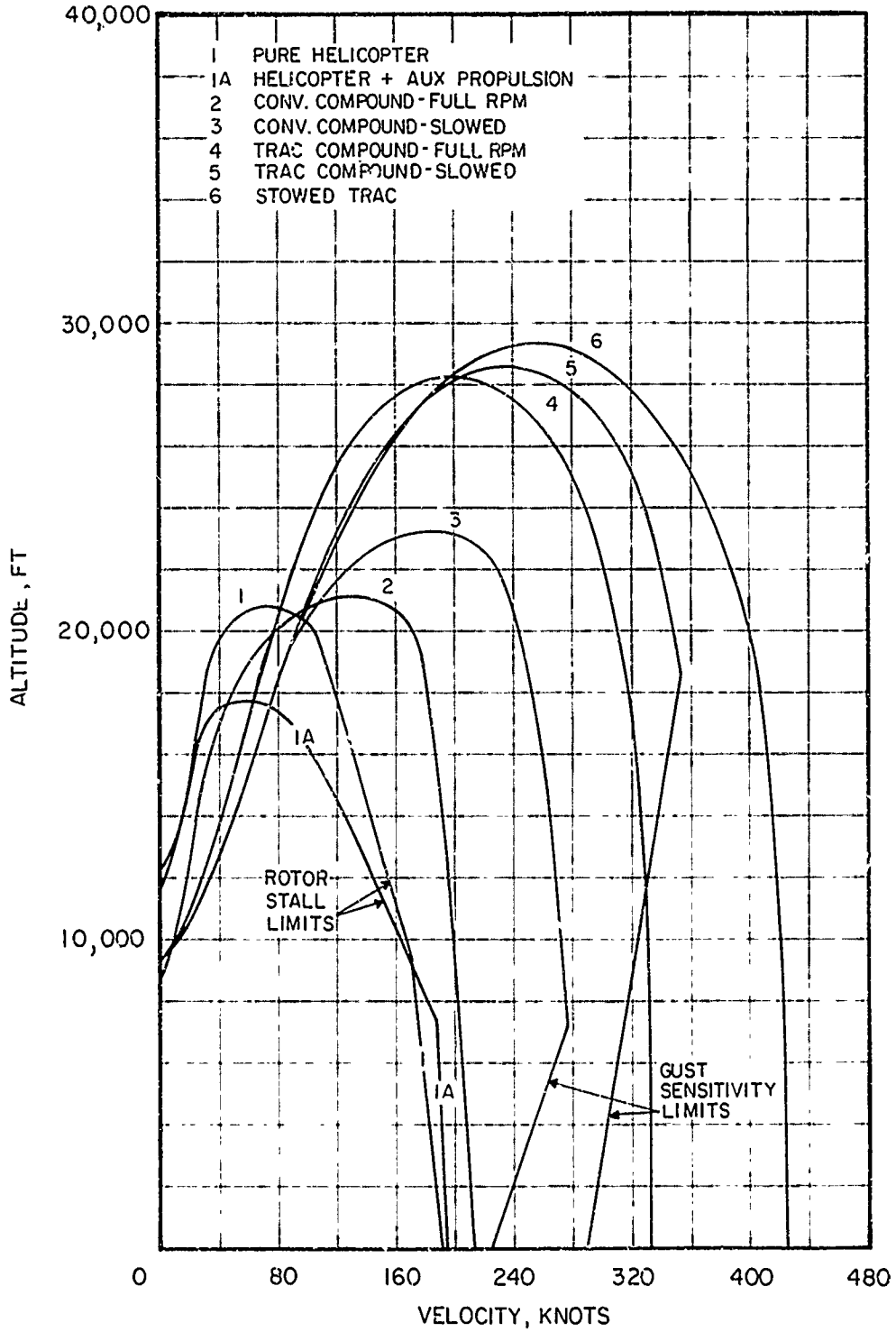

(a) Standard Day

Figure 66. Airspeed/Altitude Flight Envelopes at Design Gross Weight.

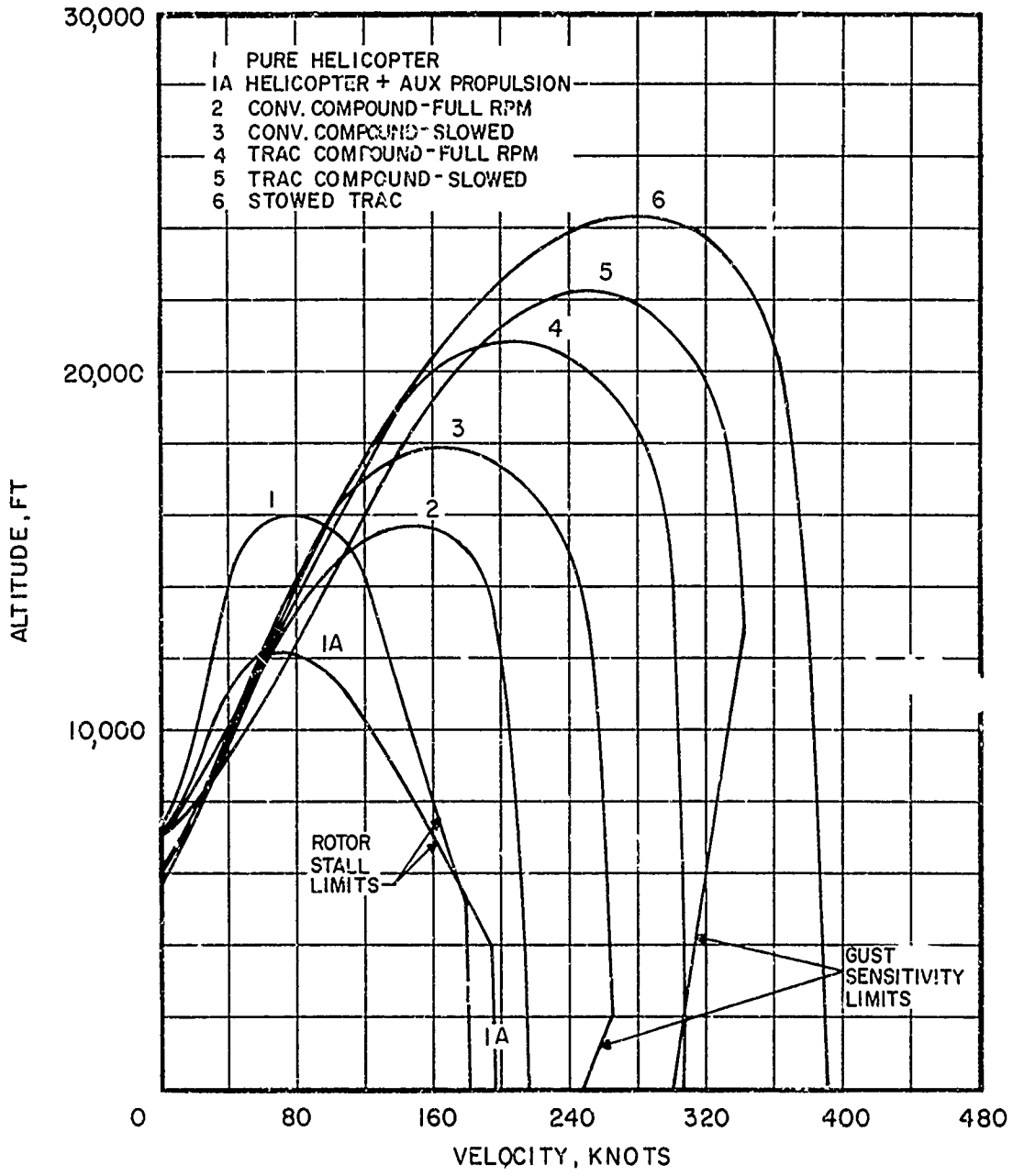

(b) Hot Day

Figure 66. Concluded.

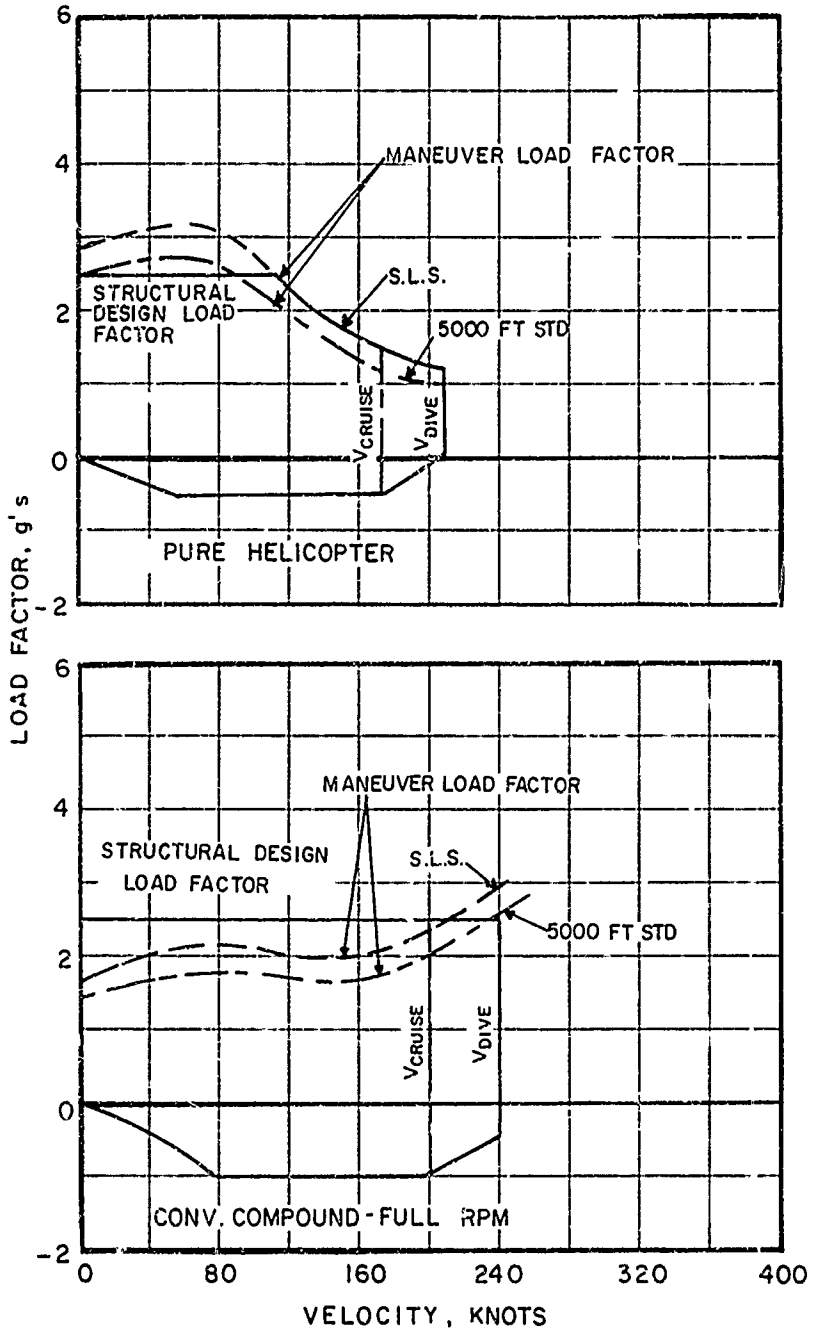

(a) Pure Helicopter and Conventional Compound - Full RPM

Figure 67. Speed/Load Factor Diagrams.

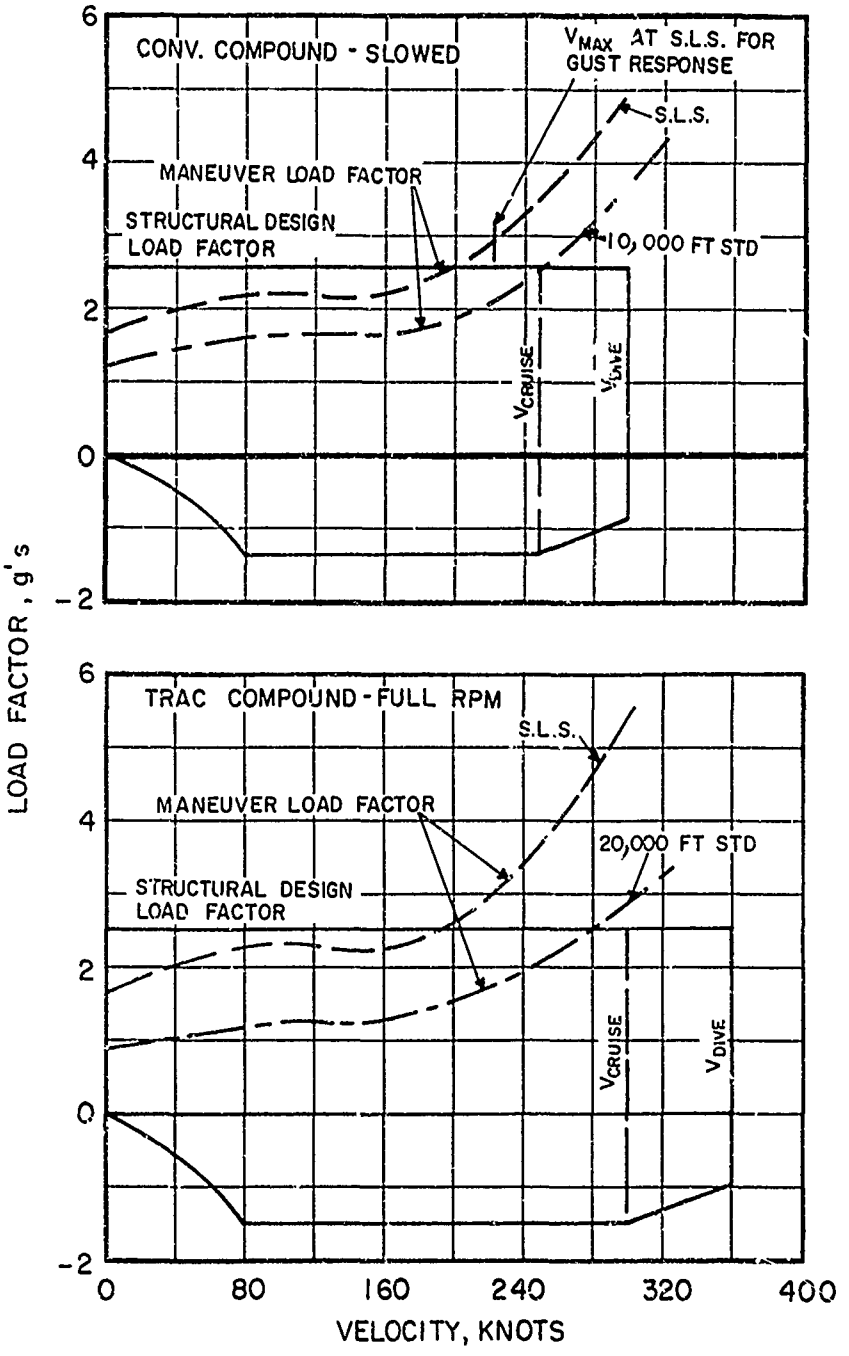

(b) Conventional Compound - Slowed, and TRAC Compound - Full RPM

Figure 67. Continued.

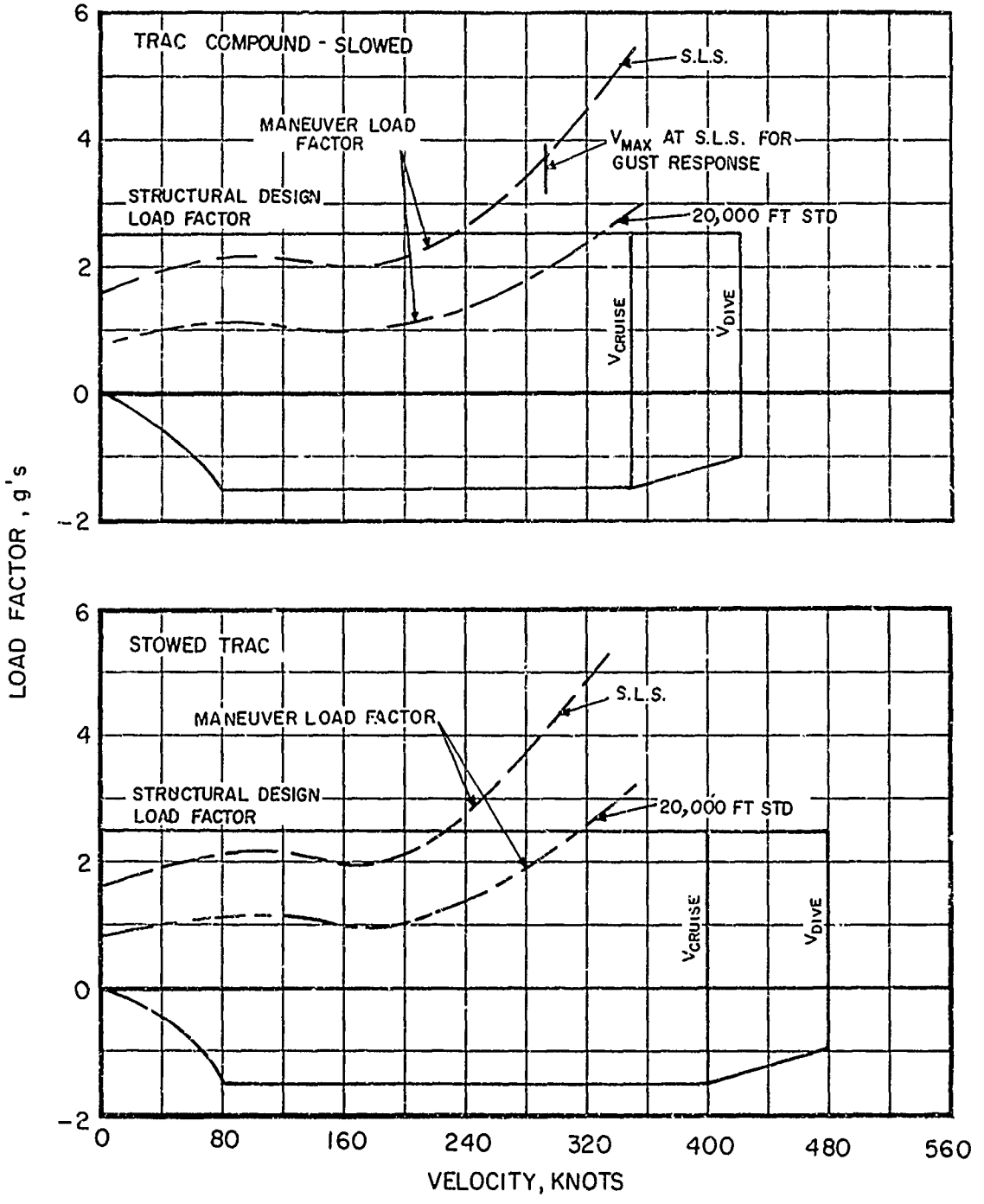

(c) TRAC Compound - Slowed, and Stowed TRAC

Figure 67. Concluded.

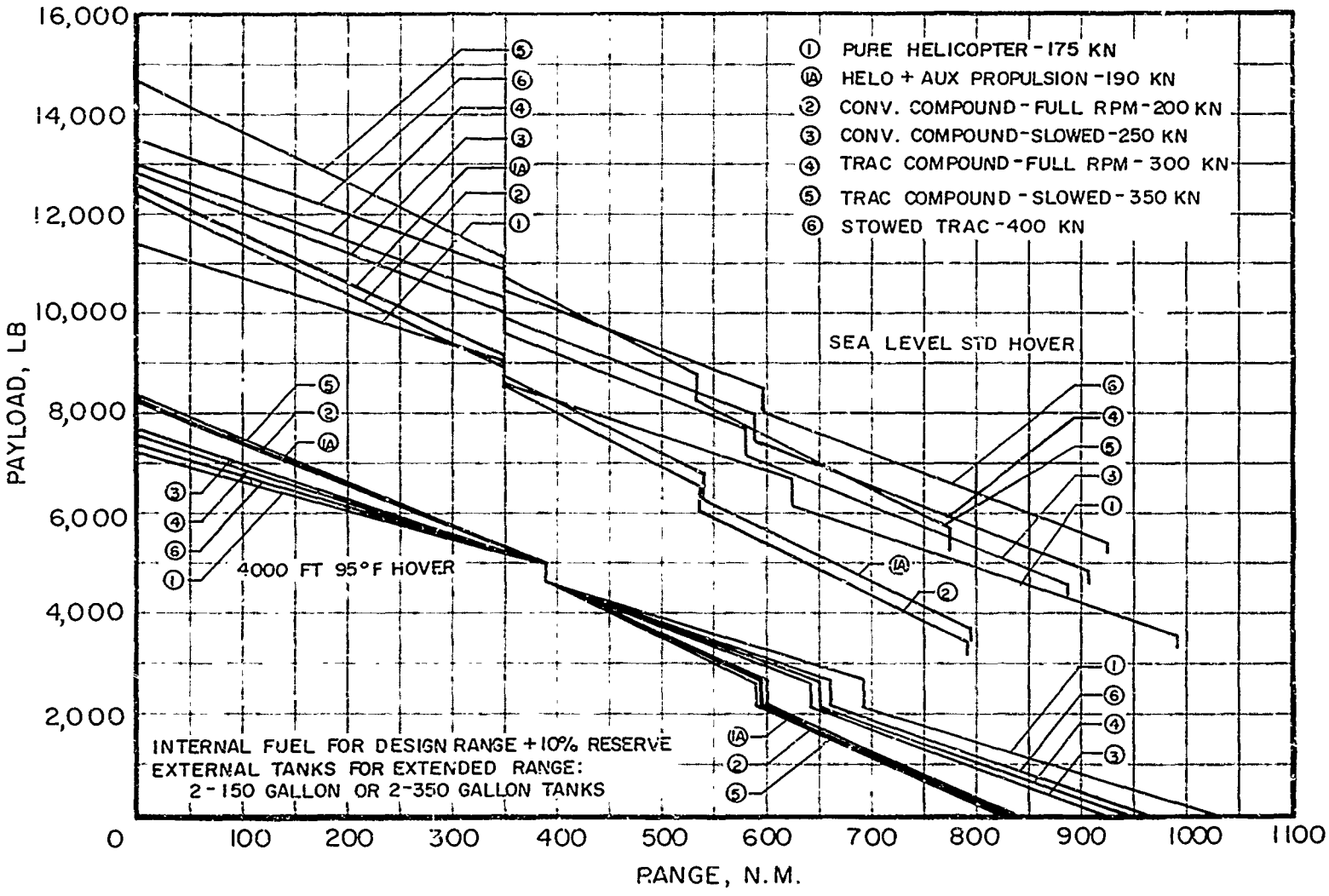

Figure 68. Payload/Range Characteristics at Design Speed and Altitude.

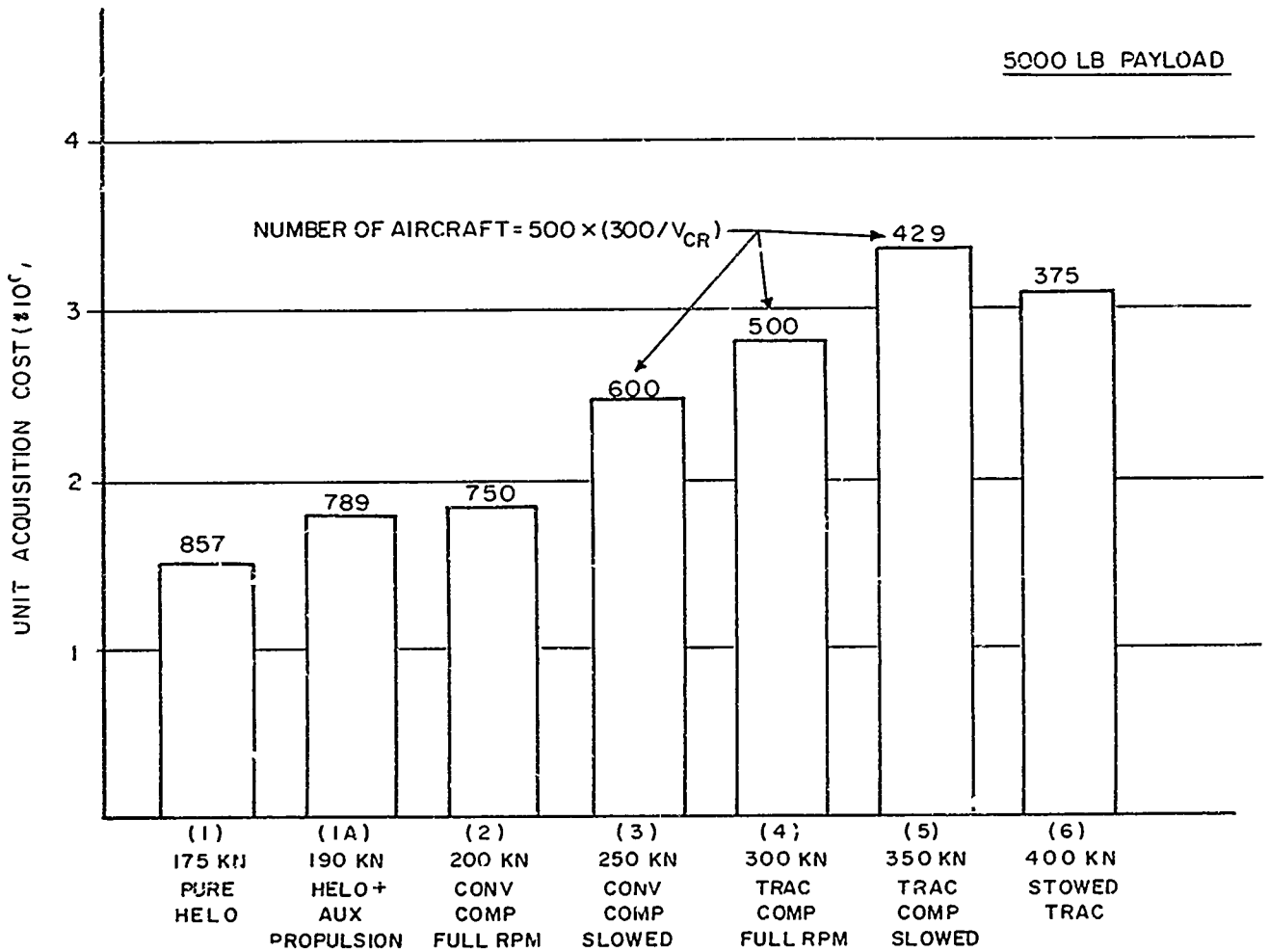

Figure 69. Aircraft Unit Acquisition Cost.

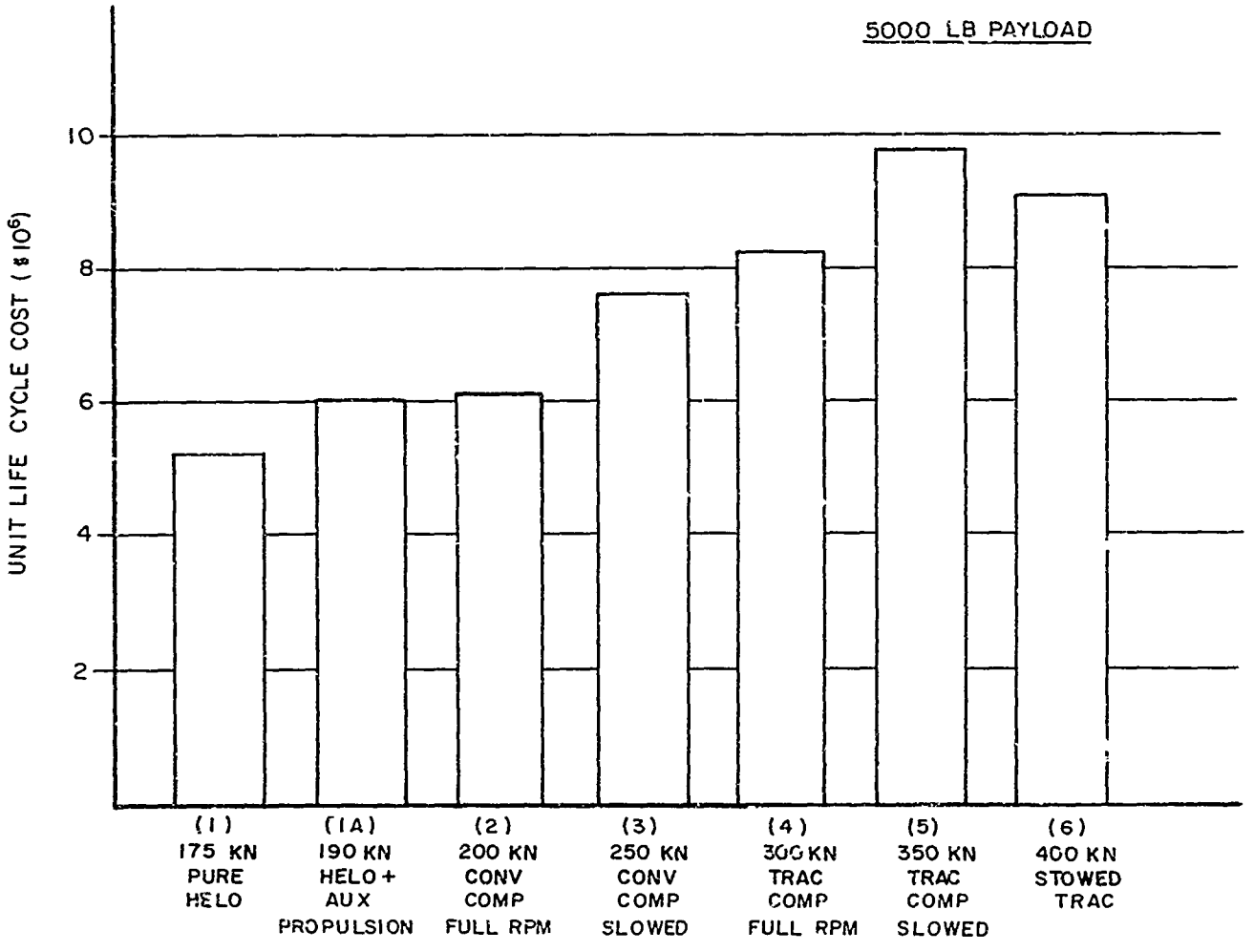

Figure 70. Aircraft Unit Life-Cycle Cost.

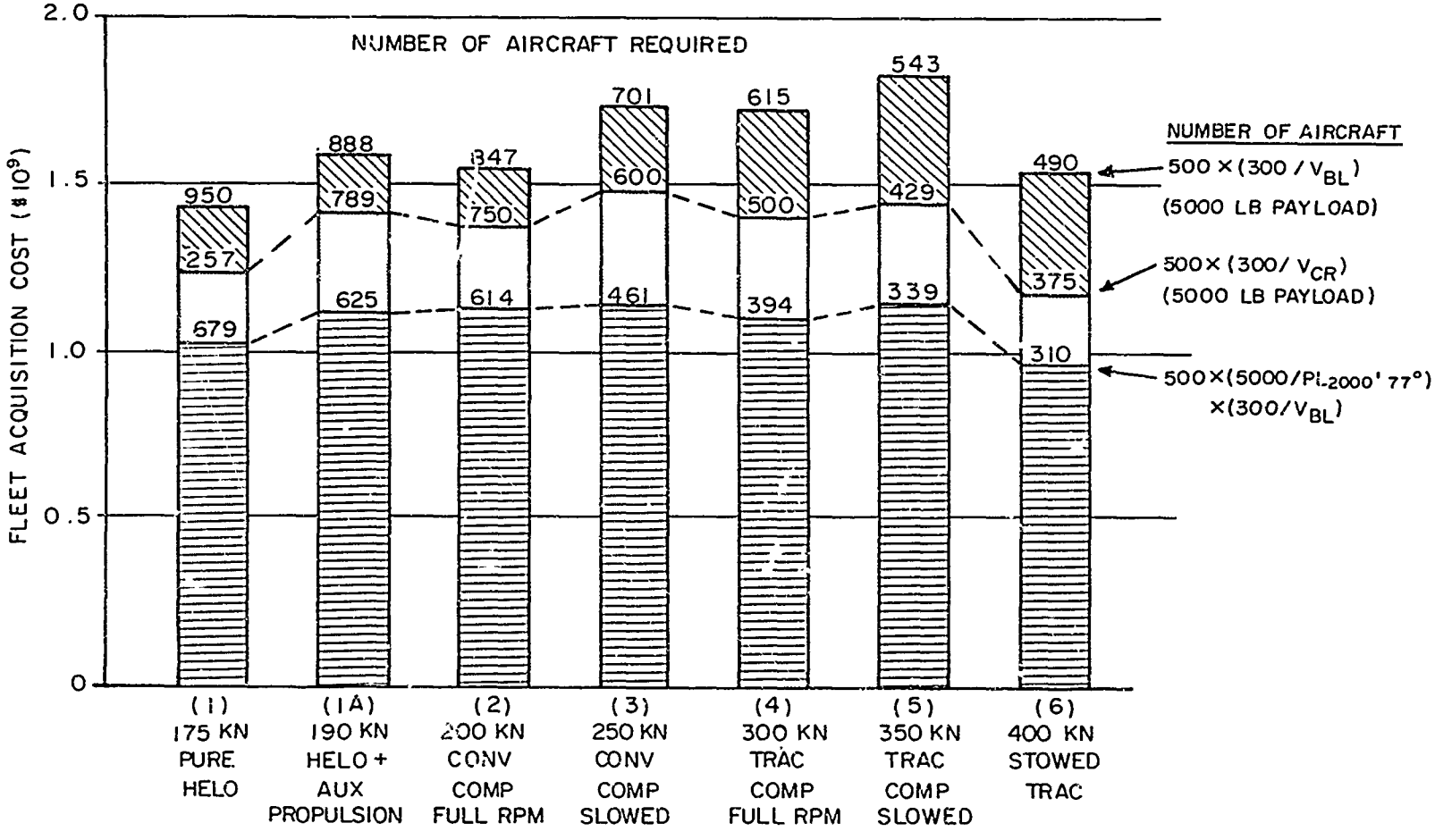

Figure 71. Fleet Acquisition Cost.

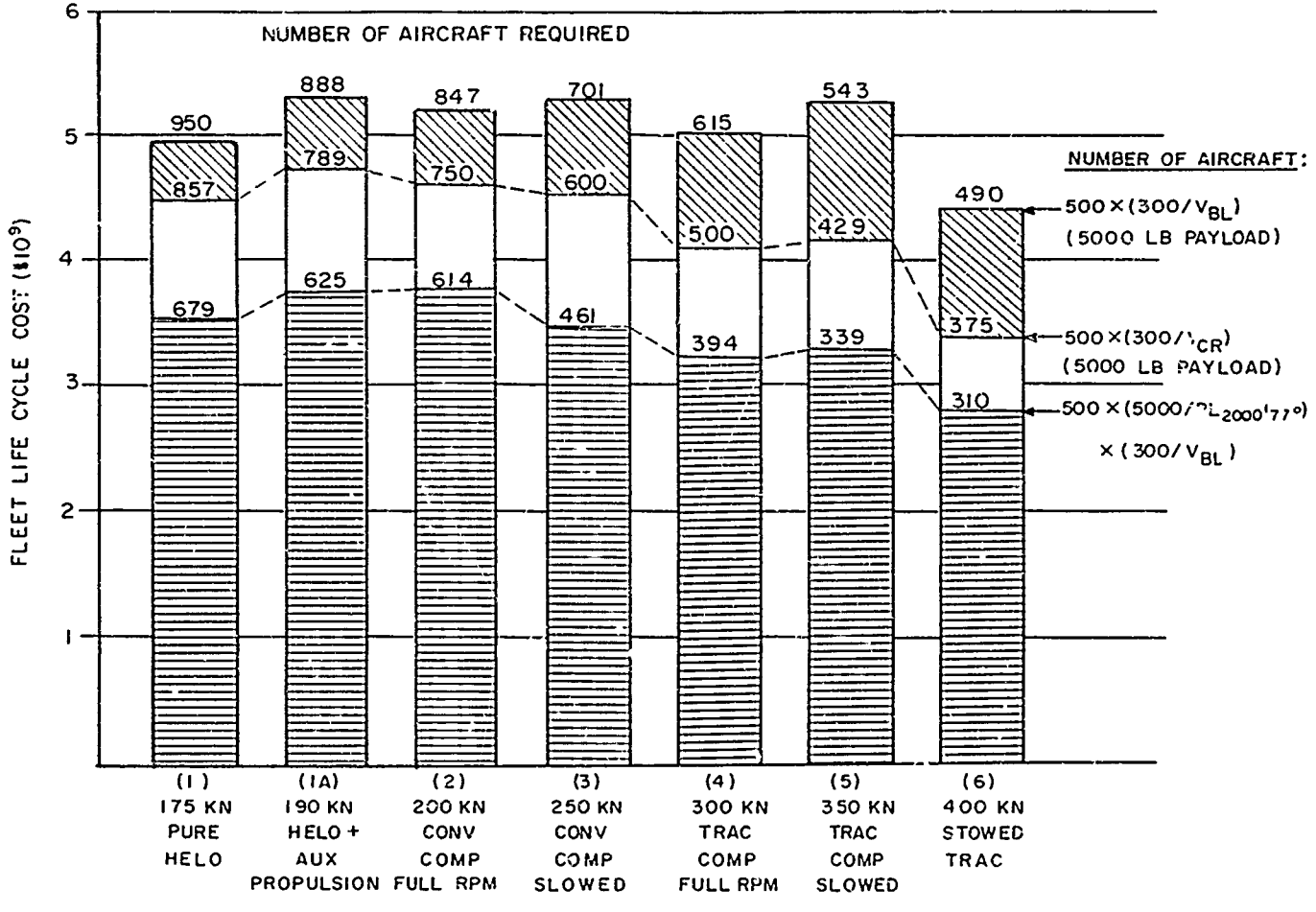

Figure 72. Fleet Life-Cycle Cost.

APPENDIX A

HELICOPTER DESIGN MODEL (HDM)

General Application

Preliminary aircraft design is an iterative procedure involving configuration, weights, performance, and handling qualities. An initial configuration is developed from such design constraints as payload volume, number of crew, number of engines, limit on rotor size, and mission equipment. This configuration is used to generate wetted area and drag estimates for Sikorsky's computerized mathematical helicopter design model, HDM (Reference 12). Other inputs to this program are derived from the system design specifications.

An intrinsic element of the aircraft design cycle (Figure A-1), HDM makes possible rapid trending studies and baseline optimization.

HDM is a digital computer program that specifies, under design constraints, rotor geometry, component weight breakdown, mission analysis, engine and gearbox sizing, speed capability, and estimated costs. These outputs provide the designer with the refinements needed for the next configuration iteration. A closed solution is achieved when consistency exists among the configuration, performance, weights, mission requirements, and system design specifications. Thus, HDM plays an important part in closing the design loop and provides early insight into design sensitivities. Aside from the derivation of the design point aircraft, the extensive trade-off and optimization capability of HDM enables trending away from the baseline configuration, such as was required in this study. The program was modified as necessary to suit the design constraints of this study and to obtain the desired level of detail in weights equations, engines and gearbox sizing criteria, and aerodynamic performance.

Program Operation

HDM has four basic loops, as shown on the flow chart of Figure A-2. The innermost loop, LO, derives the gross weight to achieve the required payload. Alternatively gross weight may be specified, in which case payload is calculated. The calculations within this loop form the nucleus of the program. The remaining three loops enable trending, for a single set of input data, on what are considered the three primary design constraints. These are blade loading C_T/σ (CTSIG), disc loading (DL), and the percent of power (PCTPR) provided at the engine shaft output that will be available for the antitorque device.

CTSIG, DL, and PCTPR can be selected as single inputs or as a required range (initial, final, and incremental values), so that repeated passes are made around the appropriate loop (L1, L2, L3) to create a matrix of design points. For each range of any of these three variables, the interpolated value to produce the optimum aircraft can be selected, based

twist, swept tips, etc. In the case of the TRAC rotor, the effects of the large root cutout were incorporated, based on the existing model test data of root cutout effects.

- Forward Flight

Forward flight rotor performance characteristics in the high-speed (greater than 180-knots) regime were derived from curve data generated by the Sikorsky Generalized Rotor Performance program, similar to that used in the preparation of the performance charts in Reference 8, except that the effects of radial flow are also included for increased accuracy. For compound configurations, it was assumed that rotor lift could be defined by an allowable maximum C_T/σ as related to the advance ratio, as described in Appendix C. The required wing lift was then the difference between the gross weight at that stage of the mission and the rotor lift so derived. By entering wing incidence/C_L/C_D curve data, wing angle of attack and profile drag and induced drag coefficients were determined. The wing area required had previously been established at an earlier stage of the program with the same maximum rotor C_T/σ approach, applied for the critical speed/altitude/temperature condition. With rotor C_T/σ, advance ratio, and tip Mach number known, and tip path plane attitude assumed, the rotor performance curve data were entered to provide rotor power required and inplane drag force. Total propulsive force required was accumulated from parasite drag, wing drag, and rotor drag components.

Performance curves for two classes of propulsive devices are included in HDM. For propellers, maps of propulsive efficiency are represented as functions of thrust coefficient, activity factor, advance ratio, and integrated lift coefficient (Reference 13). For fans, thrust/SHP ratios are calculated as functions of fan pressure ratio and flight speed. Total engine shaft horsepower required is computed as the sum of rotor power, thrust power, tail rotor/fan power, and accessory power, as affected by the mechanical inefficiencies of the drive system.

At low flight speeds (less than 180-knots), the Sikorsky Non-Dimensional Rotor Performance (NDRP) semi-empirical method was used. The analysis is based on an energy approach, modified to account for blade interference, Reynolds number, Mach number, and skewed flow effects.

- Engines

Shaft engine performance input data consist of the sea level standard SFC vs horsepower curve, and specifications of static maximum continuous, intermediate and takeoff power ratings at three altitudes and temperatures. At any general altitude and temperature, the quantity $SHP/\delta\sqrt{\theta}$ is computed, where δ is the ambient pressure ratio and θ is the absolute temperature ratio to sea level standard values. The input SFC curve is entered at this adjusted SHP value. The engine ratings are interpolated. In forward flight, engine ratings are boosted by the supercharging benefits of ram air, and SFC is reduced. These two effects are expressed by empirically-derived equations from existing engine data. In this study, a rubberized PLT-27 engine was used as the basis for fuel flow calculations.

Once the engine scale factor had been determined for the critical performance criterion, the baseline engine SFC vs horsepower curve was adjusted proportionately, so that the SFC computed subsequently was constant for a given fraction of intermediate power, regardless of required engine size.

- Cost Model

Life-cycle cost (LCC) of a military helicopter is the summation of the costs of development, prototype fabrication, production, ground support equipment, crew training, maintenance, spares, and fuel. Development and production costs are statistically trended from existing hardware, as a function of component weights already calculated. The effect of production volume on component costs (dollars per pound) is accounted by a standard learning curve technique. Prototype costs are derived from the production costs by means of the learning curve adjustment for the relatively very small number produced. Operational costs are computed mainly from published Army statistical data, Reference 14, and given operational characteristics such as utilization (flight hours per year), service life, and number of crew and maintenance personnel. An adjusted life-cycle cost was also computed on the assumption that the actual number of aircraft required was inversely proportional to the cruise speed and payload capacity, i.e., the total ton-nautical miles of work in a given time was constant. Productivity is also computed, defined as payload x block speed ÷ weight empty. Block speed was computed on the assumptions that warm-up, takeoff, and landing times were accountable towards trip time, and that climb (at 66% of cruise speed) and descent (at 90% to 93.5% of cruise speed) were accountable towards distance travelled.

A flow chart of the LCC subroutine is shown in Figure A-3. Algebraic representation of the components of each facet of life-cycle cost is discussed in the following paragraphs.

Development Cost (CDEV)

$$CDEV = [6.5 \times CFDEV \times (WE/1000)^{.8} + DCON] \times 10^6$$

Where: CFDEV = Complexity factor
WE = Weight Empty
DCON = 15.0

Prototype Cost (CPROTO) (Per Production Aircraft)

$$CPROTO = \left(\frac{QPROTO}{PBASE}\right)^{ACLF} \times CFLY \times \left(\frac{QPROTO}{PRDRUN}\right)$$

Where: QPROTO = Quantity of Prototypes
PBASE = Base Production Quantity
CFLY = Unit Flyaway Cost (See below)
PRDRUN = Production Quantity

$$ACLF = \log_{10}(ACLR)/\log_{10} 2$$

on minimum gross weight, or minimum cost.

Engine size and transmission rating can be selected from one of the following options:

1. Specified engine
2. Sufficient for the design hover point
3. Sufficient for an alternate hover point
4. Sufficient for the design cruise point
5. Greater of 2 and 3
6. Greatest of 2, 3, and 4.

In this study, the design hover requirement sized the helicopter powerplant. For the high-speed compound helicopter and TRAC configurations, the selected cruise speed, in most cases, was critical in sizing the powerplant, whereas the hover requirements sized the main gearbox.

The mission analysis routine provides sufficient flexibility for division of a mission into discrete elements at the required altitudes, temperatures, and speeds. The mission profile can contain as many as 50 segments, or many missions can be stacked to a total of 50 segments to be processed sequentially. Speed can be specified in knots, or coded as speed required to produce maximum range, maximum endurance, rotor drag divergence threshhold, or speed required to match a gearbox design power or some engine rating. Proper account is taken of fuel burn-off and the loading or offloading of passengers or cargo.

Component weights are evaluated by a set of statistical weight equations, modified to suit a specific aircraft type. Rotor group weight estimates account for blade aspect ratio, design dive speed, and hinge offset effects. The drive system is divided into individual shaft lengths and gearboxes, and weight estimates reflect the transmitted horsepower and rotational speeds of each component. Parametric weight trending equations for the TRAC rotor and stowing mechanism were developed and added to the weight subroutine, as described in Appendix IV.

Performance Methodology

- Hover

The helicopter design model utilizes the Figure of Merit Ratio (FMR) method for calculating hover performance. This semiempirical method, based on extensive hover test data, has proved to be particularly reliable at high rotor loading conditions (high C_T/σ), for which many theoretical methods give optimistic results. The FMR method can be corrected to account for special rotor physical characteristics such as nonlinear

ACLR = Learning Curve (.85)

Acquisition Cost (CACQ)

CACQ = CFLY + CGSE + CITR + CISP

Where: CGSE = Ground Support Equipment Cost
= CFLY x PCTGSE
CITR = Initial Training and Travel Cost
= (# Flight Crew Officers and Enlisted Men)
x (Respective Salaries)
CISP = Initial Spares Cost
CSTRPR = Airframe and Dynamic System Cost
CENG = Engine Cost per Aircraft
CAVI = Avionics Cost per Aircraft

Total Maintenance Enlisted Manpower Requirement

$$= (2.3178 + .000665 \times WE) \times 1.4 \times \left(\frac{UTIL}{2700}\right) \times OMHFH$$

UTIL = Annual Utilization (flt. hours/year)
OMHFH = Maintenance Burden Factor

Officer Manpower = .04 x Enlisted Manpower

CFLY = Σ (Component Weights) x (Component $/lb)
+ Engine Cost + Avionics Cost + Auxiliary Propulsion Cost

$$\text{Component \$/lb} = (\$/lb)_{PBASE} \times \left(\frac{PRDRUN}{PBASE}\right)^{ACLF}$$

$$\text{Engine Cost} = 190 \times ENG \times SHP^{.8}$$

ENG = # Engines

SHP = Installed horsepower, each engine

Auxiliary Propulsion Cost:

Propellers: CAUXP = 5600 x Propeller Diameter x (# Propellers)

Prop-Fans:

$$CAUXP = \frac{45.58 \times (\text{Design hp})^{.134}}{(\text{Pressure Ratio} - 1)^{.076}} \times \left(\frac{\#\text{ Propulsors} \times \#\text{ Aircraft}}{500}\right)^{ACLF} \times 1000 \times (\#\text{ Propulsors})$$

Operating Cost (COP)

COP = CREPL + CFC + CFUEL + CM + CRTR + CGSEM

Where:

CREPL = Replenishment Spares Cost

= (7.251 + .0073 x WE) x UTIL x SVLIFE x 1.276

SVLIFE = Service Life (years)

CFC = Flight Crew Cost

= (# Officers and Enlisted Men) x (Respective Salaries) x SVLIFE

CFUEL = Fuel Cost

$$= \frac{\text{Consumed Fuel per Mission}}{\text{Mission Time}} \times \text{UTIL} \times \text{SVLIFE} \times (\$/\text{gallon})$$

CM = CMORG + CMDEP

CMORG = Organizational Maintenance Cost

= (# Enlisted Men and Officers) x Respective Salaries x SVLIFE

CMDEP = Depot Maintenance Cost

= (.1569 + .000263 x WE) x 13.5 x UTIL x SVLIFE

CRTR = Recurring Training and Travel Cost

= [(# Enlisted Crew + # Enlisted Maintenance) x .35 x 2540 +
(# Officers Crew + # Officers Maintenance x .15 x 41580] x SVLIFE

CGSEM = Ground Support Equipment Maintenance Cost

= .03 x CM.

Life Cycle Cost (LCC)

LCC = CDEV + CPROTO + CACQ + COP

Fleet Life Cycle Cost = LCC x PRDRUN.

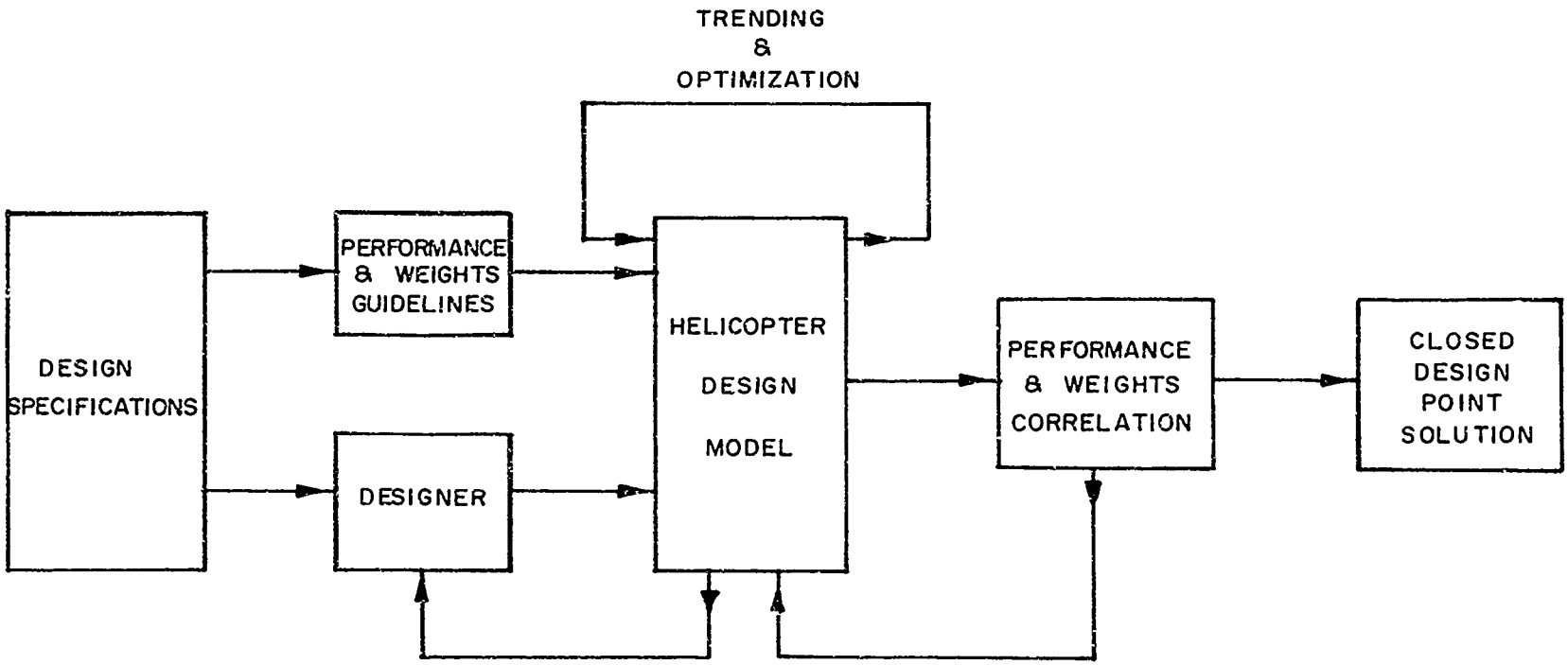

Figure A-1. Helicopter Design Model - Functional Concept.

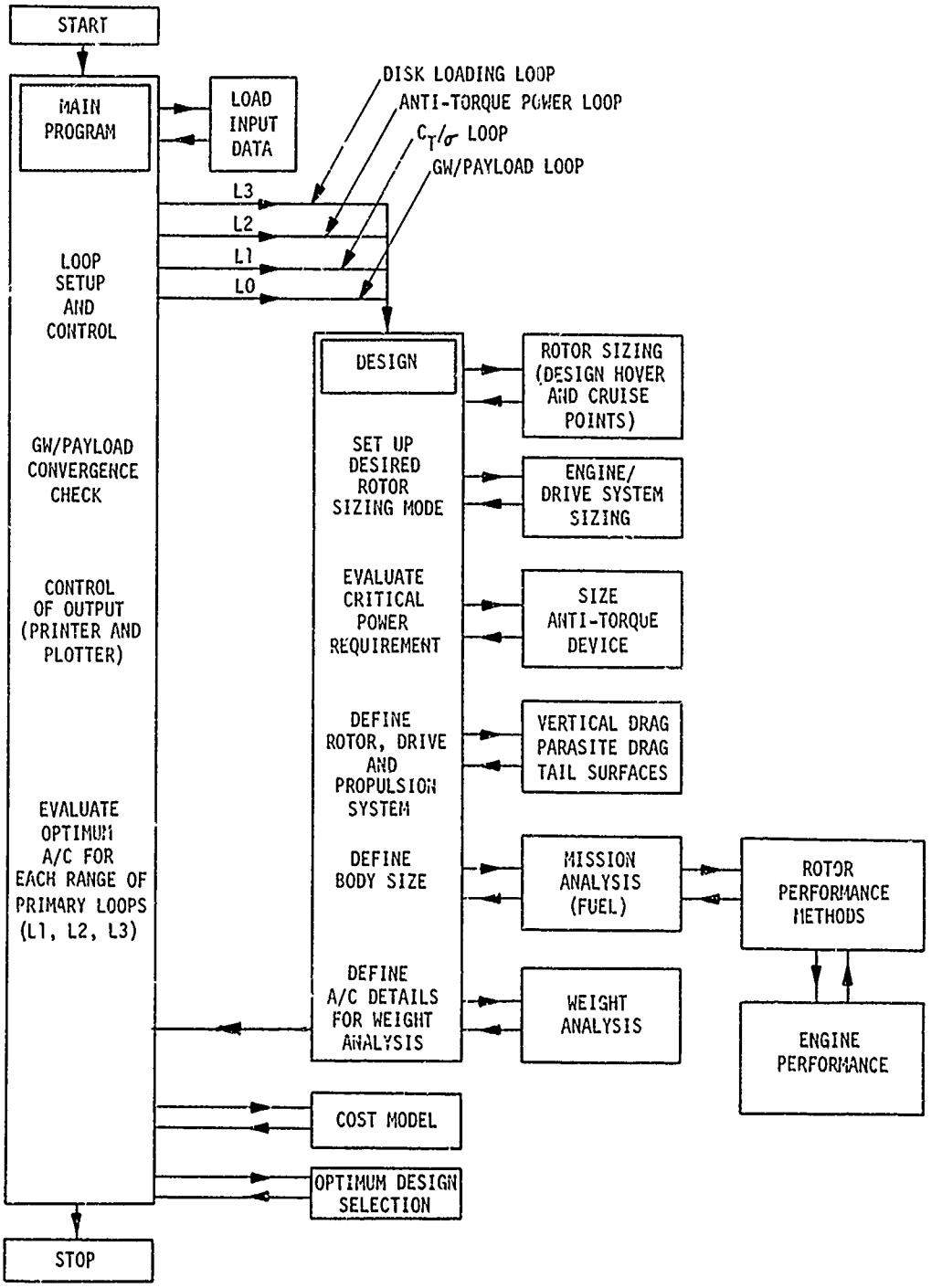

Figure A-2. HDM Flow Diagram.

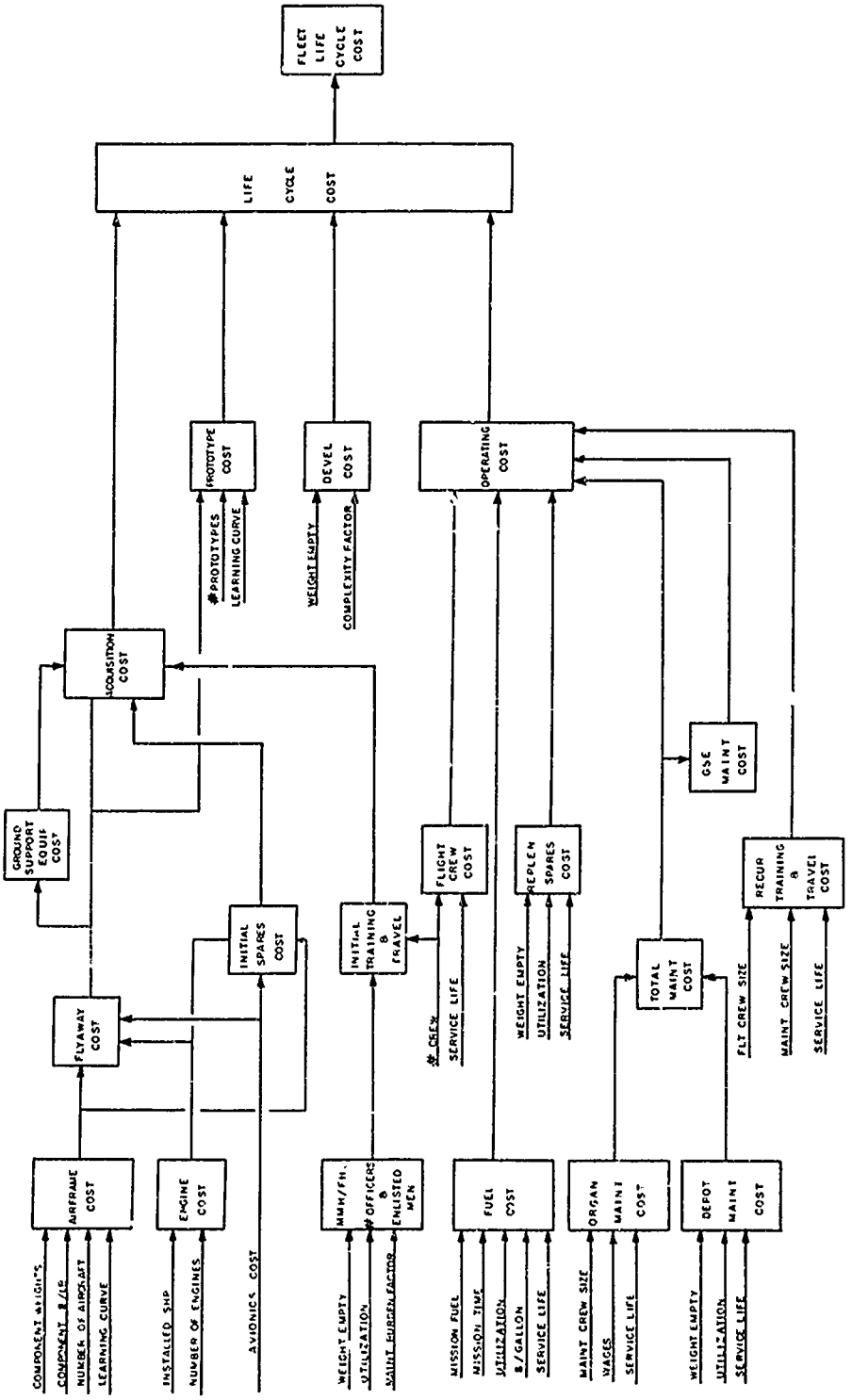

Figure A-3. Life-Cycle Cost Model.

APPENDIX B

GENERAL SPECIFICATIONS

In order to provide consistent ground rules for the parametric mission studies, a set of general specifications was established. These specifications, which influenced the studies through the mechanism of weight trending equations, fuel consumption rates, etc., were intended to be appropriate for typical Army transport mission requirements. Where applicable, UTTAS design technology was assumed, e.g., ballistic tolerance and crashworthiness requirements.

PHYSICAL CHARACTERISTICS

Rotor System

Main Rotor - Single rotor, fully articulated. Disc loading not more than 15 psf. Manual folding (power blade folding for stowed rotor configuration).

Tail Rotor - Conventional tail rotor or fan-in-fin as appropriate.

Body Group

Two crew, side-by-side. Fifth through ninety-fifth percentile aviator accommodation. Visibility per MIL-STD-850, paragraph 8. Individual ingress and egress. Cabin with load-carrying floor; access through side doors only. Mission usable cabin volume 100 ft^3 per thousand pounds of payload.

Design load factors (limit): + 2.5, - 0.5 g

Landing Gear

Wheeled main gear. Auxiliary gear either nose or tail wheel. Brakes and parking brake provided. Safe rate of sink 10 fps. Fully retractable.

Propulsion

General: Fire warning and extinguishing systems. Self-starting from -12° F to 120° F. Engine air particle separator; no IR suppression requirements. Engine anti-ice for continuous operation in moderate icing.

Engine Technology: T-700/PLT 27 level as projected for 1980 time frame.

Size: Rubberized.

Number of engines: Two.

Auxiliary propulsion: Propellers or prop-fans as appropriate.

Fuel System

Crashworthy. Gravity, pressure, and closed circuit refueling. 20% of total capacity sealed against 12.7mm, remainder 7.62mm. JP4, JP5 fuels.

Auxiliary Power Unit

Required for self-starting, ground checkout, and other functions as desired.

Flight Controls

Dual cockpit controls. Redundant controls from cockpit to power operated flight controls (including fixed wing controls and TRAC diameter control). SAS and FAS or full AFCS. No fly-by-wire for primary flight controls.

Power boost: Dual hydraulic system plus separate utility system.

Drive System

Rotor brake. Main gearbox (MGB) capable of operating 30 minutes at cruise power after sustaining a single 7.62mm hit. MGB rating 1.2 times HOGE power required at 4000 ft 95° F. Each input rated at max. engine power that may be transmitted in case of one engine failure.

TGB, IGB: grease lubricated.

Instruments

Basic and IFR per AR-95-1. Special instrumentation as required for each configuration.

Hydraulics

Per MIL-H-5440.

Electrical

Two independent power sources, each capable of supplying the full load.

Furnishings

Soundproofing, insulation for crew compartment. Two armored crew seats.

Cabin pressurization for cruise above 10,000 ft.

Environmental Systems

Heating and ventilating only for crew compartment and cabin. Windshield anti-ice, defog, defrost, and rain removal.

Anti-icing: wing leading edges and critical rotor system components as appropriate to the configuration, for moderate icing conditions.

PERFORMANCE

Design Mission

8 minutes at idle power (both engines)
2 minutes hover out of ground effect (HOGE)
Cruise (see item below), Range 200 to 500 NM.
2 minutes HOGE
Reserve fuel weight equal to 10% of the fuel weight required for the above listed mission segments.

Fuel Capacity

For design mission. Use 105% SFC.

Performance at Design Gross Weight, 4000 ft 95° F

500 fpm vertical rate of climb at zero wind and not more than 95% Intermediate Rated Power (IRP) (30 minute rating)

Performance at Cruise Altitude

Cruise at design altitude at not more than Max. Continuous Power (MCP). Cruise altitudes 4000 ft 95° F, and from SL to 20,000 ft; standard temperature.

Altitude for Takeoff and Landing

4000 ft 95° F when this condition specified for cruise.

Sea level for standard day operation, independent of cruise altitude.

Climb and Descent

Part of cruise distance. Not more than MCP and not faster than V_{cruise}.

Maximum climb and descent rates 2000 fpm.

Handling Qualities

Generally in compliance with MIL-H-8501A and MIL-F-8785B.

Weights

Payload from 2000 to 10,000 lb.

Design Gross Weight (DGW) is that required for the design mission with the appropriate payload.

Unit weights: Crew member 235 lb.
Fuel - JP-4 at 6.5 lb/gallon
Oil - 7.5 lb/gallon
Hydr. Fluid - 7.0 lb/gallon

Contingency. None for pure helicopter, 1% of weight empty for other configurations.

Technology Status. Compatible with 1980 initial operational capability (IOC).

Vibration

Not to exceed ±.05g in any direction on crew stations and cabin floor in steady cruise or hover.

Noise

Not to exceed 95 dB sideline noise at 500 feet on take-off.

EQUIPMENT

Communications (Commercial type)

Intercom

1 UHF radio

VHF radio: 1 Transmitter
2 Receivers

1 HF radio

KY 28

APX 72

Wiring, antennas, and installation

Navigation

ADF

VOR/ILS

Gyrocompass

Lights

Anti-collision

Position

Landing/Hover Light

APPENDIX C

AERODYNAMIC AND DYNAMIC CRITERIA

Allowable Blade Twist

The assumed values of blade twist are shown in Figure C-1. A high value of twist is generally desirable because of the increased hovering figure of merit it provides; however, the allowable values of blade twist generally decrease with increasing forward speed and advance ratio because of the adverse effects of twist on blade stresses, rotor-induced vibrations in forward flight, and in-plane rotor drag. The values for the conventional rotor configurations are based on previous studies and experience, and the values for the TRAC rotor configurations are based on the present full-scale preliminary design study, with trends assumed similar to those for the conventional rotor. The reduced rpm configurations have lower allowable blade twist values than do the full rpm cases, because of the increased advance ratio for a given forward speed. Although it appears that higher twist values are allowed for the TRAC rotor than for the conventional rotor, it should be noted that the TRAC twist values are the hover or extended values. In high-speed cruise, the actual twist value is only 60 percent of values shown. The twist for the stowed rotor is dependent only on the conversion speed (assumed 150 knots equivalent air speed in this study), and not on design cruise speed.

Allowable Blade Loading

Assumed values of the dimensionless blade loading parameter, $C_{T/\sigma}$, are shown in Figure C-2, along with a few typical flight test data points and some analytical limits as background information. Rotor lift capability decreases substantially with increasing advance ratio. It is also a function of the level of propulsive force produced, if any. For the configurations with wings, a relatively high value (0.12) of the blade loading parameter was assumed for hover and low speeds in order to minimize the rotor blade area and, therefore, rotor weight. At intermediate advance ratios, the assumed $C_{T/\sigma}$ values decrease in accordance with well-established trends. At the highest advance ratios, the trend was extrapolated to a constant but low level of $C_{T/\sigma}$ despite the fact that there are considerable model test data and analytical results suggesting that higher values are possible. The reason for this conservatism is that at high forward speeds, high rotor lift incurs stress and vibration penalties, and in any case the wing is a much more efficient lift producer than the rotor at high speeds.

The rotor lift capability for the configurations without wings are also indicated in Figure C-2 by the circled points. The lift capability of the pure helicopter drops quite rapidly with increasing advance ratio because of retreating blade stall, the increase of parasite drag with forward speed, the decrease in assumed blade twist with increasing advance ratio, and the concern about effect of rotor lift on blade stress and vibration. The

helicopter with auxiliary propulsion can operate at higher blade loading levels than the pure helicopter because the rotor propulsive force unloading provided alleviates the retreating blade stall problem to a certain extent.

Airframe Parasite Drag

Assumed levels of parasite area as a function of gross weight are shown in Figure C-3, along with representative curves for existing aircraft and estimates for achievable values from References 16 - 18 as background information. It should be noted that this parasite area includes the drag of the rotor head but not of the rotor blades, and does not include any wing drag, either profile or induced. The average drag of production helicopters is far higher than is permissible for truly high performance rotary-wing aircraft. There have been a few relatively low-drag helicopters, such as the Sikorsky S-67 "Blackhawk", and the assumed curve for the pure helicopters (configuration 1) in this study is representative of that state of the art. Substantial improvements beyond that level are possible, as pointed out in the references indicated, and as design cruise speed is increased, the weight penalty required to achieve still lower drag levels becomes increasingly balanced by savings in installed power and/or fuel required. Thus, the helicopter plus auxiliary propulsion and the full-rpm compound helicopter, (1A and 2) which cruise at somewhat higher speeds than the pure helicopters, are credited with lower parasite drag curves but higher weight penalties for drag reduction. The higher speed compound helicopters (configurations 3, 4 and 5) have still lower parasite drag curves because with their high design cruise speeds it pays to make the aircraft as clean as technology will permit. Note that the TRAC compound helicopters (4 and 5) are penalized relative to the conventional rotor (3) because the differential gear unit in the rotor head increases the frontal area of the rotor head somewhat. The cleanest configuration, of course, is the TRAC stowed rotor (6) which eliminates the penalty of the exposed rotor system altogether, although there is a residual drag corresponding to the stowage volume required to enclose the rotor system in cruise flight.

Although the parasite drag levels assumed in this investigation represent a challenge to the helicopter industry and the developing agencies to achieve, it is firmly believed that these levels are achievable with proper attention in the design and development stages of the aircraft. These general levels must be achieved to make high-speed rotary-wing aircraft of any kind economically attractive. The assumptions are still quite conservative relative to demonstrated achievements in the fixed-wing aircraft field, as typified by the lowest curve on Figure C-3.

Vibration Control Weight

The assumed weight fractions required to control vibration to the required values (.05 g in cruise) are shown in Figure C-4. Basic rotor-induced vibration levels increase very rapidly with speed at high forward speeds, as pointed out in References 19 and 20. At constant lift the increase with advance ratio is much greater than a linear relationship. For this reason, the assumption was made that the vibration control weight fraction increases linearly with forward speed despite the reduction in rotor lift with forward

speed that occurs in the compound helicopter configurations. The slowed rotor compound configuration was penalized 25 percent relative to the full rpm configuration to account for the higher advance ratios encountered at any given forward speed and the fact that the airframe must be "detuned" at two frequencies rather than just one. The TRAC compound configurations are assumed to require one-half of the weight allowance required by the conventional rotors. This is a conservative assumption because wind tunnel test data on the TRAC dynamically scaled rotor system, Reference 1, showed that the reduction in diameter reduced vibration levels by a factor of three, despite the corresponding increase in advance ratio. The stowed TRAC configuration has no need for a vibration control weight allowance in cruise flight, but a residual 0.5 percent of gross weight was assumed to provide an allowance for vibration control in low speed flight.

Values shown in Figure C-4 are based on 4-bladed rotors. Sikorsky experience has shown that the vibration levels are quite strongly a function of blade number, with a reasonable statistical fit provided by an inverse square relationship. Thus, in the present study, the factor $(\frac{4}{n})^2$ is applied to the Figure C-4 data for a number of blades (n) other than four.

Rotor Gust Response Criteria

The high-speed compound helicopter configurations must be designed and operated to ensure that the rotor flapping motion is stable enough in a gust environment to prevent rotor blade/airframe contact. Such contact must be prevented from happening even once during the life of the aircraft, so the gust considered must be a severe one. An unrelieved vertical gust of 50 ft/sec was assumed in the present study.

A series of calculations were made for hypothetical rotors of varying Lock number, utilizing the Sikorsky Generalized Rotor Performance computer program. Blade Lock number, proportional to the ratio of aerodynamic flapping moment to blade flapping inertia, is a primary parameter in determining flapping response to a gust. The calculations covered a range of tip speeds and advance ratios representative of the current study. A "delta-three" angle of 30 degrees, corresponding to a pitch/flap coupling ratio of -0.577, was assumed, because of the known benefits of this coupling on flapping response. In each calculation, the time history of blade flapping motion was examined after imposition of the assumed gust, and the maximum value, usually occurring in the first or second revolution, was recorded. It was established that down-flapping angles over the nose due to a down-gust were invariably larger than those over the tail due to an up-gust, so that the down-gust is more critical, assuming equal clearance angles over nose and tail. The down-gust is also the critical case with regard to lateral clearances (wing tips). Results of the calculations are presented in Figure III-5. The adverse effects of high advance ratio and the beneficial effects of low blade Lock number are evident.

The calculations also established that the maximum flapping angle was, to a resonable approximation, inversely proportional to the rotor tip speed for a given advance ratio and blade Lock number. Put another way, the product

of tip speed and flapping response angle is essentially independent of tip speed for a given advance ratio and Lock number. This relationship, which permits a simplification of the problem, is shown in Figure C-6.

The criterion for flapping selected in the present study was 12 degrees. This is a degree or two less than the clearance angles provided in the point design aircraft studies, but the margin is believed necessary for the uncertainties of blade elastic response (not considered in this analysis) or of aircraft pitching and rolling response, which could serve to reduce physical clearances during the transient following the severe gust encounters. Another condition imposed is that the rotor rpm, and therefore tip speed, be permitted to drop by 10 percent of the nominal design cruise value, because in a highly turbulent environment, rotor rpm control might be particularly difficult.

Based on the assumed flapping criterion (12° max flapping angle for a 50 ft/sec vertical gust at 90% of design cruise tip speed), the relationship between Lock number, nominal design cruise tip speed, and maximum forward speed was derived, as shown in Figure C-7. As can be seen, high design cruise speeds require either high tip speeds (with associated very high advancing tip Mach numbers) or low blade Lock numbers. In some cases investigated for the compound helicopter configurations, the cruise tip speeds desired from a performance standpoint could not be allowed because the gust reponse criteria were not met. In these cases, the design cruise tip speed was increased until the criteria were satisfied. (An alternate procedure, not investigated, would be to increase blade weight to reduce Lock number.)

One final condition was imposed because of the fact that blade Lock number changes with altitude. Neglecting any change in gust magnitude with altitude, the gust response problem is more severe at low altitudes (high Lock number) than at high altitudes (low Lock number). Requiring the aircraft to operate at the same true airspeed at sea level as at the design altitude imposes a severe minimum tip speed restriction that degrades the cruise performance at the design point. The two reduced rpm aircraft configurations (both conventional and TRAC rotor compounds) were affected by this consideration. For this reason, the condition was imposed that the aircraft must be only capable of operating at a constant <u>equivalent</u> airspeed from sea level to the design cruise altitude. (This would not impose operating difficulties for the pilot because this requirement corresponds to a constant indicated airspeed, i.e., a constant red line limit. It does however, impose operating envelope restrictions.) Even with the assumption of a constant equivalent airspeed, it was discovered that sea level operation determined the minimum allowable tip speed. For the affected aircraft, performance penalties in cruise were still encountered.

<u>Wing Aerodynamic Design Criteria</u>

Conservative assumptions were made for wing aerodynamic design. The aspect ratio was optimized for the baseline conventional slowed rotor compound helicopter design, considering the influence of hover vertical drag and cruise induced drag on the resulting design. An aspect ratio of 6 was

selected as optimum, and this value was used for all other configurations. Although this assumption may not be completely accurate, it is believed adequate to get the correct trends in the parametric study conducted. A taper ratio of 0.7 was selected, and it was assumed that the minimum profile drag coefficient is .0079, span efficiency factor is 0.8, with a maximum L/D of 21.8 at an optimum lift coefficient of 0.37. In sizing the wing, the rotor lift in cruise was first determined as previously discussed, and then the wing area selected to provide the remaining required lift at a trimmed lift coefficient of 0.52, at which the wing L/D is 18.6.

For the stowed rotor aircraft, a different wing sizing technique was required. It was assumed that the conversion speed at which the rotor is stopped and stowed is 150 knots equivalent airspeed. A 20-percent stall margin was assumed, i.e., stall speed = 150/1.2 = 125 knots EAS. A trimmed overall $C_{L_{max}}$ of 2.0 was assumed, which should be achievable with a relatively simple single-slotted flap. Lift coefficient required at 150 knots EAS is 1.39. The resultant wing loading is 106 lb/ft^2 for all of the stowed rotor designs. Cruise wing lift coefficient is then determined by flight dynamic pressure.

Block Speeds

Aircraft block speeds are less than cruise speeds because of the time spent in the mission on the ground or in hover. The mission profile specifies 12 minutes, or 0.2 hour, of such "unproductive" time. Another source of increased mission time is the reduced forward speeds assumed in climb to or descent from cruise altitude. The assumptions in this study were that rate of climb or descent is no greater than 2000 feet per minute; climb speed is 66 percent of design cruise speed; and average descent speed is 90 percent of cruise speed for cruise altitudes of 10,000 feet or less, or 93.5 percent of cruise speed for an altitude of 20,000 feet. Altitude cruise missions were assumed to start and end at sea level. With these assumptions, the variation of block speed with cruise speed and altitude is shown in Figure C-8. For the 4000 ft 95° F missions, the entire mission was assumed to be at a constant altitude, so that block speed is the same as that shown for sea level in Figure C-8.

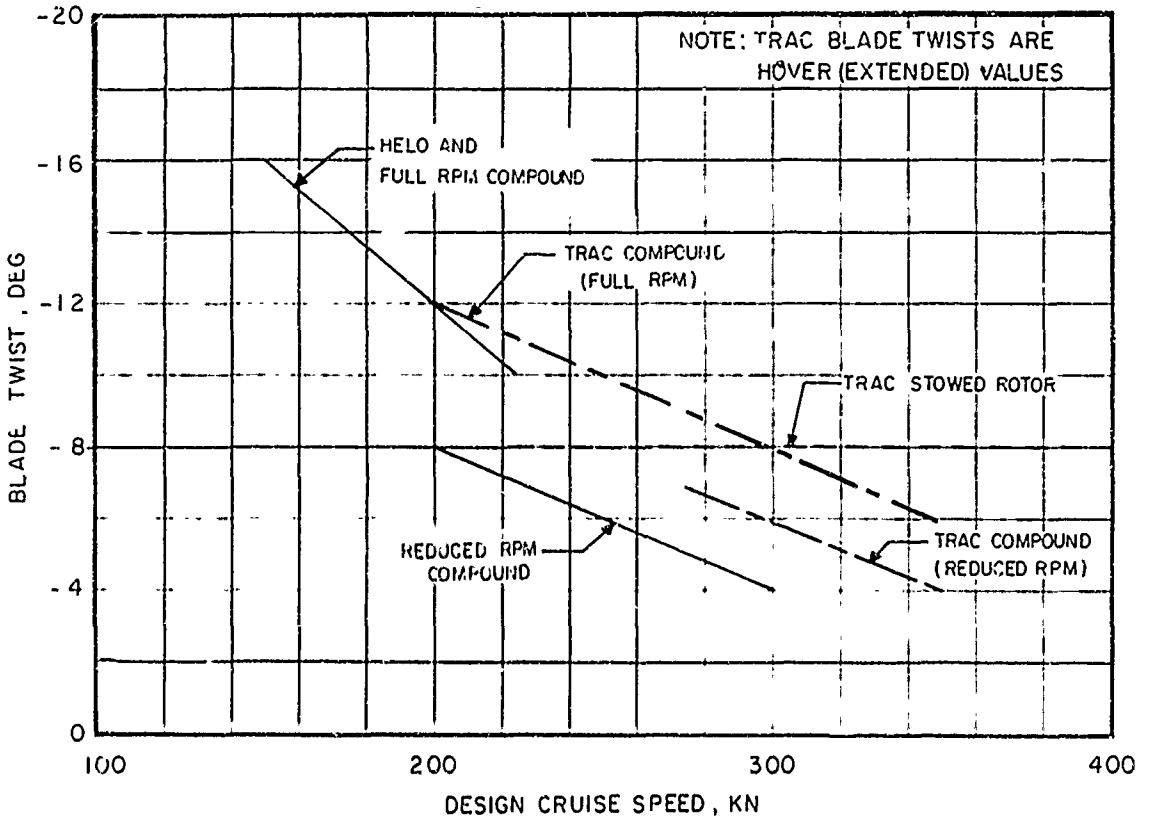

Figure C-1. Allowable Blade Twist Values.

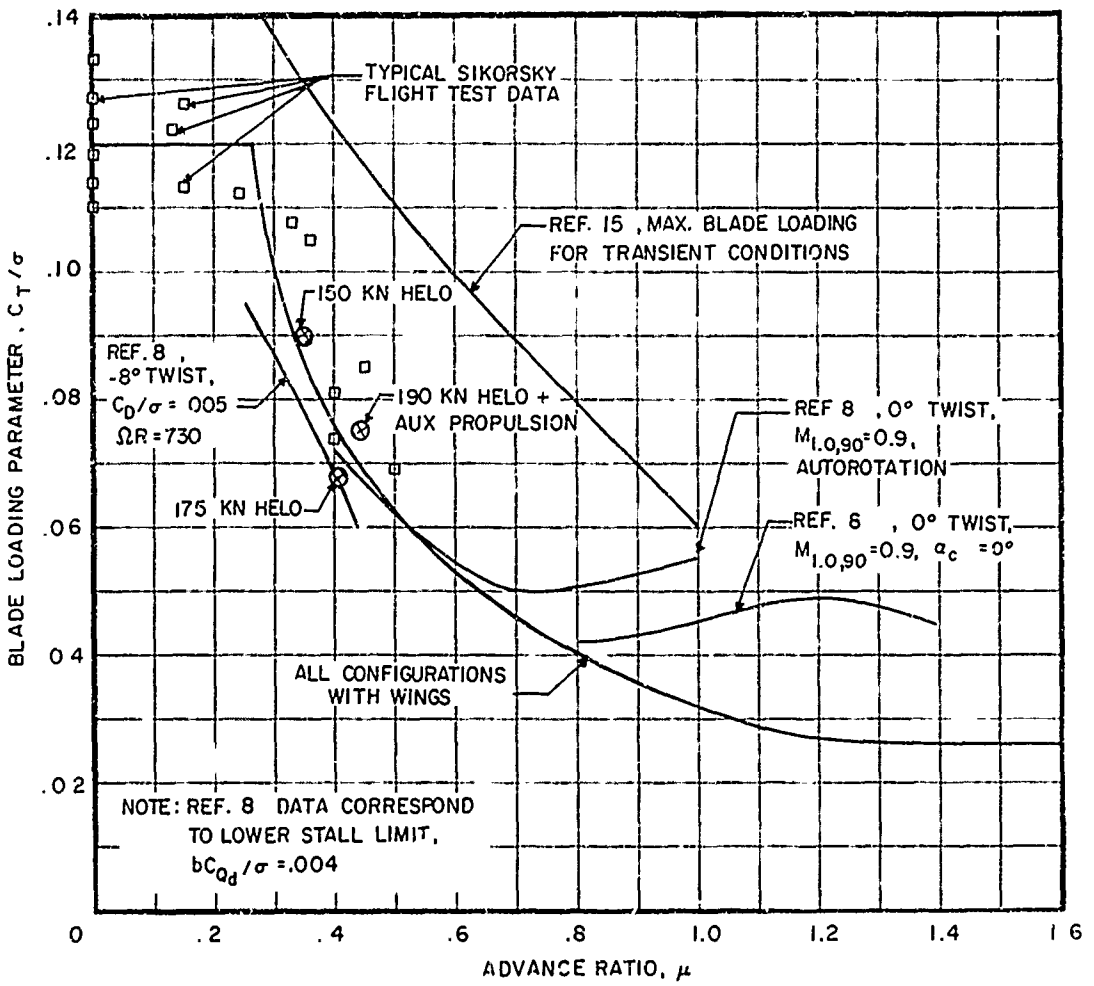

Figure C-2. Allowable Blade Loadings.

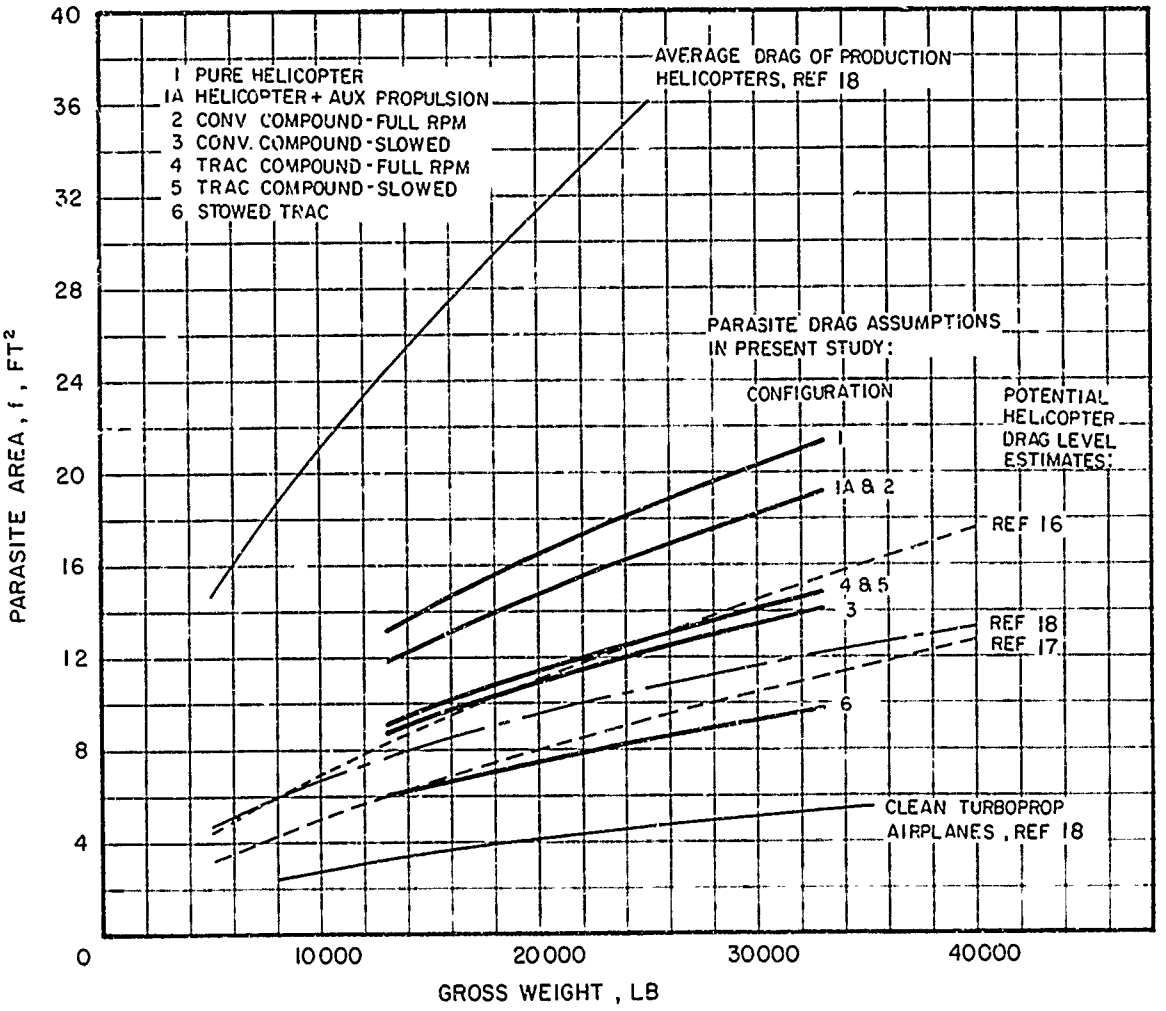

Figure C-3. Parasite Area Trends.

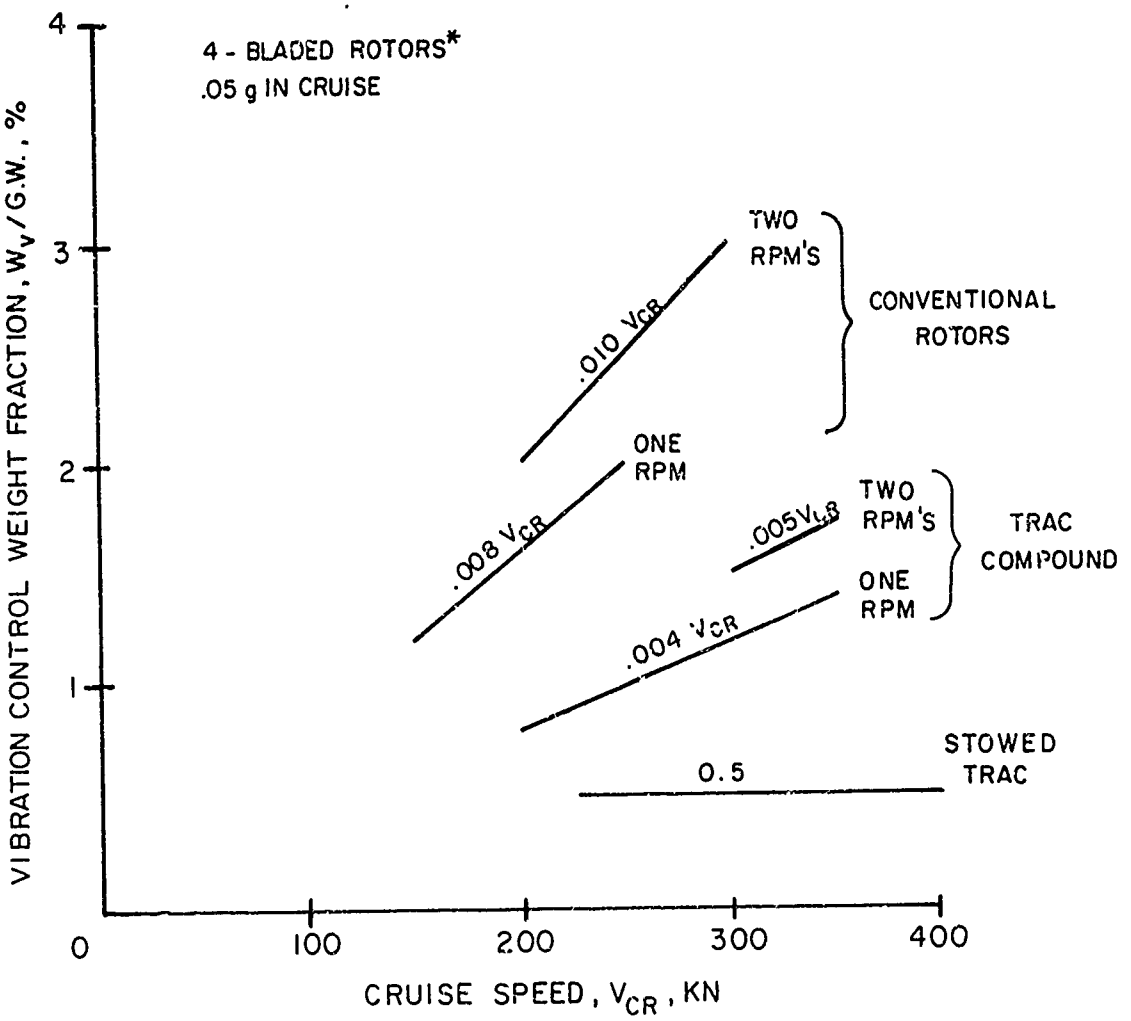

*FOR n-BLADED ROTORS, MULTIPLY ABOVE WEIGHT FRACTIONS BY $(4/n)^2$

Figure C-4. Vibration Control Weight Fractions.

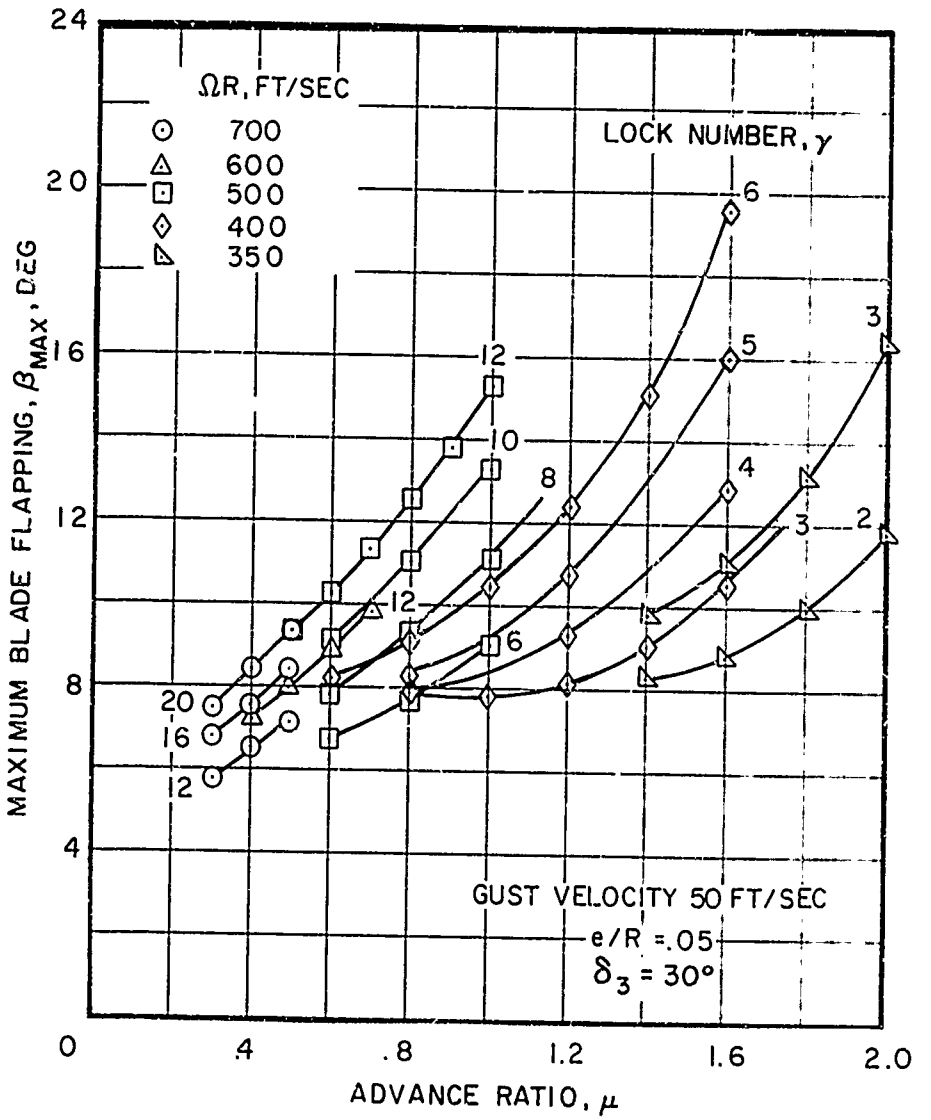

Figure C-5. Calculated Rotor Flapping Response to 50 ft/sec Gust.

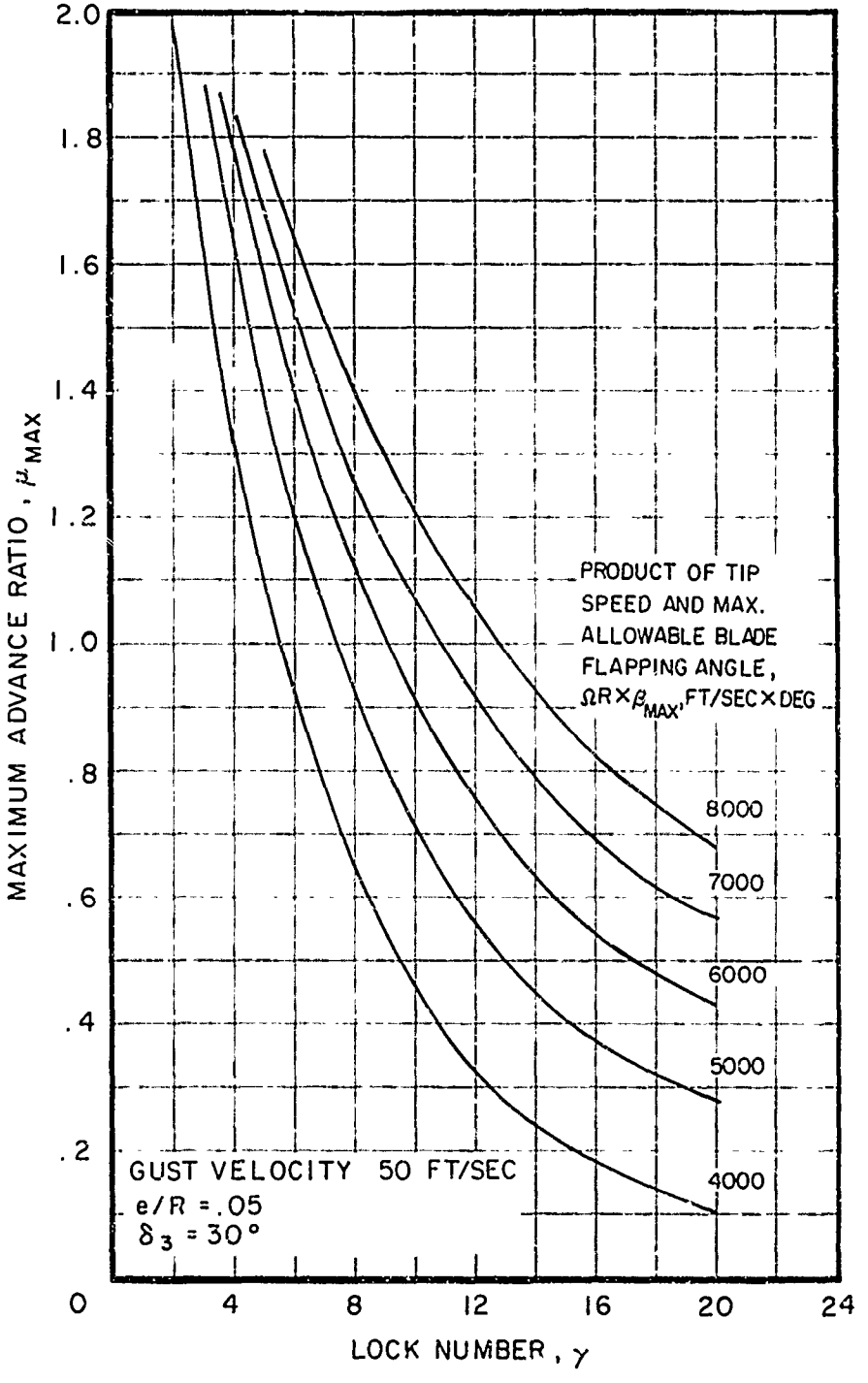

Figure C-6. Generalized Flapping Response Chart for 50 ft/sec Gust.

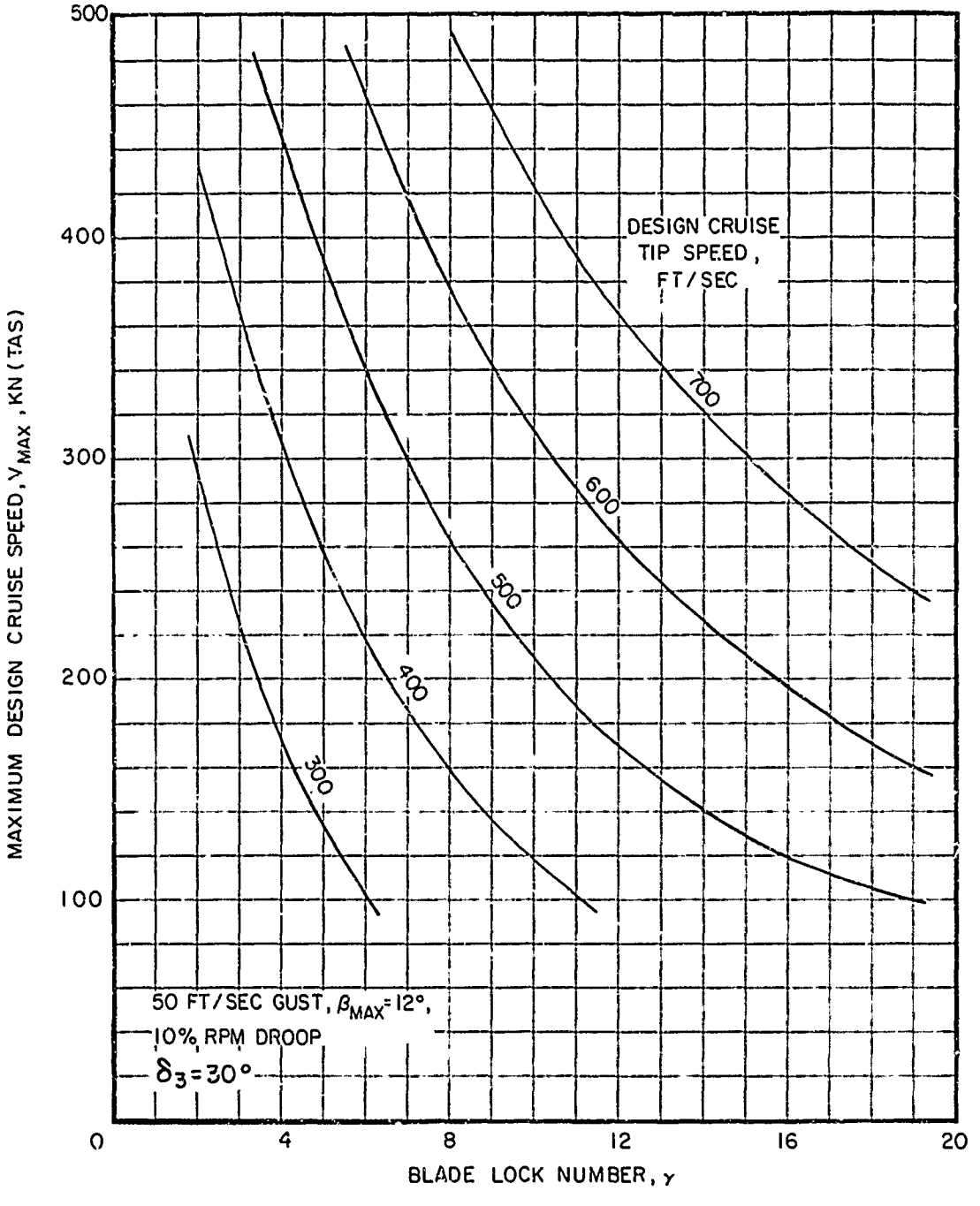

Figure C-7. Design Operating Conditions to Satisfy Gust Response Criteria.

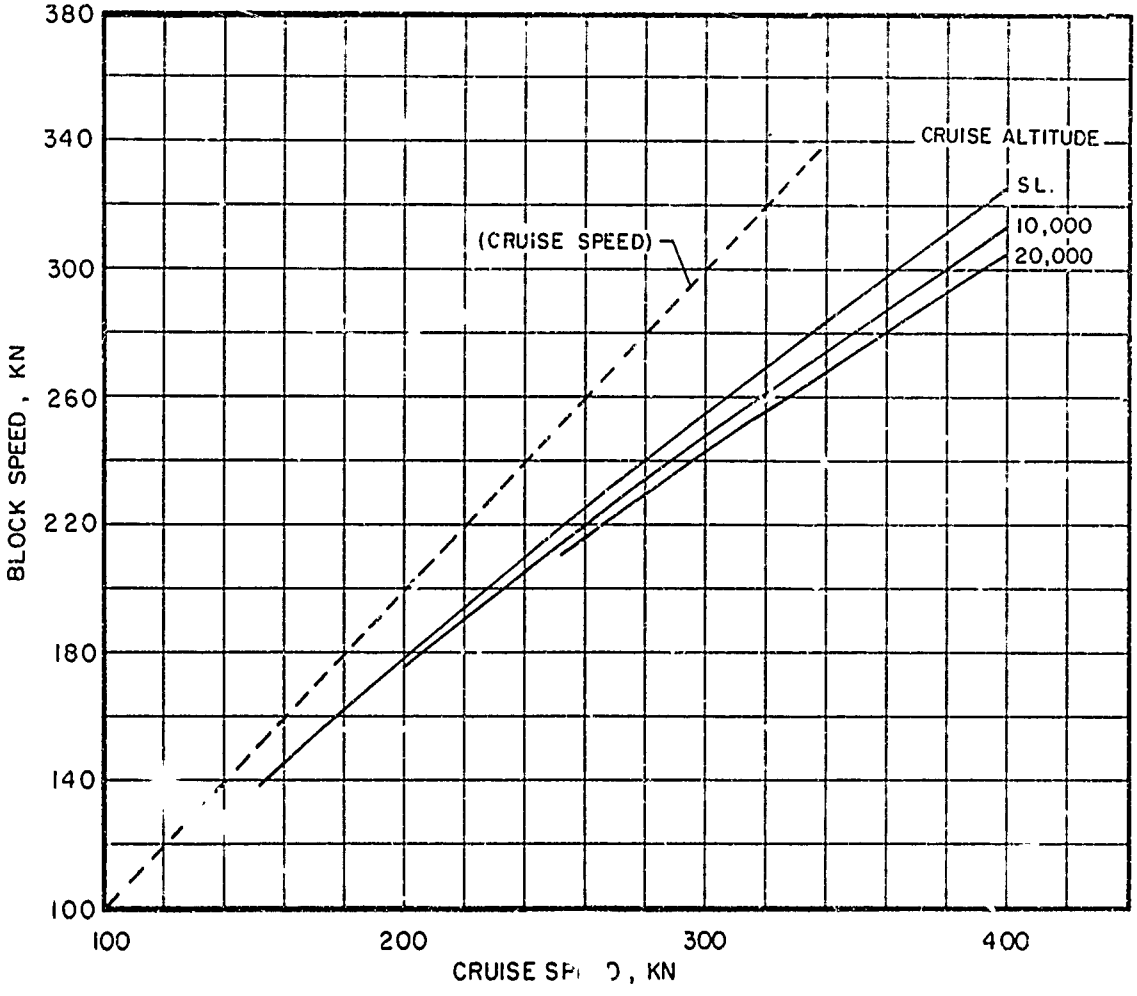

Figure C-8. Variation of Block Speed with Cruise Speed and Altitude.

APPENDIX D

PARAMETRIC WEIGHTS METHODOLOGY

Subsystem weights for pure helicopters and conventional compounds are estimated from standard Sikorsky statistical trends normalized to YUH-60A UTTAS hardware, with modifications to account for the effect of advanced technology for 1980 IOC (Initial Operating Capability). Weight estimates of rotor components unique to the TRAC concept are derived from analytical equations correlated to the 56-foot-diameter preliminary design TRAC rotor, corrected for prototype structural conservatism and technology improvements by 1980 IOC. Equipment weights are taken from UTTAS and include only minor modifications for the difference between compounds and pure helicopters and for differences noted in the general specification, Appendix B.

Subsystems whose weight trends vary with the aircraft configuration are discussed below.

1. MAIN ROTOR GROUP

   a) Pure Helicopter and Conventional Rotor Compounds - The pure helicopter and conventional rotor compound helicopters utilize articulated rotors with titanium-spar blades and elastomeric hinge/titanium head design. This rotor head concept is employed on the Sikorsky UTTAS (YUH-60A).

   The parametric equation shown uses rotor radius, blade chord, tip speed, advance ratio, blade aspect ratio, and a stress conservatism factor as parameters. Since the basic equation predicts the weight for an aluminum blade, a technology factor of 0.878 is used to reflect a 12.2% weight savings achieved on the UTTAS titanium blade. For the compound rotor the structural design advance ratio is defined at 150 knots, representative of the condition of maximum rotor structural loading. A stress conservatism factor (1+MS) of 1.66 was selected for the IRB blades, based on the CH-53 and UTTAS.

   Weight for the titanium rotor hub is derived by applying a weight savings of 14.1% over a conventional steel hub (11.1% based on UTTAS design and 3% for technology improvement by 1980). Elastomeric hinge weight is based on the UTTAS design except that the spindle is changed from steel to titanium to yield a weight saving of 11.3% in total hinge weight over UTTAS and 24.5% saving over a conventional steel hinge. Weight penalties for the articulating hub fairing for drag reduction based on the S-67 Blackhawk, and for manual blade fold at 4.3% of blade weight, based on UTTAS, are added.

b) TRAC Compound -

(1) Blades

Parametric equations derived from analysis of blade loading are used to estimate the component weights of a TRAC blade, accounted in the following groups:

- Outer blade assembly, including spar, pocket, bearing blocks attached to spar, and miscellaneous items such as paint, tips, and balance weights.
- Torque tube assembly, including outer torque tube, nut reaction tube, cuff, and bearing blocks.
- Tension-torsion straps, including tip block and hardware.
- Jackscrew assembly, including jackscrew, redundant strap, jackscrew spindle, jackscrew tip bearing and BIM.
- Retraction nut assembly.

The 56-foot TRAC rotor developed in the preliminary design section of this report is used as a base for determining coefficients to the blade equations after modifications are made to reflect technology improvements by 1980 IOC. The preliminary design weights and assumed percentage savings for 1980 are summarized in Table 6.

(i) Outer blade assembly - The outer (lifting) section of the blade is retained by internal tension straps, and so is in compression under its own centrifugal force field. The parametric weight equation for the outer blade assembly is:

$$W_b = \frac{k_1 \; x\,(1+MS)\; C_{l_m} \left(\frac{t}{c}\right) \left(\frac{Rc}{100}\right) \left(\frac{AR}{10}\right) \left(\frac{\Omega R}{100}\right)^2 R\,(.0718+0.16\mu^2) + k_2\, x \left(\frac{Rc}{100}\right)}{\left[1-.000747\;(1+MS)\left(\frac{\Omega R}{100}\right)^2\right]\left[\left(\frac{t}{c}\right)^2 + .0216\left(\frac{AR}{100}\right)^2\left(\frac{\Omega R}{100}\right)^2\right]} \qquad \text{(D-1)}$$

Where: W_b = unit weight of outer blade assy., lb

k_1 = 0.447 = correlation constant for spar weight

k_2 = 3.755 = correlation constant for pocket weight

x_1 = blade root cutout radius ratio (extended blade) = 0.5

$x = 1 - x_1$ = (length of outer blade)/R = 0.5

MS = conservatism factor, 0.891

$t/_c$ = airfoil thickness to chord ratio

R = blade radius, ft (extended blade)

c = outer blade chord, ft

AR = blade aspect ratio, $R/_c$

ΩR = normal tip speed, fps

μ = design advance ratio

C_{l_m} = mean lift coefficient = $\frac{2(C_T/\sigma)}{1/3 + 1/2\ \mu^2}$

C_T = rotor thrust coefficient

σ = rotor solidity ratio

As for conventional compound rotors, the design structural advance ratio is defined at 150 knots, representative of the condition for maximum rotor structural loading. The first term in the equation accounts for the weight of a graphite/honeycomb sandwich spar of high modulus and of constant wall thickness. A trade-off analysis shows that this spar is 11.9% lighter than an equivalent solid graphite/epoxy spar such as was used in the preliminary design. The second term in the equation accounts for the weight of a structural pocket, bearing blocks and miscellaneous items. It should be noted that composites are used to advantage here in reducing weight because blade coning is not a critical design consideration, as for conventional articulated blades for which maximum coning angle sometimes dictates minimum blade weights.

(ii) Torque tube assembly - The aluminum torque tube is a streamlined ellipse in cross section, enclosing the jackscrew. It transmits blade pitch control motion to the outboard blade and carries bending moments across the sliding joint. The inner steel torque tube reacts nut torque during retractions and provides a degree of structural redundancy. Aluminum and steel were selected for torque tube materials rather than titanium because of fabrication complexities associated with titanium. The parametric equation for estimating the weight of the torque tube assembly is:

$$W_T = \frac{k_T (x_2 - x_0)(1+MS) C_{l_m} \left(\frac{l}{b_T}\right) \left(\frac{\Omega R}{100}\right)^2 \left(\frac{Rc}{100}\right) \left(\frac{R}{10}\right)^2 (0.136 + .075\mu^2)}{1 + \frac{.0467 \left(\frac{\Omega R}{100}\right)^2 \left(\frac{AR}{100}\right)^2}{\left(\frac{t}{c}\right)^2}} \qquad \text{(D-2)}$$

Where: W_T = unit weight of torque tube assy., lb

k_T = correlation constant = 1.897

x_2 = radius ratio, radius of tip of outer torque tube to extended blade radius

x_0 = radius ratio, blade cuff radius to extended blade radius

b_T = semi-minor axis of torque tube section = $0.346(t/c)\,c$, ft

MS, C_{l_m}, ΩR, R, c, μ, AR, and t/c are blade parameters as defined for the outer blade assembly.

No weight saving over preliminary design estimates is assumed for the torque tube assembly for 1980 IOC. Torque tube design is not strongly dependent on outer blade weight because it carries only its own centrifugal loads.

(iii) Tension-torsion straps - The tension-torsion straps carry the centrifugal loads of the outboard blade. For sizing and weight estimation, a 25% rotor overspeed condition is used with a factor of safety of 1.5, with two straps failed. The straps (12 per blade) are fabricated from high strength, steel alloy (Vascomax 300) with an ultimate tensile stress allowable of 280,000 psi. The parametric weight equation is given by

$$W_s = \frac{k_s W_b \left[\frac{\Omega R}{100}\right]^2 (1-x_1^2)}{1 - 0.00452 \left[\frac{\Omega R}{100}\right]^2 (1-x_1^2)} \qquad \text{(D-3)}$$

Where: W_s = unit weight (per blade) of tension-torsion straps, lb

k_s = correlation constant = 0.00569

W_b = unit weight of outer blade, lb

ΩR = normal tip speed, fps

x_1 = blade root cutout radius ratio = 0.5

The diameter of each strap is tapered along its length to keep the centrifugal working stress constant spanwise. Weight includes root and tip reinforcements for attachment to nut and tip block, respectively.

(iv) Jackscrew assembly - The jackscrew and redundant strap carry the entire centrifugal force of the outer blade. The strap provides structural redundancy for fail-safety and is designed to carry the entire centrifugal load in case of failure in the jackscrew. High-strength steel (Vascomax 300) is used. The weight trending equation is given by

$$W_{JS} = \frac{k_{JS} \ (W_b+W_s) \ \left[\frac{\Omega R}{100}\right]^2 \ (x_2' - x_0) \ (1 + x_1)}{1 - .00452 \ (x_2'^2 - x_0^2) \ \left[\frac{\Omega R}{100}\right]^2} \qquad \text{(D-4)}$$

Where:

W_{JS} = unit weight of jackscrew assy., lb

k_{JS} = correlation constant = 0.0171

W_b = unit weight of outer blade, lb

W_S = unit weight of tension-torsion straps

ΩR = normal tip speed, fps

x_2' = radius ratio, jackscrew tip radius to extended blade radius = 0.543

x_0 = blade attachment face radius ratio = 0.0643

x_1 = blade root cutout radius = 0.5

The jackscrew assembly is also designed for an overspeed condition at 125% rpm and a factor of safety of 1.5. Weight includes 1.0 lb (per blade) for a BIM system.

(v) Retraction nut assembly - The jackscrew/nut combination uses multiple nuts (6 per blade) with individual straps (2 per nut) connected to the tip block of the outer blade. Titanium with a carbon insert and beryllium copper base is used. The parametric weight equation is based on the allowable bearing stress between the surfaces of the jackscrew and nut threads.

$$W_n = \frac{k_n \; p \; W_{JS}}{R\,(x_2' - x_0)} \cdot \qquad \text{(D-5)}$$

Where: W_n = unit weight of nut package, lb

k_n = correlation constant = 49.32

p = pitch of threads, ft

W_{JS} = unit weight of jackscrew assy., lb

R = rotor radius (extended), ft

x_2' = radius ratio = 0.543

x_0 = radius ratio = 0.0643

(2) Diameter change mechanism -

The drive mechanism is a differential gear unit located within the main rotor shaft and hub. It actuates the power screw, which, in turn, retracts or extends the nuts and straps, imparting retraction or extension motion to the outer blade. A weight summary of the drive mechanism is shown in Table 6. The weights are taken to be a function of design torque. The coefficient is determined by indexing to the 1980 IOC weight estimate (Table 6), and the exponent is taken from historical data on drive systems.

$$W_{DM} = 168.33 \left(\frac{HP_D}{RPM_J} \right)^{0.75} \qquad \text{(D-6)}$$

Where: W_{DM} = total weight of drive mechanism, lb

HP_D = design horsepower

RPM_J = output rpm of jackscrew = 1.5 main rotor rpm

The design horsepower of the drive mechanism for blade retraction is that required to overcome the average centrifugal force of the outer blade, straps, and nuts at full rotor rpm for a specified retraction time (30 seconds). It is given by:

$$HP_D = \frac{k_D}{t\, e_J} (x_1 - x_0') \left[\frac{\Omega R}{100}\right]_r^2 \left[(W_b + W_s)(1 + x_0') + W_n (x_1 + x_0')\right] \quad \text{(D-7)}$$

Where: HP_D = design horsepower

k_D = correlation constant = 3.644

x_1 = blade root cutout radius ratio = 0.50

x_o' = radius ratio, cuff outboard end radius to extended blade radius = 0.090

$(\Omega R)_r$ = retraction tip speed, fps

t = retraction time, sec.

e_J = jackscrew dynamic efficiency

W_b = unit weight of outer blade, lb

W_S = unit weight (per blade) of tension-torsion straps, lb

W_n = unit weight (per blade) of retraction nut package, lb

Weight is saved in the diameter-change mechanism if the main rotor is slowed before blade retraction to perhaps 80% rpm. Advantage of this is taken for both the slowed TRAC rotor compound and the stowed TRAC aircraft. Weight of diameter-change mechanism for stowed TRAC rotor includes corrections for increased length in the retraction, extension and locking shafts.

(3) Hub and hinges -

Weight trending equations based on UTTAS design points are used to predict hub and hinge weights for a TRAC rotor head, with coefficients modified to reflect the TRAC configuration and 1980 IOC technology. The TRAC rotor hub preliminary design consists of upper and lower titanium plates which enclose the differential gear unit and universal joint. A weight saving of 4.2% over the preliminary design value is taken for 1980 IOC in consequence to the 8.5% blade weight saving. The weight trending equation is given by:

$$W_{hub} = 16.81 \left[\left[\frac{b\, W_{bT}\, e}{100R}\right]\left[\frac{\Omega R}{100}\right]^2\right]^{0.75} \quad \text{(D-8)}$$

Where: W_{hub} = weight of hub, lb

b = number of blades

R = rotor radius, ft

ΩR = normal tip speed, fps

e = flapping hinge offset, ft

W_{bT} = unit blade weight, lb

$= W_b + W_T + W_S + W_{JS} + W_n$

The trending equation for the unit hinge weight is:

$$W_{hi} = 40.0\ L^{\frac{1}{2}} \left[\left[\frac{W_{bT}}{100R} \right] \left[\frac{\Omega R}{100} \right]^2 \right]^{0.875} \qquad \text{(D-9)}$$

Where: W_{hi} = unit hinge weight, lb

L = hinge length, ft

R = rotor radius, ft

ΩR = normal tip speed, fps

W_{bT} = unit blade weight, lb

$= W_b + W_t + W_s + W_{JS} + W_n$

For drag reduction, a weight penalty for an articulating hub fairing trended from the S-67 Blackhawk is used for the reduced and full rotor rpm TRAC compounds. For the stowed TRAC rotor aircraft, weight penalties for conventional hub fairing and for in-flight power blade fold are added. The latter is based on a preliminary design study and is given by:

$$W_{BF} = 0.247\ \frac{bW_{bT}}{L_R^2} \qquad \text{(D-10)}$$

Where: W_{BF} = weight penalty for power blade fold, lb

L_R = Retraction ratio = $\frac{\text{extended rotor diameter}}{\text{retracted rotor diameter}}$

W_{bT} = unit weight of TRAC blade, lb

b = number of blades

The weight penalty for power blade fold is less for TRAC than for conventional rotors partly because the blade area and moment arm are reduced by the diameter reduction and partly because the TRAC blades fold fore and aft about the lag hinge and do not require separate fold hinges.

2. FLIGHT CONTROLS GROUP

a) Pure Helicopter

Pure helicopter flight controls weight estimates are obtained for redundant mechanical systems from the relation

$$W_{FC} = 14.04 \left[\frac{N_z\ SGW}{1000}\right]^{0.875} \qquad \text{(D-11)}$$

Where: W_{FC} = flight controls weight, lb

N_z = ultimate load factor

SGW = structural design gross weight, lb

The equation includes dual cockpit controls, redundant controls from cockpit to power operated flight controls, SAS and FAS, and power boost. The use of composite stationary and rotating swashplates with fiberglass bellcranks saves 7% of total flight controls weight.

b) Compound

To estimate the flight controls weight for the compound, the pure helicopter equation is used as above, but with an effective N_z SGW to account for the fact that the rotor is not fully loaded at cruise speed. This is based on the CH-53 blade loading at a limit load factor of 3.0. The resulting equation is

$$W_{FC} = 14.04 \left[0.663 \left[\frac{bRc}{100}\right]\left[\frac{\Omega R}{100}\right]^2\right]^{0.875} + W_{FW} \qquad \text{(D-12)}$$

Where: W_{FC} = flight controls weight, lb

b = number of blades

R = rotor radius, ft

c = blade chord, ft

ΩR = normal tip speed, fps

W_{FW} = delta weight for fixed-wing controls, lb

Fixed-wing controls for rudder, elevator, and flaperon are scaled from the Fairchild A-10. A new coefficient is then determined for the combined helicopter and fixed-wing controls. The resulting equation is

$$W_{FC} = 18.38 \left[0.663 \left(\frac{bcR}{100}\right)\left(\frac{\Omega R}{100}\right)^2 \right]^{0.875} \qquad \text{(D-13)}$$

This equation yields a flight controls weight which is approximately 31% heavier than that of a pure helicopter.

c) Stowed TRAC

For the stowed TRAC rotor aircraft, an additional weight increment of 40 lb is added to account for increased size of stationary and rotating scissors and additional servo supports.

3. DRIVE SYSTEM

Drive system weight is broken down into contributions from individual gearboxes and shafts, each weight being calculated to take proper account of shaft rpm and transmitted horsepower, following established trends. Separate equations are used for main gearbox, intermediate gearbox, tail gearbox, main rotor shaft and tail rotor shaft. Weight trending varies among the concepts studies according to each specific drive system configuration. For example, the full rpm conventional rotor compound is unique in the family of compounds studied, in that it has a single propeller for auxiliary propulsion, driven from a gearbox common to the tail rotor, as in the AH-56. For the slowed rotor compounds, a two-speed main gearbox, scaled from corresponding gearboxes designed for the Sikorsky S-65-200 commercial compound project, was employed on the reduced rpm compounds. Drive system weights for reduced rpm compounds also include corrections for wing-mounted take-off gearboxes and wing cross-shafting. Rotor brakes, incorporated in all conventional rotor but not the TRAC rotor designs (because the diameter -change clutches can also serve the rotor brake function), are estimated from

$$W_{RB} = 1.494 \left[\left(\frac{bW_b}{1000}\right)\left(\frac{\Omega R}{100}\right)^2 \right]^{0.875} \qquad \text{(D-14)}$$

where W_b is the weight of a single rotor blade, b is the number of blades, and ΩR is the normal tip speed.

4. POWERPLANT

All rubberized engines in this study were scaled from the Lycoming PLT-27 advanced technology turboshaft engine. Assuming engines for all designs to include air particle separators and lube system, the engine weight trend can be written

$$W_{ENG} = 367.4 \ ESF^{0.70} \qquad \text{(D-15)}$$

per engine, where ESF = engine scale factor. The exponent is based on current technology engine weight versus shaft horsepower trends, and presumes that each rubberized engine developed in this study is of PLT-27 technology level, but is not necessarily of the PLT-27 family. Engine manufacturers' projected growth-engine weight relations do assume a descent from a physical engine, and thus contain exponents often significantly higher than that assumed here.

For real engine analysis, all engine weights data employed was provided to Sikorsky by the appropriate engine manufacturer, adjusted to include the weight of an inlet particle separator and integral lubrication if not included in the basic engine weight.

5. WING GROUP

The North American trending equation was used for wing weight estimation, given by

$$W_W = \frac{k_w \, S_w^{\ 0.725} \, AR^{\ 0.436} (r \, N_z \, SGW)^{\ 0.516} (10\lambda)^{\ 0.127}}{\left(100 \, \frac{t}{c}\right)^{0.186} (100 \cos \Lambda_{.25})^{\ 0.686}} \qquad \text{(D-16)}$$

Where:

W_W = wing weight, lb

k_w = correlation and technology factor = 0.686

S_w = theoretical planform area, ft^2

AR = aspect ratio = b^2/S_w

b = wing span, ft

t/c = root thickness to chord ratio

$\Lambda_{.25}$ = sweep at 25% chord, degrees

λ = taper ratio = c_t/c_r

c_t = chord at tip, ft

c_r = chord at root, ft

N_z = ultimate load factor

SGW = structural design gross weight, lb

r = wing lift ratio = $\frac{L_w}{N_z \text{ SGW}}$

L_w = ultimate wing lift, lb

For a compound helicopter, lift is shared between the main rotor and wing. The wing lift ratio represents a modification to the fixed-wing equation. The equation coefficient is determined by indexing to the current weight of the RSRA wing. A weight saving of 9% is estimated for technology improvement by 1980 IOC, with the use of composite spars and Kevlar fairings.

6. BODY GROUP

Body group weights for all configurations are estimated from standard Sikorsky body group trends, normalized to YUH-60A UTTAS. A weight saving of 9.4% is estimated for technology improvement by 1980 IOC with limited usage of composites in heavily loaded areas (such as primary structure in the transmission bay) and with the use of Kevlar fairings and titanium fittings. For the stowed TRAC rotor aircraft, weight increments are added for the following features:

a) Rotor stowage compartment doors, trended from

W_{DR} = 6.0 Rc (D-17)

Where: R = rotor radius, extended, ft

c = outer blade chord, ft

W_{DR} = weight of doors, lb

b) Enclosure for main rotor shaft.

c) Supports for stowed blades.

d) Removal of main rotor pylon from equation weight, estimated at 1.0 pound per square foot of wetted area.

7. FIXED EQUIPMENT WEIGHTS

The following equipment weights are adopted from UTTAS with minor modifications for compound configurations according to the general specifications of Appendix B.

ITEM	CONFIGURATION					
	Pure Helo.	Full RPM Convent. Comp.	Slowed RPM Convent. Comp.	Full RPM TRAC Comp.	Slowed RPM TRAC Comp.	Stowed TRAC
APU	193	193	193	193	193	193
Instruments	183	183	183	193	193	193
Hydraulics(1)	-	-	-	-	-	-
Electrical	306	310	434	310	434	310
Avionics	325	325	325	325	325	325
Furnishings	392	424(2)	424	424	424	424
Air Cond. & Anti-Ice	86	(3)	(3)	(3)	(3)	(3)
Aux. Gear	59	59	59	59	59	59
Vibration Suppress.(4)	-	-	-	-	-	-
Contingency	0	(5)	(5)	(5)	(5)	(5)

Notes (1) Based on weight trend $W_H = 12.75\left(\frac{DGW}{1000}\right)^{0.63}$

(2) For cruise flight below 10,000 feet use 392 lb

(3) Air conditioning (53 lb) plus anti-icing determined from $W_{AI} = 1.25b + 33$, where b = de-iced wing span

(4) Discussed in Appendix C.

(5) Based on 1% of weight empty

LIST OF SYMBOLS

a	airfoil lift curve slope, per radian
b	number of blades
$\frac{b\ C_{Qd}}{\sigma}$	blade stall parameter
c_f	coefficient of friction
C_L	wing lift coefficient, $\frac{\text{wing lift}}{1/2\,\rho\,V^2 S}$
C_{Qd}	drag torque coefficient for one blade, drag torque/$\pi R^2 \rho (\Omega R)^2 R$
C_T	Rotor thrust coefficient, $\frac{L}{\pi R^2 \rho\ (\Omega R)^2}$
CF	centrifugal force
c	rotor blade chord
$\bar{c}$	mean chord, $\frac{\int_0^R cr^2 dr}{\int_0^R r^2 dr}$
E	Young's modulus of elasticity
EAS	equivalent airspeed
e	flapping hinge offset
f	parasite area, parasite drag/$1/2\rho V^2$
G	shear modulus
GW	gross weight
HP	horsepower
I_B	torsional mass moment of inertia per unit length
I_{xx}	flapwise area moment of inertia
I_{yy}	edgewise area moment of inertia
I_1	blade mass moment of inertia about flapping hinge
IRP	Intermediate Rated Power

LIST OF SYMBOLS (CONTINUED)

J	torsional area moment of inertia
L	rotor lift
L/D	lift-drag ratio
MCP	Maximum Continuous Power
M_{xx}	flapwise bending moment
$M_{1.0,90}$	advancing blade tip Mach number
P	power
PF	rotor propulsive force
PL	payload
Q	jackscrew torque
R	rotor radius (extended radius for TRAC blade)
r	distance from center of rotation to spanwise station
S	wing area
SL	sea level
V	forward speed
V_{BL}	Block speed
V_{CR}	design cruise speed
W	weight
WE	empty weight
w	weight per unit length
β	blade flapping angle
γ	Lock number, $\frac{\rho c a R^4}{I_1}$
ϵ	wing span efficiency factor
η_P	propulsive efficiency
$\theta_{.75}$	collective pitch at 75% radius

LIST OF SYMBOLS (CONTINUED)

θ_1	blade twist
λ	rotor inflow ratio
μ	advance ratio, $V/\Omega R$
ρ	air density
σ	solidity, $\frac{b\bar{c}}{\pi R}$
Ω	rotor angular velocity
ω	natural frequency